UNITED STATES DEPARTMENT OF COMMERCE
DANIEL C. ROPER, Secretary
NATIONAL BUREAU OF STANDARDS
LYMAN J. BRIGGS, Director

JOURNAL OF RESEARCH

OF THE

NATIONAL BUREAU OF STANDARDS

July 1934
Vol. 13, No. 1

UNITED STATES
GOVERNMENT PRINTING OFFICE
WASHINGTON : 1934

For sale by the Superintendent of Documents, Washington, D.C. - - Price 25 cents; $2.50 per year on subscription

Beginning with the July 1934 issue of the Journal of Research of the National Bureau of Standards, the prices of the separate Research Papers appearing in the monthly issues are given on the front cover of the Journal.

This arrangement will provide a prompt and convenient method whereby readers of the Journal of Research desiring copies of separate Research Papers appearing therein may send their orders without delay to the Superintendent of Documents, United States Government Printing Office, Washington, D.C.

Engineering Library
AUG 9 1934

UNITED STATES DEPARTMENT OF COMMERCE

JOURNAL OF RESEARCH
OF THE
NATIONAL BUREAU OF STANDARDS

Vol. 13 JULY 1934 No. 1

CONTENTS

RP.	TITLE AND AUTHOR	Page
691.	A formula and tables for the pressure of saturated water vapor in the range 0 to 374 C. By Nathan S. Osborne and Cyril H. Meyers [Price 5c]	1
692.	Heats of combustion and of formation of the normal paraffin hydrocarbons in the gaseous state, and the energies of their atomic linkages. By Frederick D. Rossini [Price 5c]	21
693.	Thermal expansion of artificial graphite and carbon. By Peter Hidnert [Price 5c]	37
694.	Equilibrium volatility of motor fuels from the standpoint of their use in internal combustion engines. By Oscar C. Bridgeman [Price 10c]	53
695.	Variations in refractive index of CO_2-free dry air and a statistical correlation with solar activity. By L. W. Tilton [Price 5c]	111
696.	Corrosion of ferrous metals in acid soils. By I. A. Denison and R. B. Hobbs [Price 5c]	125
697.	Photochemical decomposition of silk. By Milton Harris [Price 5c]	151
698.	Contribution to the design of compression members in aircraft. By Wm. R. Osgood [Price 5c]	157

[The articles listed above may be purchased (see p. II) separately for the prices indicated in the table of contents]

A monthly periodical of pure and applied science published by our National Government

JOURNAL OF RESEARCH
OF THE
NATIONAL BUREAU OF STANDARDS

¶The July 1934 issue of the Journal of Research of the National Bureau of Standards begins the thirteenth semiannual volume of this periodical. The JOURNAL contains the Bureau's research papers and critical reviews in the fields of science and technology. ¶Fundamental researches always in progress in the Bureau's laboratories have their outlet in the Journal of Research of the National Bureau of Standards. If you are interested in following the new developments in science and technology, you should receive the JOURNAL. If you are already a subscriber, continue your subscription; if not, you are invited and urged to send in your subscription at once.

TECHNICAL NEWS BULLETIN

¶This is a monthly publication containing short articles reporting progress of work in the Bureau's laboratories, abstracts of papers which appear in the Journal of Research of the National Bureau of Standards, reports of scientific and technical meetings in which the Bureau has taken part, and a list of all publications by members of the staff, and other topics within the Bureau's fields. This publication is designed primarily to give its subscribers a general review of important and timely activities and accomplishments at the Bureau. The material is presented in brief, but adequate form, for the information of those who are interested in the general activities of the Bureau. It is a prompt and reliable source of official information. If you are not already a subscriber to this monthly periodical you are urged to place your subscription.

ANNUAL SUBSCRIPTION	Prices	
	United States, Canada, Cuba, Mexico, Newfoundland, Republic of Panama	Other countries
Journal of Research of the National Bureau of Standards:		
12 monthly issues (2 volumes), paper covers	$2.50	$3.25
Bound volume (½ year, 1 volume), blue buckram . . .	3.00	3.50
Technical News Bulletin, 12 monthly issues	.50	.70

Research Papers, reprinted individual articles appearing in the Journal of Research, are available from the Superintendent of Documents shortly after appearance of monthly issue of the JOURNAL.

Address orders only to
Superintendent of Documents, U. S. Government Printing Office
Washington, D.C.

U.S. DEPARTMENT OF COMMERCE NATIONAL BUREAU OF STANDARDS

RESEARCH PAPER RP691

Part of Journal of Research of the National Bureau of Standards, vol. 13, July 1934

A FORMULA AND TABLES FOR THE PRESSURE OF SATURATED WATER VAPOR IN THE RANGE 0 TO 374 C

By Nathan S. Osborne and Cyril H. Meyers

ABSTRACT

Recent experimental determinations of the vapor pressure of water have enriched our knowledge of this property sufficiently to justify revision of the accepted values.

A formulation has been developed which by a single equation represents an adjusted composite appraisal of the available data; and defines concisely and explicitly the relation of saturation pressure to temperature between the freezing point and the critical region.

Graphical comparisons of the original data with the formula indicate the degree of accord, and the confidence which may be given to the adjusted values.

Comprehensive tables of pressures, derivatives, and boiling points, computed by use of the formula are given in several customary units for convenience in compiling complete tables of thermal properties of steam. A table of conversion factors is given.

CONTENTS

		Page
I.	Introduction	1
II.	The formula	2
III.	Discussion of the accord of pressure values	3
IV.	Discussion of the accord of derivatives	6
V.	Steam condensation temperatures for thermometric calibration	8
VI.	Tables of saturation pressures, saturation temperatures, and conversion factors	10

I. INTRODUCTION

Several determinations of the relation between the temperature and pressure of saturated water vapor have recently been made in the range between the normal boiling point and the critical region. These recent determinations have contributed substantially to the knowledge of this property of steam, and have prompted a study of the available data with the object of deducing a single definitive formula that will represent a composite adjusted appraisal and serve for the numerical calculation of explicit values.

The advantage of such an interpretation of the vapor pressure data is that it provides a simple and complete method of fixing reliable definitive values of the pressure and its derivative, and furnishes a basis for coordinating other thermodynamic data.

The resulting formula here presented makes no claim to rationality or apparent simplicity, as these qualities have as yet eluded the inspiration of the authors and their colleagues. On the other hand, careful consideration has been given to the selection of a type of function with sufficient adaptability to permit its adjustment to the general trend indicated by the data, without conforming too readily to fortuitous deviations of the data from the trend characteristic of this property of water. It is evident that much depends on the discernment of the seeker for such a formula. The final choice of the type and the degree of adjustment to the experimental points is more a matter of judgment than of rigid mathematical deduction. This is especially true in a case where groups of data from various experimental sources, and over different ranges of value are to be combined in a single correlation. Consideration was also given to suitability for numerical calculation of the pressure and its derivative.

The path of approach to this problem has been the modification of a simple form of equation, long recognized as an approximation to experimental fact, by the addition of successive correction terms, each modification permitting closer accord with the data. The numerous experimental steps in this process, many of which failed to meet the above requirements, are of no further interest, since the ultimate test made by comparing observed values with those calculated from these tentative formulas left no doubt of their relative fitness to represent both the individual values and the trend of the data.

II. THE FORMULA

The equation finally selected has the form

$$\log_{10}P = A + \frac{B}{T} + \frac{Cx}{T}\,(10^{Dx^3} - 1) + E(10^{Fy^{5/4}})$$

in which P = saturation pressure in international atmospheres
t = saturation temperature in degrees of the international temperature scale
$T = t + 273.16$
$x = T^2 - K$
$y = 374.11 - t$ (374.11 taken as critical temperature),
and the parameters have the values

$A = +5.4266514$
$B = -2005.1$
$C = +1.3869(10)^{-4}$
$D = +1.1965(10)^{-11}$
$K = +293{,}700$
$E = -0.0044$
$F = -0.0057148$

The derivative dP/dt is given by the equation

$$\frac{dP}{dt} = P\left[-\frac{B + Cx(10^{Dx^2} - 1)}{T^2} + 2C\{10^{Dx^2}(1 + 2Dx^2 \log_e 10) - 1\} - \frac{5}{4}EFy^{1/4}10^{Fy^{5/4}} \log_e 10\right] \log_e 10$$

A number of values of pressure and of the derivative, computed from this formula, are given in table 1.

As an aid in judging the accord of this expression for P with the experimental data and with other proposed formulas, a graph (fig. 1) has been prepared. Deviations ($P_{obs.} - P_{calc.}$) from the values calculated by the above formula are plotted as ordinates against temperature taken as abscissa. Since a uniform scale of coordinates over the entire range would exaggerate the relative importance of some of the deviations, the scale has been arbitrarily adjusted so as to facilitate their visual appraisal. Below 1 atmosphere the unit of deviation has been taken as 0.1 mm Hg. Between 1 and 10 atmospheres the unit is 0.001 atmosphere. Above 10 atmospheres the unit is one ten-thousandth of the pressure. Use of these units brings the scale of deviations to magnitudes comparable with the precision with which they can be measured. Appropriate changes of the scale of the abscissa avoid illusion where deviations in trend occur within a narrow range of temperature, as is the case near the critical region.

The data shown on the chart are taken from four sources, namely, the Physikalisch-Technische Reichsanstalt,[1] Egerton and Callendar,[2] the Bureau of Standards,[3] and the Research Laboratory of Physical Chemistry of the Massachusetts Institute of Technology.[4] The classic data of the PTR between 0 and 100 C are still the chief experimental evidence in this range,[5] though published over 20 years ago, and their values between 100 C and the critical temperature were not approached in precision by other experimenters for nearly two decades. Since they were obtained, there have been many advances in experimental technic, and while the more recent data have in part confirmed the earlier results in the high range, they have also in part indicated the need of slight modifications.

III. DISCUSSION OF THE ACCORD OF PRESSURE VALUES.

A complete review of the experimental technic will not be undertaken here, but it may be noted that the methods of the several groups differed in many important respects, and therefore the noteworthy accord shown in the results of the more recent determinations is especially reassuring as to their reliability. The data compared have all been reduced to the basis of the present international temperature scale.

In the range of temperature below 100 C, where the determinations made by several groups of experimenters of the Reichsanstalt constitute the chief source of experimental evidence, it appears that the spread of the individual results leaves considerable to discretion in the interpretation of the most probable trend of the pressure path. The present formula gives an interpretation differing somewhat from that of the Reichsanstalt Wärmetabellen and from those of the MIT

[1] Wärmetabellen, Friedr. Vieweg & Sohn, Braunschweig, 1919. Literature: K. Scheel and W. Heuse, Ann. d. Phys., vol. 29, 723, 1909, and vol. 31, 715, 1910 (pressures at less than 50 C); L. Holborn and F. Henning, ibid., vol. 26, 833, 1908 (pressures between 50 and 200 C); L. Holborn and A. Baumann, ibid., vol. 31, 945, 1910 (pressures above 200 C); F. Henning, ibid., vol. 22, 609, 1907 (comparison of older observations of saturation pressures).

[2] A. Egerton and G. S. Callendar, Phil. Trans. Roy. Soc. of London, series A, vol. 231, p. 147, 1932.

[3] B.S.Jour. Research, vol. 10 RP 523, p. 155, 1933.

[4] Leighton B. Smith, Frederick G. Keyes, and Harold T. Gerry, Proceedings American Academy of Arts and Sciences, vol. 69, no. 3, January 1934.

[5] The vapor pressure at the triple point (+0.01° C) has recently been determined by K. Prytz, Math Fys. Meddeleisen Danske Vidensk. Selskab, vol. 11, no. 2, p. 1, 1931.

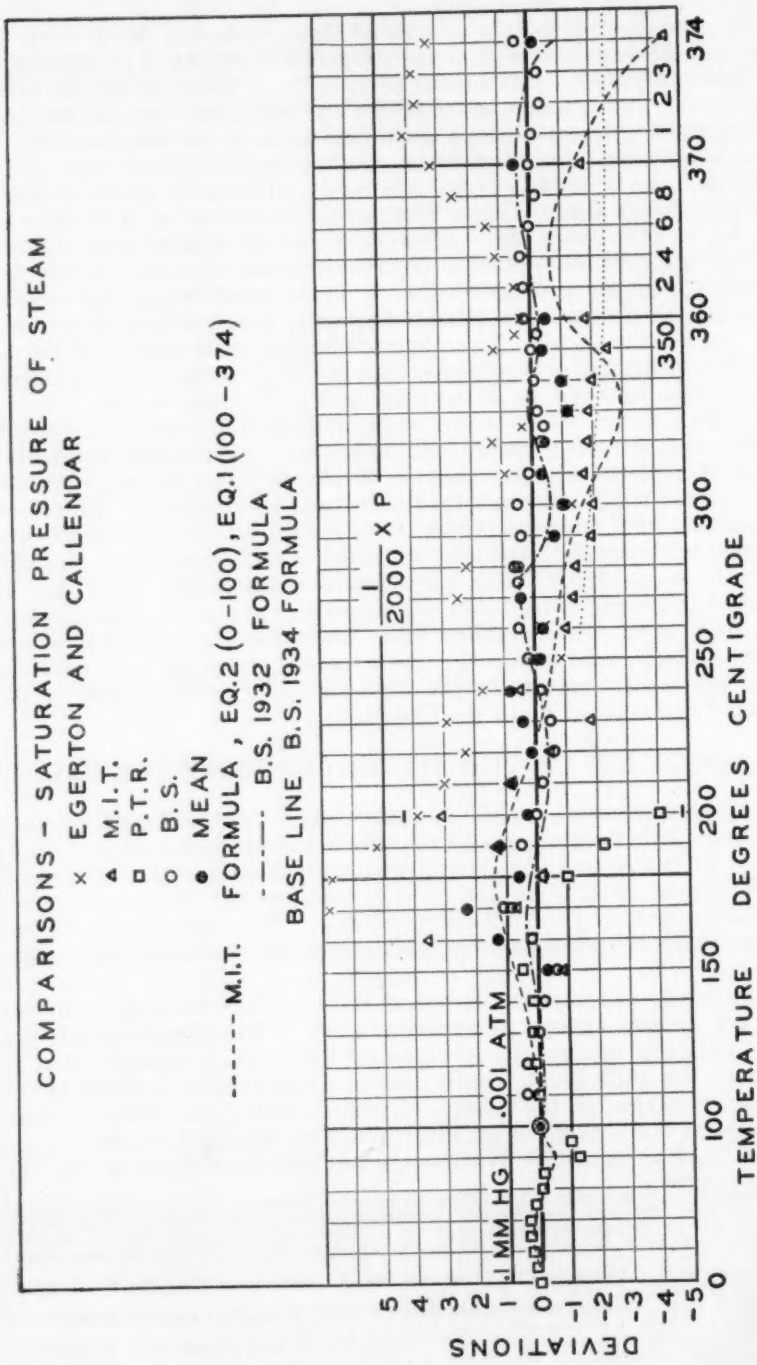
COMPARISONS – SATURATION PRESSURE OF STEAM
× EGERTON AND CALLENDAR
▲ M.I.T.
□ P.T.R.
○ B.S.
● MEAN
------ M.I.T. FORMULA, EQ.2 (0–100), EQ.1 (100–374)
-·-·- B.S. 1932 FORMULA
BASE LINE B.S. 1934 FORMULA
1/2000 × P
1 MM HG
.001 ATM
DEVIATIONS
TEMPERATURE DEGREES CENTIGRADE
5
4
3
2
1
0
-1
-2
-3
-4
-5
0
100
150
200
250
300
350
360
370
374
1 2 3
2 4 6 8

FIGURE 1

equations. In this range the degree of accord between the several interpretations and the experimental values is shown in the graph of deviations, figure 2.

By allowing a liberal tolerance to the experimental data in this region of low pressures and permitting the smoothing function to span deviations over considerable intervals, it is believed that a fairer appraisal of the true trend of the pressure curve has been obtained than would have been possible by a more rigorous adjustment. This opinion is supported by the result of a test in which experimental values of the latent heat of vaporization, the specific volumes, and the formulated vapor pressure relation were correlated by use of the Clapeyron equation. Without presenting the details of this test, it may be said that these thermodynamic data at the saturation limit in this region are in better accord with the present formula than with earlier appraisals of the pressure data.

A correlation of thermodynamic data over the entire range of the 2-phase boundary will be possible when the experimental results of the MIT program of specific volume measurements are available. The true correlation requires that temperatures be expressed on the thermodynamic scale of temperature. Therefore the actual correlation will involve such small errors as correspond to the deviation of the international scale of temperature from the true thermodynamic scale.

The Egerton and Callendar data used in the graph are their smoothed values at even temperatures except at 170, 180, and 200 C. In that range the values given by the series of measurements made in July and August 1932 have been used after a preliminary smoothing and reduction to even temperatures, since those experimenters have regarded these later measurements as more trustworthy than their earlier ones. They note that this group of their data shows a systematic deviation from the results of other observers, and they recognize the greater limitation on the accuracy of their method at the lower pressures. This deviation, although amounting to about 0.006 atmosphere from the general trend of the mean, is not serious. The effect of this departure is partly offset by the opposite though lesser deviation of the PTR values at 190 and 200 C.

The differences in trend in the extreme upper range among the Egerton and Callendar, the MIT, and the BS data are noteworthy, but perhaps not surprising when it is recalled that the properties of fluids tend to become more indeterminate as the critical region is approached.

Where there are, at the same point, values from three or more laboratories, mean values have been plotted in figure 1 in order to consider the formula with reference to the entire mass of experimental data, and thus appraise its fitness. In computing these mean values, less weight has been given to a determination consisting of but a single observation than to others, but otherwise all independent values have been regarded as of equal importance. The task of assigning to each determination a more precise estimate of relative accuracy is too difficult and delicate, and moreover proves unnecessary for the present purpose. It may be seen by inspection that the accord of these mean values with the formula, taken as a reference datum, is well within a reasonable tolerance, giving consideration to the magnitude of the deviations. No significant anomalies are indicated, there being no

important systematic deviations of the mean values. The accord of the separate determinations is naturally less perfect, but not in so much as to leave serious doubt of the suitability of the formula as a tool for the adjustment and interpolation of the pressures, and for obtaining derivatives.

IV. DISCUSSION OF THE ACCORD OF DERIVATIVES

The derivatives, being removed one step further from the original data, are proportionately more susceptible to the influence of the appraisal of the data than are the pressures. It is obvious that too rigorous an adjustment of the smoothing function to the observed points may result in a false trend and exaggerated errors in the derivative. This may be appreciated by inspection of the graph, figure 3, which shows percentage deviations of the derivative, dP/dt, calculated from different interpretations of data.

While the deviations thus shown, particularly at the extremes of pressure, correspond to minor differences in actual pressure, they are of some consequence when the derivative is used as a factor for correlating thermodynamic data. It is also possible that the actual location of the saturation limit may have an appreciable effect on the extrapolation of superheat data to the saturation limit. It should be noted that the apparent discord shown in this graphical comparison is largely artificial, due to the wide latitude possible in the individual interpretations of the data.

For example, of several formulas tested in the present study, one which was adjusted to the same mean data, using a least square method of evaluating the constants, and giving careful consideration to relative weighting of the data, showed only moderate deviations from the pressure data but gave even greater discrepancies in the derivatives than any shown in figure 3. This equation was evidently of an unsuitable type, and like several others was discarded in favor of the one finally chosen.

As a further test of the actual accord of the data as distinguished from accord in their interpretation, it was found possible to adjust the constants in the formula so that with a change of only 1 in 4,000 of the derivative the values of pressure agreed with the MIT data to within 1 in 5,000 even in the extreme upper range. This adjustment is indicated by the fine dotted line on the pressure deviation graph, figure 1. A similar adjusted interpretation could be made for the Egerton and Callendar data. This confirms the conclusion that no serious discord actually exists among the data.

In the immediate vicinity of the critical point the experimental values are not as free from doubt as could be desired to establish the true course of the pressure curve. Greater refinements in the measurements may be necessary to decide this and permit a more reliable estimate of the limiting value of the derivative at the critical state. It may be pointed out that in the MIT formulation, the formula was fitted exactly to the experimental value at 374.11 C. The authors of that formulation express the opinion that this has not led to any distortion of the trend below 374.11 C. This conclusion seems open to question. It seems not improbable that this procedure which in effect assigns to this experimental point an infinite weight is partly responsible for the discordance between the derivatives of the two

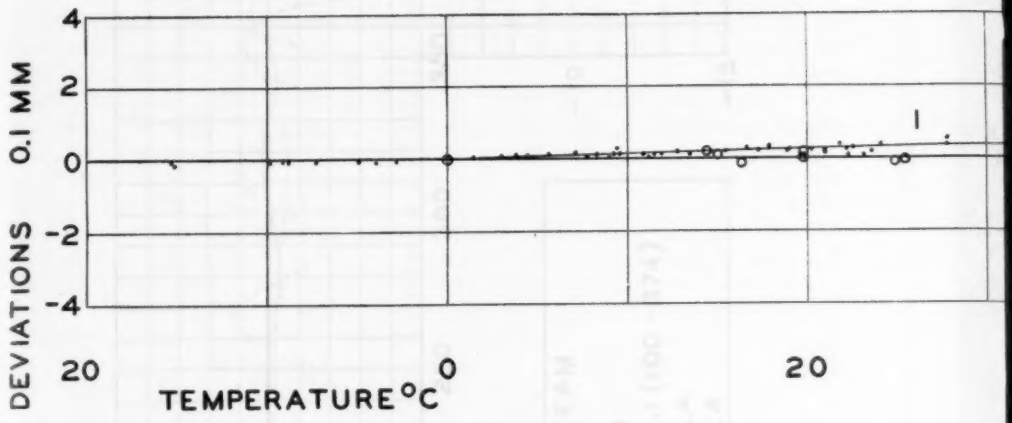

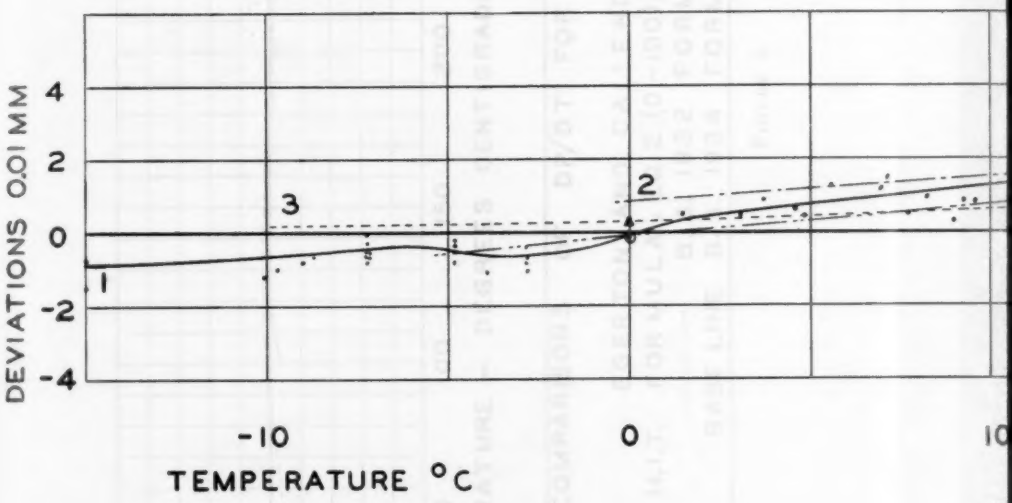

○Thiesen a
+Holborn a
• Scheel an
×Moser
△Prytz

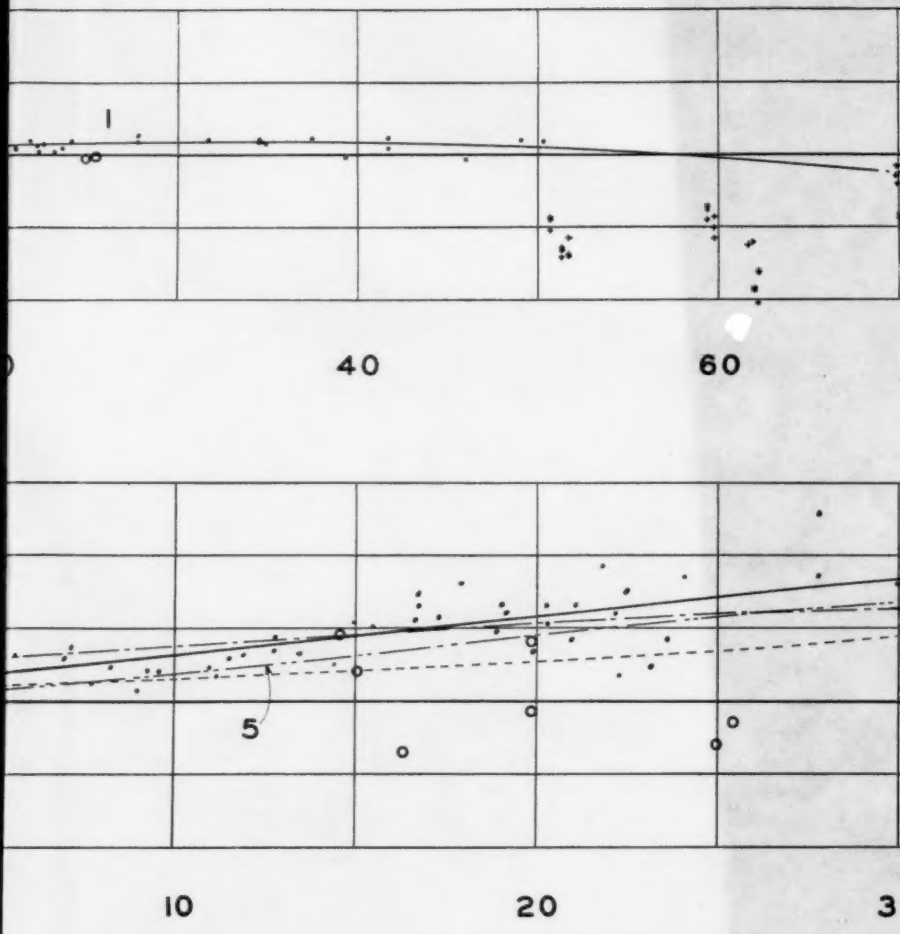

FIGURE 2.—*Vapor pressure—saturated steam: low-pressure range.*

Comparison of observed and adjusted values with B.S. formula as base line.

KEY

Observed points	*Adjusted values*
○ Thiesen and Scheel	1 ——— - - - Warmetabellen (broken where rounded to 1 m
+ Holborn and Henning	2 – — – — – MIT Eq. 2} PTR data
• Scheel and Hense	5 ——— – — – MIT Eq. 5}
× Moser	3 – – – – – – – Curve of deviation of +.01° C.
△ Prytz	

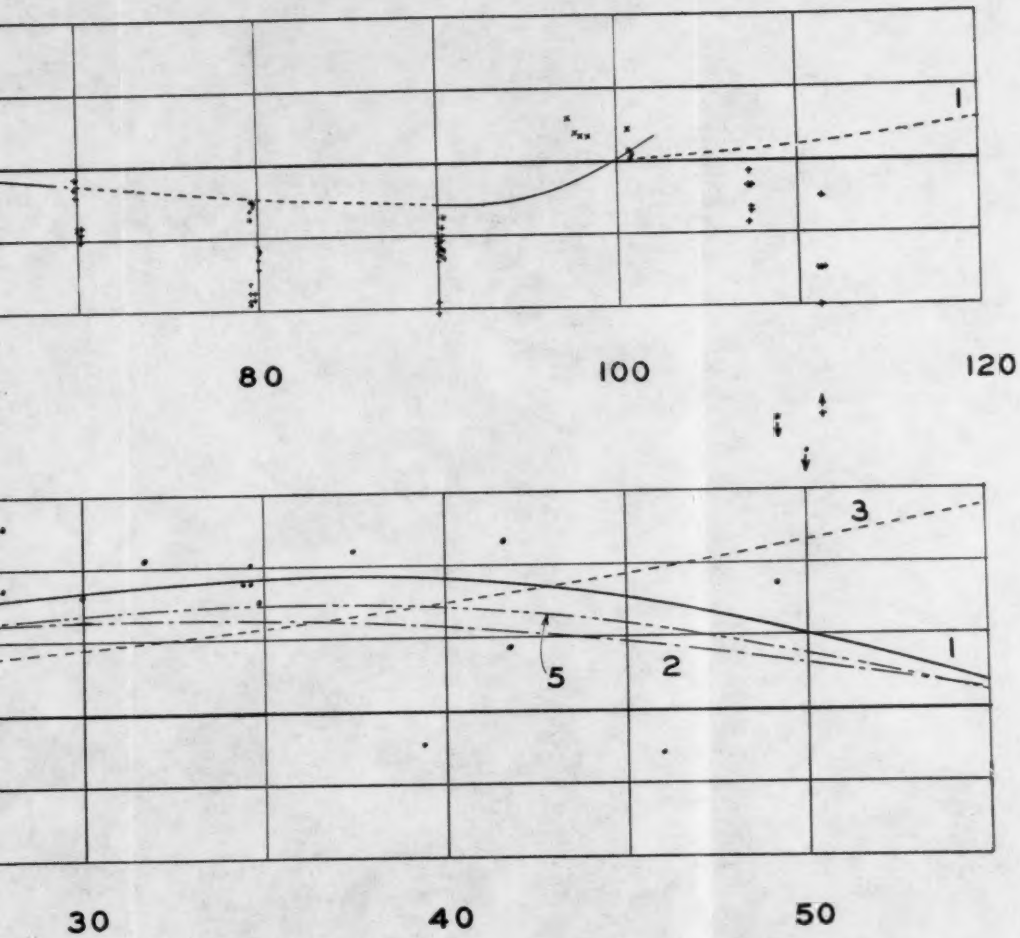

ge.

e.

64093—34. (Face p. 6.)

nded to 1 mm)

UNIV. OF MICH.

4
2
0
-2
-4
20
0
TEMPERATURE °C
DEVIATIONS 0.1 MM

4
2
0
-2
-4
-10
0
TEMPERATURE °C
DEVIATIONS 0.1 MM

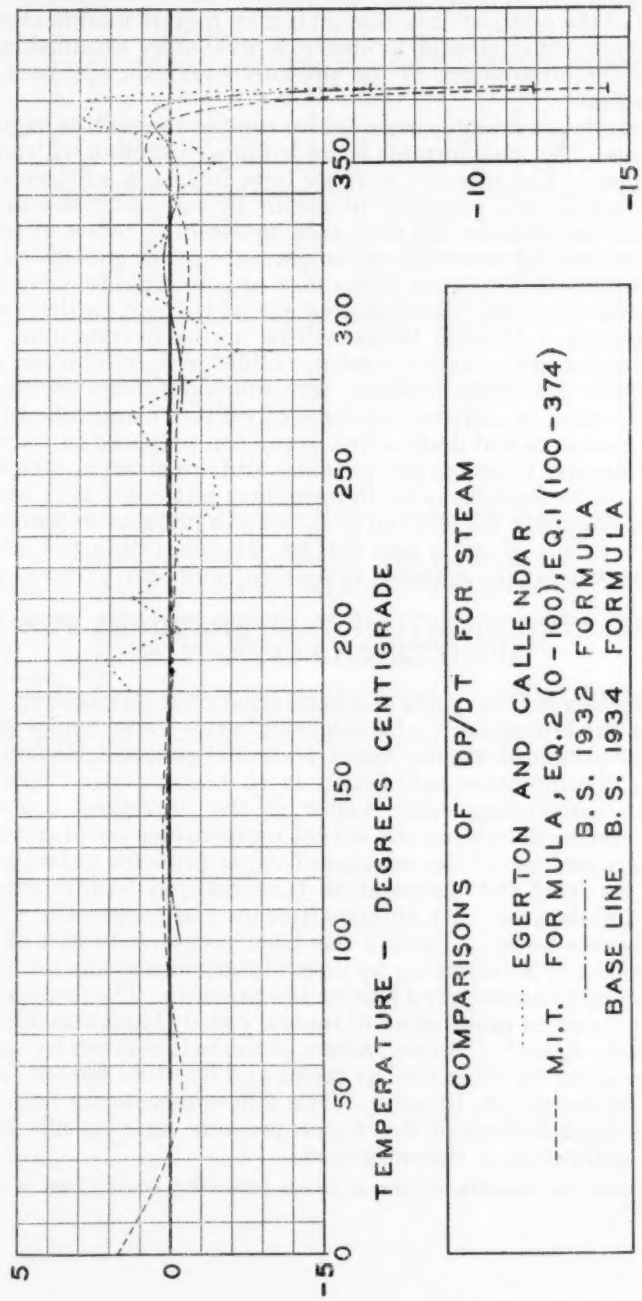
COMPARISONS OF DP/DT FOR STEAM
EGERTON AND CALLENDAR
M.I.T. FORMULA, EQ.2 (0-100), EQ.1 (100-374)
B.S. 1932 FORMULA
BASE LINE B.S. 1934 FORMULA
TEMPERATURE - DEGREES CENTIGRADE
DEVIATIONS - PARTS IN 1000
0
50
100
150
200
250
300
350
5
0
-5
-10
-15

FIGURE 3

formulations. It appears that the present formula represents a fair appraisal of the existing data though it may require modification when more precise experimental evidence is available, establishing more definitely the true course of the pressure curve on approach to the critical region.

The formula is evidently unsuited for routine use such as engineering calculations. No such formula is needed in conjunction with adequate steam tables. The primary purpose is to furnish a suitable medium for formulating this property of steam in compiling steam tables. When once the formula has been used to compute tables of pressures and derivatives, at intervals of temperature small enough to permit accurate interpolation, these tables may be converted to other systems of units, and amplified to any desired extent without further reference to the formula. All such tables will be mutually consistent. They are suitable for use as actual working tables, and in addition provide a convenient reference medium for intercomparison of numerical values expressed in different systems of units. Comprehensive base tables of pressures and derivatives have been prepared in the systems of units commonly used in steam tables and are given in tables 2 to 6, inclusive. The formula is an independent but consistent means for expressing concisely the relation of saturation pressure to temperature. Definitive values of units and factors for converting pressures and energy quantities into different systems of units are given in table 7.

V. STEAM CONDENSATION TEMPERATURES FOR THERMOMETRIC CALIBRATION

The 100-degree fixed point of the international temperature scale is defined as the temperature of condensing water vapor under the pressure of one standard atmosphere. In actual practice, the usual procedure in thermometer calibration is to observe the thermometer reading in condensing water vapor at the prevailing atmospheric pressure, and to determine the actual temperature by observation of the pressure and use of the relation of vapor pressure to temperature. Even at sea level the temperature thus realized seldom equals the value of 100 degrees. At higher altitudes the temperature is often several degrees lower. Table 8 has been prepared to furnish a convenient means of determining by direct interpolation the temperature corresponding to an observed barometric pressure. The pressures must first be reduced to millimeters of mercury at 0 C and standard gravity (980.665 cm/sec ^{2}). A comparison of the values given by this table with those given by other similar tables and by other special formulas is shown on the graph, figure 4. The differences shown indicate the range of interpretations of the vapor pressure data as affecting the practical calibration of thermometers.

NOTE.—In tables 1 to 6, inclusive, all values of pressure below 0.01 C (32.018 F) are for vapor over subcooled liquid.

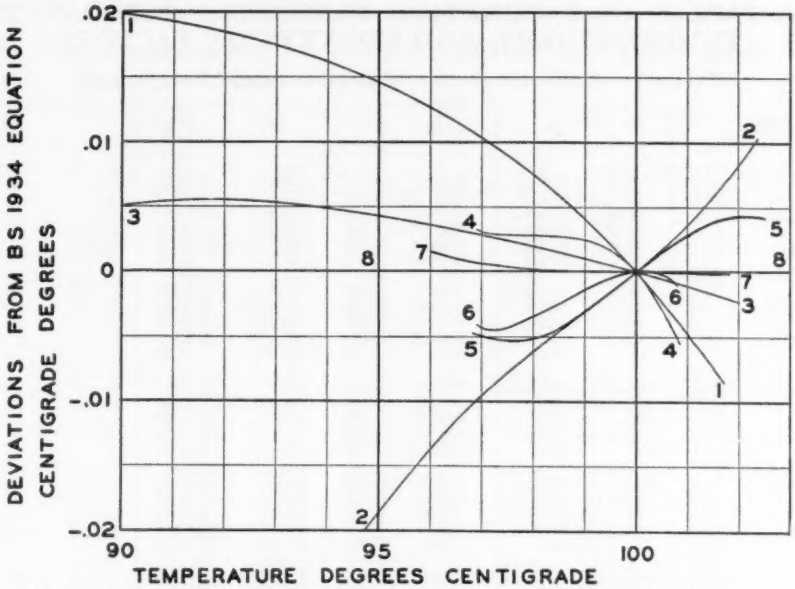

FIGURE 4.—*Steam condensation temperatures for thermometric calibration*

Comparison of various special equations and tables with B.S. 1934 formula as base line.

1. Guillaume (Broch-Reguault) Traite Pratique de Thermometrie de Precision, 1889.
2. Volet (Chappuis), Trav. Mem. Bur. Int. vol. 18, no. 4, 1930.
3. Wärmetabellen, 1919.
4. International Temperature Scale, Seventh General Conference of Weights and Measures, 1927.
5. Zmaczynski and Bonhoure, J. de Physique (ser. 7), vol. 1, p. 285, 1930.
6. Moser, Ann. d. Phys., vol. 14, p. 790, 1932.
7. Smith, Keyes and Gerry, Proc. Amer. Acad. Arts Sc., vol. 69, p. 137, 1934.
8. Holborn and Henning, Ann. d. Phys., vol. 26, p. 833, 1908 (same as base line within tolerance of rounded values given).

VI. TABLES OF SATURATION PRESSURES, SATURATION TEMPERATURES, AND CONVERSION FACTORS

TABLE 1.—*Saturation pressure of steam calculated from formula*

t	P	dP/dt	t	P	dP/dt
°C	atm	atm/°C	°C	atm	atm/°C
0	0.0060273	0.00043729	230	27.6130	0.50609
10	.012102	.00081027	240	33.0424	.58095
20	.023042	.00142704	250	39.2557	.66294
30	.041831	.0024015	260	46.3264	.75246
40	.072748	.0038796	270	54.3313	.84989
50	.121698	.0060412	280	63.3521	.95570
60	.196560	.0091004	290	73.4752	1.07045
70	.307520	.0133048	300	84.7931	1.19479
80	.467396	.0189322	310	97.4057	1.32954
90	.691923	.0262878	320	111.422	1.47572
100	1.00000	.035699	330	126.963	1.63483
110	1.41389	.047509	340	144.168	1.80896
120	1.95938	.062076	350	163.205	2.00197
130	2.66583	.079765	360	184.294	2.22115
140	3.56630	.100939	362	188.784	2.26932
150	4.69746	.125965	364	193.372	2.31938
160	6.09964	.155201	366	198.064	2.37165
170	7.81669	.188998	368	202.861	2.42656
180	9.89596	.227701	370	207.772	2.48495
190	12.3881	.271637	371	210.272	2.51588
200	15.3472	.321129	372	212.804	2.54858
210	18.8304	.376500	373	215.370	2.58412
220	22.8978	.438049	374	217.976	2.63069

TABLE 2.—*Pressure of saturated water vapor*

[1 standard atmosphere = 1.033228 kg per sq cm = standard gravity = 980.665 cm per sec per sec]

Temp t	Pressure p	Derivative dp/dt	p	dp/dt	Temp t	p	dp/dt	p	dp/dt
°C	std atm	atm/°C	kg/cm²	kg/cm² °C	°C	std atm	atm/°C	kg/cm² °C	kg/cm² °C
−5	0.004162	0.0003146	0.004300	0.0003251	55	0.15531	0.007444	0.16047	0.007691
−4	.004487	.0003364	.004637	.0003476	56	.16291	.007754	.16832	.008012
−3	.004835	.0003595	.004996	.0003715	57	.17082	.008074	.17650	.008343
−2	.005207	.0003840	.005380	.0003968	58	.17906	.008405	.18501	.008685
−1	.005604	.0004099	.005790	.0004235	59	.18764	.008747	.19387	.009038
0	.006027	.0004373	.006228	.0004518	60	.19656	.009100	.20309	.009403
+1	.006479	.0004662	.006694	.0004817	61	.20584	.009465	.21268	.009780
2	.006960	.0004968	.007192	.0005134	62	.21549	.009841	.22265	.010168
3	.007473	.0005292	.007722	.0005467	63	.22553	.010229	.23302	.010569
4	.008019	.0005633	.008286	.0005820	64	.23596	.010630	.24380	.010983
5	.008600	.0005993	.008886	.0006192	65	.24679	.011043	.25499	.011410
6	.009218	.0006372	.009525	.0006584	66	.25805	.011468	.26662	.011850
7	.009875	.0006772	.010204	.0006997	67	.26973	.011907	.27870	.012303
8	.010574	.0007193	.010925	.0007432	68	.28186	.012359	.29123	.012770
9	.011315	.0007636	.011691	.0007890	69	.29446	.012825	.30424	.013251
10	.012102	.0008103	.012504	.0008372	70	.30752	.013305	.31774	.013747
11	.012936	.0008593	.013366	.0008879	71	.32107	.013799	.33174	.014257
12	.013821	.0009109	.014280	.0009412	72	.33512	.014307	.34626	.014782
13	.014759	.0009651	.015249	.0009972	73	.34969	.014830	.36131	.015323
14	.015752	.0010220	.016276	.0010560	74	.36479	.015368	.37691	.015879
15	.016804	.0010818	.017362	.0011177	75	.38043	.015922	.39307	.016451
16	.017917	.0011445	.018512	.0011825	76	.39664	.016492	.40982	.017039
17	.019094	.0012102	.019728	.0012504	77	.41342	.017077	.42716	.017644
18	.020338	.0012792	.021014	.0013217	78	.43080	.017679	.44511	.018266
19	.021653	.0013514	.022373	.0013963	79	.44878	.018297	.46370	.018905
20	.023042	.0014270	.023808	.0014745	80	.46740	.018932	.48293	.019561
21	.024508	.0015063	.025323	.0015563	81	.48665	.019585	.50282	.020236
22	.026056	.0015891	.026922	.0016419	82	.50657	.020255	.52340	.020928
23	.027688	.0016758	.028608	.0017315	83	.52717	.020943	.54469	.021639
24	.029409	.0017665	.030386	.0018252	84	.54846	.021649	.56668	.022368
25	.031222	.0018612	.032260	.0019231	85	.57047	.022374	.58943	.023117
26	.033133	.0019602	.034234	.0020253	86	.59322	.023118	.61293	.023886
27	.035144	.0020636	.036312	.0021322	87	.61672	.023881	.63721	.024674
28	.037261	.0021715	.038500	.0022436	88	.64099	.024663	.66229	.025483
29	.039489	.0022841	.040801	.0023600	89	.66605	.025465	.68818	.026312
30	.041831	.0024015	.043221	.0024813	90	.69192	.026288	.71491	.027161
31	.044293	.0025240	.045765	.0026079	91	.71863	.027131	.74251	.028032
32	.046881	.0026516	.048439	.0027397	92	.74619	.027995	.77098	.028925
33	.049599	.0027846	.051247	.0028771	93	.77463	.028880	.80037	.029840
34	.052452	.0029230	.054195	.0030201	94	.80396	.029786	.83067	.030776
35	.055446	.0030672	.057288	.0031691	95	.83421	.030715	.86192	.031736
36	.058588	.0032172	.060535	.0033241	96	.86540	.031666	.89416	.032718
37	.061883	.0033733	.063939	.0034854	97	.89755	.032639	.92737	.033724
38	.065337	.0035356	.067508	.0036531	98	.93068	.033636	.96161	.034753
39	.068956	.0037043	.071247	.0038274	99	.96482	.034655	.99688	.035807
40	.072748	.0038796	.075165	.0040085	100	1.00000	.035699	1.03323	.036885
41	.076718	.0040618	.079267	.0041967	101	1.0362	.036766	1.0707	.037988
42	.080873	.0042509	.083560	.0043921	102	1.0735	.037858	1.1092	.039115
43	.085222	.0044472	.088054	.0045950	103	1.1120	.038974	1.1489	.040269
44	.089770	.0046510	.092753	.0048055	104	1.1515	.040115	1.1898	.041448
45	.094526	.0048624	.097667	.005024	105	1.1922	.041282	1.2318	.042654
46	.099497	.005082	.10280	.005250	106	1.2341	.042474	1.2751	.043886
47	.10469	.005309	.10817	.005485	107	1.2772	.043693	1.3196	.045145
48	.11012	.005544	.11378	.005729	108	1.3215	.044938	1.3654	.046431
49	.11578	.005788	.11963	.005981	109	1.3670	.046210	1.4125	.047746
50	.12170	.006041	.12574	.006242	110	1.4139	.047509	1.4609	.049088
51	.12787	.006303	.13212	.006513	111	1.4621	.048836	1.5106	.05046
52	.13431	.006574	.13877	.006792	112	1.5116	.05019	1.5618	.05186
53	.14102	.006854	.14571	.007082	113	1.5624	.05157	1.6144	.05329
54	.14802	.007144	.15294	.007381	114	1.6147	.05299	1.6684	.05475

TABLE 2.—*Pressure of saturated water vapor*—Continued

[1 standard atmosphere = 1.033228 kg per sq cm—standard gravity = 980.665 cm per sec per sec]

Temp t	Pressure p	Derivative dp/dt	p	dp/dt	Temp t	p	dp/dt	p	dp/dt
°C	*std atm*	*atm/°C*	*kg/cm²*	*kg/cm² °C*	°C	*std atm*	*atm/°C*	*kg/cm²*	*kg/cm² °C*
115	1.6684	0.05443	1.7239	0.05623	180	9.8960	0.22770	10.225	0.23527
116	1.7236	.05590	1.7809	.05775	181	10.126	.23185	10.462	.23956
117	1.7802	.05740	1.8394	.05930	182	10.360	.23606	10.703	.24390
118	1.8384	.05893	1.8995	.06088	183	10.598	.24032	10.950	.24830
119	1.8981	.06049	1.9612	.06250	184	10.840	.24463	11.201	.25276
120	1.9594	.06208	2.0245	.06414	185	11.087	.24899	11.456	.25727
121	2.0223	.06370	2.0895	.06582	186	11.338	.25341	11.715	.26183
122	2.0868	.06535	2.1561	.06752	187	11.594	.25789	11.979	.26646
123	2.1530	.06704	2.2245	.06927	188	11.854	.26242	12.248	.27113
124	2.2209	.06876	2.2947	.07104	189	12.119	.26700	12.522	.27587
125	2.2905	.07051	2.3666	.07285	190	12.388	.27164	12.800	.28066
126	2.3619	.07229	2.4404	.07469	191	12.662	.27633	13.083	.28551
127	2.4351	.07411	2.5160	.07657	192	12.941	.28108	13.371	.29042
128	2.5101	.07596	2.5935	.07848	193	13.224	.28589	13.664	.29539
129	2.5870	.07784	2.6730	.08043	194	13.513	.29075	13.962	.30041
130	2.6658	.07976	2.7544	.08242	195	13.806	.29567	14.265	.30549
131	2.7466	.08172	2.8378	.08443	196	14.104	.30065	14.573	.31064
132	2.8293	.08371	2.9233	.08649	197	14.407	.30568	14.886	.31584
133	2.9140	.08574	3.0108	.08858	198	14.715	.31077	15.204	.32110
134	3.0008	.08780	3.1005	.09071	199	15.029	.31592	15.528	.32642
135	3.0896	.08989	3.1923	.09288	200	15.347	.32113	15.857	.33180
136	3.1806	.09203	3.2863	.09509	201	15.671	.32640	16.192	.33724
137	3.2737	.09420	3.3824	.09733	202	16.000	.33173	16.532	.34275
138	3.3690	.09641	3.4809	.09961	203	16.334	.33711	16.877	.34831
139	3.4665	.09866	3.5817	.10193	204	16.674	.34256	17.228	.35394
140	3.5663	.10094	3.6848	.10429	205	17.020	.34806	17.585	.35963
141	3.6684	.10326	3.7903	.10669	206	17.370	.35363	17.948	.36538
142	3.7728	.10562	3.8982	.10913	207	17.727	.35925	18.316	.37119
143	3.8797	.10803	4.0086	.11162	208	18.089	.36494	18.690	.37707
144	3.9889	.11047	4.1214	.11414	209	18.457	.37069	19.070	.38301
145	4.1006	.11295	4.2369	.11670	210	18.830	.37650	19.456	.38901
146	4.2148	.11547	4.3549	.11930	211	19.210	.38237	19.848	.39508
147	4.3316	.11803	4.4755	.12195	212	19.595	.38830	20.246	.40121
148	4.4509	.12064	4.5988	.12464	213	19.986	.39430	20.651	.40740
149	4.5728	.12328	4.7248	.12738	214	20.384	.40036	21.061	.41366
150	4.6975	.12596	4.8535	.13015	215	20.787	.40648	21.477	.41999
151	4.8248	.12869	4.9851	.13297	216	21.197	.41267	21.901	.42638
152	4.9549	.13146	5.1195	.13583	217	21.613	.41892	22.331	.43284
153	5.0877	.13428	5.2568	.13874	218	22.035	.42523	22.767	.43936
154	5.2234	.13713	5.3970	.14169	219	22.463	.43161	23.209	.44595
155	5.3620	.14004	5.5402	.14469	220	22.898	.43805	23.659	.45260
156	5.5035	.14298	5.6864	.14773	221	23.339	.44456	24.115	.45933
157	5.6480	.14597	5.8357	.15082	222	23.787	.45113	24.577	.46612
158	5.7955	.14900	5.9880	.15395	223	24.241	.45777	25.047	.47298
159	5.9460	.15208	6.1436	.15713	224	24.702	.46447	25.523	.47990
160	6.0996	.15520	6.3023	.16036	225	25.170	.47124	26.007	.48690
161	6.2564	.15837	6.4643	.16363	226	25.645	.47807	26.497	.49396
162	6.4164	.16158	6.6296	.16695	227	26.126	.48498	26.995	.5011
163	6.5796	.16485	6.7982	.17032	228	26.615	.49195	27.499	.5083
164	6.7461	.16815	6.9703	.17374	229	27.110	.49898	28.011	.5156
165	6.9159	.17151	7.1457	.17721	230	27.613	.5061	28.531	.5229
166	7.0891	.17491	7.3247	.18072	231	28.123	.5133	29.057	.5303
167	7.2658	.17836	7.5072	.18429	232	28.640	.5205	29.591	.5378
168	7.4459	.18186	7.6933	.18790	233	29.164	.5278	30.133	.5454
169	7.6295	.18540	7.8830	.19156	234	29.695	.5352	30.682	.5530
170	7.8167	.18900	8.0764	.19528	235	30.234	.5426	31.239	.5607
171	8.0075	.19264	8.2736	.19904	236	30.780	.5502	31.803	.5685
172	8.2020	.19634	8.4745	.20286	237	31.334	.5578	32.376	.5763
173	8.4002	.20008	8.6793	.20673	238	31.895	.5654	32.955	.5842
174	8.6022	.20387	8.8880	.21065	239	32.465	.5732	33.544	.5922
175	8.8080	.20772	9.1006	.21462	240	33.042	.5810	34.140	.6003
176	9.0176	.21161	9.3172	.21864	241	33.627	.5888	34.745	.6084
177	9.2312	.21556	9.5379	.22272	242	34.220	.5968	35.357	.6166
178	9.4487	.21955	9.7627	.22685	243	34.821	.6048	35.978	.6249
179	9.6703	.22360	9.9916	.23103	244	35.430	.6129	36.607	.6332

TABLE 2.—*Pressure of saturated water vapor*—Continued

[1 standard atmosphere = 1.033228 kg per sq cm—standard gravity = 980.665 cm per sec per sec]

Temp t	Pressure p	Derivative dp/dt	p	dp/dt
°C	std atm	atm/°C	kg/cm²	kg/cm² °C
245	36.047	0.6210	37.244	0.6417
246	36.672	.6293	37.890	.6502
247	37.305	.6376	38.545	.6588
248	37.947	.6460	39.208	.6674
249	38.597	.6544	39.880	.6762
250	39.256	.6629	40.560	.6850
251	39.923	.6716	41.250	.6939
252	40.599	.6802	41.948	.7028
253	41.284	.6890	42.655	.7119
254	41.977	.6978	43.372	.7210
255	42.679	.7067	44.097	.7302
256	43.390	.7157	44.832	.7395
257	44.111	.7248	45.576	.7489
258	44.840	.7339	46.330	.7583
259	45.579	.7432	47.093	.7679
260	46.326	.7525	47.866	.7775
261	47.083	.7618	48.648	.7872
262	47.850	.7713	49.440	.7969
263	48.626	.7808	50.242	.8068
264	49.412	.7905	51.054	.8167
265	50.207	.8002	51.875	.8267
266	51.012	.8099	52.707	.8369
267	51.827	.8198	53.549	.8470
268	52.652	.8298	54.401	.8573
269	53.486	.8398	55.264	.8677
270	54.331	.8499	56.137	.8781
271	55.187	.8601	57.020	.8887
272	56.052	.8704	57.914	.8993
273	56.927	.8807	58.819	.9100
274	57.813	.8912	59.734	.9208
275	58.710	.9017	60.660	.9317
276	59.616	.9123	61.597	.9427
277	60.534	.9230	62.546	.9537
278	61.463	.9338	63.505	.9649
279	62.402	.9447	64.475	.9761
280	63.352	.9557	65.457	.9875
281	64.313	.9668	66.450	.9989
282	65.286	.9779	67.455	1.0104
283	66.269	.9892	68.471	1.0220
284	67.264	1.0005	69.499	1.0337
285	68.270	1.0119	70.539	1.0455
286	69.288	1.0234	71.590	1.0574
287	70.317	1.0350	72.654	1.0694
288	71.358	1.0468	73.729	1.0815
289	72.411	1.0586	74.817	1.0937
290	73.475	1.0704	75.917	1.1060
291	74.552	1.0824	77.029	1.1184
292	75.640	1.0945	78.153	1.1309
293	76.741	1.1067	79.291	1.1435
294	77.854	1.1190	80.441	1.1562
295	78.979	1.1314	81.603	1.1690
296	80.116	1.1439	82.779	1.1819
297	81.266	1.1564	83.967	1.1949
298	82.429	1.1691	85.168	1.2080
299	83.605	1.1819	86.383	1.2212
300	84.793	1.1948	87.611	1.2345
301	85.994	1.2078	88.852	1.2479
302	87.209	1.2209	90.106	1.2614
303	88.436	1.2341	91.375	1.2751
304	89.677	1.2474	92.657	1.2888
305	90.931	1.2608	93.952	1.3027
306	92.198	1.2743	95.262	1.3167
307	93.480	1.2880	96.586	1.3308
308	94.774	1.3017	97.924	1.3450
309	96.083	1.3156	99.276	1.3593

Temp t	p	dp/dt	p	dp/dt
°C	std atm	atm/°C	kg/cm² °C	kg/cm² °C
310	97.406	1.3295	100.64	1.3737
311	98.742	1.3436	102.02	1.3883
312	100.09	1.3578	103.42	1.4029
313	101.46	1.3721	104.83	1.4177
314	102.84	1.3866	106.25	1.4326
315	104.23	1.4011	107.69	1.4477
316	105.64	1.4158	109.15	1.4628
317	107.06	1.4306	110.62	1.4781
318	108.50	1.4455	112.11	1.4935
319	109.95	1.4606	113.61	1.5091
320	111.42	1.4757	115.12	1.5248
321	112.91	1.4910	116.66	1.5406
322	114.40	1.5064	118.21	1.5565
323	115.92	1.5220	119.77	1.5726
324	117.45	1.5377	121.35	1.5888
325	118.99	1.5535	122.95	1.6052
326	120.56	1.5695	124.56	1.6217
327	122.13	1.5856	126.19	1.6383
328	123.73	1.6019	127.84	1.6551
329	125.34	1.6183	129.50	1.6720
330	126.96	1.6348	131.18	1.6891
331	128.61	1.6515	132.88	1.7064
332	130.27	1.6683	134.59	1.7238
333	131.94	1.6853	136.33	1.7413
334	133.64	1.7025	138.08	1.7591
335	135.35	1.7198	139.85	1.7770
336	137.08	1.7373	141.63	1.7950
337	138.82	1.7550	143.44	1.8133
338	140.59	1.7728	145.26	1.8317
339	142.37	1.7908	147.10	1.8503
340	144.17	1.8090	148.96	1.8691
341	145.99	1.8273	150.84	1.8880
342	147.82	1.8459	152.73	1.9072
343	149.68	1.8646	154.65	1.9266
344	151.55	1.8836	156.59	1.9462
345	153.45	1.9028	158.54	1.9660
346	155.36	1.9222	160.52	1.9860
347	157.29	1.9418	162.52	2.0063
348	159.24	1.9616	164.53	2.0268
349	161.21	1.9817	166.57	2.0475
350	163.20	2.0020	168.63	2.0685
351	165.22	2.0225	170.71	2.0897
352	167.25	2.0434	172.81	2.1113
353	169.30	2.0645	174.93	2.1331
354	171.38	2.0859	177.07	2.1552
355	173.48	2.1076	179.24	2.1776
356	175.59	2.1296	181.43	2.2004
357	177.74	2.1519	183.64	2.2234
358	179.90	2.1746	185.88	2.2469
359	182.08	2.1977	188.13	2.2707
360	184.29	2.2212	190.42	2.2950
361	186.53	2.2450	192.72	2.3196
362	188.78	2.2693	195.06	2.3447
363	191.07	2.2941	197.41	2.3703
364	193.37	2.3194	199.80	2.3964
365	195.70	2.3452	202.21	2.4232
366	198.06	2.3716	204.64	2.4505
367	200.45	2.3987	207.11	2.4784
368	202.86	2.4266	209.60	2.5072
369	205.30	2.4553	212.12	2.5368
370	207.77	2.4850	214.68	2.5675
371	210.27	2.5159	217.26	2.5995
372	212.80	2.5486	219.88	2.6333
373	215.37	2.5841	222.53	2.6700
374	217.98	2.6307	225.22	2.7181

TABLE 3.—*Pressure of saturated water vapor in pounds per square inch*

Fahrenheit temperature—Standard Gravity=32.174 ft/sec²

t °F	0	1	2	3	4	5	6	7	8	9	t °F
20	.05388	.05622	.05865	.06117	.06378	.06650	.06932	.07224	.07528	.07842	20
30	.08169	.08507	.08858	.09221	.09598	.09988	.10392	.10811	.11245	.11693	30
40	.12158	.12639	.13137	.13652	.14184	.14735	.15305	.15895	.16504	.17134	40
50	.17784	.18457	.19152	.19869	.20611	.21376	.22167	.22983	.23825	.24695	50
60	.25592	.26518	.27473	.28458	.29474	.30521	.31601	.32715	.33863	.35046	60
70	.36264	.37520	.38814	.40146	.41518	.42931	.44386	.45884	.47426	.49013	70
80	.50645	.52326	.54054	.55832	.57661	.59541	.61475	.63463	.65507	.67608	80
90	.69767	.71985	.74265	.76607	.79013	.81484	.84022	.86628	.89303	.92050	90
100	.94870	.97765	1.0073	1.0378	1.0691	1.1012	1.1341	1.1679	1.2025	1.2380	100
110	1.2744	1.3117	1.3499	1.3892	1.4294	1.4705	1.5127	1.5560	1.6003	1.6456	110
120	1.6921	1.7397	1.7885	1.8384	1.8895	1.9418	1.9953	2.0501	2.1062	2.1636	120
130	2.2224	2.2825	2.3439	2.4068	2.4711	2.5369	2.6042	2.6729	2.7433	2.8152	130
140	2.8886	2.9638	3.0405	3.1190	3.1992	3.2811	3.3648	3.4503	3.5377	3.6269	140
150	3.7180	3.8110	3.9060	4.0030	4.1021	4.2032	4.3064	4.4118	4.5193	4.6290	150
160	4.7410	4.8553	4.9719	5.0908	5.2121	5.3359	5.4621	5.5908	5.7221	5.8559	160
170	5.9925	6.1316	6.2735	6.4181	6.5654	6.7156	6.8688	7.0249	7.1839	7.3459	170
180	7.5110	7.6791	7.8504	8.0250	8.2027	8.3837	8.5680	8.7558	8.9469	9.1415	180
190	9.3397	9.5414	9.7467	9.9558	10.168	10.385	10.605	10.830	11.058	11.290	190
200	11.526	11.766	12.011	12.260	12.512	12.770	13.031	13.297	13.568	13.843	200
210	14.123	14.407	14.696	14.990	15.289	15.592	15.901	16.214	16.533	16.857	210
220	17.186	17.520	17.860	18.205	18.556	18.912	19.274	19.641	20.015	20.394	220
230	20.779	21.170	21.566	21.969	22.378	22.794	23.216	23.644	24.078	24.519	230
240	24.967	25.421	25.882	26.350	26.825	27.307	27.796	28.292	28.795	29.305	240
250	29.823	30.349	30.881	31.422	31.970	32.526	33.090	33.661	34.241	34.829	250
260	35.425	36.029	36.642	37.262	37.892	38.530	39.177	39.833	40.497	41.171	260
270	41.853	42.545	43.246	43.956	44.676	45.405	46.144	46.892	47.650	48.418	270
280	49.196	49.984	50.783	51.591	52.410	53.240	54.080	54.930	55.791	56.664	280
290	57.547	58.441	59.346	60.262	61.190	62.130	63.081	64.043	65.017	66.003	290
300	67.002	68.012	69.034	70.068	71.115	72.175	73.247	74.332	75.429	76.540	300
310	77.664	78.800	79.950	81.113	82.290	83.481	84.685	85.903	87.134	88.380	310
320	89.640	90.915	92.203	93.506	94.824	96.157	97.504	98.866	100.24	101.64	320
330	103.04	104.47	105.91	107.36	108.83	110.32	111.82	113.34	114.87	116.42	330
340	117.99	119.58	121.18	122.80	124.43	126.08	127.75	129.44	131.15	132.87	340
350	134.61	136.37	138.14	139.94	141.75	143.58	145.43	147.30	149.19	151.09	350
360	153.02	154.96	156.93	158.91	160.91	162.94	164.98	167.04	169.13	171.23	360
370	173.35	175.50	177.66	179.85	182.06	184.28	186.53	188.80	191.10	193.41	370
380	195.75	198.11	200.49	202.89	205.32	207.76	210.23	212.73	215.24	217.78	380
390	220.35	222.93	225.54	228.18	230.83	233.52	236.22	238.95	241.71	244.49	390
400	247.29	250.12	252.97	255.85	258.76	261.69	264.65	267.63	270.64	273.67	400
410	276.73	279.82	282.93	286.07	289.24	292.44	295.66	298.91	302.18	305.49	410
420	308.82	312.18	315.57	318.99	322.43	325.91	329.41	332.94	336.51	340.10	420
430	343.72	347.37	351.05	354.76	358.50	362.27	366.07	369.90	373.77	377.66	430
440	381.59	385.54	389.53	393.55	397.60	401.68	405.80	409.95	414.13	418.34	440
450	422.59	426.87	431.18	435.53	439.91	444.32	448.77	453.25	457.77	462.32	450
460	466.90	471.52	476.18	480.86	485.59	490.35	495.15	499.98	504.85	509.75	460
470	514.70	519.67	524.69	529.74	534.83	539.96	545.12	550.32	555.56	560.84	470
480	566.16	571.51	576.90	582.33	587.81	593.32	598.87	604.46	610.08	615.75	480
490	621.46	627.21	633.00	638.84	644.71	650.62	656.58	662.57	668.61	674.69	490
500	680.81	686.98	693.18	699.43	705.73	712.06	718.44	724.87	731.33	737.84	500
510	744.40	751.00	757.64	764.33	771.06	777.84	784.67	791.54	798.45	805.42	510
520	812.43	819.48	826.58	833.73	840.92	848.17	855.46	862.80	870.18	877.61	520
530	885.10	892.63	900.21	907.84	915.52	923.24	931.02	938.85	946.73	954.66	530
540	962.64	970.67	978.75	986.88	995.06	1003.3	1011.6	1019.9	1028.3	1036.8	540
550	1045.3	1053.8	1062.4	1071.1	1079.8	1088.6	1097.4	1106.3	1115.2	1124.2	550
560	1133.2	1142.3	1151.5	1160.7	1169.9	1179.3	1188.6	1198.1	1207.6	1217.1	560
570	1226.7	1236.4	1246.1	1255.9	1265.7	1275.6	1285.6	1295.6	1305.7	1315.9	570
580	1326.1	1336.3	1346.6	1357.0	1367.5	1378.0	1388.6	1399.2	1409.9	1420.7	580
590	1431.5	1442.4	1453.3	1464.3	1475.4	1486.5	1497.8	1509.0	1520.4	1531.8	590
600	1543.3	1554.8	1566.4	1578.1	1589.8	1601.6	1613.5	1625.4	1637.5	1649.5	600
610	1661.7	1673.9	1686.2	1698.6	1711.0	1723.5	1736.1	1748.7	1761.4	1774.2	610
620	1787.1	1800.0	1813.1	1826.1	1839.3	1852.5	1865.8	1879.2	1892.8	1906.2	620
630	1919.8	1933.5	1947.3	1961.1	1975.1	1989.1	2003.2	2017.3	2031.5	2045.9	630
640	2060.3	2074.8	2089.3	2104.0	2118.7	2133.5	2148.4	2163.4	2178.4	2193.6	640
650	2208.8	2224.1	2239.5	2255.0	2270.6	2286.3	2302.0	2317.9	2333.8	2349.8	650
660	2366.0	2382.2	2398.5	2414.8	2431.3	2447.9	2464.6	2481.4	2498.2	2515.2	660
670	2532.2	2549.4	2566.6	2584.0	2601.5	2619.0	2636.7	2654.5	2672.3	2690.3	670
680	2708.4	2726.5	2744.9	2763.3	2781.8	2800.4	2819.2	2838.0	2857.0	2876.1	680
690	2895.3	2914.6	2934.1	2953.6	2973.3	2993.2	3013.1	3033.2	3053.4	3073.8	690
700	3094.3	3114.9	3135.7	3156.7	3177.8	3199.1	------	------	------	------	700

TABLE 4.—*Derivative of the pressure of saturated water vapor (dp/dt) in pounds per square inch per degree Fahrenheit*

t °F	0	1	2	3	4	5	6	7	8	9	t °F
20	.002294	2383	2474	2569	2666	2767	2871	2979	3090	3204	20
30	.003322	3444	3570	3700	3834	3972	4114	4260	4411	4567	30
40	.004727	4893	5063	5238	5418	5604	5794	5991	6193	6401	40
50	.006615	6836	7062	7294	7534	7779	8032	8292	8558	8832	50
60	.009114	9402	9699	10004	10316	10637	10966	11304	11651	12007	60
70	.012372	12746	13129	13522	13925	14338	14762	15196	15640	16096	70
80	.016563	17040	17530	18031	18544	19069	19607	20157	20721	21297	80
90	.021886	22490	23107	23737	24382	25042	25717	26406	27110	27831	90
100	.028567	29319	30087	30873	31675	32494	33331	34185	35058	35948	100
110	.036857	37785	38732	39699	40685	41691	42719	43766	44834	45924	110
120	.047035	48168	49323	50501	51702	52926	54173	55445	56740	58060	120
130	.05941	.06078	.06217	.06359	.06504	.06652	.06802	.06955	.07110	.07269	130
140	.07430	.07593	.07760	.07931	.08104	.08280	.08460	.08642	.08827	.09016	140
150	.09208	.09403	.09601	.09803	.10008	.10216	.10428	.10644	.10863	.11085	150
160	.11311	.11541	.11775	.12012	.12253	.12498	.12747	.13000	.13256	.13517	160
170	.13782	.14050	.14324	.14600	.14882	.15167	.15457	.15752	.16050	.16353	170
180	.16661	.16973	.17289	.17611	.17937	.18267	.18602	.18943	.19288	.19638	180
190	.19993	.20353	.20717	.21088	.21462	.21843	.22228	.22619	.23015	.23417	190
200	.23824	.24236	.24654	.25077	.25506	.25941	.26381	.26828	.27279	.27737	200
210	.28201	.28670	.29146	.29628	.30116	.30609	.31109	.31616	.32128	.32648	210
220	.33173	.33704	.34243	.34787	.35339	.35897	.36462	.37034	.37612	.38197	220
230	.38789	.39388	.39994	.40607	.41227	.41854	.42489	.43130	.43780	.44436	230
240	.45100	.45771	.46450	.47136	.47830	.48532	.49240	.49958	.50682	.51415	240
250	.5216	.5290	.5366	.5443	.5520	.5598	.5677	.5757	.5837	.5919	250
260	.6001	.6084	.6168	.6253	.6338	.6425	.6512	.6601	.6690	.6780	260
270	.6871	.6963	.7056	.7149	.7244	.7339	.7436	.7533	.7631	.7731	270
280	.7831	.7932	.8034	.8137	.8241	.8346	.8452	.8559	.8667	.8776	280
290	.8886	.8997	.9109	.9222	.9336	.9450	.9567	.9684	.9802	.9921	290
300	1.0041	1.0162	1.0284	1.0408	1.0532	1.0658	1.0784	1.0912	1.1040	1.1170	300
310	1.1301	1.1433	1.1566	1.1700	1.1836	1.1972	1.2110	1.2248	1.2388	1.2529	310
320	1.2671	1.2815	1.2959	1.3105	1.3251	1.3399	1.3548	1.3699	1.3850	1.4003	320
330	1.4157	1.4312	1.4468	1.4625	1.4784	1.4944	1.5105	1.5267	1.5431	1.5596	330
340	1.5762	1.5929	1.6097	1.6267	1.6438	1.6610	1.6784	1.6959	1.7135	1.7312	340
350	1.7491	1.7671	1.7852	1.8035	1.8219	1.8404	1.8590	1.8778	1.8968	1.9158	350
360	1.9350	1.9543	1.9738	1.9933	2.0130	2.0329	2.0529	2.0730	2.0933	2.1137	360
370	2.1342	2.1549	2.1757	2.1967	2.2178	2.2390	2.2604	2.2819	2.3036	2.3254	370
380	2.3473	2.3694	2.3916	2.4140	2.4365	2.4592	2.4820	2.5049	2.5280	2.5513	380
390	2.5746	2.5982	2.6219	2.6457	2.6697	2.6938	2.7181	2.7425	2.7671	2.7918	390
400	2.8167	2.8417	2.8669	2.8923	2.9178	2.9434	2.9692	2.9951	3.0212	3.0475	400
410	3.0739	3.1005	3.1272	3.1541	3.1811	3.2083	3.2357	3.2632	3.2909	3.3187	410
420	3.3467	3.3748	3.4032	3.4316	3.4603	3.4891	3.5180	3.5472	3.5764	3.6059	420
430	3.6355	3.6653	3.6952	3.7253	3.7556	3.7860	3.8166	3.8474	3.8784	3.9095	430
440	3.9408	3.9722	4.0038	4.0356	4.0675	4.0997	4.1320	4.1644	4.1971	4.2299	440
450	4.2629	4.2960	4.3294	4.3629	4.3966	4.4304	4.4645	4.4987	4.5331	4.5676	450
460	4.6024	4.6373	4.6724	4.7077	4.7431	4.7788	4.8146	4.8506	4.8868	4.9231	460
470	4.9597	4.9964	5.0333	5.0704	5.1077	5.1451	5.1828	5.2206	5.2586	5.2968	470
480	5.335	5.374	5.413	5.452	5.491	5.530	5.570	5.609	5.649	5.689	480
490	5.730	5.770	5.811	5.852	5.893	5.934	5.976	6.017	6.059	6.101	490
500	6.143	6.186	6.229	6.271	6.314	6.358	6.401	6.445	6.489	6.533	500
510	6.577	6.622	6.666	6.711	6.756	6.802	6.847	6.893	6.939	6.985	510
520	7.032	7.078	7.125	7.172	7.219	7.266	7.314	7.362	7.410	7.458	520
530	7.507	7.556	7.605	7.654	7.703	7.753	7.803	7.853	7.903	7.954	530
540	8.004	8.056	8.107	8.158	8.210	8.262	8.314	8.366	8.419	8.472	540
550	8.525	8.578	8.632	8.686	8.740	8.794	8.848	8.903	8.958	9.014	550
560	9.069	9.125	9.181	9.237	9.294	9.350	9.407	9.465	9.522	9.580	560
570	9.638	9.696	9.755	9.814	9.873	9.932	9.992	10.052	10.112	10.172	570
580	10.233	10.294	10.355	10.416	10.478	10.540	10.603	10.665	10.728	10.792	580
590	10.855	10.919	10.983	11.047	11.112	11.177	11.242	11.307	11.373	11.439	590
600	11.506	11.573	11.640	11.707	11.775	11.843	11.911	11.980	12.048	12.118	600
610	12.187	12.257	12.328	12.398	12.469	12.540	12.612	12.684	12.756	12.829	610
620	12.902	12.975	13.049	13.123	13.197	13.272	13.347	13.423	13.500	13.575	620
630	13.652	13.729	13.806	13.884	13.963	14.041	14.120	14.200	14.280	14.360	630
640	14.441	14.523	14.604	14.687	14.769	14.853	14.936	15.020	15.105	15.190	640
650	15.275	15.361	15.448	15.535	15.623	15.711	15.800	15.889	15.979	16.070	650
660	16.161	16.252	16.345	16.438	16.532	16.626	16.721	16.817	16.913	17.011	660
670	17.109	17.207	17.307	17.407	17.508	17.610	17.713	17.817	17.922	18.028	670
680	18.134	18.242	18.351	18.461	18.572	18.685	18.799	18.913	19.030	19.147	680
690	19.267	19.388	19.510	19.634	19.761	19.889	20.019	20.152	20.288	20.427	690
700	20.570	20.717	20.869	21.030	21.205	21.418	------	------	------	------	700

TABLE 5.—*Pressure of saturated water vapor*

Pounds per square inch—Fahrenheit temperature—Standard gravity=32.174 ft/sec²

lb/in.²	°F	lb/in.²	°F	lb/in.²	°F	lb/in.²	°F
0.10	35.030	5.4	165.510	37	262.579	97	325.627
.12	39.663	5.5	166.297	38	264.170	98	326.365
.14	43.657	5.6	167.071	39	265.728	99	327.097
.16	47.175	5.8	168.585	40	267.253	100	327.823
.18	50.324	6.0	170.054	41	268.748	101	328.544
.20	53.179	6.2	171.484	42	270.213	102	329.260
.22	55.792	6.4	172.876	43	271.651	103	329.969
.24	58.203	6.5	173.559	44	273.061	104	330.673
.25	59.343	6.6	174.232	45	274.446	105	331.371
.26	60.444	6.8	175.553	46	275.807	106	332.064
.28	62.539	7.0	176.842	47	277.143	107	332.753
.30	64.506	7.2	178.100	48	278.457	108	333.436
.32	66.361	7.4	179.330	49	279.749	109	334.114
.34	68.117	7.5	179.934	50	281.020	110	334.787
.35	68.962	7.6	180.532	51	282.270	111	335.455
.36	69.786	7.8	181.708	52	283.501	112	336.118
.38	71.375	8.0	182.858	53	284.712	113	336.778
.40	72.892	8.2	183.985	54	285.906	114	337.431
.42	74.344	8.4	185.089	55	287.082	115	338.082
.44	75.737	8.5	185.633	56	288.240	116	338.727
.45	76.414	8.6	186.172	57	289.382	117	339.368
.46	77.076	8.8	187.233	58	290.509	118	340.004
.48	78.365	9.0	188.275	59	291.620	119	340.636
.50	79.608	9.2	189.297	60	292.715	120	341.265
.55	82.536	9.4	190.301	61	293.796	121	341.889
.60	85.240	9.5	190.796	62	294.862	122	342.509
.65	87.755	9.6	191.287	63	295.916	123	343.125
.70	90.106	9.8	192.256	64	296.955	124	343.736
.75	92.317	10.0	193.209	65	297.982	125	344.344
.80	94.403	10.5	195.524	66	298.997	126	344.949
.85	96.378	11.0	197.748	67	299.998	127	345.549
.90	98.256	11.5	199.890	68	300.989	128	346.146
.95	100.045	12.0	201.956	69	301.967	129	346.739
1.00	101.755	12.5	203.951	70	302.934	130	347.329
1.10	104.964	13.0	205.881	71	303.890	131	347.915
1.2	107.930	13.5	207.751	72	304.836	132	348.497
1.3	110.689	14.0	209.564	73	305.771	133	349.076
1.4	113.272	14.5	211.323	74	306.695	134	349.651
1.5	115.701	15.0	213.034	75	307.610	135	350.223
1.6	117.994	16.0	216.319	76	308.515	136	350.792
1.7	120.167	17	219.437	77	309.411	137	351.358
1.8	122.233	18	222.407	78	310.297	138	351.920
1.9	124.203	19	225.244	79	311.175	139	352.479
2.0	126.086	20	227.961	80	312.043	140	353.034
2.2	129.622	21	230.568	81	312.903	141	353.587
2.4	132.893	22	233.075	82	313.755	142	354.137
2.6	135.939	23	235.491	83	314.598	143	354.684
2.8	138.791	24	237.821	84	315.433	144	355.227
3.0	141.475	25	240.073	85	316.260	145	355.768
3.2	144.010	26	242.253	86	317.080	146	356.305
3.4	146.414	27	244.364	87	317.891	147	356.840
3.6	148.701	28	246.413	88	318.696	148	357.372
3.8	150.883	29	248.403	89	319.493	149	357.901
4.0	152.969	30	250.338	90	320.283	150	358.428
4.2	154.969	31	252.221	91	321.067	151	358.952
4.4	156.889	32	254.054	92	321.843	152	359.472
4.6	158.737	33	255.842	93	322.613	153	359.991
4.8	160.519	34	257.586	94	323.376	154	360.506
5.0	162.238	35	259.289	95	324.133	155	361.019
5.2	163.901	36	260.953	96	324.883	156	361.529

TABLE 5.—*Pressure of saturated water vapor*—Continued

lb/in.²	°F	lb/in.²	°F	lb/in.²	°F	lb/in.²	°F
157	362.037	275	409.436	650	494.896	1500	596.199
158	362.542	280	411.059	660	496.572	1520	597.967
159	363.045	285	412.659	670	498.229	1540	599.717
160	363.545	290	414.239	680	499.868	1560	601.449
161	364.043	295	415.797	690	501.488	1580	603.165
162	364.538	300	417.334	700	503.090	1600	604.863
163	365.031	305	418.853	710	504.675	1620	606.545
164	365.522	310	420.352	720	506.243	1640	608.211
165	366.010	315	421.832	730	507.794	1660	609.861
166	366.496	320	423.295	740	509.330	1680	611.496
167	366.980	325	424.739	750	510.849	1700	613.115
168	367.461	330	426.167	760	512.353	1720	614.720
169	367.940	335	427.578	770	513.842	1740	616.310
170	368.417	340	428.973	780	515.317	1760	617.886
171	368.892	345	430.352	790	516.777	1780	619.448
172	369.364	350	431.716	800	518.223	1800	620.996
173	369.834	355	433.065	810	519.655	1820	622.531
174	370.303	360	434.399	820	521.074	1840	624.053
175	370.769	365	435.719	830	522.479	1860	625.561
176	371.233	370	437.025	840	523.872	1880	627.057
177	371.695	375	438.317	850	525.252	1900	628.540
178	372.155	380	439.596	860	526.620	1920	630.011
179	372.613	385	440.863	870	527.976	1940	631.470
180	373.069	390	442.117	880	529.320	1960	632.917
181	373.523	395	443.359	890	530.652	1980	634.353
182	373.975	400	444.588	900	531.973	2000	635.776
183	374.425	405	445.806	910	533.282	2050	639.287
184	374.873	410	447.012	920	534.581	2100	642.730
185	375.319	415	448.207	930	535.869	2150	646.107
186	375.764	420	449.391	940	537.147	2200	649.422
187	376.206	425	450.564	950	538.413	2250	652.676
188	376.647	430	451.727	960	539.670	2300	655.871
189	377.085	435	452.879	970	540.917	2350	659.010
190	377.522	440	454.021	980	542.154	2400	662.094
191	377.957	445	455.153	990	543.382	2450	665.125
192	378.391	450	456.276	1000	544.600	2500	668.105
193	378.822	455	457.388	1020	547.007	2550	671.035
194	379.252	460	458.492	1040	549.381	2600	673.916
195	379.680	465	459.586	1060	551.720	2650	676.750
196	380.107	470	460.672	1080	554.024	2700	679.537
197	380.532	475	461.748	1100	556.296	2750	682.279
198	380.955	480	462.816	1120	558.536	2800	684.977
199	381.376	485	463.875	1140	560.747	2850	687.632
200	381.796	490	464.926	1160	562.927	2900	690.245
202	382.630	495	465.969	1180	565.079	2950	692.815
204	383.458	500	467.004	1200	567.204	3000	695.344
205	383.870	510	469.050	1220	569.300	3050	697.832
210	385.906	520	471.065	1240	571.372	3100	700.278
215	387.903	530	473.051	1260	573.417	3150	702.683
220	389.865	540	475.009	1280	575.438	3200	705.044
225	391.793	550	476.939	1300	577.434		
230	393.687	560	478.842	1320	579.407		
235	395.549	570	480.719	1340	581.357		
240	397.381	580	482.571	1360	583.285		
245	398.184	590	484.399	1380	585.191		
250	400.958	600	486.203	1400	587.076		
255	402.704	610	487.985	1420	588.940		
260	404.425	620	489.744	1440	590.784		
265	406.119	630	491.482	1460	592.608		
270	407.789	640	493.199	1480	594.413		

TABLE 6.—*Pressure of saturated water vapor*

Kilograms per square centimeter—Centigrade temperature

[Standard gravity, 980.665 cm/sec²]

kg/cm²	° C	kg/cm²	° C	kg/cm²	° C	kg/cm²	° C	kg/cm²	° C
------	------	1.00	99.087	9.0	174.529	45	256.227	110	316.580
0.0075	2.590	1.10	101.764	9.2	175.461	46	257.564	112	317.929
.0100	6.707	1.20	104.247	9.4	176.377	47	258.879	114	319.260
.0125	9.996	1.30	106.564	9.6	177.278	48	260.173	116	320.573
.0150	12.749	1.40	108.739	9.8	178.164	49	261.446	118	321.868
.0175	15.123	1.5	110.789	10.0	179.036	50	262.700	120	323.146
.0200	17.217	1.6	112.730	10.5	181.158	51	263.934	122	324.408
.0225	19.091	1.7	114.573	11.0	183.201	52	265.151	124	325.653
.0250	20.791	1.8	116.330	11.5	185.172	53	266.349	126	326.883
.0275	22.349	1.9	118.009	12.0	187.078	54	267.531	128	328.098
.030	23.788	2.0	119.617	12.5	188.922	55	268.695	130	329.298
.035	26.375	2.1	121.160	13.0	190.709	56	269.844	132	330.483
.040	28.658	2.2	122.645	13.5	192.443	57	270.977	134	331.654
.045	30.705	2.3	124.075	14.0	194.128	58	272.096	136	332.812
.050	32.562	2.4	125.456	14.5	195.766	59	273.199	138	333.956
.055	34.265	2.5	126.791	15.0	197.360	60	274.288	140	335.087
.060	35.839	2.6	128.082	15.5	198.914	61	275.364	142	336.205
.065	37.302	2.7	129.335	16.0	200.429	62	276.426	144	337.311
.070	38.672	2.8	130.550	16.5	201.907	63	277.475	146	338.404
.075	39.959	2.9	131.730	17.0	203.351	64	278.512	148	339.486
.080	41.174	3.0	132.878	17.5	204.763	65	279.535	150	340.556
.085	42.326	3.1	133.995	18.0	206.143	66	280.547	152	341.614
.090	43.420	3.2	135.083	18.5	207.494	67	281.549	154	342.661
.095	44.463	3.3	136.144	19.0	208.817	68	282.538	156	343.697
.100	45.460	3.4	137.180	19.5	210.113	69	283.516	158	344.723
.11	47.331	3.5	138.192	20.0	211.383	70	284.483	160	345.738
.12	49.062	3.6	139.180	20.5	212.629	71	285.440	162	346.742
.13	50.673	3.7	140.146	21.0	213.852	72	286.387	164	347.737
.14	52.181	3.8	141.091	21.5	215.053	73	287.323	166	348.721
.15	53.599	3.9	142.017	22.0	216.232	74	288.250	168	349.696
.16	54.939	4.0	142.923	22.5	217.390	75	289.167	170	350.661
.17	56.209	4.1	143.812	23.0	218.529	76	290.075	172	351.617
.18	57.416	4.2	144.684	23.5	219.649	77	290.974	174	352.563
.19	58.568	4.3	145.538	24.0	220.750	78	291.864	176	353.501
.20	59.669	4.4	146.377	24.5	221.834	79	292.745	178	354.429
.21	60.724	4.5	147.201	25.0	222.901	80	293.618	180	355.348
.22	61.738	4.6	148.010	25.5	223.951	81	294.483	182	356.259
.23	62.713	4.7	148.805	26.0	224.986	82	295.339	184	357.161
.24	63.652	4.8	149.587	26.5	226.006	83	296.187	186	358.055
.25	64.559	4.9	150.356	27.0	227.011	84	297.028	188	358.941
.26	65.435	5.0	151.112	27.5	228.001	85	297.861	190	359.818
.28	67.106	5.2	152.589	28.0	228.978	86	298.686	192	360.687
.30	68.678	5.4	154.021	28.5	229.942	87	299.504	194	361.548
.32	70.164	5.6	155.412	29.0	230.892	88	300.315	196	362.401
.34	71.573	5.8	156.763	29.5	231.830	89	301.119	198	363.247
.35	72.252	6.0	158.078	30	232.756	90	301.916	200	364.084
.36	72.914	6.2	159.358	31	234.573	91	302.706	202	364.914
.38	74.194	6.4	160.605	32	236.345	92	303.489	204	365.737
.40	75.418	6.6	161.822	33	238.075	93	304.266	206	366.552
.45	78.267	6.8	163.010	34	239.766	94	305.036	208	367.359
.50	80.860	7.0	164.171	35	241.419	95	305.801	210	368.159
.55	83.245	7.2	165.305	36	243.035	96	306.559	212	368.951
.60	85.454	7.4	166.415	37	244.618	97	307.311	214	369.737
.65	87.514	7.6	167.501	38	246.169	98	308.057	216	370.514
.70	89.446	7.8	168.565	39	247.688	99	308.797	218	371.285
.75	91.266	8.0	169.607	40	249.178	100	309.531	220	372.048
.80	92.988	8.2	170.629	41	250.640	102	310.983	222	372 803
.85	94.622	8.4	171.631	42	252.074	104	312.413	224	373.550
.90	96.178	8.6	172.615	43	253.483	106	313.822	225	373.920
.95	97.663	8.8	173.581	44	254.867	108	315.211	---	-------

TABLE 7.—*Conversion factors*

Definitive Values

1 standard atmosphere = 760 mm mercury column (density 13.5951 g/cm³, gravity 980.665 cm/sec²).
1 meter = 39.37 inches.
1 pound = 453.59243 grams.
1,000 calories = 1/860 international kilowatt hour (definition of International Steam Conference, London 1929).
1 international electrical watt = 1.0003 absolute watts (rounded experimental value as of 1934).
1 Btu = 252.00 cal (definition evolved by usage and based on relations between mass units and thermometric scales).

PRESSURE CONVERSION FACTORS

Atm		kg/cm²		bar		mm Hg		lb/in.²
1	=	1. 03323	=	1. 01325	=	760.	=	14. 6960
. 967841	=	1	=	. 980665	=	735. 559	=	14. 2234
. 986923	=	1. 01972	=	1	=	750. 062	=	14. 5038
1. 31579	=	1. 35951	=	1. 33322	=	1000	=	19. 3369
. 680457	=	. 703067	=	. 689473	=	517. 147	=	10

ENERGY CONVERSION FACTORS

Absolute joule		international electrical		Heat		Pressure×volume				
j		*int. j*	*int. whr*	*cal*	*Btu*	$\frac{lb}{in.^2}$–ft³	$\frac{kg}{cm^2}$–m³	atm-dm³	ft-lb	
10, 000	=	9, 997	= 2. 7769 =	2, 388. 2 =	9. 4770 =	51. 2195 =	0. 101972 =	98. 6923 =	7, 375. 61	
10, 003	=	10, 000	= 2. 7778 =	2, 388. 9 =	9. 4799 =	51. 235 =	. 10200 =	98. 722 =	7, 377. 8	
36, 011	=	36, 000	= 10 =	8, 600 =	34. 128 =	184. 45 =	. 36721 =	355. 40 =	26, 560	
41, 873	=	41, 860	= 11. 628 =	10, 000 =	39. 683 =	214. 47 =	. 42699 =	413. 25 =	30, 884	
10, 552	=	10, 549	= 2. 9302 =	2, 520. 0 =	10 =	54. 046 =	. 10760 =	104. 14 =	7, 782. 6	
195, 238	=	195, 180	= 54. 217 =	46, 626 =	1, 850. 3 =	1, 000 =	1. 9909 =	1, 926. 85 =	144, 000	
98, 066. 5	=	98, 037	= 27. 233 =	23, 420 =	92. 938 =	502. 292 =	1 =	967. 841 =	72, 330. 0	
10, 132. 5	=	10, 129	= 2. 8137 =	2, 419. 8 =	9. 6026 =	51. 8982 =	. 103323 =	100 =	7, 473. 33	
13, 558. 2	=	13, 554	= 3. 7650 =	3, 237. 9 =	12. 849 =	69. 4444 =	. 138255 =	133. 809 =	10, 000	

TABLE 8.—(*Thermometric*) *Condensation temperature of steam*

[Star (*) indicates change in integer]

P	Pressure in mm mercury (standard)										P
	0	1	2	3	4	5	6	7	8	9	
	Temperature in degrees of international scale										
500	88.678	0.730	0.782	0.834	0.886	0.938	0.990	*0.042	*0.093	*0.144	500
510	89.196	.247	.298	.350	.401	.452	.502	.553	.604	.655	510
520	.705	.756	.806	.856	.907	.957	*.007	*.057	*.107	*.157	520
530	90.206	.256	.306	.355	.405	.454	.503	.553	.602	.651	530
540	.700	.749	.798	.846	.895	.944	.992	*.041	*.089	*.138	540
550	91.186	.234	.282	.330	.378	.426	.474	.521	.569	.617	550
560	.664	.712	.759	.806	.854	.901	.948	.995	*.042	*.089	560
570	92.136	.182	.229	.276	.322	.369	.415	.462	.508	.554	570
580	.600	.646	.692	.738	.784	.830	.876	.922	.967	*.013	580
590	93.058	.104	.149	.195	.240	.285	.330	.375	.420	.465	590
600	.5100	.5548	.5996	.6443	.6889	.7335	.7780	.8224	.8668	.9112	600
610	.9554	.9996	*.0438	*.0879	*.1319	*.1759	*.2198	*.2636	*.3074	*.3511	610
620	94.3948	.4384	.4820	.5255	.5689	.6123	.6556	.6989	.7421	.7852	620
630	.8283	.8713	.9143	.9572	*.0001	*.0429	*.0857	*.1284	*.1710	*.2136	630
640	95.2562	.2987	.3411	.3834	.4257	.4680	.5102	.5523	.5944	.6365	640
650	95.6785	.7204	.7623	.8041	.8459	.8876	.9293	.9709	*.0125	*.0539	650
660	96.0954	.1368	.1782	.2195	.2607	.3019	.3431	.3842	.4252	.4662	660
670	.5072	.5480	.5889	.6297	.6704	.7111	.7517	.7923	.8329	.8734	670
680	.9138	.9542	.9946	*.0349	*.0751	*.1153	*.1555	*.1956	*.2356	*.2756	680
690	97.3156	.3555	.3954	.4352	.4749	.5146	.5543	.5939	.6335	.6730	690
700	.7125	.7519	.7913	.8307	.8700	.9092	.9484	.9876	*.0267	*.0657	700
710	98.1048	.1437	.1827	.2216	.2604	.2992	.3379	.3766	.4153	.4539	710
720	.4925	.5310	.5695	.6079	.6463	.6846	.7229	.7612	.7994	.8376	720
730	.8757	.9138	.9519	.9899	*.0278	*.0657	*.1036	*.1414	*.1792	*.2170	730
740	99.2547	.2924	.3300	.3675	.4051	.4426	.4800	.5174	.5548	.5921	740
750	.6294	.6667	.7039	.7410	.7781	.8152	.8523	.8893	.9262	.9631	750
760	100.0000	.0368	.0736	.1104	.1471	.1838	.2204	.2570	.2936	.3301	760
770	.3666	.4030	.4394	.4758	.5121	.5484	.5846	.6208	.6570	.6932	770
780	.7293	.7653	.8013	.8373	.8733	.9092	.9450	.9808	*.0166	*.0524	780
790	101.0881	.1238	.1594	.1950	.2306	.2661	.3016	.3371	.3725	.4079	790
	0	1	2	3	4	5	6	7	8	9	

WASHINGTON, March 30, 1934.

U.S. DEPARTMENT OF COMMERCE NATIONAL BUREAU OF STANDARDS

RESEARCH PAPER RP692

Part of Journal of Research, of the National Bureau of Standards, vol 13, July 1934

HEATS OF COMBUSTION AND OF FORMATION OF THE NORMAL PARAFFIN HYDROCARBONS IN THE GASEOUS STATE, AND THE ENERGIES OF THEIR ATOMIC LINKAGES

By Frederick D. Rossini

ABSTRACT

From the data recently obtained in this laboratory on the heats of combustion of methane, ethane, propane, normal butane, and normal pentane, reliable values are deduced for the heats of combustion of all the other normal paraffin hydrocarbons in the gaseous state. For normal C_nH_{2n+2} (gas), with $n>5$, the heat of combustion, at a temperature of 25 C and a constant total pressure of 1 atmosphere, in gaseous oxygen to form gaseous carbon dioxide and liquid water, is $60.40+n(157.00\pm0.08)$ k$-$cal$_{15}$ per mole. (This unit of energy is a defined one and is derived from the fundamental international joule by means of the factor 1.00040/4.1850.)

The following generalization is made: In any organic molecule containing a normal alkyl group of more than 5 carbon atoms, the addition of a CH_2 group to the normal alkyl group to form the next higher normal alkyl group results in an increase in the heat of combustion of the organic molecule in the gaseous state, at a temperature of 25 C and a constant total pressure of 1 atmosphere, of 157.00 ± 0.08 k$-$cal$_{15}$ per mole.

From these and other data values are computed for the heats of formation, from hydrogen and β-graphite and diamond, respectively, of all the normal paraffin hydrocarbons in the gaseous state at temperatures of 25 C and 0 Kelvin.

The energy of dissociation, at zero Kelvin, of a gaseous normal paraffin hydrocarbon, C_nH_{2n+2}, into gaseous carbon and hydrogen atoms, is shown to be a linear function of n above, but not linear below, $n=6$. The deviations from linearity for the latter are in the direction of greater stability of the molecule and have the following values: Methane, 4.81 ± 0.08; ethane, 1.59 ± 0.14; propane, 0.83 ± 0.19; normal butane, 0.46 ± 0.27; normal pentane, 0.13 ± 0.37, k-cal per mole.

It is shown that for the normal paraffin hydrocarbons, and for carbon and hydrogen atoms in the normal state, the energy evolved in the reaction $C\,(gas)+2H(gas)+C_nH_{2n+2}\,(gas)=C_{n+1}H_{2n+4}\,(gas)$, for $n>5$, at 0 Kelvin, is $-\triangle H_0^0=(20.8\pm0.9)+D_{CO}$ k-cal$_{15}$ per mole (D_{CO} is the energy of dissociation of CO at 0 Kelvin); and any assignment of values for D_{CO}, for the energy of excitation of the carbon atom to the ^5S state, and for the energies of the 1 C–C and 2 C–H bonds formed in the reaction must satisfy this relation.

CONTENTS

		Page
I.	Introduction	22
II.	Heats of combustion	23
III.	Heats of formation from the elements	26
	1. At 25 centigrade	26
	2. At 0 Kelvin	29
IV.	Change in heat content for the reaction $nCO\,(gas)+(n+1)H_2(gas)=n/2\,O_2(gas)=C_nH_{2n+2}(gas)$	30
V.	Energies of the atomic linkages	30
VI.	References	35

I. INTRODUCTION

In this paper the writer utilizes the data on the heats of combustion of methane, ethane, propane, normal butane, and normal pentane recently obtained in this laboratory (1, 25)[1] for the following purposes: First, to predict accurate values for the heats of combustion of the normal gaseous paraffin hydrocarbons containing more than 5 carbon atoms; second, to compute values for the heats of formation of all the normal paraffin hydrocarbons in the gaseous state; and third, to test the accuracy of the postulate of the constancy of the energies of the atomic linkages in these molecules.

Because of the increasing industrial importance of vapor phase reactions involving the paraffin hydrocarbons, there is great need for values of the heats of formation of these substances in the gaseous state, for making calculations of the chemical equilibria involved.

The heats of combustion of hydrocarbons have been of considerable interest to the physical chemist for many years. Speculation concerning the influence of structure and of the number of carbon atoms upon the energy content of hydrocarbon molecules began as early as 1869, when Hermann (2) utilized for this purpose the data on heats of combustion obtained by Favre and Silbermann (4) about 15 years earlier.

From the results of his own measurements, reported in 1886 in the fourth volume of his monumental treatise on thermochemistry, Thomsen (3) showed that, in general, the addition of a CH_2 group to any molecule in the gaseous state resulted in an increase in its heat of combustion of about 158 kilocalories per mole. And, in particular, Thomsen's values for methane, ethane, propane, isobutane, and tetramethylmethane showed constant successive differences in the heats of combustion, at constant pressure and a temperature of 18 C, of 158.34 ± 0.20 kilocalories per mole.

Except for the meager data of Berthelot and Matignon (5) on ethane and propane, and the isolated value of Roth and Machlett (6) on pentane, no data on the heats of combustion of the gaseous paraffin hydrocarbons above methane were reported during the half century following Thomsen's measurements. Thus it was only natural that Thomsen's data were used to substantiate the almost universally accepted postulate of the constancy of the energies of the C–C and C–H linkages in the saturated hydrocarbon molecules.

Many calculations have been made in recent years concerning the postulate of the constancy of bond energies in the paraffin hydrocarbons. In his recent book on "The Covalent Link in Chemistry", published in 1933, Sidgwick (7) writes: " * * * and so the values of the heats of formation of the [atomic] links [in the paraffin hydrocarbons] should be independent of the number of atoms in the molecule, as in fact they are found to be."

In particular, one may cite the recent, 1932, calculations of Pauling (8) who showed that, using the values given by Kharasch [2] (9) for the heats of combustion of methane, ethane, propane, butane, hexane, and heptane, the energies of formation from gaseous atoms calculated on the assumption of constant energies for the C–H and C–C

[1] Figures in parentheses here and throughout the text refer to the references at the end of this paper, p. 35.
[2] The values given by Kharasch (9) for methane, ethane, propane, and butane are based on the calorimetric data of Thomsen (3).

bonds were practically identical with the values computed from heats of combustion plus some auxiliary data.[3] The differences between the values calculated by the two methods were such as to be equivalent to errors of less than 0.1 percent in the heats of combustion, or about 0.2 kilocalorie per carbon atom. This agreement is quite extraordinary because it borders on the very limit of the calorimetric precision obtainable by Thomsen (3), and there must be superimposed upon his calorimetric uncertainty errors due to the large corrections for impurities in the samples of hydrocarbons burned by him. This latter uncertainty is probably much greater than Thomsen's calorimetric error because his various samples had the following empirical formulas: Ethane, $C_2H_{6.054}$, $C_2H_{6.033}$; propane, $C_3H_{7.991}$; isobutane, $C_4H_{9.748}$, $C_4H_{9.899}$; tetramethylmethane; $C_5H_{11.78}$, $C_5H_{11.64}$. Thomsen assumed that his last sample of pentane was, in mole percent, 78.5 C_5H_{12} + 21.5 C_4H_8.

Because of these facts, it has seemed desirable that an accurate test be made of the postulate of the constancy of the energies of the atomic linkages in the simple paraffin hydrocarbon molecules, by discovering, if possible, any real deviation from linearity in the heats of combustion of the members of the series. With the data on heats of combustion recently obtained in this laboratory (1), it is now possible to submit the postulate to a more rigorous test.

II. HEATS OF COMBUSTION

According to prevailing ideas, the heats of combustion of the paraffin hydrocarbons in the gaseous state should show constant differences between successive members of the series. That is to say, the heat of combustion will be a linear function of the number of carbon atoms,

$$Qc = A + Bn \tag{1}$$

where Qc is the heat of combustion of a gaseous normal paraffin hydrocarbon containing n carbon atoms, B is the constant increment per carbon atom or CH_2 group, and A is a constant. This relation may be expressed also as

$$(Qc - A)/n = B \tag{2}$$

The following are the data recently obtained in this laboratory (1) on the heats of combustion of the gases at a temperature of 25 C and a constant total pressure of 1 atmosphere, in k-cal_{15} per mole: [4]

Methane	212. 79 ± 0. 07
Ethane	372. 81 ± 0. 11
Propane	530. 57 ± 0. 12
Normal butane	687. 94 ± 0. 15
Normal pentane	845. 27 ± 0. 21

Examination of these values shows that the successive differences are 160.02, 157.76, 157.37, and 157.33, respectively. These differences are quite significantly not constant, but are apparently approaching a

[3] The nature of the calculation is such that the use of different values for the subsidiary data changes only the actual values of the C–H and C–C bond energies, not their constancy from one molecule to another. The postulate of the constancy of the energies of the atomic linkages in the normal gaseous paraffin hydrocarbons may be said to be practically substantiated if the heats of combustion of all the successive members of the series show constant differences within the limits of experimental error.

[4] These values are given in k-cal_{15}, which is a defined unit and is taken as equivalent to 4.1850/1.00040 international kilojoules. The fundamental unit of energy in this work is the international joule based upon standards of emf and resistance maintained at this Bureau. See p. 736 of reference (25).

constant value with increasing number of carbon atoms. In figure 1 is plotted, against the number of carbon atoms, the function $(Qc-60.40)/n$. The value of the constant, 60.40, has been chosen so that the values of $(Qc-60.40)/n$ will approach a constant value at about $n=6$. That this relation adequately represents the data is corroborated by the values which have been included on the plot for gaseous normal heptane and gaseous normal octane.

The values for the heats of combustion of gaseous normal heptane and gaseous normal octane are, respectively, 1159.5 ± 0.6 and 1316.3 ± 0.7, k-cal$_{15}$ per mole at a temperature of 25 C and a constant total pressure of 1 atmosphere. These values are based upon the recent accurate data obtained by Jessup (10), in the heat division of this Bureau, on the heats of combustion of the liquid hydrocarbons at a temperature of 30 C and constant volume in a bomb calorimeter. Jessup's data have been converted according to the method of Washburn (11) to give the energy of the reaction at a pressure of 1 atmosphere. After converting to a temperature of 25 C and a constant pressure of 1 atmosphere, the writer has added the heat of vaporization, using the values 8.75 and 9.85, k-cal per mole, for normal heptane and normal octane, respectively. These values of the heat of vaporization, which are uncertain by about 0.5 percent, were obtained by the present writer from a review of the existing data which will be published in a subsequent paper. Jessup's data on the heats of combustion of liquid normal heptane and liquid normal octane are accurate to about ± 0.03 percent.

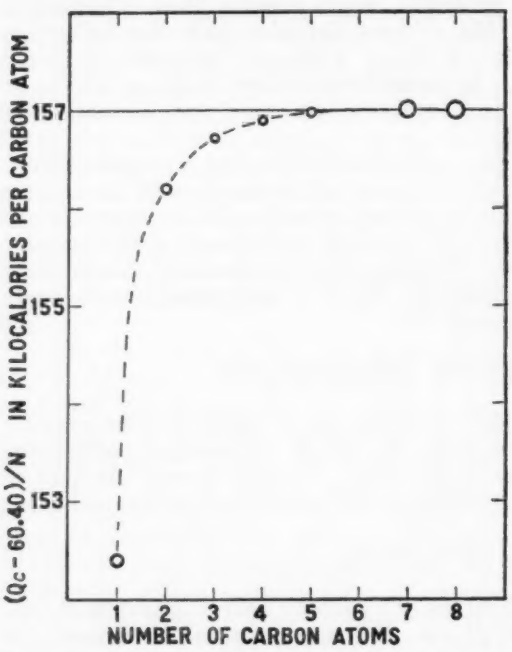

FIGURE 1.—*Relation between the heats of combustion of the normal paraffin hydrocarbons and the number of carbon atoms in the molecule.*

The scale of ordinates gives the function $(Qc-60.40)/n$, where Qc is the heat of combustion of gaseous normal C_nH_{2n+2} at a temperature of 25 C and a constant total pressure of 1 atmosphere, in k-cal$_{15}$ per mole, and n is the number of carbon atoms in the molecule. The scale of abscissae gives the number of carbon atoms in the molecule. The circles are drawn with radii representing the estimated uncertainties in the various values.

From the data displayed in figure 1, one can say that the heat of combustion of any gaseous normal paraffin hydrocarbon containing more than 5 carbon atoms is given by the following relation:

For $n>5$

$$Qc = 60.40 + n\ (157.00 \pm 0.08)\ \text{k-cal}_{15}\ \text{per mole}\ ^{5} \qquad (3)$$

[5] See footnote to table 1.

at a constant total pressure of 1 atmosphere and a temperature of 25 C. Here Qc is the heat of the reaction

$$C_nH_{2n+2}\ (\text{gas}) + \frac{3n+1}{2} O_2\ (\text{gas}) = nCO_2\ (\text{gas}) + (n+1)\ H_2O\ (\text{liquid}) \quad (4)$$

and n is the number of carbon atoms, which must be greater than 5. The uncertainty in the values of Qc obtained from the foregoing relation is about ± 0.05 percent.

In table 1 are summarized the values for the heats of combustion of the normal paraffin hydrocarbons in the gaseous state.

TABLE 1.—*Summary of the values for the heats of combustion of the normal paraffin hydrocarbons in the gaseous state*

$C_{n2}H_{n+2}$ (gas)	Heat [1] of combustion at 25 centigrade and a constant total pressure of 1 atmosphere
	K-cal$_{15}$ per mole.
Methane	212.79±0.07
Ethane	372.81± .11
Propane	530.57± .12
Normal butane	687.94± .15
Normal pentane	845.27± .21
Normal hexane	1,002.40± .48
Normal heptane	1,159.40± .56
Normal octane	1,316.40± .64
Normal nonane	1,473.40± .72
Normal decane	1,630.40± .80
Normal undecane	1,787.40± .88
Normal dodecane	1,944.40± .96
Normal pentadecane	2,415.4±1.2
Normal C_nH_{2n+2} (for $n>5$)	60.40+n (157.00±.08)

[1] The k-cal$_{15}$ used here is a defined unit, and is derived from the fundamental international kilojoule by means of the factor 1.00040/4.1850. The values are independent of the atomic weight of carbon; 1 mole of C_nH_{2n+2} is taken as equivalent to $(n+1)$ (18.0156) grams of H_2O. The values for the first 5 members of the series are directly measured ones, the values for the others are calculated.

It will be noted that the actual heats of combustion of the first 5 members of the series differ from the values expected from the linear relation given by equation 3, by the following amounts: Methane, -4.61 ± 0.07; ethane, -1.59 ± 0.11; propane, -0.83 ± 0.12; normal butane, -0.46 ± 0.15; normal pentane, -0.13 ± 0.21, k-cal per mole, at a constant total pressure of 1 atmosphere and a temperature of 25 C.

The writer believes that it is now possible to make the following accurate generalization concerning the heats of combustion of all organic compounds containing normal alkyl groups of more than 5 carbon atoms:

In any organic molecule containing a normal alkyl group of more than 5 carbon atoms, the addition of a CH_2 group to the normal alkyl group to form the next higher normal alkyl group results in an increase in the heat of combustion of the organic molecule in the gaseous state, at a temperature of 25 C and a constant total pressure of 1 atmosphere, of 157.00 ± 0.08 k-cal$_{15}$ per mole.

III. HEATS OF FORMATION FROM THE ELEMENTS

1. AT 25 CENTIGRADE

It is conventional, in tabulating thermodynamic data concerning the free energies, heats, and entropies of formation of chemical compounds, to use as reference or standard states for the elemental substances those states in which the elements naturally exist at the standard temperature of 25 C.

Because the synthesis of the hydrocarbon molecules cannot be carried out under conditions which permit accurate calorimetric measurement, the heats of formation of these substances are computed most accurately from their heats of combustion. For this purpose it is necessary to know the heats of formation of liquid water and gaseous carbon dioxide. The standard state usually chosen for carbon is that of graphite, but this reference state is a somewhat uncertain one because Roth and his coworkers (12) have found that the heats of combustion of various graphites differ by amounts which are very much greater than the calorimetric errors. Roth found that the heats of combustion of various samples of graphite naturally grouped themselves more or less closely about two values. The samples giving the higher value had much the less spread, and Roth chose this as the more definite of the two kinds, labeling it β-graphite and the other α-graphite. Another standard state that has been proposed for carbon is that of diamond, which, though a perfectly definite state, has the apparent disadvantage that it is practically inaccessible on account of its cost. However, it may be more desirable to deal with a certain fixed reference state, even though it is practically inaccessible, than to select as standard an accessible state which is naturally variable and whose position must therefore be fixed arbitrarily. For these reasons, the present calculations on the heats of formation of the normal paraffin hydrocarbons in the gaseous state are made with reference to two standard states for carbon, β-graphite and diamond.

The heat of formation of liquid water from gaseous hydrogen and oxygen has been determined in this laboratory (1):

$$H_2\,(\text{gas}) + \tfrac{1}{2}O_2\,(\text{gas}) = H_2O\,(\text{liquid}),\quad \Delta H^0_{298\cdot1} = -68.313 \pm 0.010 \text{ k-cal}_{15} \text{ per mole.} \tag{5}$$

The best values for the heat of formation of carbon dioxide can be determined from the work of Roth and his coworkers (12), who measured the heats of combustion of β-graphite and of diamond at constant volume in a bomb calorimeter. The precision of their calorimetric measurements was about ± 0.03 percent, but this does not represent the uncertainty in the values deduced for the heat of formation of 1 mole of carbon dioxide, for the following reasons:

(a) The desired changes in heat content are those for the reactions

$$C(\beta\text{-graphite}) + O_2\,(\text{gas}) = CO_2\,(\text{gas}) \tag{6}$$

and

$$C(\text{diamond}) + O_2\,(\text{gas}) = CO_2\,(\text{gas}) \tag{7}$$

at a temperature of 25 C and a constant pressure of 1 atmosphere. The heat effect actually measured in the bomb is that for the process of burning a mixture of carbon with liquid paraffin in oxygen at an

initial pressure of about 30 or 35 atmospheres. From this heat effect is subtracted the heat of combustion of the liquid paraffin which is determined in separate but similar experiments. As Washburn (11) has shown, the heat of combustion of carbon as determined under the conditions of the bomb process will be quite significantly different from the value of $-\Delta U$ (the decrease in internal or intrinsic energy) for reactions 6 or 7. Applying Washburn's equations to the data of Roth and Wallasch (12), who, however, do not give as complete information as is desirable for this purpose, one finds that the values of $-\Delta U$ for reactions 6 and 7 at 1 atmosphere are less than the observed heats of combustion as measured in the bomb process by about 0.10 percent, which is nearly four times the calorimetric uncertainty.

(b) The amount of reaction in the experiments of Roth and his coworkers was determined from the mass of carbon placed in the bomb. Because of the possible presence of incombustible impurities in the sample of carbon the experiment carried out in this manner may result in a low heat effect per unit mass of carbon. The uncertainty in this regard can be eliminated by determining the amount of reaction from the mass of carbon dioxide formed.

(c) Because the atomic weight of carbon [6] is uncertain to about 0.03 percent, the value deduced for the heat of combustion per mole of carbon will be uncertain to the same extent whenever the amount of reaction is determined from the mass of carbon. Determination of the amount of reaction from the mass of carbon dioxide formed reduces the uncertainty in this regard to about ± 0.007 percent, if the uncertainty in the atomic weight of carbon is ± 0.03 percent.

From the data of Roth and his coworkers (12) the following values are obtained for the heats of combustion of carbon at a temperature of 18 C and at constant volume in their bomb calorimeter: β-graphite, 7.856 ± 0.002 and diamond, 7.873 ± 0.005, k-cal$_{15}$ per gram, weighed in air. The densities of these samples of carbon were 2.22 and 3.50 g per cm^3, respectively, and the corresponding factors for correcting the observed weights in air to true masses are 1.0004 and 1.0002. If the atomic weight of carbon is taken as 12.007 ± 0.003, and the Washburn correction of Q to 1 atmosphere as -0.10 ± 0.03 percent, then for reactions 6 and 7 one calculates, respectively, $\Delta H^0_{298.1} = -94.20 \pm 0.08$ and -94.42 ± 0.10, k-cal$_{15}$ per mole.[7] The effect of the presence of undetected incombustible impurities in the samples of carbon used by Roth and his coworkers would be to raise these values by the amount corresponding to the weight percent of incombustible impurity. The foregoing value for the heat of formation of 1 mole of carbon dioxide from β-graphite and oxygen is to be compared with the present accepted value, 94.24, which was obtained (14) from Roth's value by converting his weights in air to true masses and using 12.00 as the atomic weight of carbon.

The existing data on the heat of formation of carbon dioxide may therefore be said to be quite unsatisfactory, and an accurate determination of this fundamental thermal constant is urgently needed. Any new determination of the heat of formation of carbon dioxide

[6] The value for the atomic weight of carbon given in the 1934 report of the International Committee on Atomic Weights (13) is 12.00. A large body of evidence has been accumulated which indicates that this value is low by about 0.04 to 0.08 percent. Presumably the changing of the old value to a new one has been delayed until such time as the uncertainty in the new value becomes significantly less than the difference between the present value and what will be the new one.

[7] For reactions 6 and 7 at 1 atmosphere, ΔH differs from ΔU by 0.003 k-cal per mole.

carried out by combustion of carbon in a bomb calorimeter should provide (a) for the accurate specification of the conditions of the bomb process in order that the Washburn (11) correction may be made accurately, and (b) for the accurate determination of the amount of the reaction, preferably from the mass of carbon dioxide formed, in order to make insignificant the uncertainty in the value of the atomic weight of carbon and to eliminate the effect of the possible presence of incombustible impurities in the samples of carbon.

Because the uncertainty in the present value for the heat of formation of carbon dioxide is relatively so large, there is no advantage to be gained in changing the present accepted value, 94.24, to the value deduced above, 94.20 ± 0.08, and, accordingly, for reaction 6, the value

$$\Delta H^0_{298.1} = -94.24 \pm 0.10 \text{ k-cal}_{15} \text{ per mole} \quad (8)$$

is used in this paper.

The data of Roth and his coworkers yield for the transition

$$\text{C}(\beta\text{-graphite}) = \text{C(diamond)}, \Delta H^0_{298.1} = 0.22 \pm 0.07 \text{ k-cal}_{15} \text{ per mole.} \quad (9)$$

Hence to be consistent with equation 8 one must use for the reaction given by equation 7

$$\Delta H^0_{298.1} = -94.46 \pm 0.10 \text{ k-cal}_{15} \text{ per mole.} \quad (10)$$

Combination of equations 5, 6, and 8 with the values for the heats of combustion of the normal paraffin hydrocarbons yields for the reaction,

$$n\text{C}(\beta\text{-graphite}) + (n+1)\text{H}_2 \text{ (gas)} = \text{C}_n\text{H}_{2n+2} \text{ (gas)}, \quad (11)$$

$$\Delta H^0_{298.1} = Qc_{298.1} - n(162.55 \pm 0.10) - (68.313 \pm 0.010) \text{ k-cal}_{15} \text{ per mole.} \quad (12)$$

Here $\Delta H^0_{298.1}$ is the increase in heat content for the reaction of forming the normal gaseous paraffin hydrocarbon from β-graphite and gaseous hydrogen, $Qc_{298.1}$ is the heat evolved in the combustion of the hydrocarbon gas at a temperature of 25 C and a constant total pressure of 1 atmosphere, and n is the number of carbon atoms in the hydrocarbon molecule. For $n > 5$

$$\Delta H^0_{298.1} = -(7.913 \pm 0.010) - n(5.55 \pm 0.13) \text{ k-cal}_{15} \text{ per mole.} \quad (13)$$

With diamond as the standard state for carbon the analogous equations are:

$$n\text{C(diamond)} + (n+1)\text{H}_2 \text{ (gas)} = \text{C}_n\text{H}_{2n+2} \text{ (gas)}, \quad (14)$$

$$\Delta H^0_{298.1} = Qc_{298.1} - n(162.77 \pm 0.10) - (68.313 \pm 0.010) \text{ k-cal}_{15} \text{ per mole;} \quad (15)$$

and for $n > 5$,

$$\Delta H^0_{298.1} = -(7.913 \pm 0.010) - n(5.77 \pm 0.13) \text{ k-cal}_{15} \text{ per mole.} \quad (16)$$

The values computed from these equations are given in table 2.

TABLE 2.—*The heats of formation, from the elements, of the gaseous normal paraffin hydrocarbons, at 25 centigrade and 0 Kelvin*

C_nH_{2n+2} (gas)	$nC(\beta\text{-graphite})+(n+1)H_2$ (gas) $=C_nH_{2n+2}$ (gas)		$nC(\text{diamond})+(n+1)H_2$ (gas) $=C_nH_{2n+2}$ (gas)	
	$\Delta H^0_{298.1}$ *K-cal*$_{15}$ *per mole*	ΔH^0_0 *K-cal*$_{15}$ *per mole*	$\Delta H^0_{298.1}$ *K-cal*$_{15}$ *per mole*	ΔH^0_0 *K-cal*$_{15}$ *per mole*
Methane	−18.07±0.12	−16.18±0.13	−18.29±0.12	−16.53±0.13
Ethane	−20.60± .23	−16.99± .24	−21.04± .23	−17.69± .24
Propane	−25.39± .32	−20.27± .34	−26.05± .32	−21.32± .34
Normal butane	−30.57± .43	−23.93± .46	−31.45± .43	−25.33± .46
Normal pentane	−35.79± .54	−27.64± .60	−36.89± .54	−29.39± .60
Normal hexane	−41.21± .72	−31.52± .81	−42.53± .72	−33.62± .81
Normal heptane	−46.76± .84	−35.55± .97	−48.30± .84	−38.00± .97
Normal octane	−52.31± .96	−39.58±1.12	−54.07± .96	−42.38±1.12
Normal nonane	−57.86±1.08	−43.61±1.26	−59.84±1.08	−46.76±1.26
Normal decane	−63.41±1.20	−47.64±1.40	−65.61±1.20	−51.14±1.40
Normal undecane	−68.96±1.32	−51.67±1.54	−71.38±1.32	−55.52±1.54
Normal dodecane	−74.51±1.44	−55.70±1.68	−77.15±1.44	−59.90±1.68
Normal pentadecane	−91.2 ±1.8	−67.8 ±2.1	−94.5 ±1.8	−73.0 ±2.1
Normal C_nH_{2n+2} (for $n>5$)	$-7.91-n(5.55\pm0.12)$	$-7.34-n(4.03\pm0.14)$	$-7.91-n(5.77\pm0.12)$	$-7.34-n(4.38\pm0.14)$

NOTE.—The estimated uncertainties given here represent the absolute error in each of the values. The accuracy of the difference between any two values in a given column is equal to $\pm0.12\,\Delta n$ at 25 centigrade and to $\pm0.14\Delta n$ at 0 Kelvin.

2. AT 0 KELVIN

With the recent development of methods for calculating accurate values of thermodynamic quantities from spectroscopic data, it has been especially convenient to compute, for a given substance, values of the free energy function $(F^0-E^0_0)/T$, where F^0 is the free energy of the substance at the temperature T and E^0_0 (or U^0_0) is the internal energy of the substance at the absolute zero (15). Combination of the values of this function at any given temperature for all the substances participating in a given reaction yields the value of $(\Delta F^0-\Delta E^0_0)/T$. In order to obtain a value for the free energy of the reaction it is necessary to have values for ΔE^0_0, which in the large majority of cases must be obtained from calorimetric data on heats of reaction. For this reason there is included here a tabulation of the values of ΔE^0_0 (or ΔU^0_0), which is equal to ΔH^0_0, and is the increase in internal or intrinsic energy at the absolute zero accompanying the formation of the gaseous normal hydrocarbon from its elements, carbon and hydrogen, all in their standard states.

For this calculation there are needed the values of $H^0_{298.1}-H^0_0$ for carbon, hydrogen, and the gaseous hydrocarbons, which are, in k-cal$_{15}$ per mole: $C(\beta\text{-graphite})$, 0.251 ± 0.006; $C(\text{diamond})$, 0.125 ± 0.013; H_2 (gas), 2.023 ± 0.001; CH_4 (gas), 2.395 ± 0.001; C_nH_{2n+2} (gas) (for $n>1$), $1.445+n$ $(0.754\pm n\%)$.

The values for carbon are taken from Rodebush's compilation in the International Critical Tables (16); that for hydrogen from Giauque (15); that for methane from Kassel (17); and those for the normal hydrocarbons above methane from unpublished calculations by Kassel (18).

For the reaction given by equation 11

$$\Delta H^0_0 = Qc_{298.1} - n(160.28\pm0.10) - (66.290\pm0.010) - (H^0_{298.1}-H^0_0)\ [C_nH_{2n+2}\ (\text{gas})]\ \text{k-cal}_{15}\ \text{per mole}, \quad (17)$$

and for $n>5$

$$\Delta H^0_0 = -(7.335\pm0.032) - n(4.03\pm0.14)\ \text{k-cal}_{15}\ \text{per mole}. \quad (18)$$

For the reaction given by equation 14

$$\Delta H^0_0 = Qc_{298.1} - n(160.63 \pm 0.10) - (66.290 \pm 0.010) - (H^0_{298.1} - H^0_0)\ [C_nH_{2n+2}\ (\text{gas})]\ \text{k-cal}_{15}\ \text{per mole}, \quad (19)$$

and for $n > 5$

$$\Delta H^0_0 = -(7.335 \pm 0.032) - n(4.38 \pm 0.14)\ \text{k-cal}_{15}\ \text{per mole} \quad (20)$$

The values calculated from these equations are given in table 2.

IV. CHANGE IN HEAT CONTENT FOR THE REACTION: nCO (gas) + $(n+1)$ H_2 (gas) = $n/2$ O_2 (gas) + C_nH_{2n+2} (gas)

From data obtained in this laboratory (1), it is possible to evaluate accurately the change in heat content at a temperature of 25 C. for the reaction

$$n\text{CO (gas)} + (n+1)\ H_2\ (\text{gas}) = n/2\ O_2\ (\text{gas}) + C_nH_{2n+2}\ (\text{gas}): \quad (21)$$

$$\Delta H^0_{298.1} = Qc_{298.1} - n\ (135.936 \pm 0.032) - (68.313 \pm 0.010)\ \text{k-cal}_{15}\ \text{per mole}; \quad (22)$$

for $n > 5$

$$\Delta H^0_{298.1} = n(21.06 \pm 0.09) - (7.913 \pm 0.010)\ \text{k-cal}_{15}\ \text{per mole}. \quad (23)$$

In order to evaluate the change in heat content for reaction 21 at the absolute zero, values of $H^0_{298.1} - H^0_0$ are needed for the gaseous hydrocarbons, hydrogen, carbon monoxide, and oxygen. The data for hydrogen and the hydrocarbons are given in the preceding section; the values for carbon monoxide and oxygen, respectively 2.066 ± 0.001 and 2.068 ± 0.001 k-cal$_{15}$ per mole, are taken from the calculations of Johnston and his coworkers (19).

For the reaction given by equation 21

$$\Delta H^0_0 = Qc_{298.1} - n\ (132.880 \pm 0.032) - (66.290 \pm 0.010) - (H^0_{298.1} - H^0_0)\ [C_nH_{2n+2}\ (\text{gas})]\ \text{k-cal}_{15}\ \text{per mole}; \quad (24)$$

and for $n > 5$

$$\Delta H^0_0 = n(23.37 \pm 0.11) - (7.335 \pm 0.032)\ \text{k-cal}_{15}\ \text{per mole}. \quad (25)$$

The values computed from equations 24 and 25 are, respectively, in k-cal$_{15}$ per mole: Methane, 11.22 ± 0.08; ethane, 37.81 ± 0.14; propane, 61.93 ± 0.19; normal butane, 85.67 ± 0.27; normal pentane, 109.36 ± 0.37; normal hexane, 132.88 ± 0.57; normal heptane, 156.25 ± 0.72; normal octane, 179.62 ± 0.86; normal nonane, 202.99 ± 0.99; normal decane, 226.36 ± 1.10; normal undecane, 249.73 ± 1.21; normal dodecane, 273.10 ± 1.32.

V. ENERGIES OF THE ATOMIC LINKAGES

The energy required to dissociate a molecule into its constituent atoms is a quantity possessing considerable importance in determining the thermodynamic stability of the molecule. The amount of this energy of dissociation is a function of the number and kind of atoms and the nature of their respective linkages.

For molecules in which the atomic linkages can be characterized as covalent, Pauling (8) has shown that the energy of dissociation of the

gaseous molecule into its constituent atoms can, as a first approximation, be expressed as the sum of constant terms which are assigned to represent the energies of the various atomic linkages in the molecule. That is to say,

$$(Da)^0_0 = \Sigma m_i l_i, \tag{26}$$

where $(Da)^0_0$ is the energy absorbed at the absolute zero in the reaction of dissociating the gaseous molecule, in its normal state, into its constitutent atoms, each in the normal state, and l_i is the value assigned to represent the energy of each atomic linkage of the kind i, the number of which is m_i. If the atoms at the instant of dissociation are not in their normal or ground states, then, as pointed out by Mecke (22), there must be added to equation 26 a term for correcting the atoms to their normal states. This gives

$$(Da)^0_0 + \Sigma m_a E_a = \Sigma m_i l_i, \tag{27}$$

where E_a is the energy, referred to the normal state, of the state of the atom at the instant of dissociation, and m_a is the number of atoms.

At the instant of dissociation of the molecule C_nH_{2n+2} into its constituent atoms, the hydrogen atoms are in their normal ^2S state, while the carbon atoms are in the tetravalent ^5S state, which has an energy [8] of about 35 kilocalories above that of the bivalent normal ^3P state. If E_c is the difference in energy between the ^5S and the ^3P states of the carbon atom, and a and b are the energies to be assigned respectively to the C–H and C–C bonds, then for the molecule C_nH_{2n+2}

$$(Da)^0_0 + nE_c = (2n+2)\ a + (n-1)\ b. \tag{28}$$

$(Da)^0_0$ is the energy absorbed in the reaction,

$$C_nH_{2n+2}\ (\text{gas}) = nC\ (\text{gas}) + (2n+2)\ H\ (\text{gas}), \tag{29}$$

when all the substances are in the normal state.

Since the term nE_c is linear in n, the postulate of the constancy of the bond energies in the paraffin hydrocarbons may be said to be substantiated if the value of $(Da)^0_0$ is a linear function of n.

If D_{CO}, D_{O_2}, and D_{H_2} are the values for the energy absorbed in the reaction of dissociating, at 0 Kelvin, the gaseous molecules, CO, O_2, and H_2, in their normal states, into their respective gaseous atoms each in its normal state, then for the reaction given by equation 29.

$$(Da)^0_0 = -Qc_{298.1} + n\ (132.880 \pm 0.032) + (66.290 \pm 0.010) + (H^0_{298.1} - H^0_0)\,[C_nH_{2n+2}\ (\text{gas})] - \frac{n}{2} D_{O_2} + nD_{CO} + (n+1)D_{H_2}$$

$$\text{k-cal}_{15} \text{ per mole}; \tag{30}$$

and for $n > 5$

$$(Da)^0_0 = -n\ (23.37 \pm 0.11) + (7.335 \pm 0.032) - \frac{n}{2} D_{O_2} + nD_{CO} + (n+1)\ D_{H_2}\ \text{k-cal}_{15} \text{ per mole}. \tag{31}$$

[8] The difference in energy between the ^5S state and the ^3P state of the carbon atom is known only approximately. Pauling (8) uses the value 23, while Heitler and Herzberg (23) estimate 37 kilocalories per mole.

The value for the energy of dissociation of CO is at the time of this writing the subject of much controversial opinion and of some apparently contradictory facts. The values for the energies of dissociation of H_2 and O_2 into normal atoms are (20, 21):

$$H_2 \text{ (gas)} = 2 \text{ H (gas)}, \ \Delta H_0^\circ = 102.9 \pm 0.7 \text{ k-cal}_{15} \text{ per mole} \quad (32)$$

$$O_2 \text{ (gas)} = 2 \text{ O (gas)}, \ \Delta H_0^\circ = 117.4 \pm 0.7 \text{ k-cal}_{15} \text{ per mole} \quad (33)$$

Until an accurate value for the energy of dissociation of CO is available no accurate calculation can be made of the energy of dissociation of hydrocarbon molecules into gaseous normal carbon and hydrogen atoms. And, further, until an accurate value for the difference in energy between the ^5S and ^3P states of the carbon atom is available no accurate calculation can be made of the absolute values of the energies of the C–H and C–C linkages.

However, it is possible to deduce from equations 28, 30, and 31 certain relations concerning the energies of the atomic linkages in the normal paraffin hydrocarbons, because the values of the energies of dissociation of CO, O_2, and H_2, and the value of E_c, enter linearly into the evaluation of $\Sigma m_i l_i$, and their absolute values are not required in testing the constancy of the bond energies from one molecule to another.

In the first place it is readily evident that the relation expressed by equation 28 is not true for values of n less than 6, but is true for values of n greater than 5. If $(Da)_0^\circ$ is the actual energy absorbed by the dissociation of normal C_nH_{2n+2} (gas) into gaseous normal carbon and hydrogen atoms, and $(2n+2)\ a+(n-1)\ b-nE_c$ is the value calculated by assuming constant values for a and b, the energies of the C–H and C–C bonds, respectively, then one obtains the following values for Δ, the deviation of $(Da)_0^\circ$ from linearity with n:

Normal C_nH_{2n+2} (gas)	$\Delta=(Da)_0^\circ-[(2n+2)a+(n-1)b-nE_c]$	
	K-cal per mole	*K-cal per carbon atom*
Methane	4.81±0.08	4.81±0.08
Ethane	1.59±0.14	0.80±0.07
Propane	0.83±0.19	0.28±0.06
Normal butane	0.46±0.27	0.12±0.07
Normal pentane	0.13±0.37	0.03±0.07
Normal $C_nH_{2n+2}(n>5)$	0.00±0.11n	0.00±0.11

These values are plotted in figure 2.

From the above facts one can say that, within the accuracy of the present experimental data, the energy of dissociation of normal C_nH_{2n+2} (gas) into gaseous carbon and hydrogen atoms is not a linear function of n below, but is a linear function of n above, $n=6$.

If the energies of all the C—H and all the C—C linkages are assumed to be respectively equivalent throughout a given molecule then one must conclude that, below $n=6$, the strength of one or the other or both linkages increases with decreasing n.

But a better explanation may be in the distinction between various kinds of C—H and of C—C bonds in the normal paraffin hydrocarbon.

For example, one can distinguish three kinds of C—H linkages, a_0, a_1, and a_2, in the normal paraffin molecule

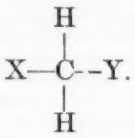

a_0 is the C—H bond when X = Y = H,
a_1 is the C—H bond when [9] X = H and Y = R, and
a_2 is the C—H bond when X = Y = R.

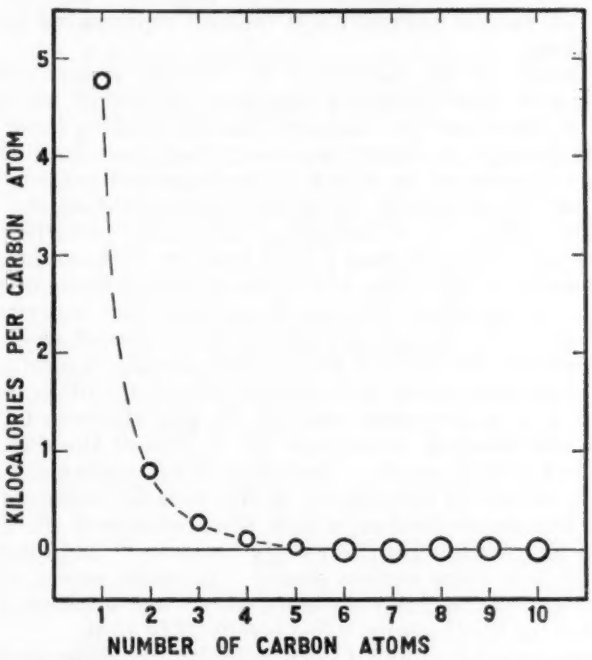

FIGURE 2.—*Deviations from linearity with the number of carbon atoms of the energy of dissociation of the normal paraffin hydrocarbon molecule into atoms.*

The scale of ordinates gives Δ, the deviation from linearity in the relation between n and the energy of dissociation, at the absolute zero, of normal C_nH_{2n+2} into gaseous carbon and hydrogen atoms, in k-cal per carbon atom. The scale of abscissae gives the number of carbon atoms in the molecule.

Similarly one can distinguish three kinds of C–C bonds, b_0, b_1, and b_2, in the normal paraffin molecule

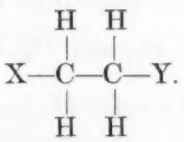

b_0 is the C–C bond when X = Y = H,
b_1 is the C–C bond when X = H and Y = R, and
b_2 is the C–C bond when X = Y = R.

[9] R represents a normal alkyl radical.

On this basis the energies of the atomic linkages in the various molecules can be represented as follows:

Methane	$4a_0$.
Ethane	$6a_1+b_0$.
Propane	$6a_1+2a_2+2b_1$.
Normal butane	$6a_1+4a_2+2b_1+b_2$.
Normal pentane	$6a_1+6a_2+2b_1+2b_2$.
Normal C_nH_{2n+2}, for $n>2$	$6a_1+2(n-2)a_2+2b_1+(n-3)b_2$.

And the difference between successive members becomes constant and equal to $2a_2+b_2$ when n is greater than 3. This approximates what the experimental data indicate. In a more exact sense, however, one would need to take cognizance of the kind of atoms which are attached to the carbon atoms once removed from the bond, that is, to distinguish between various normal alkyl radicals represented by R in the above notation.

Differentiation of the various C–H linkages is not new. From measurements of the infrared absorption spectra of liquid paraffin hydrocarbons, Brackett (24) deduced that the binding force of a "primary" C–H linkage (a_1 above) is greater than that of a "secondary" C–H linkage (a_2 above) by about 3.2 percent and greater than that of a "tertiary" C–H linkage (a_3 in the above notation) by about 5.6 percent. By means of calculations involving potential energies, Eyring (26) has computed that a C–H bond in methane becomes progressively weaker as the other hydrogen atoms are replaced by methyl groups. In our notation, Eyring found that the successive differences between a_0, a_1, a_2, and a_3 were about 3.1 kilocalories.

If the bonds at the ends of the normal paraffin molecule are considered, as indicated above, to be different from the other bonds, then the addition of 1 carbon atom and 2 hydrogen atoms to C_nH_{2n+2} corresponds to the creation, at or near the middle of the molecule, of 1 C–C bond and 2 C–H bonds. And since the experimental data indicate that the energy of this process is constant for values of n greater than 5, one can conclude that, within the accuracy of the data, there is no interaction, with regard to energy between C, H groups that are separated by 2 or more carbon atoms. In other words, the methyl group at the end of the chain of carbon atoms has a sphere of influence that includes the C, H group twice removed from it.

For the reaction of adding 1 carbon and 2 hydrogen atoms to any normal paraffin hydrocarbon above pentane to form the next higher normal paraffin hydrocarbon one finds from equation 31 that, when $n>5$, for the reaction,

$$C\ (gas)+2H\ (gas)+C_nH_{2n+2}\ (gas)=C_{n+1}H_{2n+4}\ (gas), \qquad (34)$$

the energy evolved at 0 degree K is

$$-\Delta H_0^0=(-23.37\pm0.11)-1/2\ D_{O_2}+D_{CO}+D_{H_2}\ \text{k-cal}_{15}\ \text{per mole}. \qquad (35)$$

Substituting the values for D_{O_2} and D_{H_2} from equations 32 and 33 gives

$$-\Delta H_0^0=(20.8\pm0.9)+D_{CO}\ \text{k-cal}_{15}\ \text{per mole}. \qquad (36)$$

When corrected for the energy of excitation of the carbon atom from the normal ^3P state to the ^5S state, the values given by equations 35 and 36 may be said to represent the energy associated with 1 C–C and 2 C–H linkages at or near the middle of any gaseous normal paraffin

hydrocarbon molecule above pentane. Then using the notation already defined.

$$2a_2 + b_2 = (20.8 \pm 0.9) + D_{co} + E_c \text{ k-cal}_{15} \text{ per mole.} \quad (37)$$

And any assignment of values for D_{co}, for the energy of excitation of the carbon atom to the ^5S state, and for a_2 and b_2, the energies of the C–C and C–H bonds formed in reaction given by equation 34, must satisfy the relation expressed by equation 37. In general, any assignment of values must satisfy the relation

$$\Sigma m_i l_i = (110.2 \pm 0.7) + n(20.8 \pm 0.9) + n(D_{co} + E_c) + \Delta \text{ k-cal}_{15} \text{ per mole.} \quad (38)$$

VI. REFERENCES

1. Rossini, F. D., B.S. Jour. Research, vol. 6, pp. 1 and 37, 1931; vol. 7, p. 329, 1931.
2. Hermann, L., Chem. Zentr., vol. 14, p. —, 1869. See p. 239 in reference 3.
3. Thomsen, J., "Thermochemische Untersuchungen", vol. 4, Barth, Leipzig, 1886.
4. Favre, P. A., and Silbermann, J. T., Ann. chim. phys., vol. 34, p. 357, 1852.
5. Berthelot, M., and Matignon, C. A., Ann. chim. phys., vol. 30, p. 547, 1893.
6. Roth, W. A., and Machlett, unpublished. The value appears in Landolt-Börnstein-Roth-Scheel Tabellen, 5th ed., vol. 2, p. 1588. Springer, Berlin, 1923.
7. Sidgwick, N. V. "The Covalent Link in Chemistry", Cornell University Press, Ithaca, New York, 1933.
8. Pauling, L., J. Am. Chem. Soc., vol. 54, p. 3570, 1932.
9. Kharasch, M. S., B.S. Jour. Research, vol. 2, p. 359, 1929.
10. Jessup, R. S. The data will appear in the Journal of Research of the National Bureau of Standards.
11. Washburn, E. W., B.S. Jour. Research, vol. 10, p. 525, 1933.
12. Roth, W. A., and Wallasch, H., Ber., vol. 46, p. 896, 1913; Z. Elektrochem., vol. 21, p. 1, 1915; Roth, W. A., and Naeser, W., Z. Elektrochem., vol. 31, p. 461, 1925.
13. Baxter, G. P., Curie, M., Hönigschmid, O., Le Beau, P., and Meyer, R. J., Jour. Am. Chem. Soc., vol. 56, p. 753, 1934.
14. Parks, G. S., and Huffman, H. M., "The Free Energies of Some Organic Compounds", Chemical Catalog Company, New York, 1932.
15. Giauque, W. F., J. Am. Chem. Soc., vol. 52, pp. 4808 and 4816, 1930.
16. International Critical Tables, vol. 5, p. 87. McGraw-Hill Book Company, New York, 1929.
17. Kassel, L. S., J. Am. Chem. Soc., vol. 55, p. 1351, 1933.
18. Kassel, L. S., private communication.
19. Johnston, H. L., and Walker, M. K., J. Am. Chem. Soc., vol. 55, p. 172, 1933; Johnston, H. L., and Davis, C. O., ibid., vol. 56, p. 271, 1934.
20. Richardson, O. W., and Davidson, P. M., Proc. Roy. Soc. (London), vol. 123A, p. 466, 1929.
21. Herzberg, G., Z. physik. Chem., vol. 10B, p. 189, 1930.
22. Mecke, R., Z. Elektrochem., vol. 36, p. 589, 1930.
23. Heitler, W., and Herzberg, G., Z. Physik., vol. 53, p. 52, 1929.
24. Brackett, F. S., Proc. Natl. Acad. Sci., vol. 14, p. 857, 1928.
25. Rossini, F. D., B.S. Jour. Research, vol. 12, p. 735, 1934.
26. Eyring, H., J. Am. Chem. Soc., vol. 54, p. 3191, 1934.

WASHINGTON, April 17, 1934.

U.S. DEPARTMENT OF COMMERCE NATIONAL BUREAU OF STANDARDS

RESEARCH PAPER RP693

Part of Journal of Research of the National Bureau of Standards, vol. 13, July 1934

THERMAL EXPANSION OF ARTIFICIAL GRAPHITE AND CARBON

By Peter Hidnert

ABSTRACT

The linear thermal expansion of longitudinal sections cut from 14, 3, 1¼, and 1 inch artificial graphite electrodes and of transverse sections cut from 14 and 3 inch electrodes, were investigated at various temperatures between 20 and 1,000 C. A comparison of the average expansion curves of the longitudinal and transverse sections is shown in figure 3, and the ranges of the coefficients of expansion for various temperature ranges are given in table 4. The coefficients of expansion of the transverse sections are larger than the coefficients of expansion of the longitudinal sections. For example, for the range from 20 to 1,000 C, the linear expansion of the transverse sections cut from 3-inch graphite is about 110 percent greater than the expansion of the longitudinal sections cut from 3-inch graphite electrodes. Other conclusions are listed in section V of this paper.

The linear thermal expansion of two types of carbon which are used for expansion elements in temperature regulators for domestic gas ovens, were investigated at various temperatures between 20 and 350 C. The coefficients of expansion of carbon made with lampblack are about three times as large as the coefficients of carbon made with petroleum coke.

CONTENTS

	Page
I. Introduction	37
II. Materials investigated	39
III. Apparatus	40
IV. Results	40
1. Artificial graphite	40
2. Carbon	49
V. Conclusions	50
1. Artificial graphite	50
2. Carbon	51

I. INTRODUCTION

During the past few years there has been a demand for data on the thermal expansion of artificial graphite at elevated temperatures for the following purposes:

1. To calculate the volumes of graphite crucibles used in determining the specific volumes of molten metals and alloys.

2. For a reference standard in the determination of the thermal expansion of refractory materials. During the past few years, expansion data to 600 C by Hidnert and Sweeney [1] have been extrapolated and used for these purposes.

[1] Hidnert and Sweeney B.S. Technologic Paper 335.

In 1927 Hidnert and Sweeney published in B.S. Technologic Paper 335 a table of data on the thermal expansion of graphite (natural [2] and artificial) and of other forms of carbon by Fizeau, Muraoka, Dewar, Day and Sosman, and Sieglerschmidt. Available data by other observers are given in table 1.

TABLE 1.—*Expansion data by previous observers on graphite and other forms of carbon* [a]

Observer	Date	Material	Temperature or temperature range	Coefficient of linear expansion per degree centigrade	Remarks
			°C	$\times 10^{-6}$	
Fizeau [b]	1865	Diamond	20	0.85	
			30	1.00	
			40	1.14	
			50	1.29	
Fizeau [c]	1866	do	40	1.18	Same diamond as used by Fizeau in 1865.
Monckman [d]	1888	Carbon	13–614	6.66	Experiment 1.
			14–645	6.6	Experiment 2.
			15–300	5.6	Experiment 3.
			300–645	8	
			15–143	4.5	Experiment 4.
			143–263	7.7	
			263–282	14.0	
			282–602	9	
Joly [e]	1898	Diamond	0–400	[f] 2.8	At a temperature of 850 C the diamond began to burn rapidly. Its surface soon became stepped in a manner characteristic of certain crystals. Once commenced, the combustion continued till the oven was cooled down to about 712 C.
			400–580	[f] 4.4	
			580–686	[f] 6.8	
			686–750	[f] 11.4	
Stewart [g]	1908	Carbon in the form of films made of commercial lampblack and a lacquer called "zapon L".			The result obtained shows the coefficient of carbon in the form of lampblack to be about 0.0002, which is from 10 to 30 times that of the pure metals.
National Carbon Co. [h]	1911	Electrodes:			
		Coal	220–1,820	11.0	
		Coke	180–1,920	7.2	
		Graphite	440–1,720	10	
		Arc carbon of lampblack.	25–1,000	6.0	
Röntgen [i]	1912	Diamond	−188 to −79	0.18	
			−79 to 0	.58	
			0 to +23	.97	
			+23 to 55	1.17	
			55 to 78	1.45	

[a] For data by other observers (Fizeau, Muraoka, Dewar, Day and Sosman, and Sieglerschmidt), see Hidnert and Sweeney, B.S. Technologic Paper 335, table 1.
[b] Fizeau, Comptes Rendus, vol. 60, p. 1161, 1865.
[c] Fizeau, Comptes Rendus, vol. 62, pp. 1101, 1133, 1866.
[d] Monckman, Proc. Royal Society of London, vol. 44, p. 220, 1888.
[e] Joly, Scientific Trans. Royal Dublin Society, vol. 6 (series 2), p. 283, 1898.
[f] Computed by Hidnert in 1934 from expansion data given by Joly.
[g] Stewart, Physical Review, vol. 26, p. 333, 1908.
[h] See Chaney, International Critical Tables, vol. 2, p. 303, 1927.
[i] Röntgen, Sitzungsberichte der mathematisch-physikalischen Klasse der K. B. Akademie der Wissenschaften zu München, vol. 42, p. 381, 1912.

[2] For graphite from Batongol, Fizeau (Comptes Rendus, vol. 68, p. 1125, 1869) reported 7.86×10^{-6} for the coefficient of linear expansion at 40 C, and for graphite from Cumberland, Dewar (Proc. Roy. Soc. London, vol. 70, p. 237, 1902) obtained 73.3×10^{-6} for the average coefficient of cubical expansion between −186 and +17 C.

In the present investigation, thermal expansion measurements were made on longitudinal and transverse sections of artificial graphite at various temperatures between 20 and 1,000 C. A neutral atmosphere was used in order to prevent oxidation of the graphite samples at elevated temperatures. Two other types of carbon which are of importance from the standpoint of expansion, were included in this investigation.

The author expresses his appreciation to H. D. Batchelor of the National Carbon Co., Cleveland, Ohio, and M. S. May of the Speer Carbon Co., Saint Marys, Pa., for their cooperation in this investigation. Acknowledgment is also due to the following members of the staff of the National Bureau of Standards: H. W. Bearce, W. Souder, and C. G. Peters, for valuable suggestions; to H. S. Krider for assistance during the measurements; and to S. Alpher for aid in the preparation of the figures.

II. MATERIALS INVESTIGATED

The following materials were investigated: (1) artificial graphite, longitudinal and transverse sections; and (2) carbon. A description of these materials is given in tables 2, 3, and 5. Information about the preparation of 14-inch artificial graphite electrode, chemical composition and density, have been published[3] in 1927.

In 1927, Chaney[4] stated "Manufactured carbon articles in the form of rods, plates, blocks, tubes, etc., in a wide variety of shapes are made by molding or extruding specially prepared mixtures of pulverized carbon 'flours' with binding materials of tar or pitch, and subsequently carbonizing the binder at high temperatures. The resulting products always consist of a porous mass of carbon particles knit together by the residual carbon resulting from the decomposition of the binding materials. Because of the variations inherent in all manufacturing processes the physical properties of commercial carbons are subject to characteristic variations, the allowable range of which is determined by the service and cost requirements of the consumer. A high degree of precision in the individual determinations is therefore valueless, the typical range of variation being alone significant. Individual values where given must be regarded merely as representative."

Mantell[5] in 1928 described the manufacture and uses of graphite and other forms of carbon. He stated that "The particular field of graphite is that of electrolytic work, where its low resistance and long life are very important. Graphite electrodes are extensively used in the electrolytic production of chlorine and caustic, the chlorination of gold ores, the recovery of copper, nickel, and zinc, the production of hypochlorites and many other similar applications." In a later publication, Mantell[6] stated that "carbon has shown its suitability in equipment employed in five different fields: (1) Acid manufacture, (2) papermaking, (3) the electrochemical industries, (4) combustion equipment, and (5) machinery operating under corrosive conditions."

[3] See footnote 1.
[4] Chaney, Commercial Carbons for Electrical Uses, International Critical Tables, vol. 2, p. 303, 1927.
Mantell, Industrial Carbon, Industrial Chemical Monographs, D. Van Nostrand & Co., Inc., 1928.
[6] Mantell, Industrial and Engineering Chemistry, vol. 24, p. 1255, 1932.

III. APPARATUS

Figure 1 of B.S. Scientific Paper 524 shows part of the apparatus used in the investigation. The samples of artificial graphite were investigated at various temperatures between 20 and 1,000 C in the white furnace shown at the left end of the figure. The same furnace was used for the samples of carbon which were investigated at various temperatures between 20 and 350 C. Micrometer microscopes were sighted on fine wires suspended from the ends of the sample. The samples of graphite were mounted in the furnace as illustrated in figure 5 of the paper mentioned, but the samples of carbon were mounted as shown in figure 4 of the same paper. Each sample was 300 mm long.

Since graphite oxidizes in air at about 640 C, it was necessary to use a neutral atmosphere in the furnace at elevated temperatures. The neutral atmosphere consisted of a mixture of nitrogen and hydrogen gas (about 5 percent hydrogen). A combination reducing valve and flow meter was attached to the cylinder containing the mixture of nitrogen and hydrogen gas. The large gage indicated the pressure (pounds per square inch) of the gas in the cylinder and the small gage indicated the flow (liters per minute) of the gas from the cylinder. The gas was passed through copper gauze contained in a long copper tube supported horizontally in a tube furnace heated electrically to about 700 C, in order to remove oxygen. The hot gas was cooled by passing it through a copper coil surrounded by flowing water. The cooled gas was then passed through bottles or drying tubes containing calcium chloride and magnesium perchlorate trihydrate, in order to remove moisture. The dry gas was passed through another flow meter and finally into the furnace at both ends. The reducing valve was adjusted so that the gas flowed at a rate of about 5 liters per minute. The gas was allowed to flow into the furnace containing the graphite sample, during the time the sample was heated from 400 to 1,000 C and cooled to 600 C or less.

The samples of carbon were not heated in a neutral atmosphere, for measurements were only made to 350 C.

IV. RESULTS

The results obtained on artificial graphite and carbon are given in subsections 1 and 2, respectively.

1. ARTIFICIAL GRAPHITE

The linear thermal expansion of longitudinal sections cut from 14-, 3-, 1¼-, and 1-inch graphite electrodes and of transverse sections cut from 14- and 3-inch graphite electrodes, were investigated at various temperatures between 20 and 1,000 C. The results obtained on the longitudinal sections are given in figure 1 and in table 2, and the results on the transverse sections in figure 2 and table 3.

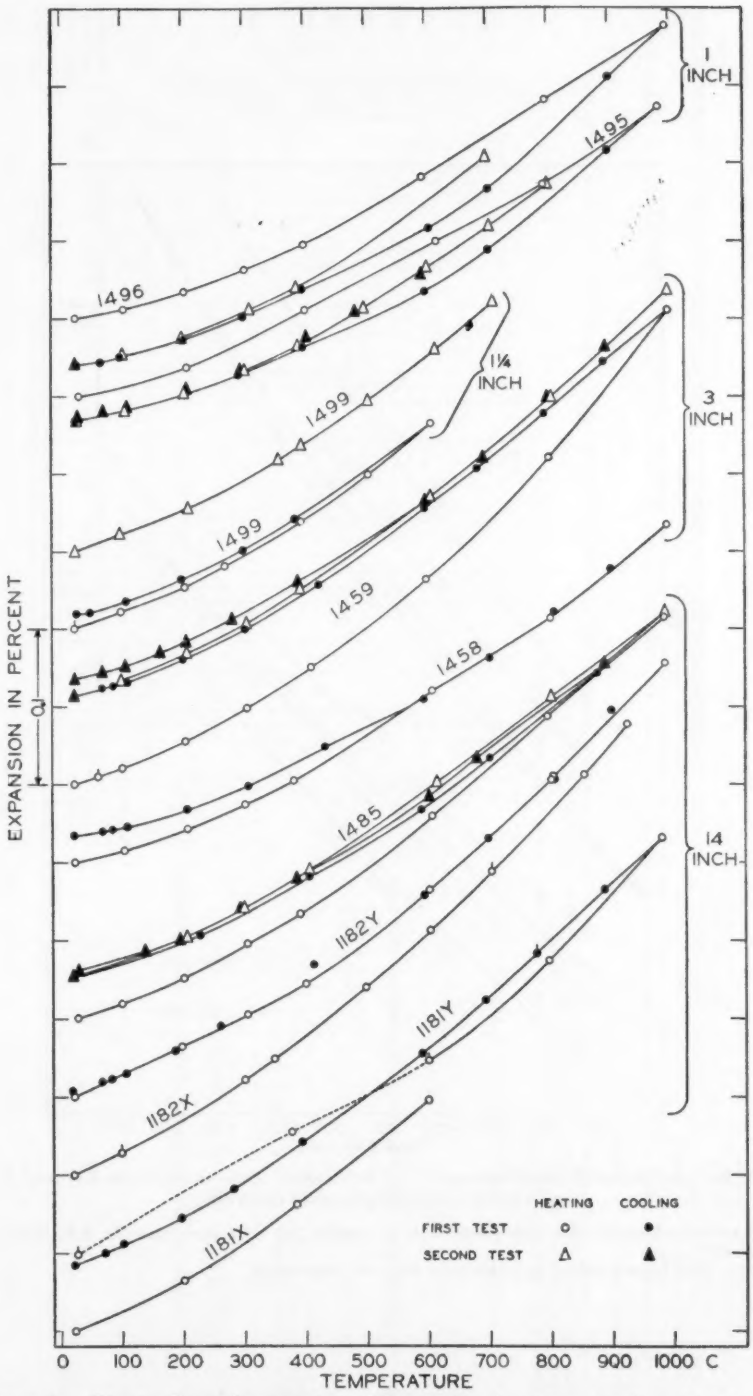

FIGURE 1.—*Linear thermal expansion of longitudinal sections cut from 14-, 8-, 1¼-, and 1-inch diameter artificial graphite electrodes.*

NOTE.—A tagged symbol indicates more than one observation.

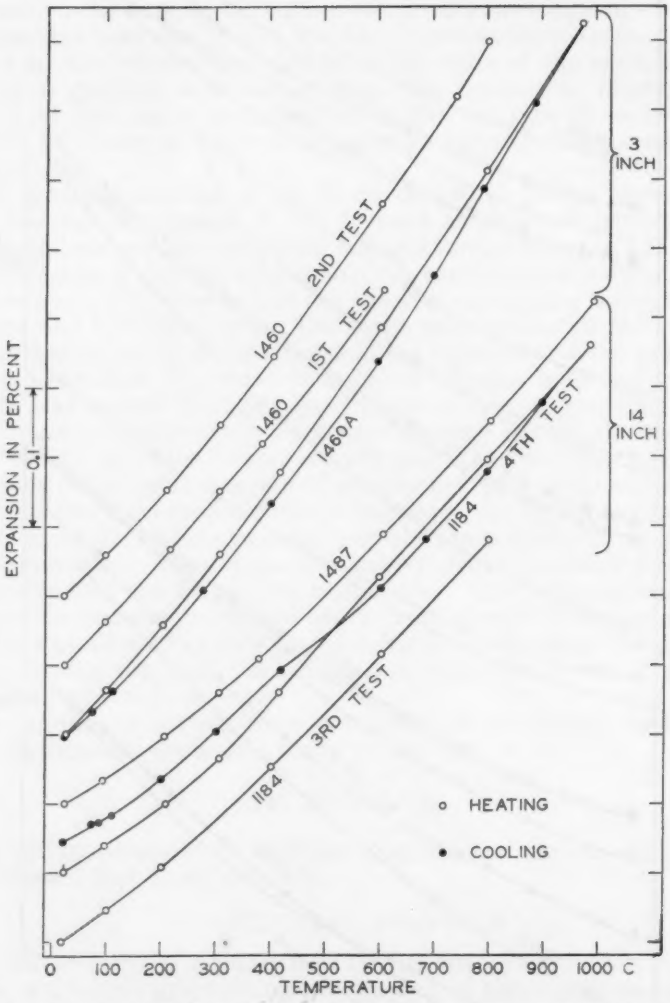

FIGURE 2.—*Linear thermal expansion of transverse sections cut from 14- and 3-inch diameter artificial graphite electrodes.*

(Expansion curves for first and second tests of sample 1184 have been given in B.S. Technologic Paper 335.)

NOTE.—The tagged symbol indicates more than one observation.

TABLE 2.—*Average coefficients of expansion of longitudinal sections of artificial graphite*

Sample	Description	Test number	Average coefficients of expansion per degree centigrade										Change[1] in length after heating and cooling
			20 to 100 C	20 to 200 C	20 to 300 C	20 to 400 C	20 to 500 C	20 to 600 C	20 to 700 C	20 to 800 C	20 to 900 C	20 to 1,000 C	
			×10⁻⁶	×10⁻⁶	×10⁻⁶	×10⁻⁶	×10⁻⁶	×10⁻⁶	×10⁻⁶	×10⁻⁶	×10⁻⁶	×10⁻⁶	*Percent*
1180 A[2]	Longitudinal section cut from 14-inch graphite electrode	1	1.9	2.0	2.2	2.4							(3)
		2	1.9	2.0	2.2	2.4	2.6						
		3			2.1		2.5	2.7					
1181[2]	do	1	2.2	2.1	2.3	2.4							
1181 X[4]	do	1		1.8		2.3		2.6		(5)			
1181 Y[4]	do	1				2.2		2.2		2.4		2.8	−.006
		[6] 1	1.6	1.7	1.9	2.1		2.4	2.5	2.7	2.8	2.8	
1182[2]	do	1	1.8	1.9	2.1	2.3							
1182 X[7]	do	1	1.8		2.2		2.5	2.7	2.8		3.1	(5)	
1182 Y[7]	do	1		1.8	1.8	1.9		2.3		2.6		2.9	+.004
1485[8]	do	1	1.3	1.4	1.7	1.8		2.2		2.5		2.7	+.027
		[6] 1		1.2		1.6		1.9	2.0		2.3	2.4	
		2		1.4	1.6	1.8		2.1		2.3		2.4	+.003
		[6] 2		1.2	1.5	1.6		1.9	2.1		2.3	2.4	
1458[10]	Longitudinal section cut from 3-inch graphite electrode	1	0.9	1.1	1.3	1.5		1.9		2.0		2.2	+.017
		[6] 1	.6	0.9	1.1	1.3		1.5	1.7	1.8	2.0	2.1	
1459[11]	do	1	1.3	1.5	1.7	1.9		2.3		2.7		3.1	+.057
		[6] 1	1.0	1.3	1.5	1.7		2.1	2.2	2.4	2.5	2.6	
		2	1.4	1.5	1.7	1.9		2.2		2.5		2.7	+.012
		[6] 2	0.9	1.3	1.5	1.7		2.0	2.1	2.3	2.5	2.6	
1499[12]	Longitudinal section cut from 1¼-inch graphite electrode	1	1.4	1.5	1.7	1.9	2.0	2.2					+.009
		[6] 1	0.9	1.3	1.5	1.7		2.1					
		2	1.5	1.5	1.6	1.9	2.0	2.2	2.3				

[1] The plus (+) sign indicates an increase in length and the minus (−) sign a decrease in length.
[2] Data by Hidnert and Sweeney, B.S. Technologic Paper 335.
[3] Less than 0.012 percent (Hidnert and Sweeney, B.S. Technologic Paper 335, p. 226).
[4] Cut from sample 1181 after first test (cross section of original sample, semicircle, diameter 63 mm; cross section of sample 1181 X, 22 mm diameter, and of sample 1181 Y, 14 × 10 mm).
[5] Observation wire (Pt – Ir) broke at about 800 C.
[6] Cooling.
[7] Cut from sample 1182 after first test (cross section of original sample, semicircle, diameter 63 mm; cross section of sample 1182 X, 21 mm, and of sample 1182 Y, 14×10 mm).
[8] Observation wires (Pt – Os) broke below 1,000 C.
[9] Graphite electrode manufactured recently, submitted by Acheson Graphite Corporation, Niagara Falls, N.Y. in 1932.
[10] Graphite electrode purchased in 1930 from Acheson Graphite Corporation. Density 1.528 g/cm³, determined by E. L. Peffer of the National Bureau of Standards, by same method as described in footnote 4 of table 2, B.S. Technologic Paper 335.
[11] Graphite electrode purchased from Acheson Graphite Corporation. (Different date from that mentioned in footnote [10].)
[12] Graphite (grade 580) submitted by Speer Carbon Co., Saint Marys, Pa., in 1932. Made by hot extrusion process. Composed of artificial graphite throughout, formed partly by the graphitization of the pitch coke acting as the bonding material. Baked to approximately 2,500 C. Used as anodes in large mercury arc rectifiers developed for the conversion of alternating to direct current for railway service and in other applications where an unusually strong artificial graphite product is required. The maximum operating temperature in rectifiers is understood to be in the neighborhood of 760 C.

TABLE 2.—*Average coefficients of expansion of longitudinal sections of artificial graphite*—Continued

Sample	Description	Test number	Average coefficients of expansion per degree centigrade										Change[1] in length after heating and cooling
			20 to 100 C	20 to 200 C	20 to 300 C	20 to 400 C	20 to 500 C	20 to 600 C	20 to 700 C	20 to 800 C	20 to 900 C	20 to 1,000 C	
			×10⁻⁶	×10⁻⁶	×10⁻⁶	×10⁻⁶	×10⁻⁶	×10⁻⁶	×10⁻⁶	×10⁻⁶	×10⁻⁶	×10⁻⁶	*Percent*
1495[13]	Longitudinal section cut from 1-inch graphite electrode	1		1.0		1.5		1.7		1.8		2.0	−.016
		[6] 1			1.1	1.3		1.4	1.6		2.0	2.1	
		2	0.8	1.0	1.2	1.3	1.5	1.7	1.8	2.0			+.003
		[6] 2	.7	1.0	1.1	1.4	1.5	1.6		1.9			
1496[14]	do	1	.7	0.9	1.1	1.3		1.6		1.8		1.9	−.030
		[6] 1	.7	.9	1.1	1.3		1.5	1.7		2.1	2.3	
		2	.9	1.0	1.2	1.4			2.0				

[1] The plus (+) sign indicates an increase in length and the minus (−) sign a decrease in length.
[6] Cooling.
[13] Graphite electrode purchased from Acheson Graphite Corporation, in 1932.
[14] Graphite electrode purchased from Acheson Graphite Corporation, before 1932.

TABLE 3.—*Average coefficients of expansion of transverse sections of artificial graphite*

Sample	Description	Test number	Average coefficients of expansion per degree centigrade										Change[1] in length after heating and cooling
			20 to 100 C	20 to 200 C	20 to 300 C	20 to 400 C	20 to 500 C	20 to 600 C	20 to 700 C	20 to 800 C	20 to 900 C	20 to 1,000 C	
			×10⁻⁶	×10⁻⁶	×10⁻⁶	×10⁻⁶	×10⁻⁶	×10⁻⁶	×10⁻⁶	×10⁻⁶	×10⁻⁶	×10⁻⁶	*Percent*
1183[3]	Transverse section cut from 14-inch graphite electrode	1	3.1	3.2	3.4	3.6							[7]
		[3] 1	2.8	3.0	3.2	3.4							
		[3] 2	2.9	2.8	3.1	3.4	3.6	3.7					
1184	do	3	2.8	2.9		3.3		3.5		3.7	[4]		
		4	2.6	2.6	2.9	3.2		3.7		3.8		3.9	+.022
		[6] 4	2.2	2.5	2.9	3.1		3.1	3.3	3.4	3.6	3.7	
1487[8]	do	1	2.4	2.6	2.8	2.9		3.3		3.5		[7] 3.7	
1460	Rod composed of 7 transverse sections[8] cut from same 3-inch graphite electrode as sample 1459 (table 2)	1	4.2	4.3	4.4	4.4		4.6		[9]			
		2	3.9	4.0	4.3	4.5		4.8		5.1		[10]	
1460 A	Duplicate of sample 1460	1	4.3	4.4	4.6	4.8		5.1		5.3		5.4	−.001
		[6] 1	3.7		4.2	4.4		4.7	4.9	5.2	5.3	5.4	

[1] The plus (+) sign indicates an increase in length and the minus (−) sign a decrease in length.
[2] Data by Hidnert and Sweeney, B.S. Technologic Paper 335.
[3] Less than 0.012 percent (Hidnert and Sweeney, B.S. Technologic Paper 335, p. 226).
[4] Observation wire (Pt – Rh) broke below 900 C.
[5] Cooling.
[6] Cut from same electrode as sample 1485 (table 2).
[7] Observation wire (Pt – Rh) broke at 900 C. on cooling.
[8] One end of each section was threaded, and the other end drilled and tapped. These sections were screwed together. It is believed that the expansion data obtained on this sample are reliable, for expansion determinations on an iron-chromium alloy (1427 P) composed of 7 sections machined and screwed together in a similar manner, agreed satisfactorily with results obtained on a duplicate alloy (1427) in a single piece. The following coefficients of expansion were obtained:

Temperature range	Average coefficients of expansion per degree centigrade	
	Sample 1427 P	Sample 1427
°C		
20 to 200	10.7×10^{-6}	10.4×10^{-6}
20 to 300	11.1	10.7
20 to 400	11.3	11.1
20 to 600	11.9	11.6
20 to 700	12.1	11.8
20 to 800	12.6	12.2
20 to 900	13.1	12.8

[9] Observation wire (Pt – Rh) broke at 800 C.
[10] Observation wire (Pt – Rh) broke at 1,000 C.

Some of the tests could not be carried to 1,000 C, for one or both observation wires broke before this temperature was reached. Platinum-osmium (6 percent osmium), platinum-iridium (20 percent iridium), and platinum-rhodium (20 percent rhodium) wires, 0.002-inch diameter, were tried. None of these wires gave entire satisfaction. The platinum-rhodium (20 percent rhodium) wire was found to give the best results under the conditions of the test which required

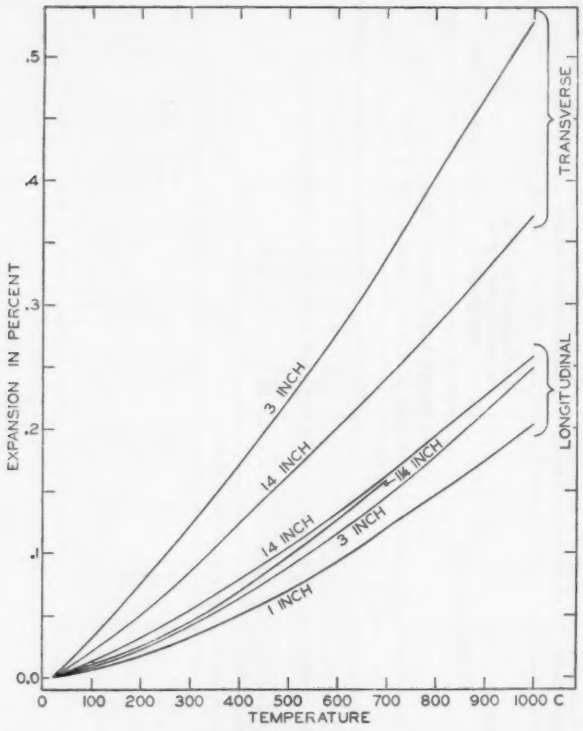

FIGURE 3.—*Comparison of average expansion curves of longitudinal and transverse sections of artificial graphite electrodes.*

that each observation wire should sustain a load of about 15 grams at temperatures up to 1,000 C in an atmosphere consisting of nitrogen and hydrogen.

From the coefficients of expansion in tables 2 and 3, average expansion curves shown in figure 3 were derived for the various longitudinal and transverse sections of graphite. A comparison of the range of coefficients of expansion of the longitudinal and transverse sections is given in table 4.

TABLE 4.—*Comparison of average coefficients of expansion of longitudinal and transverse sections of artificial graphite*

Material	Average coefficients of expansion per degree centigrade			
	20 to 100 C	20 to 200 C	20 to 300 C	20 to 400 C
	×10⁻⁶	×10⁻⁶	×10⁻⁶	×10⁻⁶
Longitudinal sections:				
Cut from 14-inch electrode	1.3 to 2.2(7)	1.2 to 2.1(11)	1.5 to 2.3(11)	1.6 to 2.4(12)
Cut from 3-inch electrode	0.6 to 1.4(6)	0.9 to 1.5(6)	1.1 to 1.7(6)	1.3 to 1.9(6)
Cut from 1¼-inch electrode	0.9 to 1.5(3)	1.3 to 1.5(3)	1.5 to 1.7(3)	1.7 to 1.9(3)
Cut from 1-inch electrode	0.7 to 0.9(5)	0.9 to 1.0(6)	1.1 to 1.2(6)	1.3 to 1.5(7)
Transverse sections:				
Cut from 14-inch electrode	2.2 to 3.1(7)	2.5 to 3.2(7)	2.8 to 3.4(6)	2.9 to 3.6(7)
Cut from 3-inch electrode	3.7 to 4.3(4)	4.0 to 4.4(3)	4.2 to 4.6(4)	4.4 to 4.8(4)

Material	Average coefficients of expansion per degree centigrade		
	20 to 500 C	20 to 600 C	20 to 700 C
	×10⁻⁶	×10⁻⁶	×10⁻⁶
Longitudinal sections:			
Cut from 14-inch electrode	2.5 to 2.6(3)	1.9 to 2.7(10)	2.0 to 2.8(4)
Cut from 3-inch electrode		1.5 to 2.3(6)	1.7 to 2.2(3)
Cut from 1¼-inch electrode	2.0(2)	2.1 to 2.2(3)	2.3(1)
Cut from 1-inch electrode	1.5(2)	1.4 to 1.7(6)	1.6 to 2.0(4)
Transverse sections:			
Cut from 14-inch electrode	3.6(1)	3.1 to 3.7(5)	3.3(1)
Cut from 3-inch electrode		4.6 to 5.1(4)	4.9(1)

Material	Average coefficients of expansion per degree centigrade		
	20 to 800 C	20 to 900 C	20 to 1,000 C
	×10⁻⁶	×10⁻⁶	×10⁻⁶
Longitudinal sections:			
Cut from 14-inch electrode	2.3 to 2.7(5)	2.3 to 3.1(4)	2.4 to 2.9(7)
Cut from 3-inch electrode	1.8 to 2.7(6)	2.0 to 2.5(3)	2.1 to 3.1(6)
Cut from 1¼-inch electrode			
Cut from 1-inch electrode	1.8 to 2.0(4)	2.0 to 2.1(2)	1.9 to 2.3(4)
Transverse sections:			
Cut from 14-inch electrode	3.4 to 3.8(4)	3.6(1)	3.7 to 3.9(3)
Cut from 3-inch electrode	5.1 to 5.3(3)	5.3(1)	5.4(2)

NOTE.—The number in the parenthesis following each range of coefficients of expansion, indicates the number of determinations.

The following general conclusions may be drawn from an examination of the data:

1. The coefficients of expansion of the longitudinal and transverse sections of graphite increase with temperature.

2. The coefficients of expansion of the transverse sections are larger than the coefficients of expansion of the longitudinal sections. Figure 3 indicates that for the range from 20 to 1,000 C, the linear expansion of the transverse sections cut from 3-inch graphite is about 110 percent greater than the expansion of the longitudinal sections cut from 3-inch graphite electrodes.

3. There appears to be a tendency for the coefficients of expansion of a longitudinal section to increase [7] with increase in the diameter

[7] The longitudinal section cut from 1¼-inch graphite electrode prepared by Speer Carbon Co., is an exception. The other longitudinal sections from 1-, 3-, and 14-inch electrodes, were prepared by Acheson Graphite Co. After an examination of these results, M. S. May of the Speer Carbon Co., recently stated that the 1¼-inch graphite does not fall in line with the Acheson product because it is made by a somewhat different process.

of the graphite electrode from which the longitudinal section has been cut.

4. The coefficients of expansion of the transverse sections cut from the 3-inch graphite electrodes are larger than the coefficients of expansion of the transverse sections cut from the 14-inch electrodes. For example, for the range from 20 to 1,000 C the average coefficient of expansion of the transverse sections from the 3-inch graphite is about 40 percent greater than the coefficient of expansion of the transverse sections from the 14-inch graphite electrodes.

5. The difference between the expansion of the transverse and longitudinal sections cut from the 3-inch graphite electrodes is considerably greater than the difference between the expansion of the transverse and longitudinal sections cut from the 14-inch electrodes. Figure 3 indicates that the former difference is about 145 percent greater than the latter difference for the linear expansion between 20 and 1,000 C.

6. The coefficients of expansion of the longitudinal sections cut from the 1-inch graphite electrodes are in good agreement with the data obtained by Day and Sosman [8] on ½-inch [9] graphite electrode.

7. The longitudinal and transverse sections of graphite indicate changes in length after heating to elevated temperatures and cooling to room temperature. A second heating and cooling cause smaller changes.

It has been indicated in a previous publication [10] that the differences in expansion and tensile strength between the transverse and longitudinal sections of a 14-inch graphite electrode may be due to the fact that the graphite electrode in the process of manufacture has been compressed differently in the two directions. Attention was also directed to statements of Taylor [11] on the effects of the extrusion process by which the "green" electrodes are formed. He stated that during extrusion the outer portions are retarded by friction with the walls of the die. There is therefore a good deal of internal motion parallel to the axis of the forming electrode. This internal motion causes a marked difference in the structure in the two directions. There is a tendency for the material to have a laminated structure in the transverse direction. The aggregate particles and cell walls are more firm and continuous in a lengthwise direction of the electrode than in a crosswise direction. Voids or pores tend to form with their longer axes lengthwise of the electrode. It seems quite probable that this has an effect on expansivity in the two directions. The longitudinal increment is practically a measure of the linear expansion of the material, and the transverse change is the linear expansion plus an increment of distortion due to increased spring in the arches formed by the cell walls of the voids and pores. Taylor also believed that the lower tensile strength in the transverse direction is due to the laminated structure mentioned.

As appreciable differences were found in the thermal expansion of sections cut from different size electrodes, an endeavor was made to obtain information about the ratio of the coke and plastic organic material, and the approximate grain size of the different electrodes. Referring to the graphite electrodes prepared by Acheson Graphite

[8] Day and Sosman, Jour. Ind. and Eng. Chem., vol. 4, p. 490, 1912, or J. Wash. Acad. Sci., vol. 2, p. 284, 1912 (see also Day, Sosman, and Hostetter, Amer. Jour. Sci., vol. 37, 4th series, p. 1, 1914).
[9] Hidnert and Sweeney, B.S.Technologic Paper 335, table 1, footnote 5.
[10] Hidnert and Sweeney, B.S.Technologic Paper 335, p. 228.
[11] See reference, footnote 10.

Co., H. D. Batchelor, director of research of the National Carbon Co., Inc., Cleveland, Ohio, stated the following:

"The ratio of coke and plastic organic material is approximately the same for all sizes of graphite electrodes. It varies somewhat according to size but not to exceed 10 percent. The grain sizes of different size electrodes do vary in accordance with their size. The coarsest particles in 3- and 4-inch electrodes will all pass through a 20-mesh screen and a greater proportion of them will pass through a 200-mesh screen. In a 14-inch electrode the coarse particles are between 0.03 and 0.06 inch in diameter, the next closest lie between 0.03 and 0.015 and finally, here again, the larger portion of the particles will pass through the 200-mesh screen.

"In addition to the difference in grain size above mentioned, possibly one should take into consideration the normal variation to be expected in commercial electrodes. As to just what this variation is in terms of thermal expansion, we have no information, * * *."

M. S. May of the Speer Carbon Co., recently stated: "It appears probable that the difference in expansion between the different sized Acheson rods is because they are made from flours of different finenesses rather than because of the difference of diameter itself." As insufficient data on grain sizes of the different size electrodes are available, it was not possible to definitely determine the relation between expansion and grain size.

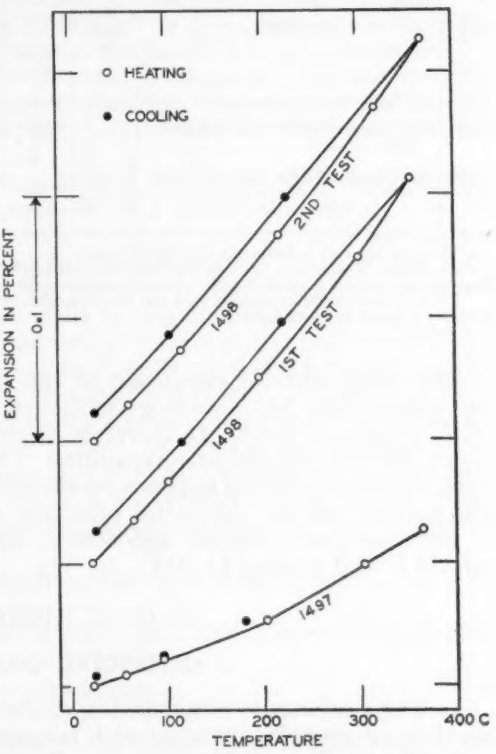

FIGURE 4.—*Linear thermal expansion of two types of carbon.*

1497 — Composed of petroleum coke, bonded with coal tar pitch coke. 1498 — Composed of lampblack bonded with coal tar pitch coke.

The linear thermal expansion of artificial graphite electrode depends on various factors indicated in this section. The direction (longitudinal or transverse) along which expansion measurements are made, appears to be the most important factor. Graphite should therefore be used with caution for the purposes indicated in the introduction of this paper.

2. CARBON

Two types of carbon [12] which are important from the standpoint of thermal expansion were included in this investigation. These types

[12] Submitted by Speer Carbon Co., Saint Marys, Pa., in 1932. Made by hot extrusion process.

of carbon are used for expansion elements [13] in temperature regulators for domestic gas ovens.

Measurements of linear thermal expansion were made [14] at various temperatures between 20 and 350 C. Figure 4 and table 5 show the results obtained.

TABLE 5.—*Average coefficients of expansion of carbon*

Sample	Description	Test number	Average coefficients of expansion per degree centigrade					Change in length after heating and cooling
			20 to 60 C	20 to 100 C	20 to 200 C	20 to 300 C	20 to 350 C	
			×10⁻⁶	×10⁻⁶	×10⁻⁶	×10⁻⁶	×10⁻⁶	*Percent*
1497	Carbon, grade 2079,[b] 5/16-inch diameter	1	1.4	1.5	1.4	1.7	1.8	+0.004
1498	Carbon, grade 2095,[c] 5/16-inch diameter	1	4.0	4.1	4.3	4.5	4.7	+.012
		[d] 1	-------	3.9	4.2	-------	4.3	
		2	4.1	4.0	4.3	4.5	4.7	+.011
		[d] 2	-------	3.8	4.2	-------	4.4	

[a] The plus (+) sign indicates an increase in length.
[b] Composed of petroleum coke, bonded with coal tar pitch coke; carries about 0.5 percent ash (mineral matter) and under 1 percent volatile. Baked to about 1,000 C.
[c] Composed of lampblack bonded with coal tar pitch coke; carries about 1 percent ash and under 1 percent volatile. Baked to about 1,000 C.
[d] Cooling.

The coefficients of expansion of the carbon made with lampblack are about three times as large as the coefficients of the carbon made with petroleum coke. It therefore appears that the latter carbon is more suitable for the low expanding element of temperature regulators, for the regulation depends on the difference of expansion between the carbon rod and the metal tube into which the rod is inserted.

Both samples of carbon indicated an increase in length after heating to 350 C and cooling to 20 C.

V. CONCLUSIONS

1. ARTIFICIAL GRAPHITE

1. The coefficients of expansion of the longitudinal and transverse sections of graphite increase with temperature.

2. The coefficients of expansion of the transverse sections are larger than the coefficients of expansion of the longitudinal sections. For the range from 20 to 1,000 C, the linear expansion of the transverse sections cut from 3-inch graphite is about 110 percent greater than the expansion of the longitudinal sections cut from 3-inch graphite electrodes.

3. There appears to be a tendency for the coefficients of expansion of a longitudinal section to increase with increase in the diameter of the graphite electrode from which the longitudinal section has been cut.

4. The coefficients of expansion of the transverse sections cut from the 3-inch graphite electrodes are larger than the coefficients of expansion of the transverse sections cut from the 14-inch electrodes. For example, for the range from 20 to 1,000 C, the average coefficient

[13] Maximum temperature in service 600 F (316 C).
[14] In the longitudinal direction.

of expansion of the transverse sections from the 3-inch graphite is about 40 percent greater than the coefficient of expansion of the transverse sections from the 14-inch graphite electrodes.

5. The difference between the expansion of the transverse and longitudinal sections from the 3-inch graphite electrodes is considerably greater than the difference between the expansion of the transverse and longitudinal sections from the 14-inch electrodes. Figure 3 indicates that the former difference is about 145 percent greater than the latter difference for the linear expansion between 20 and 1,000 C.

6. The coefficients of expansion of the longitudinal sections cut from the 1-inch graphite electrodes are in good agreement with the data obtained by Day and Sosman on ½-inch graphite electrode.

7. The longitudinal and transverse sections of graphite indicate changes in length after heating to elevated temperatures and cooling to room temperature. A second heating and cooling cause smaller changes.

8. The differences in expansion and tensile strength between the transverse and longitudinal sections of a graphite electrode may be due to the fact that the electrode in the process of manufacture has been compressed differently in the two directions. Taylor has indicated that during extrusion the outer portions of the electrode are retarded by friction with the walls of the die. There is a tendency for the material to have a laminated structure in the transverse direction. The aggregate particles and cell walls are more firm and continuous in lengthwise direction. Voids or pores tend to form with their longer axes lengthwise of the electrode. It seems probable that this has an effect on the expansion in the two directions. Taylor stated that the longitudinal increment is practically a measure of the linear expansion of the material, and the transverse change is the linear expansion plus an increment of distortion due to the laminated structure.

9. The grain sizes of the different size electrodes appear to have an effect on expansion.

10. Graphite should be selected with care for the purposes indicated in section I of this paper.

2. CARBON

The coefficients of expansion of carbon made with lampblack are about three times as large as the coefficients of carbon made with petroleum coke. It therefore appears that the latter carbon is more suitable for the low expanding element of temperature regulators.

WASHINGTON, April 21, 1934.

U.S. DEPARTMENT OF COMMERCE NATIONAL BUREAU OF STANDARDS

RESEARCH PAPER RP694

Part of Journal of Research of the National Bureau of Standards, vol. 13, July 1934

EQUILIBRIUM VOLATILITY OF MOTOR FUELS FROM THE STANDPOINT OF THEIR USE IN INTERNAL COMBUSTION ENGINES

By Oscar C. Bridgeman

ABSTRACT

One of the larger problems in connection with the relation between fuel characteristics and engine performance is concerned with fuel volatility. For many years, the National Bureau of Standards conducted an investigation of fuel volatility, in cooperation with the automotive and petroleum industries, and the present paper covers the experimental data obtained and the conclusions reached in this investigation. An apparatus and method are described for the measurement of the equilibrium volatility of motor fuels, and experimental data are presented on 38 gasolines and blends covering a wide range of volatility. A correlation is shown to exist betwen equilibrium volatility data and distillation data obtained by the standard A.S.T.M. method. By use of the equations deduced, it is possible to obtain from distillation data all of the equilibrium volatility data of interest in connection with engine performance.

CONTENTS

	Page
I. The practical problem of motor fuel volatility	54
1. The automotive industry problem	54
2. The petroleum industry problem	55
3. The cooperative fuel research and the practical volatility problem	55
4. Scope of the present paper	56
II. Analysis of the volatility problem	56
1. Choice of variables	56
2. Ranges over which variables require investigation	57
3. Subdivision of the volatility investigation	58
III. Definitions of technical terms used	59
IV. A.S.T.M. evaporation data on fuels used in volatility work	60
V. Equilibrium air-evaporation apparatus and method of use	63
1. Description of apparatus	64
2. Calibration of apparatus	65
(a) Calibration of gasoline displacement system	65
(b) Calibration of flowmeter	68
(c) Calibration of vaporization coil	68
3. General experimental procedure	72
VI. Method of treatment of experimental data	73
1. Partial volatility and dew-point data	73
2. Bubble-point data	77
VII. Correlation of volatility data with A.S.T.M. distillation data	81
1. Preliminary method of correlation	81
2. Final method of correlation	84
(a) General method	84
(b) Application to partial volatility data	85
(c) Application to dew-point data	88
(d) Application to bubble-point data	91

Page

VIII. Accuracy of volatility data and of correlation with A.S.T.M. distillation data 94
1. Consideration of partial volatility 94
2. Consideration of dew points 96
3. Consideration of bubble points 97
IX. Detailed method for evaluation of volatility data from A.S.T.M. distillation data 98
1. Computation from volatility equations 98
(a) Partial volatility data 98
(b) Dew-point data 99
(c) Bubble-point data 100
(d) Volatility data at other percentages evaporated and for other mixtures 100
2. Graphical evaluation of volatility data 101
(a) Chart for evaluation of parameter C 101
(b) Chart for evaluation of 16:1 temperatures 102
(c) Duplex scale for temperature differences between resultant mixture lines 104
3. Special chart for dew-point data 104
4. Complete example of evaluation of volatility data 105
X. Volatility data at a total pressure lower than standard atmospheric pressure 106
XI. Conclusions 108

I. THE PRACTICAL PROBLEM OF MOTOR FUEL VOLATILITY

The advent of the automobile and the phenomenal growth of the automotive industry changed the status of gasoline from a byproduct of little commercial value to the major product of the petroleum industry. The new market for gasoline, thus created, stimulated the rapid expansion of the petroleum industry, resulting in extensive development of the national oil resources and improvements in refinery technology. Thus the last two decades have seen the rise concurrently of two of the major industries of the country, each dependent upon the other, but until recently neither industry has been in possession of requisite information for satisfying the requirements of the other. The immediate problem confronting the industries, therefore, was to secure adequate knowledge of the best engine design for operation with existing fuels and of the most satisfactory fuel for use with existing engines. The ideal solution, hoped for, was the acquisition of sufficient information to permit that mutual adaptation of engine design and fuel characteristics which would result in maximum economies for both industries.

1. THE AUTOMOTIVE INDUSTRY PROBLEM

One of the major problems of the automotive industry has always been to design engines which would give the desired performance with current fuels. The engine should start readily even in cold weather and should keep on running without too many interruptions. The induction system should take care of adequate distribution of the charge to the various cylinders and should permit the automobile to accelerate rapidly. Heating of the intake manifold should be sufficient to vaporize most of the fuel in order to minimize dilution of the crankcase oil. The fuel feed system should be constructed so that the fuel is fed in the desired amounts to the intake manifold without serious interruption of flow due to vapor lock.

In order to design equipment which will satisfy these requirements, the automotive engineer must know how the fuel behaves in the engine and what characteristics of the fuel determine this behavior. He is also interested in specifying the type of fuel for which his engine is designed and on which it will operate satisfactorily, and in having information on the ability of the oil refiner to supply an adequate amount of such fuel at a reasonable price.

2. THE PETROLEUM INDUSTRY PROBLEM

The petroleum technologist also should know how the fuel behaves in the engine in order that he may intelligently produce the most satisfactory fuel for use in engines of current design. He should know, still further, the characteristics of fuels which determine their performance in the engine and he should have adequate routine tests for the evaluation of these characteristics. Then with knowledge of what gasoline for use in existing types of engines ought to be and with sufficient information to enable him to determine when he has such a fuel, the oil refiner is in a position to develop his refinery technique to the point where he can produce a consistently satisfactory fuel from the minimum amount of crude oil.

3. THE COOPERATIVE FUEL RESEARCH AND THE PRACTICAL VOLATILITY PROBLEM

In 1922 the automotive and petroleum industries combined in financing cooperative fuel research at the National Bureau of Standards on important problems of common interest under the supervision of a steering committee composed of representatives from the three cooperating groups. This fuel research has had for its one guiding principle the mutual adaptation of the fuel to the engine and the engine to the fuel. Insofar as has been feasible, work on the various projects undertaken has been conducted simultaneously from the standpoint of the fuel characteristics and the behavior in the engine.

One of the larger problems investigated was the relation between fuel volatility and engine performance. When a fuel is used in the engine, there are two portions of the fuel system in which volatility is of interest in connection with performance. These may be characterized as the fuel feed system, including all parts up to the carburetor jet, and the induction system, in which the fuel is in contact with air. In the former, volatility is connected with vapor-locking tendency; whereas, in the latter, volatility is linked with starting, acceleration, and crankcase dilution. In both of these cases, the optimum volatility is dependent to a greater or less extent upon the individual characteristics of each engine and equipment and upon the conditions of use.

Accordingly, a practical investigation of fuel volatility from the automotive standpoint should involve (1) an evaluation of those fuel characteristics which affect the various phases of engine performance under conditions of operation, and (2) the development of test methods for the determination of these volatility characteristics.

4. SCOPE OF THE PRESENT PAPER

Those properties of fuels which determine their tendency to cause vapor lock in the fuel feed system will not be considered in the present paper, and reference will be made only to those characteristics which affect vaporization in the presence of air. Because the extent of vaporization in the induction system is specific for each type of equipment, the first step in the study of fuel volatility should yield results of general applicability and independent of the particular conditions existing in any one induction system. Data so obtained for an ideal manifold represent limiting values approximated to varying degrees by different systems, and furnish the fundamental information necessary for an intelligent investigation of volatility under actual operating conditions.

The volatility work has been confined to this first step in the study of vaporization in the presence of air. Until a study of the application of these data to actual manifolds is undertaken, the somewhat plausible assumption is necessary that the order of the volatilities of a series of fuels under equilibrium conditions is unchanged when these fuels are used in any given engine induction system.

II. ANALYSIS OF THE VOLATILITY PROBLEM

1. CHOICE OF VARIABLES

Volatility is a measure of the tendency of a substance to evaporate or to change from liquid to vapor under given conditions. It may be expressed in terms of the pressure exerted by the vapor under each set of specified conditions. One of the conditions which must be specified is the temperature, for the vapor pressures of all substances increase with temperature. Another condition which must be specified in the case of composite liquids, like gasolines, is the composition of the liquid at the time when the vapor pressure is measured.

With a one-component substance, such as water, the vapor pressure at a given temperature remains constant regardless of how much water evaporates. When more than one component is present, this is no longer true, since the more volatile constituents evaporate more readily, leaving the residual liquid less and less volatile as evaporation progresses. With a substance like gasoline, containing possibly several hundred hydrocarbons, the change in vapor pressure as evaporation progresses is very marked, since the less volatile components have a lower vapor pressure and since the proportion of these less volatile components in the residual liquid becomes greater as more of the liquid evaporates. This means that not only must the temperature be specified in the case of gasolines, but the composition of the liquid must also be specified.

Specification of the chemical composition of a gasoline is in general almost impossible at present, due to the indeterminate number of hydrocarbons present in unknown amounts. While it may be feasible to separate a simple natural gasoline into various groups by fractional distillation and thereby arrive at its approximate composition, even this method is not practicable for the average refinery product. With any specific gasoline, it is not necessary to know the chemical composition for, at any given temperature, the vapor pressure is defined at each point when the percentage evaporated is specified. If per-

centage evaporated is thus used to indicate composition, it is necessary to have some means of identifying each gasoline. Such identification is furnished by the distillation curve.

When a gasoline is delivered by the carburetor to the induction system, it is mixed with air in the requisite proportions. The mixture supplied is expressed in terms of the weight of air per unit weight of gasoline, which is commonly called the air-fuel ratio. The resultant mixture formed when part or all of the liquid evaporates is also expressed in terms of the weight of air per unit weight of gasoline vapor. Hence although the pressure of the vapor is the fundamental variable involved at any temperature and percentage evaporated, a more convenient variable, related to pressure, is the resultant mixture ratio of air and gasoline vapor formed at this temperature and percentage evaporated. In this case, it is necessary to specify the total pressure of the mixture and this has been fixed at one atmosphere, which is equal to 760 mm of mercury under standard conditions or 14.7 lb/in.^{2}

By the use of these variables, volatility is specified in terms of the practical units used by the industry. Volatility is therefore defined for the present purpose in terms of the temperature at which a given air-vapor mixture is formed under equilibrium conditions at a pressure of one atmosphere, when a given percentage is evaporated. According to this definition, one gasoline is more volatile than another for any given percentage evaporated if it forms the given air-vapor mixture at a lower temperature.

2. RANGES OVER WHICH VARIABLES REQUIRE INVESTIGATION

In order that an engine may start and run without interruption, it is necessary that an explosive mixture of air and fuel vapor be supplied to the cylinders at all times during the period of operation. The practical range of explosive air-vapor mixtures is from 4:1 to 20:1 by weight. Accordingly, at each percentage evaporated, this limits the range of resultant mixtures which require investigation.

When an engine is being started in cold weather, a very rich mixture must be supplied by the carburetor since the percentage of the fuel which evaporates under these conditions is small and enough must be evaporated to produce an explosive mixture. As the engine warms up, a larger percentage evaporates and accordingly a leaner mixture can be supplied by the carburetor. Finally, when the engine is being run under steady operating conditions, the resultant air-vapor mixture is not much leaner than the supplied mixture because most of the fuel evaporates.

Hence, since different percentages of the fuel evaporate under different operating conditions, the mixture supplied by the carburetor must be adjusted so that the resultant mixture is always in the explosive range from 4:1 to 20:1. The limits of the percentage of fuel evaporated under operating conditions range from very small percentages to complete evaporation, so that the study of fuel volatility should include measurements at values of the percentage evaporated covering the range from 0 to 100 percent.

3. SUBDIVISION OF THE VOLATILITY INVESTIGATION

A diagrammatic example for one gasoline of the volatility field of interest in connection with automotive engines is shown in figure 1. The hatched area, labeled "Automotive Volatility Field", covers a range for this gasoline of air-vapor mixtures bounded by the 4:1 to 20:1 air-vapor lines and of percentages evaporated from 0 to 100 percent. For gasolines with different evaporation curves, similar volatility fields will be obtained but displaced to an extent dependent

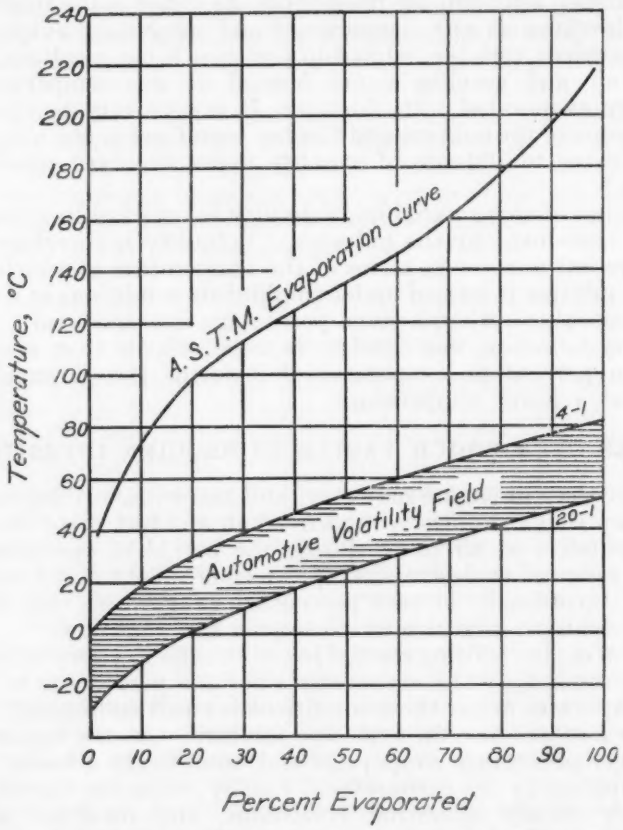

FIGURE 1.—*Illustration of the volatility field of interest in connection with engine performance as compared with the A.S.T.M. evaporation curve.*

upon the differences in distillation characteristics. Each point in the field represents the resultant air-vapor mixture formed under equilibrium conditions at that temperature and at the given percentage evaporated for a total pressure of one atmosphere. Each air-vapor line is a volatility curve and is called the resultant equilibrium air-evaporation curve. It represents an equilibrium distillation or evaporation in the presence of air under such conditions that all of the vapor formed is confined in the presence of the residual liquid under a total pressure of one atmosphere. The upper curve in the figure is the A.S.T.M. evaporation curve of the fuel (see definition,

sec. III). It represents a nonequilibrium distillation or evaporation at atmospheric pressure under such conditions that the vapor formed is removed in a specified manner from contact with the residual liquid under a total pressure of one atmosphere. The A.S.T.M. evaporation curve is used to identify the gasoline.

The vertical line of 100 percent evaporated represents the temperatures corresponding to complete equilibrium vaporization of the various supplied air-fuel mixtures. This line also represents the temperatures at which liquid would just separate out under equilibrium conditions on cooling the superheated resultant air-vapor mixtures. Hence temperatures along this line are called dew points, and the chemical composition of the gasoline vapor is the same at every temperature, being identical with the composition of the unvaporized liquid gasoline. The composition of the liquid which separates out will, however, vary with temperature.

The vertical line of 0 percent evaporated represents the temperatures at which a bubble would form under equilibrium conditions in the liquid gasoline saturated with air under a total pressure of one atmosphere. Hence temperatures along this line are called bubble points. At different temperatures, the ratio of air to fuel vapor in the bubble will be different and the chemical composition of the fuel vapor will vary. The composition of the liquid gasoline will, however, be the same at all temperatures.

At every intermediate percentage between 0 and 100 percent, where both liquid and vapor are present simultaneously in more than infinitesimal amounts, the chemical composition of each is different at every temperature and neither liquid nor vapor has the same composition as the original gasoline. Data at intermediate percentages are called partial volatility data.

III. DEFINITIONS OF TECHNICAL TERMS USED

A summary of definitions of a number of the technical terms used in this paper is given below:

Volatility is the tendency of a substance to evaporate or to change from liquid to vapor under given conditions. For the present purpose, it is expressed quantitatively in terms of the temperature at which a given resultant air-vapor mixture will be formed under equilibrium conditions at a pressure of one atmosphere, when a given percentage is evaporated.

Supplied air-fuel mixture (supplied mixture or air-fuel mixture) is the ratio by weight of the amount of air to that of liquid fuel supplied. As used in this paper, the total pressure is one atmosphere, unless otherwise stated.

Resultant air-vapor mixture (resultant mixture or air-vapor mixture) is the ratio by weight of the amount of air to that of fuel vapor formed from the supplied mixture. The total pressure of air and fuel vapor is taken to be one atmosphere, unless otherwise stated.

Equilibrium vaporization is the vaporization under such conditions that all of the vapor formed is confined in the presence of the residual liquid for a period of time sufficiently long so that any increase in the time would not increase the amount which evaporates under otherwise unchanged conditions.

Equilibrium air-evaporation is the vaporization under equilibrium conditions in the presence of air. The total pressure is one atmosphere, unless otherwise stated.

Equilibrium air-evaporation curves are the curves obtained by plotting temperature against percentage evaporated for a constant resultant air-vapor mixture.

A.S.T.M. evaporation curves are curves obtained by plotting the temperatures recorded in the standard A.S.T.M. distillation test against the percentage evaporated, which is obtained by adding the distillation loss to the percentage distilled at each point.

Percentage evaporated is the amount of liquid which evaporates under given conditions, expressed in percent. When used in this paper in connection with the volatility data, it is expressed in weight percent. When used in connection with A.S.T.M. evaporation data, it is expressed in volume percent.

Dew point is the temperature corresponding to initial liquid formation under equilibrium conditions on cooling a given superheated resultant air-vapor mixture. It is also the temperature corresponding to complete equilibrium vaporization of a given supplied air-fuel mixture. It is the point at which a given equilibrium air-evaporation curve intersects the line of 100 percent evaporated. Unless otherwise stated, it refers to a total pressure of one atmosphere.

Bubble point is the temperature at which a bubble, composed of a given air-vapor mixture, is in equilibrium with the unvaporized liquid gasoline, saturated with air under a total pressure of one atmosphere. It is the point at which a given equilibrium air-evaporation curve intersects the line of 0 percent evaporated. Unless otherwise stated, it refers to a total pressure of one atmosphere.

Partial volatility data are data applying to percentages evaporated intermediate between 0 and 100 percent.

IV. A.S.T.M. EVAPORATION DATA ON FUELS USED IN VOLATILITY WORK

A.S.T.M. evaporation data were obtained on all of the fuels used in the volatility work. These data were primarily intended for identification but after volatility results on a number of fuels had been obtained, a relation was found to exist between the A.S.T.M. evaporation and the volatility data. Accordingly, extreme care was taken in making the A.S.T.M. distillations.

For all the gasolines, the American Society for Testing Materials Standard Method D86–27 was employed [1] and all detailed directions were carefully followed. In two respects, temperature was controlled more closely than required by the standard A.S.T.M. method. By using a mixture of finely shaved ice and water, the temperature of the condenser was maintained as closely as possible at 0 C, rather than at temperatures within the permissible range of 0 to 4.5 C. Further, in the initial measurement of the sample, the actual temperature of the gasoline, within the permissible range of 12.8 to 18.3 C, was noted and throughout the entire distillation the temperature of the liquid

[1] A.S.T.M. Standards, 1927, p. 378, published by the American Society for Testing Materials, Philadelphia, Pa. This method was revised to a minor extent in 1930, under the designation D86–30, but this revision does not affect the conclusions reached in the present paper.

bath surrounding the receiver was kept at this value within 1° C. In this manner, better reproducibility was obtained and greater precision in the determination of distillation loss was possible.

The magnitude of the possible error in distillation loss by taking advantage of the extreme temperature range, permitted by the A.S.T.M. method, can be shown by an example. Suppose a gasoline of specific gravity 0.720 at 60 F/60 F has 2.0 percent distillation loss when measured and collected at 15.6 C. If the sample is measured at 18.3 C, and is collected at 12.8 C, the apparent loss will be 2.6 percent. If, however, it is measured at 12.8 C and collected at 18.3 C, the apparent loss will be 1.4 percent. In either of these cases, there will be an error of 0.6 percent, and there may be a difference of 1.2 percent in duplicate determinations. While the errors may compensate in some cases, the example indicates the possible deviations by the A.S.T.M. method. A control of the temperature so that the sample is measured and collected at temperatures differing by not more than 1° C, reduces the error from this source to 0.1 percent. A more satisfactory procedure would be to measure and collect the sample at 0 C.

Thermometer readings were taken when the first drop fell from the end of the condenser; at every 5 percent recovered throughout the distillation; and when the thermometer reading reached its maximum value. With every gasoline, an A.S.T.M. evaporation curve was obtained by plotting the distillation temperatures against the corresponding percentages evaporated. The percentage evaporated at any point is equal to the percentage recovered plus the distillation loss up to that point. Since the vapor pressure drops very rapidly as the distillation progresses, most of the loss should occur towards the beginning of the distillation. It was therefore assumed that, within experimental error, all of the loss occurred before 10 percent of the sample had been recovered in the receiver, and accordingly the percentage evaporated at every point was considered to be equal to the percentage recovered plus the total distillation loss. Since temperatures below 10 percent evaporated were not used in the correlation with the volatility data, the error introduced in this procedure of correcting for distillation loss should be negligible.

The evaporation curve is simply the ordinary distillation curve displaced to the right by an amount equal to the distillation loss. If the loss is 2 percent and the thermometer reading at 10 percent recovered is 60 C, then in plotting the curve, a mark is made at 12 percent evaporated and 60 C. From the smooth curve through the plotted points for each gasoline, the temperatures were read at every 10 percent evaporated from 10 to 90 percent. These values were then used for the correlation with the volatility data.

Plotting the A.S.T.M. data as evaporation curves places all gasolines on a comparable basis, which is not true of the distillation curves. Further, the method used in obtaining the equilibrium volatility curves precludes any loss, so that the comparison with the A.S.T.M. curves is more logical when the A.S.T.M. data are corrected for loss in the manner indicated.

A description of the 38 fuels used in the volatility experiments is given in table 1. The gasolines contributed by the various oil com-

panies were experimental samples, in many cases prepared specially for the cooperative fuel research work, and they should not be considered as representative of the commercial products sold by these companies. It is believed, however, that the general conclusions drawn from the data on these samples are applicable to commercial gasolines and blends. The list includes 5 aviation gasolines, 5 cracked gasolines, 6 natural gasoline blends, 3 benzol blends, and 3 ethyl ether blends. Identification data on the fuels are given in table 2.

TABLE 1.—*Description of fuels*

Fuel no.	Source	Composition
1, 2, 3	Atlantic Refining Co	Straight run fuel.
1A, 2A, 3A, 4A	do	Special blends for starting tests.
A	National Bureau of Standards	U.S. motor gasoline.
B	Army Air Corps	Domestic aviation gasoline.
C	National Bureau of Standards	Equal parts A and B.
D, E, F	The Texas Co	Special blends for acceleration tests.
RH	Vacuum Oil Co	Fuel from Grozny crude.
L	Standard Oil Co. of N.J	Laurel oil.
6	National Bureau of Standards	U.S. motor gasoline.
G	do	Fuel 6, 60 percent; motor benzol, 40 percent.
H	do	Fuel A, 80 percent; benzene, 20 percent.
I	do	Fuel A, 60 percent; benzene, 40 percent.
RPC	Universal Oil Products Co.; (cracked by Dubbs process)	Fuels from midcontinent crude.
J		Fuels from Smackover crude.
K		Fuels from Panhandle crude.
N		Fuels from California crude.
O		Fuels from Wyoming crude.
M	National Bureau of Standards	Fuel A, 80 percent; kerosene, 20 percent.
B3	Army Air Corps	Domestic aviation gasoline.
101	Naturaline Co. of America	Natural gasoline aviation fuel.
111	Phillips Petroleum Co	Do.
121	Virginian Gasoline & Oil Co	Do.

		Natural gasoline	375 C end-point cracked gasoline
		Percent	*Percent*
S1	Shell Petroleum Corporation	12	88
S2		16	84
S3		22	78
S4		26	74
S5		32	68
S6		52	48

		Ethyl ether	Fuel B3
EB1	National Bureau of Standards	25	75
EB2		50	50
EB3		75	25

TABLE 2.—*Identification data on fuels*

Fuel	A.S.T.M. temperatures at stated percentages evaporated			Loss	Residue	60 F/60 F specific gravity
	10 percent	50 percent	90 percent			
	°C	°C	°C	Percent	Percent	
1	114	155	199	1.3	1.7	0.764
2	62	111	195	1.4	1.6	.730
3	91	158	197	1.8	1.2	.755
1A	80	139	195	2.3	1.7	.733
2A	84	139	195	1.5	1.5	.739
3A	93	140	193	1.0	2.0	.738
4A	90	140	186	1.5	1.5	.731
A	75	135	196	1.2	1.3	.768
B	63	101	132	2.0	1.0	.714
C	69	115	174	1.2	1.3	.741
D	89	122	200	.8	1.2	.754
E	84	137	199	.7	1.8	.762
F	72	163	198	1.0	1.0	.766
RH	85	126	168	.5	1.1	.739
RL	72	104	147	.3	1.2	.724
L	117	126	152	.3	1.2	.751
6	92	139	190	1.0	1.0	.768
G	86	107	178	1.0	1.5	.807
H	73	113	186	1.8	1.2	.776
I	76	94	177	1.7	1.3	.805
RPC	66	134	198	1.0	1.5	.747
J	54	135	207	1.6	1.4	.751
K	65	122	176	1.0	1.2	.735
N	96	150	204	.6	1.2	.771
O	82	147	200	.6	1.4	.755
M	89	152	222	.7	1.3	.776
B3	65	105	148	1.6	1.2	.709
101	42	61	106	2.3	1.2	.678
111	53	70	115	1.7	1.3	.684
121	72	79	110	1.1	1.4	.696
S1	64	115	165	.8	1.2	.743
S2	64	114	166	.8	1.2	.735
S3	60	104	161	1.4	1.1	.731
S4	54	103	161	1.3	1.2	.725
S5	52	99	159	1.3	1.2	.719
S6	44	86	154	1.2	1.3	.708
EB1	46	83	128	1.9	1.1	.714
EB2	40	53	124	1.9	1.1	.718
EB3	36	40	112	2.4	.8	.722

V. EQUILIBRIUM AIR-EVAPORATION APPARATUS AND METHOD OF USE

When an engine is being run, a mixture of liquid gasoline and air is supplied by the carburetor to the intake manifold, in which vaporization occurs to an extent dependent upon the design of the manifold, the conditions of operation and the characteristics of the fuel. The most direct method of obtaining volatility data in terms of the variables used in automotive practice is to employ an apparatus in which the process of vaporization is analogous to that occuring in the intake manifold. Such an apparatus was designed by T. S. Sligh [2] at the commencement of this work and was employed throughout essentially in its original form. Known mixtures of air and gasoline are supplied to a vaporization coil maintained at definite temperatures and the amounts of gasoline evaporated are measured. The data thus obtained, when corrected to equilibrium conditions, represent values which would be obtained in an ideal engine manifold. A manifold of this type would be equivalent to a tube, maintained at

[2] Sligh, SAE Jour., p. 393, April 1926, and p. 151, August 1926.

uniform temperature, of such length that any increase in the length would not increase the amount of fuel vaporized.

1. DESCRIPTION OF APPARATUS [3]

Diagrams of the Sligh equilibrium air-evaporation apparatus are shown in figures 2 and 3. In the earlier stages of the work, the temperature range covered did not go below 0 C and the simpler apparatus shown in figure 2 was employed. For extension of the temperature range below 0 C, the more complicated apparatus shown in figure 3 was used. Identical lettering is used for similar parts in the two figures.

The essential part of the equilibrium air-evaporation apparatus is the vaporization coil A, which is a 16-ft length of copper tubing of 7/16 in. outside diameter formed into a helix. Liquid gasoline and preheated air in definite proportions are fed at uniform rates into the

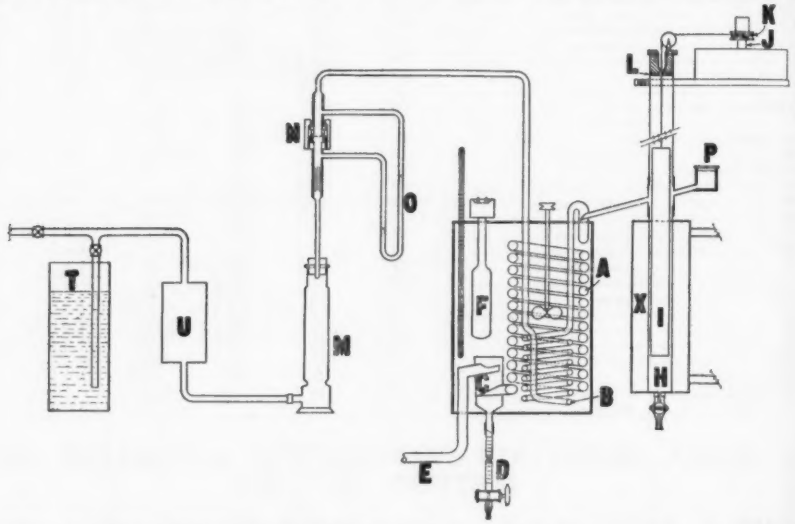

FIGURE 2.—*Equilibrium air-evaporation apparatus for measurements above 0 C.*

top of this coil which is immersed in a well-stirred constant temperature bath. After passage through the coil the unvaporized liquid is separated from the air-vapor mixture in the chamber C and is collected and measured in the burette D, while the vapor passes out through the exhaust pipe E. The flow of gasoline into the vaporization coil is controlled by displacement from the reservoir H by means of the hollow plunger I operated by clockwork. Partial stoppage by the plunger of the overflow tube into the vaporization coil is avoided by providing an offset in the reservoir wall at this point. The plunger is suspended by a fine nichrome wire, 0.008 in. in diameter, which passes through a packing gland L at the top of the reservoir and thence over an idler pulley to connect to a drum K mounted on the spindle of the clock J. The packing gland consists of a thin piece of leather, pierced by a very fine hole for the wire, and mounted between two metal disks which serve to compress the leather and force it tightly

[3] Preliminary descriptions have been given by Bridgeman and Cragoe, A.P.I. Bull., Jan. 31, 1928, p. 54 and by Bridgeman, SAE Jour., April 1928, p. 437.

around the wire. A recess is provided at the top which was filled with mercury to prevent leakage. The mainspring was removed from the clock, which is driven by the weight of the plunger acting through the drum mounted on the main shaft. The gear train and escapement serve to regulate the motion and to maintain a constant rate of fall of the plunger. To permit rewinding, a ratchet clutch is placed on the top of the clock and engages a gear on the drum. Four drums were used permitting variations in the rate of feed from 1 to 4 ml per minute. The reservoir H was filled through the cup P which was closed with a tight-fitting screw cap during the runs. In the later experiments, a water jacket X was placed around the reservoir in order to control the temperature of the gasoline.

The air used in the experiments was supplied under a slight positive pressure. It was dried by passage through a tower M containing

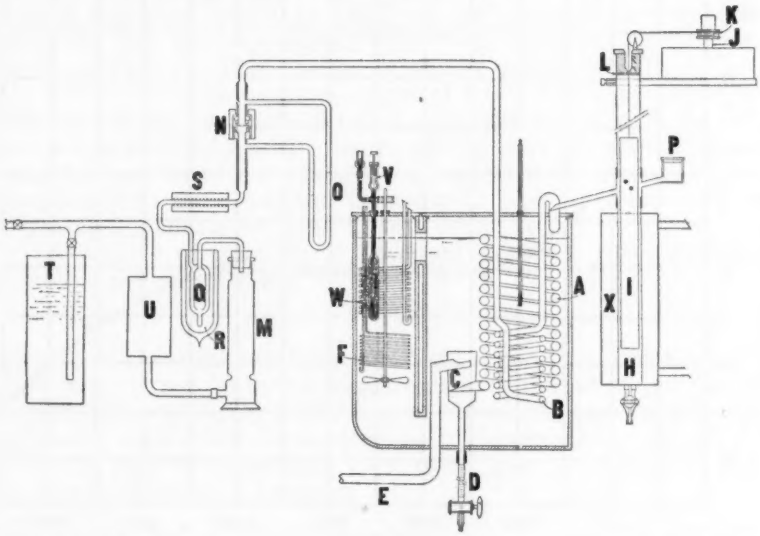

FIGURE 3.—*Equilibrium air-evaporation apparatus for measurements both above and below 0 C.*

calcium chloride and for the work below 0 C any residual moisture was frozen out by passing the air through a drying tube Q (fig. 3) immersed in a low temperature bath R. This bath was filled either with carbon dioxide slush or liquid air, depending upon the available supply of these refrigerants. The dried air was then heated to about room temperature by means of the electric heater S before passing into the flow meter N. Flat plate orifices were employed to control the air flow, and to reduce turbulence on the high pressure side of the orifice, a number of tubes are placed lengthwise in the air passage as shown in figure 2. The water manometer O indicated the pressure drop across the orifice. Five different orifices were employed, permitting considerable variation in the air flow. For convenience in the interchange of orifices, the flow meter was constructed in two parts joined together by a large threaded union. From the flow meter, the air passed upwards through a small copper coil B for final adjustment of the air temperature before it came in contact with the gasoline.

Fluctuations in the air pressure were smoothed out by means of the pressure regulator T and the 5 liter surge tank U. The pressure regulator consisted simply of a tube immersed in a tank containing water, and regulation of the valve at the top of the tube varied the amount of air by-passed against a predetermined head of water.

For work above 0 C, the bath containing the vaporization coil was filled with water and manual temperature regulation was employed using the electrical immersion heater F (fig. 2). At temperatures below 0 C, and in some of the later experiments above 0 C, the bath liquid consisted of a mixture in equal parts of carbon tetrachloride and gasoline. The temperature was automatically controlled by means of a mercury-in-glass thermoregulator V (fig. 3), the excess cooling by means of a carbon dioxide expansion coil W being com-

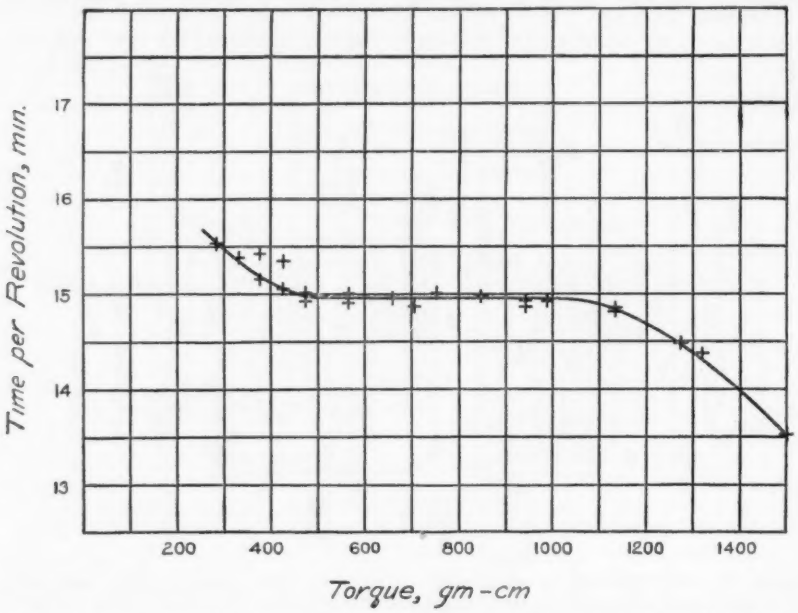

FIGURE 4.—*Calibration curve for mechanism controlling rate of gasoline feed.*

pensated for by the addition of electrical energy through the heating coil F. In some of the earlier experiments, a mixture of finely shaved ice and water was used to obtain a temperature of 0 C.

2. CALIBRATION OF APPARATUS

(a) CALIBRATION OF GASOLINE DISPLACEMENT SYSTEM

The volume of gasoline supplied to the vaporization coil is dependent upon the displacement of the plunger, upon the size of the drum on the clock spindle, and upon the clock rate. The plunger was a uniform cylinder of outside diameter 2.540 cm and displacement 5.067 ml per cm immersion. The clock rate was checked for a wide range of weights with each of the four drums. For each measurement, the torque was computed by multiplying the weight of the plunger in grams by the effective radius of the drum in centimeters. The

effective radius was taken to be the actual radius plus that of the wire. The calibration data are shown in graphical form in figure 4, in which the time per revolution, in minutes, is plotted against the torque in g–cm. Over a considerable range, the clock rate is constant, but the departure from constancy is very marked toward each end of the curve.

Appropriate weights for each drum were computed from the torque required for the same clock rate in all cases, namely, one revolution in 14.95 minutes. In choosing these values, allowance was made for the decrease in torque due to increasing loss of weight with depth of immersion. For example, no. 2 drum had an effective radius of 0.943 cm and with a plunger weighing 1,000 g, the torque equals 943 g–cm and the clock rate is 14.95 min per revolution. The weight of the plunger would have to drop below 500 g before the clock rate is affected. If the plunger were immersed to a depth of 25 cm, the volume displaced would be 126.7 ml and the loss in weight due to buoyancy in a gasoline having a 60 F/60 F specific gravity of 0.720 would be 91.2 g. This change in weight would not affect the clock rate and therefore a plunger weight of 1,000 g is appropriate for use with no. 2 drum. Adjustment of the plunger weight with the different drums was accomplished by means of lead shot put into or withdrawn from the interior of the plunger. In some cases a second wire was wound around the drum and thence over an idler pulley to a weight to supply an additional load on the drum.

The volume of gasoline F displaced per unit time, expressed in milliliters per minute, is

$$F = k\pi DrA \tag{1}$$

where D is the effective diameter of the drum in centimeters, r is the clock rate in rpm, A is the displacement in milliliters per centimeter length of the plunger, while k is a constant equal to 1.000027, to transform from cubic centimeters to milliliters, and π equals 3.1416. With the present apparatus, $r = 1/14.95$, and $A = 5.067$, so that the relation in equation 1 becomes

$$F = 1.065D \tag{1A}$$

The data on the four drums are given in table 3.

TABLE 3.—*Constants of the drums used in the gasoline displacement system*

Number	Effective diameter	Gasoline displacement		Weight on drum
	cm	*ml/rev*	*ml/min*	*g*
1	0.943	15	1.003	1,500
2	1.885	30	2.006	1,000
3	2.827	45	3.010	500
4	3.769	60	4.013	500

The weight of gasoline displaced per unit time is the product of the volume and the density of the gasoline at the temperature existing in the reservoir H at the time of displacement. Hence

$$W_g = Fd \tag{2}$$

where W_g is the weight of gasoline in grams per minute and d is the density. Values of the density at the desired temperatures were obtained from the measured gravity at 60 F making use of the national standard petroleum oil tables,[4] for the change of density with temperature.

(b) CALIBRATION OF FLOWMETER

The orifices used in the flowmeter were calibrated by comparison with a master orifice of known characteristics. The flow of air W_a in grams per minute is given by the formula

$$W_a = k\sqrt{H} \tag{3}$$

where k is the orifice constant for air at 25 C and 760 mm pressure, and H is the pressure drop across the orifice, expressed in centimeters of water. Within the experimental error of the volatility measurements k can be considered constant, since the variations in air temperature and pressure were small. Data on the five orifices used are given in table 4.

TABLE 4.—*Constants of the orifices used in the flowmeter*

Number	Approximate orifice diameter	Orifice constant
	Inch	
1	1/16	1.12
2	3/32	2.25
3	1/8	4.66
4	5/32	7.11
5	3/16	10.58

The pressure drop H across the orifice to give any desired air-fuel mixture for a specific rate of gasoline feed is obtained by combining equations 2 and 3, which leads to the relation

$$H = \left(\frac{M_s F d}{k}\right)^2 \tag{4}$$

where M_s is the supplied air-fuel mixture and is equal to W_a/W_g. The pressure drop H is the difference in level, in centimeters of water, between the two arms of the manometer across the orifice.

(c) CALIBRATION OF VAPORIZATION COIL

The degree of vaporization under flow conditions is a function not only of the thermodynamic variables, temperature, pressure and mixture ratio, but also in general a function of the rate of flow and the characteristics of the specific apparatus used. Hence, for vaporization data by a dynamic method to be general and a function of the thermodynamic variables only, it is necessary that the apparatus be calibrated to evaluate the effect of the rate of flow on the measurements. With a well-designed apparatus, carefully manipulated, the amount of liquid evaporated into the air stream from a constant supplied air-fuel mixture will vary continuously with the rate of flow through the vaporization coil, and the change in the amount evapo-

[4] N.B.S. Miscellaneous Publication No. 154, 1924.

rated with rate of flow will become successively less as the flow decreases. The value approached with each constant mixture and temperature as the rate of flow becomes zero is the equilibrium percentage evaporated. Hence if the percentages evaporated are measured for a number of sufficiently slow rates, which are determined by the particular apparatus, the extrapolated value at zero rate of flow is independent of the apparatus and represents the equilibrium value for vaporization from the specific mixture being studied at the specific temperature. Measurements with other mixtures and at a number of temperatures serve to establish the departure from equilibrium with this specific fuel under all conditions of use in the apparatus. Similar investigations with other fuels are necessary to determine whether a general relation for departure from equilibrium can be obtained which is independent of the particular fuel used.

An experimental investigation was made of the effect of temperature and mixture ratio on the change in the percentage evaporated with rate of gasoline flow in the case of a number of gasolines. Temperatures ranging from +45 to −30 C were employed and air-fuel mixtures from 0.5:1 to 16:1 were supplied to the vaporization coil. Experiments were made with 5 fuels and rates of gasoline feed of 1, 2, 3, and 4 ml per min were used. Under each set of conditions, the values of the amounts evaporated, expressed in weight percent, were plotted against the rate of gasoline feed and the line through these points was extrapolated to zero rate of feed. This extrapolated value was considered to be the equilibrium percentage evaporated.

A study of the data showed that the departure from equilibrium vaporization was independent of the specific fuel, the temperature and the supplied air-fuel mixture, and was dependent only upon the rate of feed and the percentage evaporated. The following relation was found to hold for all of the measurements:

$$P = P_o(1 + 0.0125F) \tag{5}$$

where P is the equilibrium percentage evaporated and P_o is the experimentally determined value at the feed F in milliliters per minute.

The departure from equilibrium vaporization is illustrated graphically in figure 5, in which deviations from equation 5 are plotted against P employing different symbols for the four rates of gasoline feed used, approximately 1, 2, 3, and 4 ml per min. The agreement of the data with equation 5 is further illustrated in table 5 for fuels *B*3 and 111, in which are recorded values of P at various temperatures and with a number of supplied air-fuel mixtures. The values of P were computed from the experimental values of percentages evaporated P_o by means of equation 5 and hence if the equation is valid, P should be constant at each temperature and with each mixture. The deviations from constancy are listed in the table and no trend of the deviations with either temperature or mixture ratio is noted. The grand average deviation from equation 5 is 1 percent evaporated. At small percentages evaporated, the departure from equilibrium vaporization is less than the average deviation from the equation, so that in this range, the results indicate the degree of reproducibility of the measurements, which is one unit in the percentage evaporated.

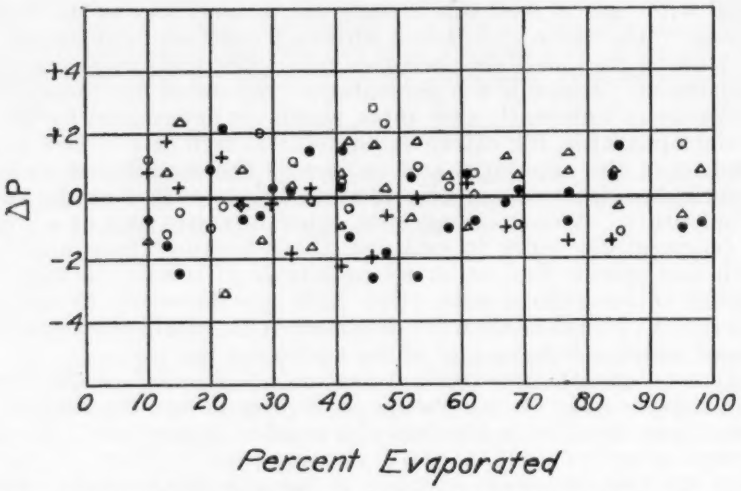

FIGURE 5.—*Deviation plot showing lack of trend in deviations from equation 5.*

TABLE 5.—*Test of equation 5 for correction to equilibrium vaporization*

(1) DATA FOR FUEL B3

Feed	P for $M_s=4$	ΔP	P for $M_s=8$	ΔP	P for $M_s=12$	ΔP	P for $M_s=16$	ΔP
				(*a*) TEMPERATURE=15 C				
1.003	47.2	−0.6	66.2	−1.0	75.7	−1.4	82.1	−1.4
2.006	46.0	−1.8	67.0	−.2	77.2	+.1	84.1	+.6
3.010	48.1	+.3	68.5	+1.3	78.5	+1.4	84.3	+.8
4.013	50.1	+2.3						
Average	47.8	±1.3	67.2	±.8	77.1	±1.0	83.5	±.9
				(*b*) TEMPERATURE=0 C				
1.003	36.1	+0.3	43.6	−1.9	53.2	0.0	61.1	+0.4
2.006	37.3	+1.5	42.9	−2.6	50.6	−2.6	61.4	+.7
3.010	34.2	−1.6	47.2	+1.7	55.0	+1.8	59.7	−1.0
4.013	35.7	−.1	48.3	+2.8	54.1	+.9		
Average	35.8	±.9	45.5	±2.2	53.2	±1.3	60.7	±.7
				(*c*) TEMPERATURE=−15 C				
1.003	14.8	+1.8	24.6	−0.2	31.6	−1.8	38.4	−2.2
2.006	11.5	−1.5	24.1	−.7	33.6	+.2	42.1	+1.5
3.010	13.8	+.8	25.7	+.9	33.7	+.3	41.4	+.8
4.013	11.8	−1.2	24.6	−.2	34.5	+1.1		
Average	13.0	±1.3	24.8	±.5	33.4	+.6	40.6	±1.5
				(*d*) TEMPERATURE=−30 C				
1.003	10.3	+0.8	15.4	+0.3	23.0	+1.3	30.0	−0.2
2.006	8.8	−.7	12.7	−2.4	23.9	+2.2	30.5	+.3
3.010	8.1	−1.4	17.5	+2.4	18.6	−3.1		
4,013	10.7	+1.2	14.6	−.5	21.4	−.3		
Average	9.5	±1.0	15.1	±1.4	21.7	±1.7	30.2	±.3

Grand average deviation=±1.1.

TABLE 5.—*Test of equation 5 for correction to equilibrium vaporization*—Continued

(2) DATA FOR FUEL 111

Feed	P for $M_s=4$	ΔP	P for $M_s=8$	ΔP	P for $M_s=12$	ΔP	P for $M_s=16$	ΔP
			(*a*) TEMPERATURE=0 C					
2.006	61.3	−0.8	86.5	±1.6	94.2	−1.1	96.8	−0.9
3.010	62.2	+.1	84.6	−.3	94.7	−.6	98.5	+.8
4.013	62.8	+.7	83.7	−1.2	96.9	+1.6		
Average	62.1	±.5	84.9	±1.0	95.3	±1.1	97.7	±.9
			(*b*) TEMPERATURE=−15 C					
2.006	40.6	−1.3	57.3	−1.0	69.2	+0.2	76.6	−0.8
3.010	43.7	+1.8	59.0	+.7	69.7	+.7	78.2	+.8
4.013	41.5	−.4	58.6	+.3	68.0	−1.0		
Average	41.9	±1.1	58.3	±.7	69.0	±.6	77.4	±.8
			(*c*) TEMPERATURE=−30 C					
2.006	20.8	+0.9	27.3	−0.6	41.6	+0.3	52.1	+0.6
3.010			26.5	−1.4	40.4	−.9	50.8	−.7
4.013	18.9	−1.0	29.9	+2.0	41.8	+.5		
Average	19.9	±1.0	27.9	±1.3	41.3	±.6	51.5	±.7

Grand average deviation=±0.9.

Verification of the conclusion that the corrected experimental results represent equilibrium conditions, was obtained by experiments on pure toluene. In this case, the known molecular weight and vapor pressure data permit a computation of the volatility. Determinations were made with a considerable number of supplied air-toluene mixtures and at the four temperatures 0, 15, 25, and 35 C. From the plot of these experimental data, the temperatures corresponding to four resultant air-vapor mixtures covering the range of interest were obtained and a comparison is made in table 6 with the calculated temperatures. The details of this procedure for obtaining both the experimental and calculated values will be explained later in this paper. The agreement between the two sets of values substantiates the conclusion that, within the experimental error of the measurements, the corrected results obtained with the Sligh volatility apparatus closely approximate equilibrium conditions.

TABLE 6.—*Comparison of observed and calculated temperatures for various resultant mixtures of air and toluene vapor*

Mixture	Observed temperature	Calculated temperature
	° *C*	° *C*
8:1	23	25
12:1	17	17
16:1	12	12
20:1	8	8

All values obtained in the study of fuel volatility were corrected to equilibrium values by means of equation 5.

3. GENERAL EXPERIMENTAL PROCEDURE

The method of using the equilibrium air-evaporation apparatus is comparatively simple. In making an experiment, the drum on the clock spindle was rotated so as to raise the plunger to the top of the reservoir, which was then filled with the gasoline. For most purposes, the 2 or 3 ml per min drums were found to be the most convenient. After the temperature of the bath was adjusted, the air supply was turned on, the manometer head was regulated to the value computed from equation 4 for the desired air-fuel mixture and the clock was started. A few minutes were allowed for constancy to be attained and measurements were then made of the amount unvaporized. After several check readings, the experimental conditions were varied and other readings were taken. With each fuel, a sufficient number of supplied mixtures were employed over a range of temperature to cover the desired volatility field.

In determining the volume of gasoline unvaporized, two different sizes of burettes were found to be convenient. For large amounts unvaporized, the volume collected per unit time was large and a burette of 5 ml capacity was used; whereas, for small amounts unvaporized, one of 1 ml capacity was employed. Drainage errors in the burette were avoided by starting a stop watch when the liquid passed a given mark, by draining the gasoline into a calibrated flask of 1 or 5 ml capacity until full and then stopping the watch when the meniscus passed the mark on the burette a second time. The accuracy of the stop watch was checked periodically.

It is necessary to know the specific gravities of the original fuel and of the residual liquid after partial vaporization, in order to express the experimental results on a weight basis. Accordingly, the specific gravities of the original gasoline and of each residue were determined at 60 F. by means of a pycnometer. The gravities at other temperatures were obtained from the national standard petroleum oil tables.[5]

The percentage by weight of gasoline evaporated during an experiment is given by the relation

$$P_0 = \frac{Fd_1 - Vd_2}{Fd_1} \times 100 \qquad (6)$$

where F is the volume of liquid in milliliters supplied per minute, computed from equation 1A; d_1 is the specific gravity of the original gasoline at room temperature; V is the measured volume of the liquid residue collected per minute; and d_2 is the specific gravity of the residue at the temperature of the bath containing the vaporization coil. It has been found that the small difference in temperature between the residue collected in the burette and that in the bath introduces a negligible error. In every case the values of P_0 were corrected to equilibrium values by means of equation 5.

A sample data sheet indicating the details of computation is shown in table 7.

[5] See reference 4.

TABLE 7.—*Sample data sheet — fuel S3*

Temperature	Supplied mixture M_s	Feed F	Orifice size	Pressure drop H	Specific gravity of residue		Time for collection of 1 ml of residue	Obs. weight percent evaporated, P_o	Corr. to equilibrium, vaporization	Equilibrium wt percent evaporated, P
					60 F/60 F	t°/160 F				
° C			*Inch*				*Sec.*			
15	4	3.010	1/8	3.5	0.765	0.765	37.6	43.9	1.6	45.5
	8	3.010	5/32	6.0	.772	.772	53.3	60.1	2.3	62.4
	12	3.010	3/16	6.0	.777	.777	65.4	67.2	2.5	69.7
	16	2.006	5/32	10.6	.782	.782	123.6	73.8	1.8	75.6
0	4	3.010	1/8	3.5	.755	.767	30.2	29.9	1.1	31.0
	8	3.010	5/32	6.0	.763	.775	35.2	39.3	1.5	40.8
	12	3.010	3/16	6.0	.765	.777	42.8	49.9	1.9	51.8
	16	2.006	5/32	10.6	.771	.783	72.0	55.0	1.4	45.4
−15	4	3.010	1/8	3.5	.749	.773	27.4	22.2	.8	23.0
	8	3.010	5/32	6.0	.754	.778	29.0	26.0	1.0	27.0
	12	3.010	3/16	6.0	.758	.782	32.8	34.3	1.3	35.6
	16	2.006	5/32	10.6	.763	.786	52.2	37.7	.9	38.6
−30	4	3.010	1/8	3.5	.739	.776	24.2	11.5	.4	11.9
	8	3.010	5/32	6.0	.744	.780	26.0	17.3	.6	17.9
	12	3.010	3/16	6.0	.750	.786	26.9	19.4	.7	20.1
	16	2.006	5/32	10.6	.755	.791	43.0	23.9	.6	24.5

Specific gravity of original gasoline (77 F/60 F) = 0.723.

VI. METHOD OF TREATMENT OF EXPERIMENTAL DATA

1. PARTIAL VOLATILITY AND DEW-POINT DATA

In the preliminary treatment of the experimental data, values of the volatility, in terms of the temperature required to produce a given resultant air-vapor mixture, were obtained graphically for each such resultant mixture. The corrected percentages evaporated were plotted against the corrresponding temperatures for each supplied air-fuel mixture and smooth curves were drawn through the points. This gave a temperature-percentage evaporated curve for every supplied mixture. The percentage evaporated P which would produce a given resultant air-vapor mixture M_R from each supplied mixture M_S was computed by means of the relation

$$P = \frac{M_S}{0.01\ M_R} \tag{7}$$

Values of P thus computed were used to locate temperatures on the supplied mixture curves, corresponding to the various resultant mixtures of interest. Smooth curves were then put through these points, so that a temperature-percentage evaporated curve was obtained for each desired resultant air-vapor mixture.

A sample diagram is shown in figure 6 for fuel S1. The circles represent the experimentally observed values corrected to equilibrium by means of equation 5. The continuous lines through these points correspond to the four supplied air-fuel mixtures of 4:1, 8:1, 12:1, and 16:1. The dotted lines indicate temperatures along resultant air-vapor mixture lines of 8:1, 12:1, 16:1, and 20:1. From equation 7, it is found that a 20:1 resultant mixture will be formed from a 16:1 supplied mixture when 80 percent of the fuel is evaporated. The same resultant mixture will be formed from an 8:1 supplied mixture at 40 percent evaporated and from a 4:1 mixture at 20 percent evaporated. By drawing a smooth curve through these points

corresponding to the same resultant mixture, it is possible to determine the temperatures at various percentages evaporated which will produce this constant air-vapor mixture. Thus at 80 percent evaporated, a temperature of 24 C is required to produce a 20:1 air-vapor mixture. At temperatures below this, at the same percentage evaporated, leaner mixtures are formed; at higher temperatures, the resultant mixtures are richer.

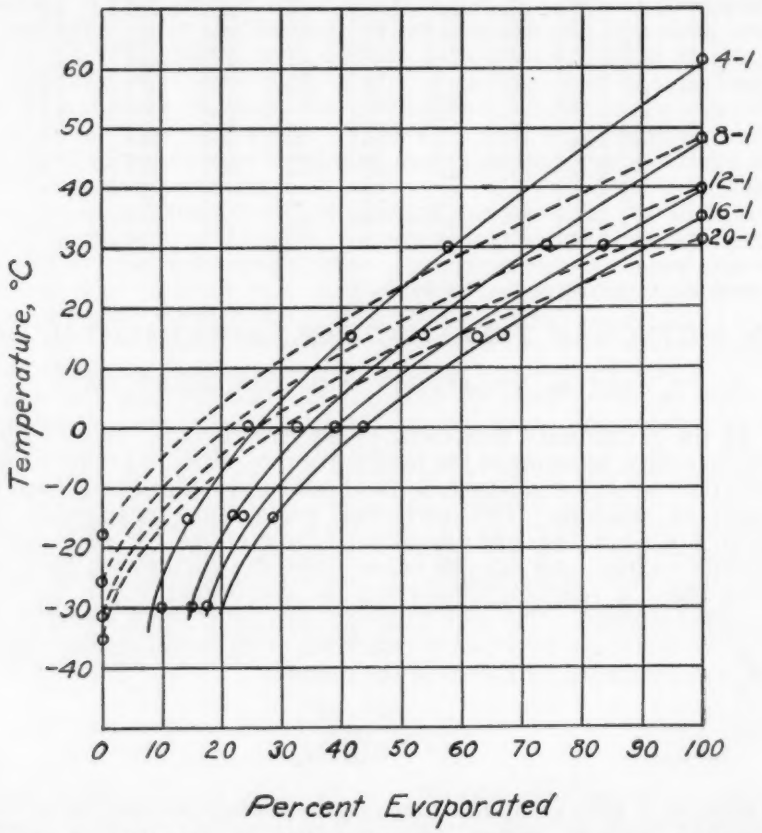

FIGURE 6.—*Volatility curves for fuel S1. The solid lines correspond to designated air-liquid fuel ratios, while the dashed lines correspond to designated air-vapor ratios.*

The dew points of the various mixtures are the intercepts of the extrapolated mixture lines with the vertical line of 100 percent evaporated. Each intercept is rendered more certain by the fact that analogous supplied and resultant mixture lines must intersect at the dew point, which essentially amounts to a double smoothing of the data, thereby increasing the accuracy. Thus, with reference to figure 6, the continuous and dotted lines for 16:1 supplied and resultant mixtures respectively cross at 100 percent evaporated at a temperature of 35 C, which is the 16:1 dew point of this gasoline.

Plots similar to that shown in figure 6 were made for each fuel studied. The evaluation of the bubble points of these mixtures will be discussed in the following section.

While the method outlined was fairly satisfactory for the evaluation of the volatility data from the experimental results, two graphical smoothings of the data were involved and there was some latitude for personal judgment in drawing the curves. Accordingly, it was considered desirable to develop a method in which all of the points on each fuel would be considered simultaneously in drawing any one line. Inspection of the original curves for the entire set of data on the 38 fuels showed that the difference in temperature between any two

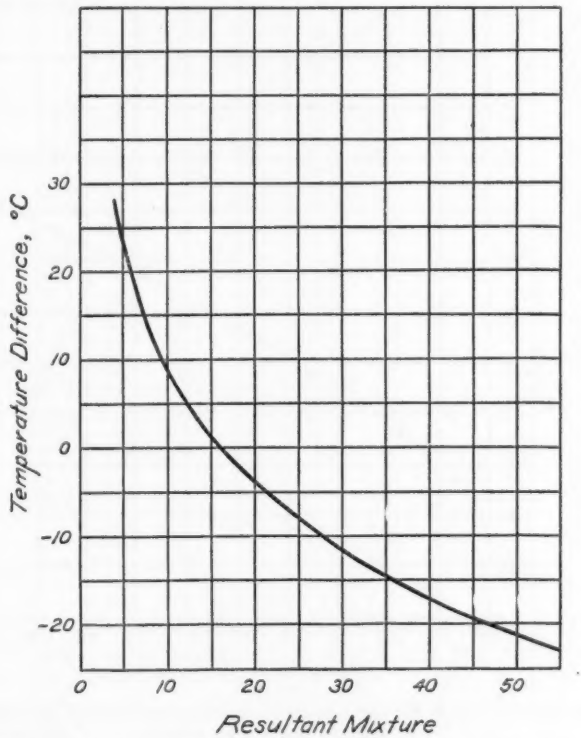

FIGURE 7.—*Curve showing differences in temperature between lines for various resultant air-vapor mixtures.*

resultant mixtures lines from 8:1 to 20:1 was the same at every percentage evaporated and for each gasoline studied, the average deviation from constancy being considerably less than 1° C.

The differences in temperature between various resultant air-vapor mixture lines are shown in figure 7, referred to a 16:1 mixture as standard. Thus, if the temperature on a 16:1 mixture line at 90 percent evaporated is 40 C, the temperature on a 20:1 line at the same percentage evaporated will be obtained by adding −4° C, giving 36 C. On the other hand, if the 16:1 temperature at 10 percent evaporated is −20 C, the 8:1 temperature at 10 percent evaporated will be (−20+13) °C or −7 C. Values for other mixtures at any percentage evaporated can be obtained in a similar manner.

The constant temperature difference between any two resultant mixture lines, over the range of interest, made it possible to transform all of the data on any one gasoline to temperatures along a 16:1 resultant mixture line. Thus, for each experimental value of supplied mixture and percentage evaporated, the value of the resultant mixture formed was computed from equation 7. Then by means of the curve in figure 7, the experimental temperature to which the above data apply was corrected to the value corresponding to the 16:1 resultant mixture at the same percentage evaporated. For example, assume that the equilibrium percentage evaporated is 80 percent at 50 C when supplying a 16:1 air-fuel mixture. From

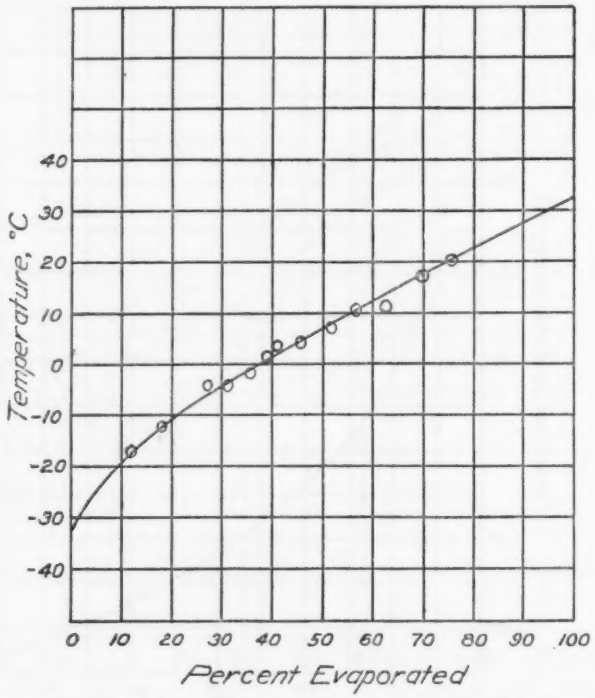

FIGURE 8.—*Volatility curve for resultant mixture containing 16 parts of air and 1 part of fuel S3 by weight.*

equation 7 the resultant air-vapor mixture, M_R equals 20:1, and from the curve in figure 7, the temperature difference between a 20:1 and a 16:1 resultant air-vapor mixture is 4° C. Therefore at 80 percent evaporated, a 16:1 resultant mixture would be formed at 50 − 4° C = 46 C.

Temperatures, thus corrected to values on a 16:1 resultant mixture line, were plotted against the corresponding percentages evaporated and a smooth curve was drawn through these points. An example is shown in figure 8 for fuel S3. The value at 0 percent evaporated was obtained in a manner described in the following section. Similar curves were drawn for the 38 fuels and the temperatures at every 10 percent evaporated from 10 to 100 percent inclusive read from these curves are shown in table 8. The values from 10 to 90 percent

represent partial volatility data while the temperatures at 100 percent evaporated represent dew points. The dew-point values for fuels 1A, 2A, 3A, and 4A are in parentheses, because these values were obtained by extrapolation over a much longer range than usual.

TABLE 8.—*16:1 temperatures from experimental curves, °C at stated percentages evaporated*

Fuel	10	20	30	40	50	60	70	80	90	100
1	15	23	29	34	39	43	48	51	55	59
3	4	19	29	35	40	44	47	50	53	56
1A	−5	5	13	20	27	33	38	44	49	(54)
2A	−1	8	16	23	29	34	39	44	49	(53)
3A	1	10	17	23	29	34	39	44	48	(53)
4A	2	11	18	23	29	33	37	41	45	(49)
A	−8	5	15	20	25	31	36	43	49	56
B	−17	−8	−4	−1	1	4	6	9	11	14
C	−13	−3	4	9	13	17	22	27	33	40
D	2	8	12	15	17	20	25	33	45	57
E	−2	9	17	22	27	33	39	45	51	58
F	−10	10	26	36	42	46	50	52	55	57
RH	−3	5	11	16	20	24	27	31	34	37
L	17	18	19	20	21	22	23	24	25	27
RPC	−15	−1	10	19	27	34	40	47	53	59
2	−20	−12	−5	2	9	17	26	36	46	56
6	5	12	18	22	27	32	36	41	47	53
G	−2	0	2	5	8	12	17	24	24	44
H	−11	−3	4	9	14	20	27	34	42	50
I	−10	−6	−5	−4	0	6	14	23	33	44
J	−22	−7	6	16	26	34	42	50	58	65
K	−15	−4	4	11	17	23	28	33	38	42
M	2	16	26	32	38	45	52	59	67	75
N	7	17	24	31	38	43	49	54	59	64
O	−2	11	20	28	35	41	47	52	58	63
B3	−15	−9	−4	0	5	9	13	16	20	24
101	−34	−31	−29	−26	−24	−21	−18	−14	−10	−4
111	−26	−24	−22	−20	−18	−16	−13	−10	−5	1
121	−14	−13	−12	−12	−11	−10	−8	−6	−4	−1
S1	−15	−6	2	8	13	18	23	27	31	35
S2	−15	−7	0	6	11	16	21	26	31	35
S3	−19	−11	−5	0	6	11	17	22	28	34
S4	−23	−14	−7	−1	4	10	15	21	27	33
S5	−26	−17	−10	−4	1	6	12	18	25	31
S6	−30	−23	−19	−14	−8	−2	5	12	20	28
EB1	−30	−27	−23	−18	−12	−4	1	5	8	10
EB2	−35	−34	−33	−31	−29	−24	−17	−6	2	8
EB3	−38	−38	−38	−38	−37	−37	−36	−32	−9	0

A 16:1 air-vapor mixture was chosen as a standard of reference since it is essentially the leanest mixture which it is feasible to employ in the engine. However, the method works equally well for other reference mixtures from 4:1 to 20:1, which covers the range of interest in automotive work.

2. BUBBLE-POINT DATA

When the curve representing any given air-vapor mixture is extrapolated back to cut the vertical line of 0 percent evaporated, the point of intersection is the bubble point and represents the limiting temperature below which this given mixture cannot be formed. In general, the determination of bubble points of air-vapor mixtures by extrapolation of these equilibrium air-evaporation curves is not feasible, due to increasing curvature at smaller percentages evaporated. Bubble points may, however, be computed from the vapor pressures of the gas-free gasolines over a range of temperatures and from the molecular weights of the hydrocarbon vapors present in the small bubbles which form in the gasolines at the bubble points. Direct determination of the molecular weights of the vapors formed under these conditions is difficult so an indirect method was employed

involving computation from measurements of the molecular weights of the liquid residues at various percentages evaporated obtained by means of the equilibrium air-evaporation apparatus.

From the 16:1 air-vapor curves of the fuels studied, the temperatures were read at 20, 40, 60, and 80 percent evaporated. Then using equation 7, the air-fuel mixtures which must be supplied in each case to produce a 16:1 resultant mixture were computed. With every fuel, each computed air-fuel mixture was run through the equilibrium air-evaporation apparatus at the appropriate temperature to give the desired resultant mixture at the chosen percentage evaporated. About 50 ml of residue was collected under each set of conditions and the molecular weights of these samples and of the original gasolines were

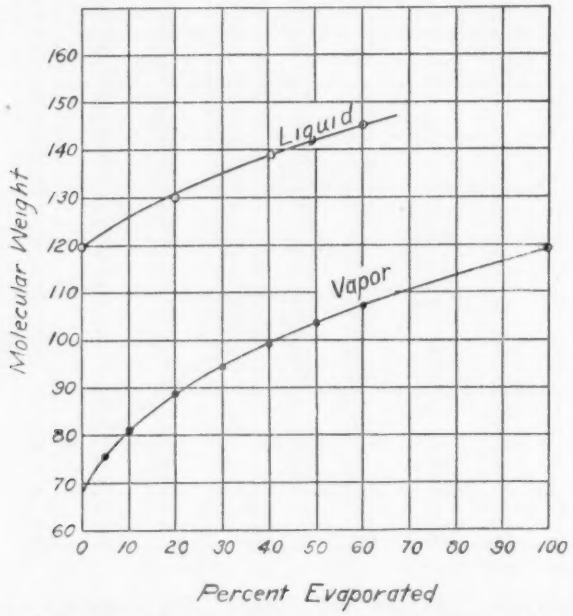

FIGURE 9.—*Molecular weight curves of liquid and vapor for fuel A at various percentages evaporated.*

determined by measuring the lowerings in the freezing point of pure benzene on addition of known amounts of the residues.[6] These data were then plotted against the percentage evaporated and a smooth curve drawn through the plotted points, as illustrated in the upper curve of figure 9 for fuel A. From this curve, the molecular weights were obtained at 5 percent evaporated and thereafter at every 10 percent evaporated up to 60 or 80 percent, and were used to compute the molecular weights of the vapors formed under each set of conditions.

Since the number of moles of gasoline in the residue plus those of the vapor in the resultant mixture at any percentage evaporated are necessarily equal to the number of moles of gasoline supplied, it follows that

$$\frac{100-P}{M_L}+\frac{P}{M_r}=\frac{100}{M_a} \tag{8}$$

[6] Bridgeman, SAE Jour., Nov. 1928, p. 478.

where P is the percentage evaporated by weight, and M_L, M_F, and M_G are the molecular weights, respectively, of the liquid residue, of the vaporized fuel, and of the original gasoline.

Rearranging equation 8, it becomes

$$M_F = \frac{M_L}{1 + \frac{100}{P} \cdot \frac{\Delta M}{M_G}} \tag{9}$$

where $\Delta M = M_L - M_G$. For each value of the molecular weight of the residue, M_L, obtained from the curve, the corresponding value of the molecular weight of the gasoline vapor, M_F, at the same percentage evaporated, was computed from equation 9. For example, if the molecular weight of the original gasoline is 100 and the molecular weight of the residue at 50 percent evaporated is 120, then $\Delta M = 20$, and $M_F = 120/1.4 = 86$ at 50 percent evaporated.

The computed values of the molecular weights of the vapors were plotted against the percentage evaporated and a smooth curve was drawn through the points, as illustrated in the lower curve of figure 9. The extrapolated value at 0 percent evaporated is the desired molecular weight of the vapor in the first small bubble which forms in the gasoline under equilibrium conditions corresponding to a 16:1 resultant air-vapor mixture.

The next step is the determination of the bubble point temperature, which involves a knowledge of the gasoline vapor pressure necessary for the formation of a 16:1 resultant mixture. Assuming that both the gasoline vapor and the air obey the perfect gas laws, which is closely true, then

$$\frac{p_A}{p_F} = \frac{W_A M_F}{W_F M_A} \tag{10}$$

where p_A and p_F are the respective partial pressures of air and fuel vapor in the resultant mixture, expressed in millimeters of mercury; W_A and W_F are their respective masses in grams; and M_A and M_F are their respective molecular weights. Further, since the total pressure of the mixture is 760 mm of mercury

$$p_A = 760 - p_F. \tag{11}$$

Combining equations 10 and 11, and substituting the resultant mixture ratio M_R for W_A/W_F, there results

$$p_F = \frac{760}{1 + M_R \cdot \frac{M_F}{M_A}}. \tag{12}$$

Substituting 16 for M_R and taking the molecular weight of air as 28.96, the relation becomes

$$p_F = \frac{760}{1 + 0.553 M_F}. \tag{13}$$

Using the molecular weights of the gasoline vapors, M_F, obtained from the extrapolated molecular weight curve for each fuel, the values of the vapor pressures of the gasolines, p_F, necessary to form 16:1 air-vapor mixtures in the small bubbles were computed from equation 13.

The last step involves the evaluation of the temperature with each gasoline at which the vapor pressure has the value computed above. For this purpose, the gasolines were dried and freed from dissolved gases and their vapor pressures were measured over a range of temperatures under conditions such that a small bubble of vapor was present in each case. The details of the methods used in the preparation of the gasoline samples and in the vapor-pressure measurements will be presented in a later paper.[7] It was found that the vapor-pressure data on each gasoline could be accurately reproduced by an equation of the form

$$\log_{10}\frac{p_F}{760}=A\left[1-\frac{T_n}{T}\right] \tag{14}$$

where T is the temperature in absolute centigrade degrees corresponding to the vapor pressure p_F in millimeters of mercury; T_n is the temperature in absolute centigrade degrees at which the vapor pressure is equal to 760 mm of mercury; and A is a specific constant evaluated from the data on each fuel. Using the values of p_F obtained from equation 13 and the appropriate values of the constant A, equation 14 was used to compute the desired bubble point temperatures ($T-273.1$) corresponding to 16:1 resultant mixtures of air and vapor from the various gasolines.

An example for fuel A will illustrate the method of computation. From the curve of molecular weight of the vapor in the 16:1 resultant air-vapor mixture, the value of the molecular weight at 0 percent evaporated is found on extrapolation to be 68. Substituting this value for M_F in equation 13, the partial pressure p_F of gasoline vapor in the mixture is computed to be 19.7 mm of mercury. From vapor pressure measurements on this fuel, the temperature at which the vapor pressure equals 760 mm is 74.0 C, and the constant A equals 3.87. T_n is therefore $74.0+273.1=347.1$ K. Substituting these values for p_F, T_n and A in equation 14, T is found to be 246 K. The desired bubble point is then equal to $246-273=-27$ C.

Molecular weight and vapor pressure data were obtained on 5 gasolines and their 16:1 bubble points evaluated in the manner indicated are given in table 9.

TABLE 9.—*Evaluation of 16:1 bubble points*

Fuel	Molecular weight of vapor for 16:1 mixture, M_F	Partial pressure of gasoline vapor, p_F	Normal bubble point	Vapor pressure constant A	16:1 bubble point
			° C		° C
A	68	19.7	74.0	3.87	−27
B	68	19.7	63.0	3.97	−33
C	68	19.7	68.7	3.96	−29
J	66	20.3	55.4	3.84	−40
M	76	17.7	88.7	3.96	−16

[7] Preliminary information is given by Bridgeman, Aldrich, and White, SAE Jour., p. 488, May 1929; and A.P.I. Bull., section 3, p. 4, Jan. 2, 1930.

VII. CORRELATION OF VOLATILITY DATA WITH A.S.T.M. DISTILLATION DATA

1. PRELIMINARY METHOD OF CORRELATION [8]

Although the equilibrium air-evaporation apparatus seems to be satisfactory for the determination of gasoline volatility, nevertheless it is not convenient for testing a large number of gasolines rapidly, due to the time required in obtaining complete information on each sample. On the other hand, the A.S.T.M. distillation test is simple, reproducible and in cómmon use, so that an attempt was made to interpret the A.S.T.M. evaporation curves in terms of volatility, on the basis of the data obtained on the 38 diverse fuels.

A scheme of correlation of the results obtained by the two methods is suggested by the Clapeyron equation for pure substances which is

$$\frac{dp_F}{dT} = \frac{L}{T(V_1 - V_2)} \tag{15}$$

where p_F is the vapor pressure at the temperature T in absolute degrees; L is the latent heat of vaporization per mole; V_1 is the molal volume of the vapor and V_2 is the molal volume of the liquid.

For the conditions involved in the present work, where the pressure is below atmospheric, the volume of the liquid is negligible in comparison with that of the vapor and it can be assumed without much error that the vapor obeys the perfect gas law, namely, $p_F V_1 = RT$, where R is the gas constant per mole. Under these conditions, the Clapeyron equation 15 becomes

$$\frac{1}{p_F} \cdot \frac{dp_F}{dT} = \frac{L}{RT^2} \tag{16}$$

Integration yields the relation

$$\log_e \frac{p_F}{760} = \frac{L}{RT_n}\left[1 - \frac{T_n}{T}\right] \tag{17}$$

where L is assumed to be independent of temperature and T_n is the boiling point in absolute degrees corresponding to a pressure of 760 mm of mercury. Experimental evidence has shown that L/RT_n has approximately the same value for substances like the hydrocarbons, which have similar properties, so that it can be replaced by the symbol a. In this case, equation 17 becomes

$$\log_e \frac{p_F}{760} = a\left[1 - \frac{T_n}{T}\right] \tag{18}$$

If a mixture of hydrocarbon vapor and air in a space of volume V are both assumed to obey the perfect gas law, then

$$p_A = W_A RT/M_A V \tag{19}$$

and

$$p_F = W_F RT/M_F V \tag{20}$$

[8] See reference 3; also, Bridgeman, A.P.I. Bull., section 2, p. 124, Jan. 3, 1929; and SAE Jour., p. 137, August 1929.

where p_A and p_F are the respective partial pressures in millimeters of mercury of the air and hydrocarbon vapor in the mixture; W_A and W_F are their respective masses in grams; M_A and M_F are their respective molecular weights; V and T are the volume and absolute temperature of the mixture; and R is the gas constant per mole. Combination of equations 19 and 20 gives

$$\frac{p_A}{p_F}=\frac{W_A M_F}{W_F M_A} \tag{21}$$

Further, if the total pressure of the mixture is one atmosphere or 760 mm of mercury, then

$$p_A+p_F=760 \tag{22}$$

Substituting in equation 21 the value $(760-p_F)$ for p_A, and the mixture ratio M_R for W_A/W_F, there results

$$\frac{760}{p_F}=1+M_R\cdot\frac{M_F}{M_A} \tag{23}$$

Taking logarithms of both sides, equation 23 becomes

$$\log_e\frac{p_F}{760}=-\log_e\left[1+M_R\cdot\frac{M_F}{M_A}\right] \tag{24}$$

A combination of equations 18 and 24 gives

$$a\left[1-\frac{T_n}{T}\right]=-\log_e\left[1+M_R\cdot\frac{M_F}{M_A}\right]=-2.3\log_{10}\left[1+M_R\cdot\frac{M_F}{M_A}\right]$$

which on rearrangement becomes

$$\frac{T_n}{T}=1+\frac{2.3}{a}\log_{10}\left[1+M_R\cdot\frac{M_F}{M_A}\right] \tag{25}$$

The average molecular weight of the hydrocarbons in gasoline is about that of octane, namely 114, so that M_F can be replaced by $(114+\Delta M_F)$, where ΔM_F is the difference in molecular weight of octane and any other hydrocarbon which might be considered. The average molecular weight of air M_A is 28.96 and confining attention to a 16:1 resultant mixture M_R, equation 25 can be written

$$\frac{T_n}{T_{16}}=1+\frac{2.3}{a}\log_{10}\left[1+0.553(114+\Delta M_F)\right]$$

where T_{16} is the temperature in absolute degrees corresponding to a resultant 16:1 mixture.
Rearranging,

$$\frac{T_n}{T_{16}}=1+\frac{4.154}{a}+\frac{2.3}{a}\log_{10}(1+0.0086\Delta M_F)$$

For normal paraffin hydrocarbons, $2.3/a$ is approximately equal to 0.2 so that the equation becomes

$$\frac{T_n}{T_{16}} = 1.36 + 0.2 \log_{10}(1 + 0.0086\Delta M_p) \tag{26}$$

The temperature ratio T_n/T_{16} in equation 26 is equal to 1.36 in the case of octane, since $\Delta M_p = 0$. For nonane, $\Delta M_p = 14$, in which case T_n/T_{16} equals 1.37. . It is seen that T_n/T_{16} is essentially constant for hydrocarbons having a molecular weight close to that for octane and that the ratio is not very sensitive to changes in molecular weight.

With a group of similar gasolines, the molecular weights of the vapors in 16:1 mixtures should not be very different at the same percentage evaporated. Under these conditions, equation 26 suggests that the ratio of the absolute A.S.T.M. evaporation temperature to the absolute temperature of a 16:1 resultant mixture should be essentially constant at the same percentage evaporated. The ratios would, however, be different at each constant percentage evaporated. Accordingly, the ratio T_{ASTM}/T_{16} was evaluated for each of the 38 fuels at every 10 percent evaporated from 10 to 90 percent inclusive. At each constant percentage evaporated, the ratios were found to be approximately constant, as can be seen by comparing the average ratio at the bottom of the columns in table 11 with the observed values.

The correlation of dew point values with the A.S.T.M. data in the manner outlined above for partial volatility data is not feasible. It is impossible to obtain directly the temperature at 100 percent evaporated on the A.S.T.M. evaporation curve in the case of those gasolines which cannot be distilled dry, and it is impracticable to obtain this temperature by extrapolation due to the increasing curvature of the evaporation curve near the end point. Further, the temperatures recorded by the distillation thermometer near the end point are subject to considerably larger experimental error than are those between 10 and 90 percent evaporated. It was observed, however, that the 16:1 dew points were closely related to the temperatures at 90 percent evaporated on the A.S.T.M. evaporation curves. For each gasoline, the 90 percent point in absolute degrees was divided by the 16:1 dew point in absolute degrees and the ratios $T_{90\%}/T_{DP16}$ were found to be fairly constant, as can be seen from table 12, where the average ratio is given at the bottom of the column of observed ratios.

In correlating the bubble points with the A.S.T.M. data, the temperatures at 0 percent evaporated on the A.S.T.M. evaporation curves cannot, in general, be determined. There is ordinarily some distillation loss, so that the initial boiling point of the gasoline becomes the temperature at some percentage higher than 0 percent evaporated. Further, extrapolation to the temperature at 0 percent evaporated is not feasible, due to the increasing curvature at small percentages evaporated. Work on vapor pressures of gasolines indicated that there was a relation between the vapor pressure data and the A.S.T.M. evaporation temperatures at 10 percent evaporated, and this suggests an analogous relation for bubble points of 16:1 air-vapor mixtures. Accordingly, for each fuel the 10 percent point in degrees absolute

was divided by the 16:1 bubble point in degrees absolute and the ratios $T_{10\%}/T_{BP16}$ were found to be very constant for the 5 fuels studied, as seen from table 13.

It should be pointed out that, while the A.S.T.M. and volatility data were compared at the same numerical percentages evaporated, the A.S.T.M. evaporation data are expressed in terms of volume percent, whereas the volatility data are expressed in terms of weight percent. The difference between the two types of percentage is appreciable, but not very large, and a correction to a common basis could be made if the density of the distillate in the A.S.T.M. tests were determined for a number of percentages evaporated. Since this requires additional experimentation and since each of the two types of percentage are in extensive use, the comparison was made in the somewhat illogical manner using the accepted variables, thereby permitting an interpretation of the A.S.T.M. evaporation curves directly in terms of the temperatures corresponding to various resultant air-vapor mixtures.

2. FINAL METHOD OF CORRELATION [9]

(a) GENERAL METHOD

A study of the temperature ratios showed that there was a trend with the volatility of the gasoline. Thus, for example, the ratios for a natural gas gasoline were lower than those for U.S. motor gasoline. This could be predicted from equation 25, for the molecular weights of the vapors from the two types of gasolines will differ considerably. Further, the constant a becomes smaller as the molecular weight M_r decreases. Equation 25 could be modified to take into account the variation of a with molecular weight in the case of pure hydrocarbons, but the application to the volatility data would be involved since the molecular weights of the vapors in air-gasoline mixtures are, in general, not known and their determination is difficult. Accordingly, a different type of relation was deduced for pure hydrocarbons.

From the data of Young [10] on the boiling points of pure hydrocarbons, use was made of the vapor pressure equation of Cragoe [11] to calculate the temperatures at which the vapor pressures corresponded in each case to a 16:1 air-vapor mixture, as given by equation 13. These data are tabulated in table 10. Values of $t_n - t_{16}$ were computed and it was found that these values could be expressed as a function of t_n by means of the equation $t_n - t_{16} = 65 + t_n/3$ which on arranging becomes

$$\frac{T_n}{T_{16}} = 1.5 - \frac{39}{T_{16}} \tag{27}$$

This equation relates temperature ratio and volatility, but does not take into consideration the fact that the distillation curve for a pure hydrocarbon is a straight horizontal line, while that for a gasoline in general shows curvature over the whole distillation range.

[9] Briefly described by Bridgeman, SAE Jour., p. 345, October, 1929.
[10] Young, Proc. Royal Irish Acad., vol. 38, 65, 1928.
[11] Cragoe, Int. Crit. Tables, vol. 3, p. 228, 1928.

TABLE 10.—*16:1 Temperatures for pure hydrocarbons*

Hydrocarbon	Boiling point	16:1 temperatrue		Hydrocarbon	Boiling point	16:1 temperature	
		Cragoe equation	Equation 27			Cragoe equation	Equation 27
	°C	°C	°C		°C	°C	°C
C_4H_{10}	−1.0	−67	−66	C_9H_{20}	149.8	35	35
C_5H_{12}	36.1	−42	−41	$C_{10}H_{22}$	173.2	51	50
C_6H_{14}	68.8	−20	−19	$C_{11}H_{24}$	194.7	66	65
C_7H_{16}	98.4	0	1	$C_{12}H_{26}$	215.1	79	78
C_8H_{18}	125.3	19	18	$C_{13}H_{28}$	233.9	92	91

It seemed apparent that, in the limiting case of zero slope, a general relation for the temperature ratios of gasolines would reduce to equation 27. Thus, the relation for gasolines would be of the general form

$$\frac{T_{\text{ASTM}}}{T_{16}} = 1.5 - \frac{C}{T_{16}} \tag{28}$$

where C is a function of the slope of the A.S.T.M. evaporation curve and of the percentage evaporated, and reduces to 39 for pure hydrocarbons.

(b) APPLICATION TO PARTIAL VOLATILITY DATA

Analytical treatment of all of the partial volatility data on the 38 fuels showed that the parameter C of equation 28 could be expressed by means of the relation

$$C = \sqrt{460\ S}\ .\ \log_{10}\left[\frac{100-P}{50}\right] + 39 \tag{29}$$

where S is the slope of the A.S.T.M. evaporation curve at any given percentage evaporated P. The slope is expressed in terms of degrees centigrade change per unit change in the percentage evaporated.

When $S=0$, the first term of equation 29 drops out leaving $C=39$, regardless of the percentage evaporated. This is the condition for pure hydrocarbons. When $P=50$, the first term again drops out leaving $C=39$, this time independent of the slope. This deduction from the equation appears to be accurately substantiated by the experimental data, namely, that with respect to temperature ratios over the range from 8:1 to 20:1 along a line of 50 percent evaporated, a gasoline behaves as if it were a pure hydrocarbon with a boiling point equal to the A.S.T.M. 50 percent point.

The slopes of the A.S.T.M. evaporation curve at every 10 percent evaporated from 10 to 90 percent were obtained for each fuel from the plotted curves, and the value of T_{ASTM}/T_{16} was computed for every point according to the relation in equations 28 and 29. These computed ratios are compared in table 11 with the ratios obtained from the experimental volatility data. The observed ratios are shown in the upper row of figures for each fuel and the computed ratios in the lower row.

TABLE 11.—*Comparison of observed and calculated temperature ratios for 16:1 mixtures*

Fuel number	For various percentages evaporated								
	10	20	30	40	50	60	70	80	90
1[1]	1.344	1.348	1.355	1.365	1.372	1.383	1.390	1.407	1.439
	1.339	1.348	1.359	1.365	1.372	1.383	1.390	1.407	1.448
2	1.324	1.322	1.329	1.342	1.362	1.386	1.407	1.427	1.467
	1.319	1.326	1.333	1.342	1.357	1.372	1.394	1.418	1.454
3	1.314	1.340	1.358	1.370	1.377	1.385	1.396	1.412	1.442
	1.320	1.340	1.358	1.366	1.377	1.385	1.393	1.408	1.446
1A	1.318	1.341	1.354	1.365	1.373	1.383	1.395	1.414	1.454
	1.318	1.337	1.348	1.356	1.369	1.383	1.395	1.414	1.458
2A	1.313	1.341	1.350	1.355	1.364	1.379	1.395	1.414	1.454
	1.318	1.341	1.350	1.355	1.369	1.383	1.395	1.414	1.458
3A	1.335	1.350	1.355	1.361	1.368	1.381	1.395	1.414	1.451
	1.327	1.346	1.351	1.357	1.372	1.381	1.395	1.410	1.455
4A	1.320	1.348	1.358	1.368	1.368	1.383	1.396	1.414	1.444
	1.320	1.344	1.353	1.360	1.372	1.383	1.392	1.405	1.453
A	1.314	1.331	1.337	1.355	1.369	1.381	1.404	1.421	1.456
	1.314	1.331	1.342	1.355	1.369	1.377	1.396	1.417	1.452
B	1.312	1.325	1.338	1.349	1.365	1.371	1.384	1.394	1.426
	1.312	1.325	1.338	1.349	1.355	1.362	1.375	1.389	1.426
C	1.316	1.330	1.336	1.344	1.357	1.370	1.384	1.413	1.460
	1.316	1.330	1.341	1.349	1.361	1.370	1.384	1.413	1.460
D	1.317	1.334	1.344	1.351	1.363	1.366	1.370	(1.385)	1.487
	1.321	1.339	1.349	1.355	1.363	1.370	1.383	(1.418)	1.487
E	1.318	1.330	1.341	1.356	1.367	1.376	1.394	1.421	1.457
	1.318	1.335	1.350	1.360	1.367	1.376	1.394	1.417	1.457
F	1.312	1.322	1.338	1.362	1.384	1.398	1.400	1.409	1.436
	1.307	1.331	1.346	1.362	1.380	1.385	1.391	1.405	1.445
RH	1.326	1.338	1.345	1.353	1.362	1.370	1.386	1.401	1.436
	1.326	1.338	1.345	1.353	1.362	1.375	1.382	1.406	1.445
L	1.345	1.345	1.346	1.352	1.357	1.366	1.375	1.395	1.426
	1.349	1.355	1.355	1.361	1.361	1.370	1.375	1.395	1.436
6	1.313	1.330	1.340	1.359	1.374	1.384	1.398	1.414	1.448
	1.327	1.339	1.345	1.364	1.369	1.379	1.389	1.410	1.452
G	1.325	1.334	1.338	1.346	1.352	1.365	1.389	1.427	1.469
	1.329	1.338	1.343	1.350	1.357	1.365	1.389	1.414	1.460
H	1.321	1.329	1.329	1.330	1.345	1.365	1.390	1.424	1.457
	1.316	1.334	1.343	1.344	1.359	1.375	1.395	1.415	1.453
I	1.326	1.330	1.340	1.345	1.345	1.355	1.381	1.419	1.470
	1.322	1.335	1.340	1.345	1.349	1.360	1.385	1.419	1.461
RPC	1.314	1.320	1.332	1.343	1.356	1.368	1.390	1.416	1.445
	1.314	1.330	1.336	1.347	1.365	1.377	1.394	1.416	1.449
J	1.303	1.316	1.326	1.349	1.365	1.388	1.406	1.428	1.450
	1.303	1.321	1.340	1.349	1.369	1.379	1.402	1.415	1.446
K	1.310	1.327	1.339	1.352	1.362	1.371	1.389	1.409	1.444
	1.310	1.327	1.339	1.352	1.362	1.371	1.385	1.409	1.444
N	1.318	1.331	1.346	1.353	1.360	1.374	1.388	1.410	1.436
	1.327	1.340	1.351	1.357	1.374	1.378	1.397	1.414	1.441
O	1.310	1.320	1.335	1.349	1.364	1.379	1.394	1.412	1.429
	1.315	1.335	1.349	1.354	1.373	1.384	1.398	1.408	1.438
M	1.316	1.325	(1.335)	1.351	1.367	1.377	1.398	1.422	1.456
	1.320	1.339	(1.348)	1.355	1.371	1.381	1.398	1.422	1.465
B3	1.310	1.326	1.341	1.355	1.361	1.369	1.381	1.405	1.437
	1.306	1.326	1.337	1.346	1.361	1.369	1.381	1.405	1.441
101	1.318	1.322	1.328	1.328	1.341	1.353	1.372	1.397	1.441
	1.312	1.322	1.322	1.332	1.341	1.353	1.368	1.393	1.441
111	1.320	1.321	1.326	1.332	1.346	1.362	1.380	1.406	1.448
	1.320	1.320	1.332	1.337	1.346	1.356	1.371	1.392	1.442
121	1.332	1.334	1.337	1.340	1.344	1.350	1.359	1.379	1.425
	1.328	1.334	1.341	1.340	1.344	1.350	1.364	1.385	1.439
S1	1.306	1.322	1.335	1.341	1.356	1.375	1.389	1.414	1.440
	1.310	1.322	1.339	1.345	1.360	1.371	1.389	1.410	1.436
S2	1.306	1.323	1.332	1.348	1.362	1.376	1.394	1.418	1.444
	1.310	1.323	1.332	1.348	1.362	1.372	1.390	1.409	1.444
S3	1.310	1.320	1.331	1.344	1.351	1.370	1.386	1.410	1.442
	1.310	1.326	1.337	1.344	1.347	1.370	1.382	1.406	1.442
S4	1.308	1.316	1.327	1.340	1.356	1.368	1.392	1.415	1.447
	1.312	1.322	1.332	1.340	1.352	1.368	1.388	1.411	1.451
S5	1.315	1.312	1.319	1.335	1.357	1.372	1.393	1.412	1.450
	1.311	1.318	1.330	1.339	1.348	1.363	1.389	1.408	1.450
S6	1.305	1.311	1.326	1.343	1.355	1.373	1.388	1.417	1.457
	1.309	1.317	1.326	1.343	1.346	1.364	1.384	1.408	1.453
EB1	1.313	1.321	1.324	1.341	1.364	1.375	1.387	1.399	1.426
	1.313	1.321	1.324	1.331	1.348	1.360	1.372	1.389	1.433
EB2	1.315	1.322	1.325	1.326	1.336	1.350	1.394	(1.416)	1.444
	1.315	1.322	1.325	1.326	1.336	1.350	1.377	(1.395)	1.439
EB3	1.315	1.319	1.323	1.327	1.327	1.335	1.341	1.370	1.458
	1.314	1.319	1.323	1.327	1.331	1.335	1.341	1.374	1.458
Average of observed ratios	1.317	1.328	1.337	1.348	1.359	1.372	1.388	1.410	1.447

[1] The upper row of figures for each fuel is the observed ratio; the lower row, the calculated.

The effect of slope of the A.S.T.M. evaporation curves at the 10, 50, and 90 percent points on the temperatures of 16:1 resultant mixtures is shown in figure 10 for three hypothetical fuels which have identical A.S.T.M. temperatures at these three points. At the 10 percent point, fuel I, with the largest slope, shows a 16:1 temperature 6° C. higher than fuel III with the smallest slope; at the 50 percent point, all three fuels have the same 16:1 temperature regardless of

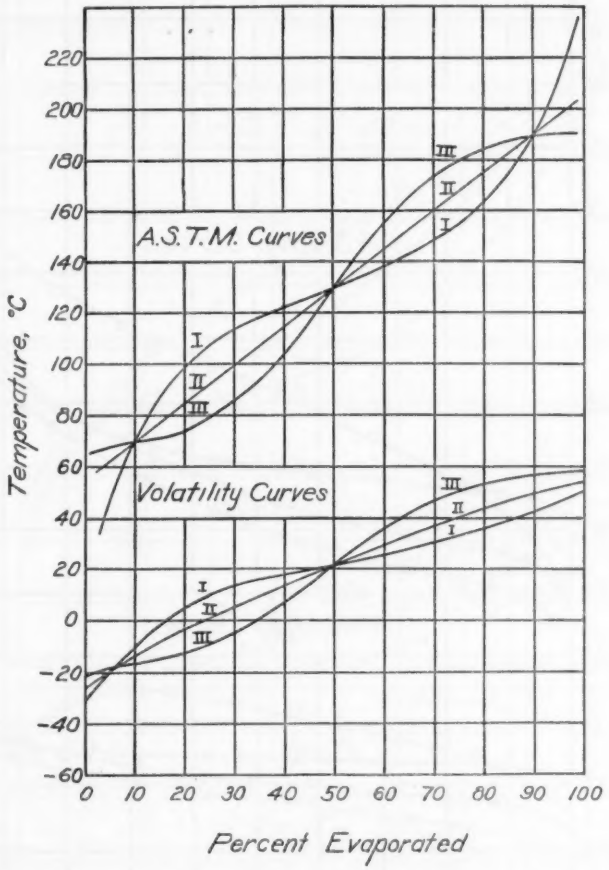

FIGURE 10.—*Volatility and A.S.T.M. evaporation curves for 3 hypothetical fuels showing the effects of variation in slope of the A.S.T.M. curves at 10, 50, and 90 percent evaporated.*

the slope; and at 90 percent, fuel I, with the largest slope, shows a 16:1 temperature 15° C. lower than fuel III, with the smallest slope.

The types of volatility curves obtained with aviation fuels, benzene blends and ethyl ether blends are shown respectively in figures 11, 12, and 13. In each figure, the upper set of curves are the A.S.T.M. evaporation curves of the fuels, while the lower set are volatility curves representing the temperatures corresponding to 16:1 resultant air-vapor mixtures formed from the above fuels. Descriptions of these fuels, including the composition of the blends, have been given in table 1.

(c) APPLICATION TO DEW-POINT DATA

In the preliminary correlation of the dew points with the A.S.T.M. data, it was found that a relation existed between the dew-point temperatures and the A.S.T.M. evaporation temperatures at 90

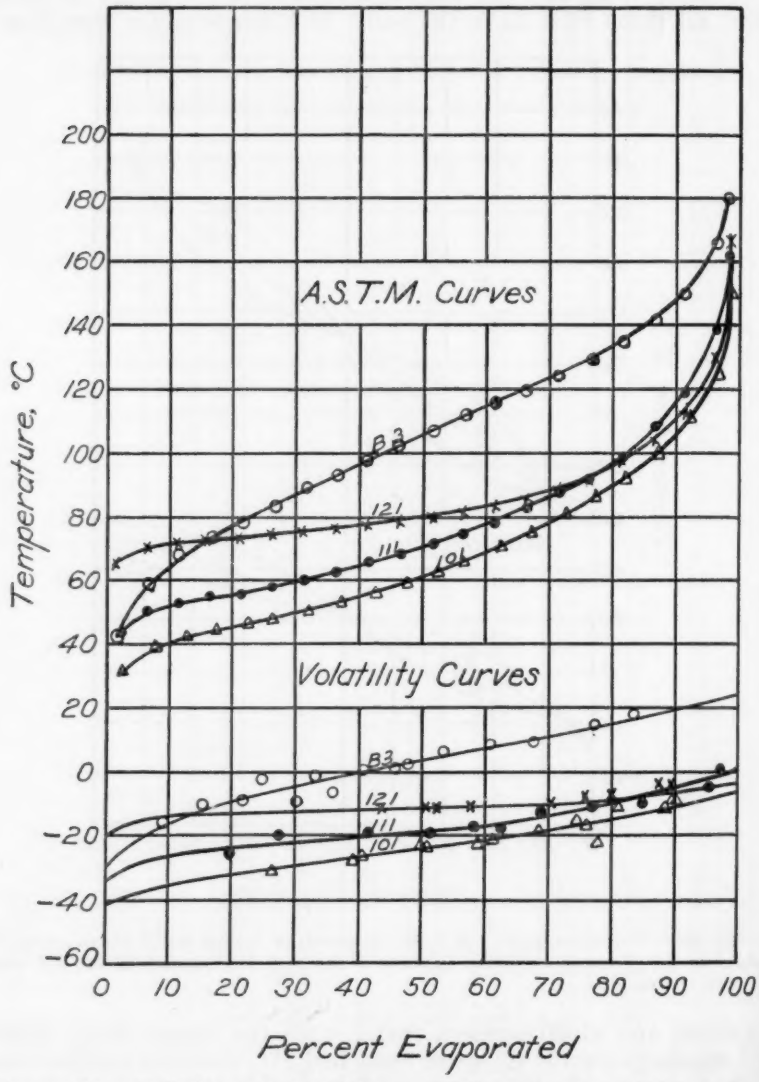

FIGURE 11.—*Volatility and A.S.T.M. evaporation curves for aviation fuels.*

percent evaporated. Accordingly, the following relation analogous to equation 28 should hold for dew points.

$$\frac{T_{90\%}}{T_{DP16}} = 1.5 - \frac{C}{T_{DP16}} \tag{30}$$

where the temperatures are in absolute centigrade degrees, and C is a function of the slope S of the A.S.T.M. evaporation curve at the 90 percent point, expressed as degrees centigrade change per unit change

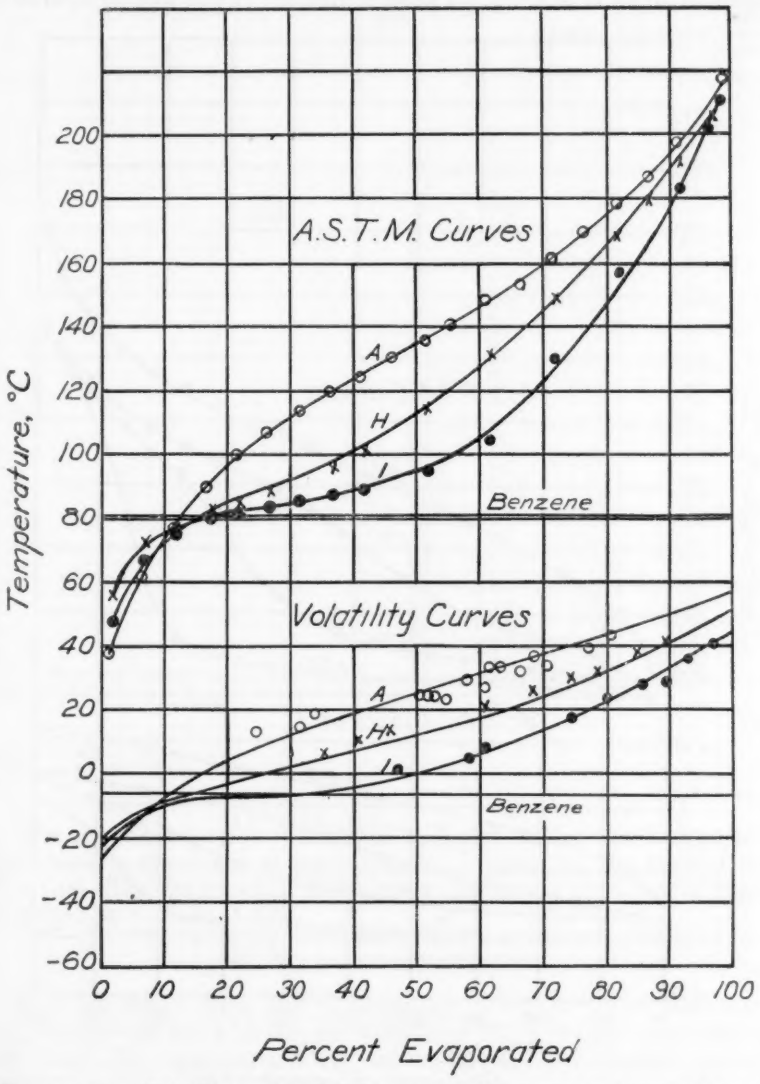

FIGURE 12.—*Volatility and A.S.T.M. evaporation curves for benzene blends.*

in the percentage evaporated. The relation between C and the slope S is

$$C = -10\sqrt{S} + 39 \tag{31}$$

Equations 30 and 31 may be combined and rearranged to give

$$1.5\, t_{DP_{16}} = t_{90\%} - 10\sqrt{S} + 39 \tag{32}$$

where the temperatures are in centigrade degrees. These equations are applicable to pure hydrocarbons, conditioned by $S=0$.

For each gasoline, the value of the ratio $T_{90\%}/T_{DP16}$ was computed using equations 30 and 31. These computed ratios are compared in

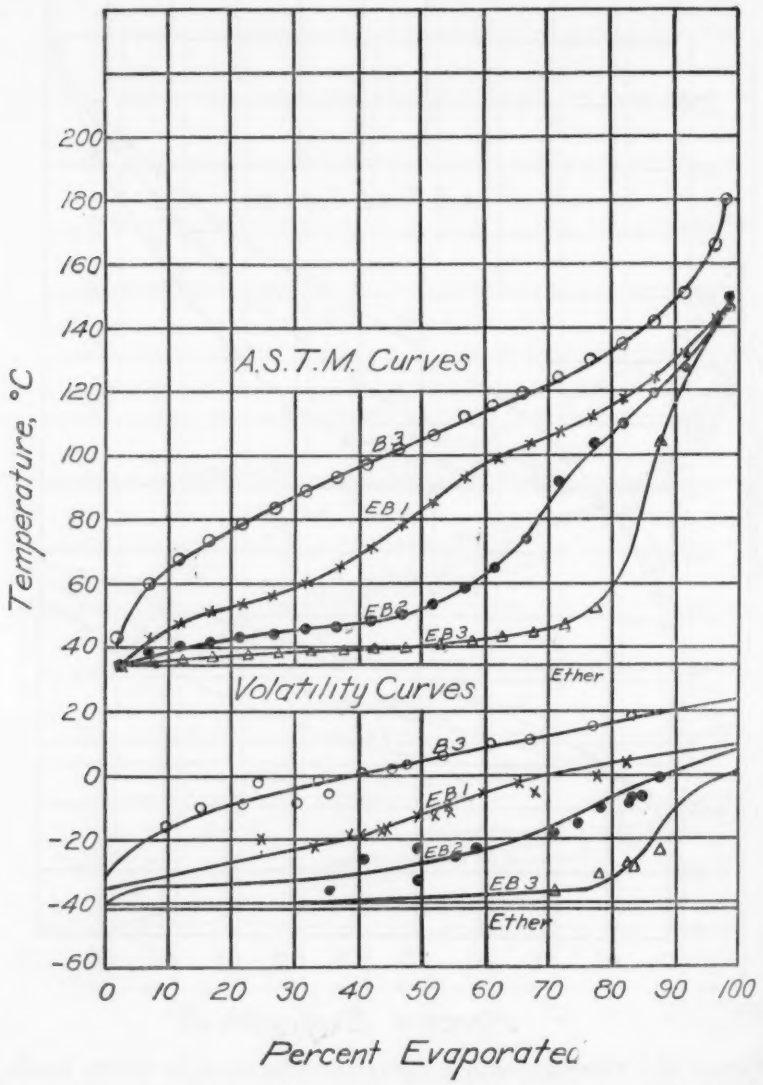

FIGURE 13.—*Volatility and A.S.T.M. evaporation curves for ethyl ether blends.*

table 12 with the ratios obtained from the experimentally determined dew points. The data for fuels 1A, 2A, 3A, and 4A, are shown in parentheses, because they were obtained by extrapolation over a much longer range than usual.

TABLE 12.—*Dew-point data for 16:1 mixtures*

Fuel number	90 percent point	Slope	$T_{10\%}/T_{DP_{16}}$		Difference between observed and calculated temperature
			Observed	Calculated	
					°C
1	199	2.1	1.422	1.426	1
2	195	2.4	1.423	1.427	1
3	197	2.1	1.429	1.425	−1
1A	195	2.8	(1.431)	1.431	0
2A	195	2.7	(1.436)	1.431	−1
3A	193	2.4	(1.430)	1.426	−1
4A	186	2.3	(1.426)	1.426	0
A	196	2.3	1.426	1.426	0
B	132	1.7	1.411	1.406	−1
C	174	3.2	1.428	1.428	0
D	200	5.4	1.434	1.447	3
E	199	2.4	1.426	1.426	0
F	198	2.0	1.428	1.424	−1
RH	168	2.2	1.423	1.419	−1
L	152	1.8	1.417	1.417	0
6	190	2.5	1.420	1.424	1
G	178	3.2	1.423	1.432	2
H	186	2.5	1.421	1.425	1
I	177	3.4	1.420	1.429	2
RPC	198	2.2	1.419	1.423	1
J	207	2.0	1.420	1.424	1
K	176	2.2	1.425	1.421	−1
N	204	1.7	1.415	1.419	1
O	200	1.7	1.408	1.420	3
M	222	3.0	1.423	1.435	3
B3	148	2.0	1.418	1.418	0
101	106	2.5	1.409	1.409	0
111	115	2.5	1.416	1.411	−1
121	110	2.3	1.408	1.408	0
S1	165	1.7	1.422	1.413	−2
S2	166	1.8	1.425	1.416	−2
S3	161	2.0	1.414	1.418	1
S4	161	2.4	1.418	1.423	1
S5	159	2.5	1.421	1.421	0
S6	154	2.8	1.419	1.423	1
EB1	128	1.8	1.417	1.407	−2
EB2	124	2.1	1.413	1.413	0
EB3	112	3.8	1.410	1.420	2
Average observed ratio=1.421					
Grand average deviation=					1.0

The effect of slope is illustrated in figure 14 for three hypothetical fuels having the same 90 percent point, slopes varying from 0 to 5.0. The fuel with the greatest slope has a dew point 13° C lower than the fuel with zero slope.

(d) APPLICATION TO BUBBLE-POINT DATA

In accordance with the preliminary relation found between the 16:1 bubble points and the temperatures at 10 percent evaporated on the A.S.T.M. evaporation curves, equation 28 becomes for bubble points:

$$\frac{T_{10\%}}{T_{BP16}} = 1.5 - \frac{C}{T_{BP16}} \tag{33}$$

where the temperatures are in absolute centigrade degrees. The relation between C and the slope of the A.S.T.M. evaporation curve at the 10 percent point is as follows:

$$C = -10\sqrt{S} + 39 \tag{34}$$

It is interesting that equation 34 is formally identical with equation 31, relating C and S at the 90 percent point in the evaluation of dew points.

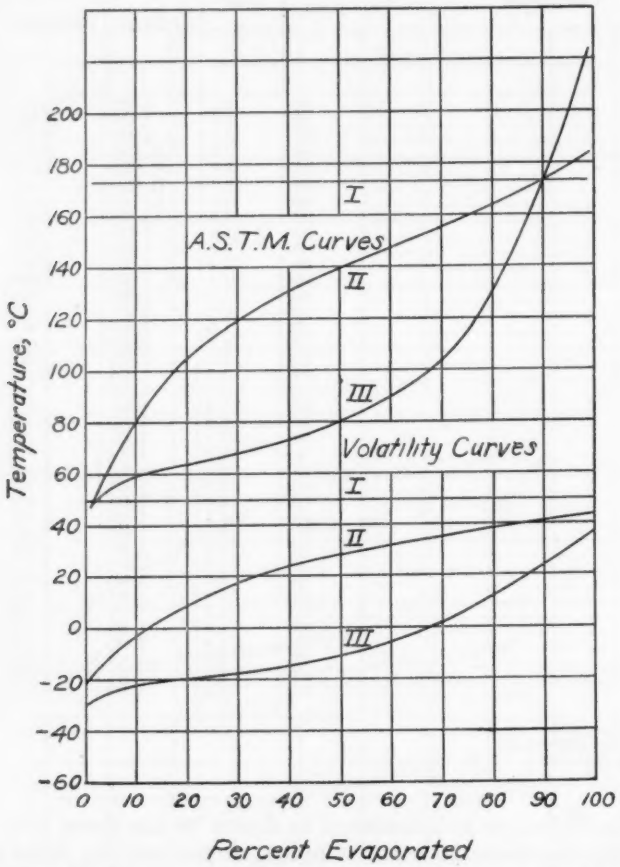

FIGURE 14.—*Volatility and A.S.T.M. evaporation curves for 3 hypothetical fuels showing the effect on the dew point of variation in the slope of the A.S.T.M. curve at 90 percent evaporated.*

The ratio $T_{10\%}/T_{BP16}$ was computed for each fuel by means of equations 33 and 34 and a comparison is made in table 13 between these computed ratios and those obtained from the experimentally determined bubble points.

TABLE 13.—*Bubble-point data for 16:1 mixtures*

Fuel	$T_{10\%}/T_{EP16}$		S	10% point
	Obs.	Comp.		
				° C
A	1.410	1.414	3.0	75
B	1.400	1.400	2.1	63
C	1.401	1.402	2.2	69
J	1.408	1.402	2.5	54
M	1.409	1.410	2.5	89

Average observed ratio = 1.406.

The effect of slope at the 10 percent point is illustrated in figure 15 for three hypothetical fuels having the same 10 percent point, but

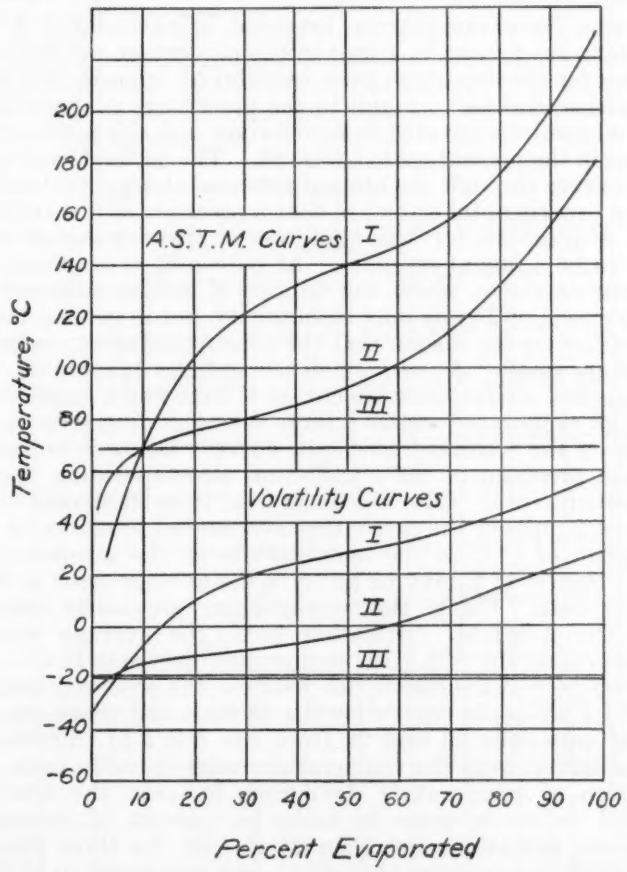

FIGURE 15.—*Volatility and A.S.T.M. evaporation curves for 3 hypothetical fuels showing the effect on the bubble point of variation in slope of the A.S.T.M. curve at 10 percent evaporated.*

slopes varying from 0 to 5.0. The fuel with the greatest slope has a bubble point 14° C lower than the pure hydrocarbon with zero slope.

VIII. ACCURACY OF VOLATILITY DATA AND OF CORRELATION WITH A.S.T.M. DISTILLATION DATA

1. CONSIDERATION OF PARTIAL VOLATILITY

The accuracy of the partial volatility data is largely determined by the precision of calibration of the equilibrium air-evaporation apparatus and accessories and by the sensitivity of the method. The estimated precisions of the various parts of the apparatus and of the factors affecting the accuracy of the results, based on the calibration data and on experimental checks, are as follows:

Air feed	0.2 percent
Gasoline feed	0.2 percent
Volume of residue	0.2 percent
Specific gravity determinations	0.1 percent
Evaporation bath temperature	0.1 C
Time for collection of residue	0.3 percent

Considering the various factors involved, it is estimated that the observed data are precise to 1 unit in the percentage evaporated. The correction for the departure from equilibrium vaporization was found to be precise likewise to 1 unit in the percentage evaporated, so that individual results, corrected to equilibrium, may be considered precise to 2 units in the percentage evaporated. The method used of drawing smooth curves through the plotted experimental points tends to minimize the experimental errors, so that a precision of 2 units in the percentage evaporated for the equilibrium air-evaporation apparatus appears to be a liberal estimate. At percentages evaporated around 95 percent or above, where the volume of residue collected is small, errors in excess of 2 units may be obtained, but in general the slope of the volatility curves is such that the corresponding errors in the temperature are small. At very small percentages evaporated, the slope of the supplied air-fuel mixture curves is large and a small error in the percentage evaporated causes a large corresponding error in the temperature on the resultant air-vapor curve. Below 5 percent evaporated, the precision of the equilibrium air-evaporation apparatus is very unsatisfactory. Over the range from 10 to 90 percent evaporated an error of 2 units in the percentage evaporated produces on the average an error of 1° C in the temperatures on the resultant air-vapor curves. Hence, 1° C may be taken as the average error in the partial volatility data. Using the precautions, previously outlined, in making the A.S.T.M. distillation tests, the average error in the temperatures on the A.S.T.M. evaporation curves is 1° C.

The accuracy of the correlation between the observed temperatures on the 16:1 air-vapor curves for the 38 fuels and those computed by means of equations 28 and 29 from the A.S.T.M. distillation data can be observed from the temperature ratios listed in table 11. The distribution of temperature deviations between the observed and calculated values is given in table 14. About 87 percent of the points show deviations less than 2° C. Of the three points which showed deviations greater than 3° C, two amounted to 4° C and the other to 7° C. It is believed that the deviations at these three points are without significance, being attributable to experimental error, and for this reason the ratios at these three points are shown in parentheses in table 11. For further comparison, the temperature deviations between the observed and computed 16:1 temperatures are shown graphically in figures 16, 17, and 18 for 10, 50, and 90 percent evap-

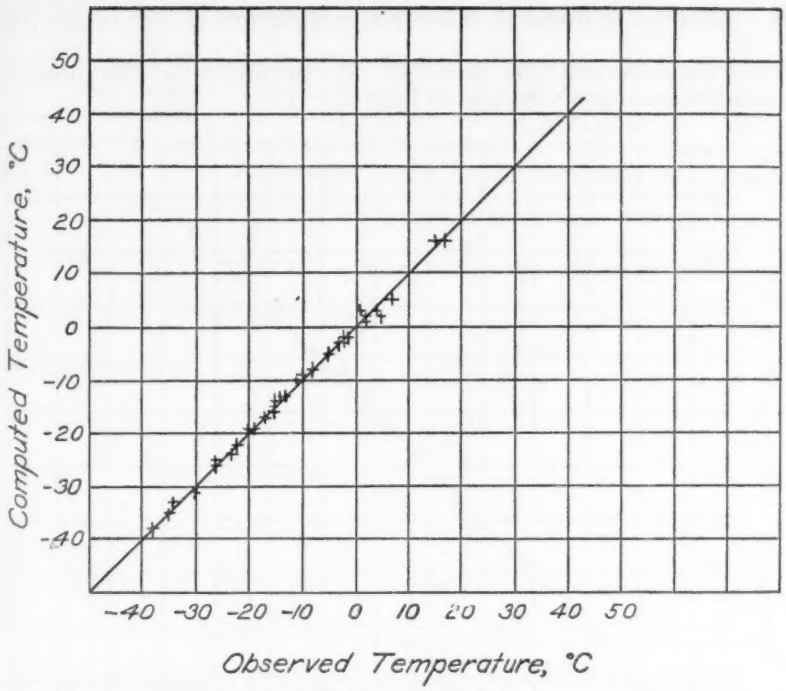

FIGURE 16.—*Plot showing agreement between observed and computed volatility data at 10 percent evaporated.*

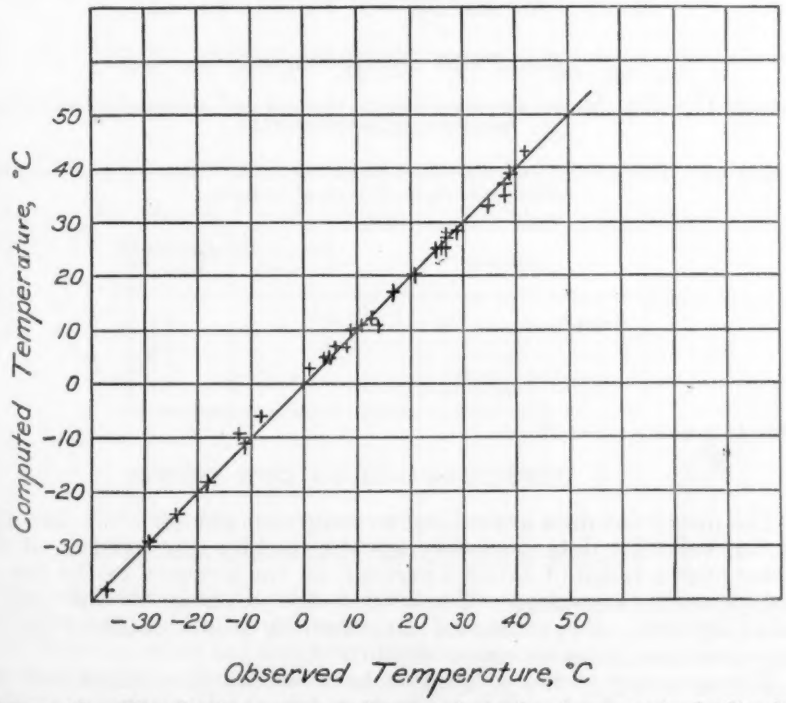

FIGURE 17.—*Plot showing agreement between observed and computed volatility data at 50 percent evaporated.*

orated respectively. The grand average deviation between observed and computed values for the 38 fuels is 1° C.

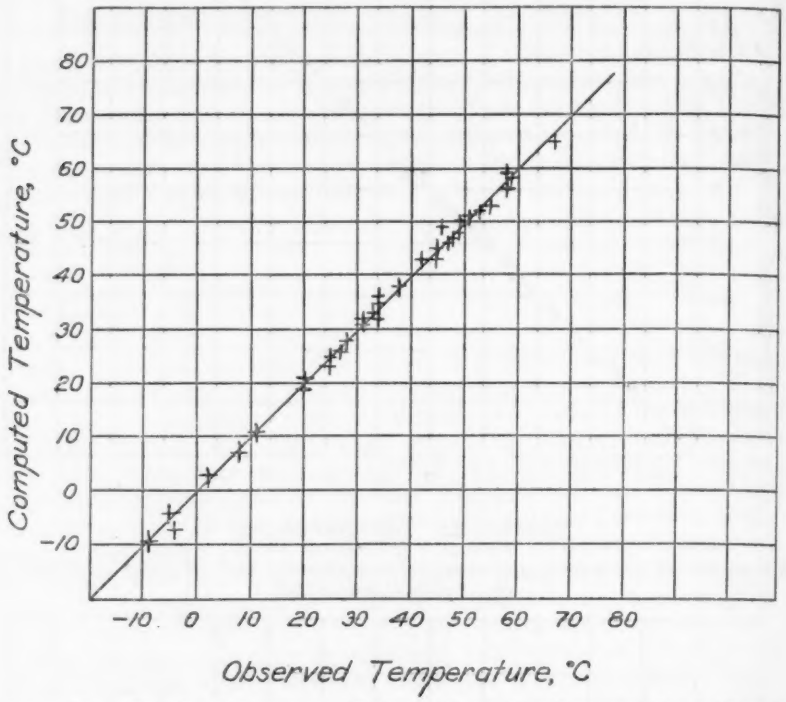

FIGURE 18.—*Plot showing agreement between observed and computed volatility data at 90 percent evaporated.*

TABLE 14.—*Distribution of temperature deviations between observed and computed values from 10 to 90 percent inclusive.*

Deviation ° C	Number of points	Percent of points
Above 3	3	0.9
3	22	6.4
2	50	14.6
1	150	43.9
0	117	34.2

Grand average deviation=1° C.

2. CONSIDERATION OF DEW POINTS

The dew-point data are subject to somewhat greater error than the partial volatility data since they are obtained by extrapolation of the latter over a range of about 5 percent, on the average, to the line of 100 percent evaporated. Considering the accuracy of the partial volatility data, it is estimated that the dew points obtained by the extrapolation process are accurate to 2° C.

The accuracy of the correlation between the dew points and the 90-percent A.S.T.M. points is illustrated in the last column of table

12 which lists the temperature differences between the observed and computed values. The distribution of temperature deviations is given in table 15. About 74 percent of the points show deviations less than 2° C., and only 3 out of the 34 fuels show deviations amounting to 3° C. For further comparison, the temperature deviations

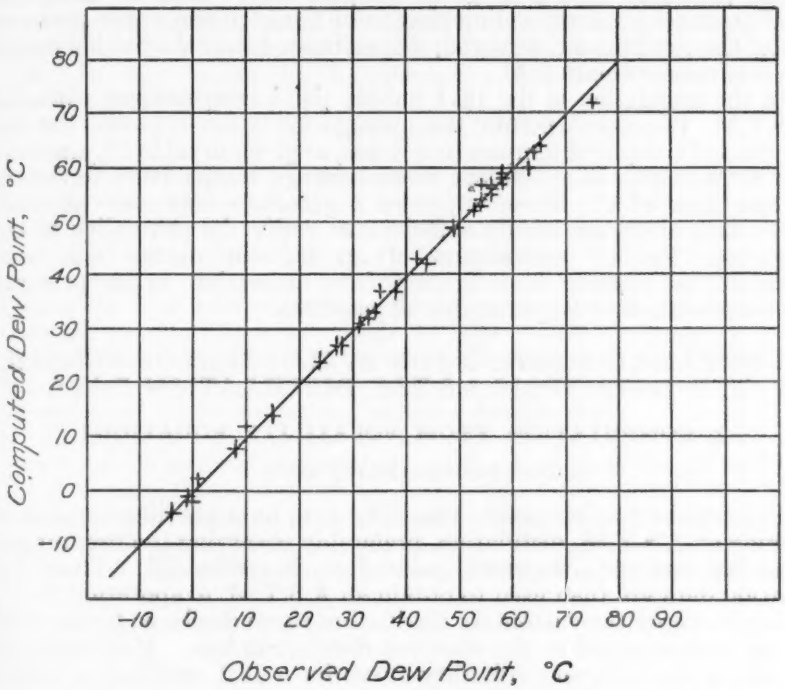

FIGURE 19.—*Plot showing agreement between observed and computed dew points.*

between the observed and computed 16:1 dew points are shown graphically in figure 19.

TABLE 15.—*Distribution of temperature deviations between observed and computed dew-point values.*

Deviation ° C	Number of points	Percent of points
3	3	8.8
2	6	17.6
1	16	47.1
0	9	26.5

3. CONSIDERATION OF BUBBLE POINTS

The accuracy of the bubble-point data depends upon the accuracy of the molecular weight values for the gasoline vapors present in the small bubbles, upon the accuracy of the vapor-pressure values for the gas-free gasolines, and upon how closely the gasoline vapors obey the perfect gas laws at the low pressures under consideration.

The indirect evaluation of the molecular weights of the vapors has an estimated accuracy of 5 units in molecular weight. Considering the probable deviations from the perfect gas laws, the corresponding error in the vapor pressure of the gasoline amounts to 2 mm of mercury. This is also the accuracy of the experimentally determined vapor pressures over a range of temperatures. Since a change of 1° C produces a corresponding change of 1 mm in the vapor pressure under the conditions considered, it is estimated that the bubble points are accurate to about 2° C.

In the correlation of the 16:1 bubble point temperatures with the A.S.T.M. 10-percent points, the average deviation between the observed and computed temperature ratios, as given in table 13, amounts to 0.0024. This is equivalent to an average temperature deviation of less than 1° C. However, since 5 gasolines only were studied, these data alone are hardly sufficient to verify the generality of the relations. Further verification of an indirect nature has been obtained in another investigation from extensive vapor pressure measurements on a large number of gasolines.

IX. DETAILED METHOD FOR EVALUATION OF VOLATILITY DATA FROM A.S.T.M. DISTILLATION DATA

1. COMPUTATION FROM VOLATILITY EQUATIONS

(a) PARTIAL VOLATILITY DATA

The first step in obtaining volatility data on a gasoline consists in making an A.S.T.M. distillation, preferably observing the precautions regarding temperature control pointed out in section IV. These distillation data are then used to obtain an A.S.T.M. evaporation curve, which is simply the customary distillation curve displaced to the right by an amount equal to the observed distillation loss. If it is desired to obtain the complete volatility curve for a 16:1 resultant mixture, the slope of the A.S.T.M. evaporation curve at every 10 percent evaporated is evaluated, by either of two methods. One of these is to employ the customary graphical method of laying a straight edge tangent to the curve at the point under consideration and reading the temperature difference along the line thus formed for a change of 10 percent in the percentage evaporated. The temperature difference, in degrees centigrade, divided by 10 is the desired slope. A second, less accurate method consists in reading the temperatures on the curve at 5 percent more and 5 percent less than the percentage evaporated under consideration, in subtracting the latter from the former, and finally dividing by 10. The second method ordinarily gives sufficient accuracy for the purpose if there is not a very marked change in curvature in the 10 percent range considered. For example, it is desired to find the slope of an A.S.T.M. evaporation curve at 40 percent evaporated. The temperature at 45 percent evaporated is found to be 130 C and at 35 percent evaporated, it is 110 C. Subtracting 110 from 130 gives 20, which when divided by 10 gives 2 as the slope at 40 percent evaporated.

The values of the slope at every 10 percent evaporated are then used to compute values of the parameter C at each value of the percentage evaporated P by means of equation 29.

$$C = \sqrt{460S} \cdot \log_{10}\left[\frac{100-P}{50}\right] + 39 \tag{29}$$

The next step is to read the temperatures on the plotted A.S.T.M. evaporation curve of the gasoline at every 10 percent evaporated from 10 to 90 percent. These temperatures together with the corresponding values of C, obtained from equation 29, at the same percentages evaporated, are used to compute the 16:1 temperatures by means of equation 28. In order to simplify the calculation, equation 28 may be written as follows:

$$1.5t_{16} = t_{\text{ASTM}} - (136.6 - C) \tag{34}$$

where t_{16} and t_{ASTM} are in centigrade degrees. The value of C at the percentage evaporated under consideration is subtracted from 136.6 and the resulting number is subtracted from the temperature on the A.S.T.M. evaporation curve at the same percentage evaporated as was used for the evaluation of C. This difference divided by 1.5 gives the 16:1 temperature at the particular percentage evaporated. Similar computations are made for the values at every 10 percent evaporated from 10 to 90 percent. It should be emphasized that the values of S, C, t_{ASTM} and t_{16} always refer to a common percentage evaporated when computing partial volatility data.

Example: A gasoline has an A.S.T.M. evaporation temperature of 100 C at 30 percent evaporated and has a slope of 2.0 at 30 percent evaporated. It is desired to know the temperature at which a mixture of 16 parts of air and 1 part of vapor from this gasoline will form at 30 percent evaporated. Equation 29 gives 43.4 as the value of C at 30 percent evaporated. Substituting in equation 34 the above value of C and 100 for t_{ASTM}, the 16:1 temperature at 30 percent evaporated is found to be 4.5 C.

(b) DEW-POINT DATA

The first step in obtaining dew point data on a gasoline consists in determining the value of the slope of the A.S.T.M. evaporation curve at 90 percent evaporated. From this value of the slope, C is computed by means of equation 31

$$C = -10\sqrt{S} + 39 \tag{31}$$

The next step consists in reading the temperature on the A.S.T.M. evaporation curve at 90 percent evaporated. This temperature together with the value of C from equation 31 is used to obtain the 16:1 dew point by means of equation 30, which may be written in the simpler form

$$1.5t_{DP16} = t_{90\%} - (136.6 - C) \tag{35}$$

where t_{DP16} and $t_{90\%}$ are in centigrade degrees.

When computing dew point data, S and $t_{90\%}$ refer to 90 percent evaporated whereas C and t_{DP16} refer to 100 percent evaporated.

Example: A gasoline has an A.S.T.M. evaporation temperature of 200 C at 90 percent evaporated and the A.S.T.M. evaporation curve has a slope of 2.0 at 90 percent evaporated. It is desired to know the dew point of a 16:1 mixture of air and this gasoline. From equation 31, C is found to have a value of 24.9. Substituting this value of C

in equation 35 together with 200 for $t_{90\%}$ and dividing the resultant summation by 1.5 gives 58.9 C. This is the desired 16:1 dew point.

(c) BUBBLE-POINT DATA

The first step in obtaining bubble-point data on a gasoline consists in determining the slope of the A.S.T.M. evaporation curve at 10 percent evaporated. From this value of the slope, C is computed by means of equation 33

$$C=-10\sqrt{S}+39 \tag{33}$$

The next step consists in reading the temperature on the A.S.T.M. evaporation curve at 10 percent evaporated. This temperature together with the value of C from equation 33 is used to obtain the 16:1 bubble point by means of equation 32, which may be written:

$$1.5t_{BP16}=t_{10\%}-(136.6-C) \tag{36}$$

where t_{BP16} and $t_{10\%}$ are in centigrade degrees.

When computing bubble-point data, S and $t_{10\%}$ refer to 10 percent evaporated, whereas C and t_{BP16} refer to 0 percent evaporated.

Example: A gasoline has an A.S.T.M. evaporation temperature of 60 C at 10 percent evaporated and the A.S.T.M. evaporation curve has a slope of 2.0 at 10 percent evaporated. It is desired to know the bubble point of a 16:1 mixture of air and this gasoline. From equation 33, C is found to have a value of 24.9. Substituting this value of C in equation 36 together with 60 for $t_{10\%}$, the desired bubble point $t_{BP_{16}}$ is -34.5 C.

(d) VOLATILITY DATA AT OTHER PERCENTAGES EVAPORATED AND FOR OTHER MIXTURES

Having the 16:1 temperatures at every 10 percent evaporated from 0 to 100 percent, the value at any intermediate percentage evaporated may be obtained by plotting the computed temperatures against the corresponding percentages evaporated, by drawing a smooth curve through the plotted points and by reading off this curve the temperatures at the desired percentages evaporated.

From the 16:1 values, the temperatures may readily be obtained corresponding to the formation, under equilibrium conditions, of any other desired mixture of air and gasoline vapor from 8:1 to 20:1. A method for making such transformations was indicated in figure 7, where the differences in temperature found between the various resultant mixture lines were shown as a curve. The equation of this curve can be written as follows:

$$t_{M_R}-t_{16}=52.5-43.5\log_{10}M_R \tag{37}$$

where M_R is the resultant air-vapor mixture and t_{M_R} is the temperature in centigrade degrees corresponding to the formation of the mixture M_R. In this equation, t_{M_R} and t_{16} refer to the same percentage evaporated, but the difference $t_{M_R}-t_{16}$ is the same at all percentages evaporated, being only dependent within experimental error on the value of M_R. Hence having the value of t_{16}, the temperature for any other mixture within the limits stated, may be computed.

Example: A gasoline has a 16:1 temperature of 4.5 C at 30 percent evaporated. It is desired to know the temperature corresponding to the formation of an 8:1 mixture at 30 percent evaporated. Substituting 8 for M_R in equation 37, $t_8 - t_{16}$ equals 13.1. Adding 13.1 to 4.5 gives 17.6 C which is the desired 8:1 temperature.

While equation 37 holds with sufficient accuracy for all of the gasolines studied, the difference between any two resultant mixture lines does depend to a slight extent upon the volatility of the gasoline. A more precise equation is as follows:

$$t_{M_R} - t_{16} = [0.132 - 0.109 \log_{10} M_R](t_{\text{ASTM}} + 273) \qquad (38)$$

Equation 38 reduces to equation 37 for a value of t_{ASTM} equal to 125 C.

2. GRAPHICAL EVALUATION OF VOLATILITY DATA

The detailed computation of partial volatility, dew-point and bubble-point data on gasolines from the A.S.T.M. distillation data may be avoided by the use of charts. Equations 29, 31, and 33 for the evaluation of the parameter C may be combined in one alinement chart. Equations 34, 35, and 36 may be combined in another alinement chart to give directly the temperatures corresponding to the formation of 16:1 resultant air-vapor mixtures. A duplex scale, based on equation 37, can be used to indicate the differences in temperature between 16:1 mixture lines and other mixture lines of interest. Accordingly, two alinement charts and a duplex scale have been designed so that they are as accurate as is justified from the experimental work on which they are based, namely, 1° C.

(a) CHART FOR EVALUATION OF PARAMETER C

The alinement chart for the evaluation of C from the slope of the A.S.T.M. evaporation curve and the percentage evaporated is shown in figure 20. The scale on the left, marked P, represents percentages evaporated. The horizontal scale, marked S, represents the slope of the A.S.T.M. evaporation curve. The scale on the right, marked C, represents values of the parameter C. The identical points, marked D.P. and B.P., on the P scale slightly above 80 percent evaporated are for the evaluation of C in connection with dew points and bubble points.

In using the chart, connect by means of a straight edge the appropriate mark on the P scale with the corresponding value of the slope of the A.S.T.M. evaporation curve on the S scale. The intersection of this line with the C scale gives the desired value of C. Three precautions should be observed in using this chart:

(1) In evaluating C for partial volatility data, the value of S refers to the percentage evaporated P under consideration.

(2) For dew point data, S refers to the slope at 90 percent evaporated.

(3) For bubble point data, S refers to the slope at 10 percent evaporated.

Solutions for a number of cases are given below:

P scale	S scale	Intersection on C scale
10	2.0	47
50	Any value	39
Any value	0.0	39
90	2.0	18
D.P.	2.0	25
B.P.	1.0	29

It is to be noted that when $P=50$, the slope of the A.S.T.M. evaporation curve has no effect and $C=39$ in all cases. Further, when $S=0$, C has the same value, namely, 39, at all percentages evaporated.

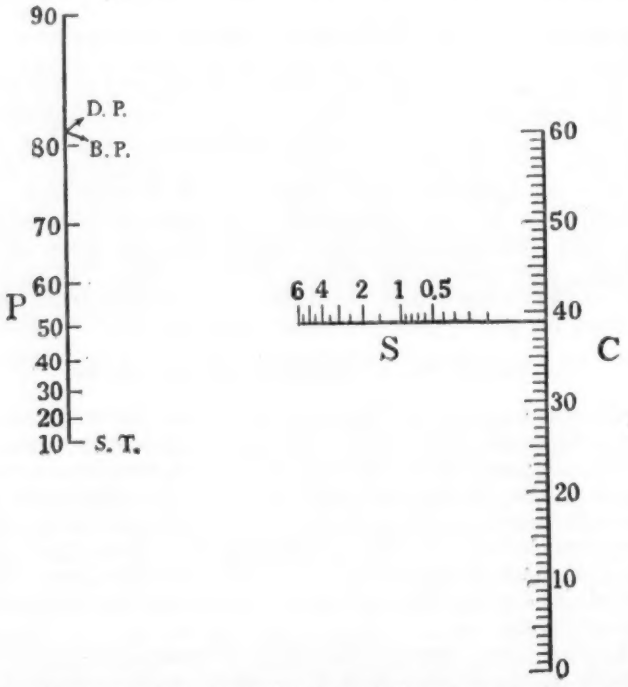

FIGURE 20.—*Alinement chart for evaluation of the parameter C in equations 29, 31, and 33 from the percentage evaporated P and the slope S of the A.S.T.M. evaporation-curve.*

(b) CHART FOR EVALUATION OF 16:1 TEMPERATURES

The chart for the evaluation of the temperatures on a 16:1 resultant air-vapor line from the values of C and the A.S.T.M. evaporation temperature is shown in figure 21. The scale on the left represents A.S.T.M. evaporation temperatures in centigrade degrees; the middle scale represents values of the parameter C; whereas the scale on the right represents temperatures in centigrade degrees for a 16:1 resultant mixture of air and gasoline vapor.

In using the chart, connect by means of a straight edge the appropriate mark on the A.S.T.M. temperature scale with the correspond-

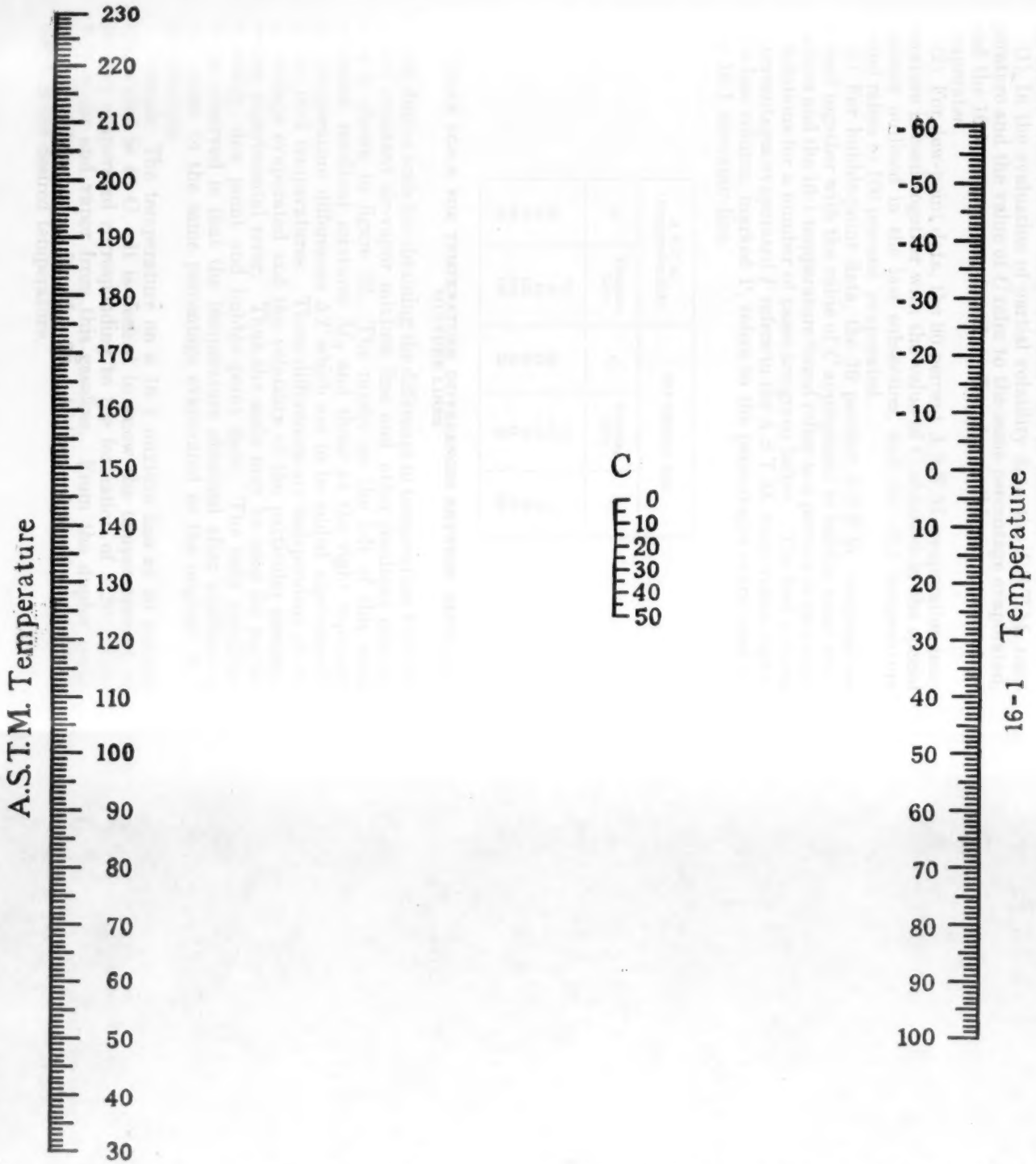

FIGURE 21.—*Alinement chart for evaluation of 16:1 temperatures on the volatility curve from the temperature on the A.S.T.M. evaporation curve and the value of the parameter C obtained from figure 20.*

64093—34. (Face p. 102)

UNIV. OF MICH.

-40
-30
-20
-10
0
10
20
30
40
50
60
70
80
90
100
110
120
130
140
150
160
170
180
190
200
210
220
230

ing value of C on the middle scale, and extrapolate the line thus formed to cut the 16:1 temperature scale. The intersection of the line with the scale gives the desired 16:1 temperature. The precautions which should be observed in using this chart are as follows:

(1) In the evaluation of partial volatility data, the A.S.T.M. temperature and the value of C refer to the same percentage evaporated, and the 16:1 temperature found applies also to this same percentage evaporated.

(2) For dew-point data, the 90 percent A.S.T.M. evaporation temperature is used together with the value of C obtained in the special manner outlined in the last subsection, and the 16:1 temperature found refers to 100 percent evaporated.

(3) For bubble-point data, the 10 percent A.S.T.M. temperature is used together with the value of C appropriate to bubble point evaluations and the 16:1 temperature found refers to 0 percent evaporated.

Solutions for a number of cases are given below. The first column of percentages evaporated P refers to the A.S.T.M. evaporation curve. The last column, marked P, refers to the percentages evaporated on the 16:1 air-vapor line.

A.S.T.M. evaporation data		16:1 volatility data		
P	Temperature	C	Temperature	P
	°C		°C	
10	60	29	−32	0
10	60	47	−20	10
50	125	39	18	50
90	180	18	41	90
90	180	25	46	100

(c) DUPLEX SCALE FOR TEMPERATURE DIFFERENCES BETWEEN RESULTANT MIXTURE LINES

The duplex scale for obtaining the difference in temperature between a 16:1 resultant air-vapor mixture line and other resultant mixture lines is shown in figure 22. The marks on the left of this scale represent resultant mixtures M_R and those at the right represent the temperature differences ΔT which are to be added algebraically to the 16:1 temperatures. These differences are independent of the percentage evaporated and the volatility of the particular gasoline, within experimental error. Thus the scale may be used for partial volatility, dew point and bubble point data. The only condition to be observed is that the temperature obtained after addition of ΔT refers to the same percentage evaporated as the original 16:1 temperature.

Example: The temperature on a 16:1 mixture line at 90 percent evaporated is 40 C. It is desired to know the temperature at 90 percent evaporated corresponding to the formation of a 20:1 mixture of air and vapor from this gasoline. From the duplex scale, ΔT is found to be -4 for $M_R=20$. Adding -4 to 40 gives 36 C, which is the desired temperature.

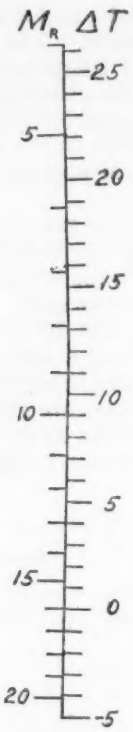

FIGURE 22.—*Duplex scale showing temperature differences between volatility curves for various resultant air-vapor mixtures*

3. SPECIAL CHART FOR DEW-POINT DATA

Although the charts shown in figures 20 and 21 are satisfactory for the evaluation of dew points, a more convenient graphical method for such data is illustrated in figure 23.

Duplex scale I gives the dew points directly for a gasoline having a slope of 2.0 at 90 percent evaporated on the A.S.T.M. evaporation curve, which represents an average value. The temperatures in centigrade degrees at 90 percent evaporated are placed on the left side of this scale whereas the corresponding dew points, in centigrade degrees, for a 16:1 mixture are placed on the right side of the scale.

Duplex scale II indicates the temperature correction for the 16:1 dew point of the gasoline if it has a slope other than 2.0 at 90 percent evaporated. The marks on the left side of scale II represent slopes at 90 percent evaporated, whereas those on the right represent corrections which are to be added algebraically to the dew-point values from scale I.

Example: A gasoline has a temperature of 150 C at 90 percent evaporated and a slope of 4.0 at this point on the A.S.T.M. evaporation curve. It is desired to know the 16:1 dew point of this gasoline. From scale I, a 90 percent point of 150 C corresponds to a 16:1 dew point of 25 C. From scale II, a slope of 4.0 indicates a correction of plus 4. Therefore the desired dew point is 29 C.

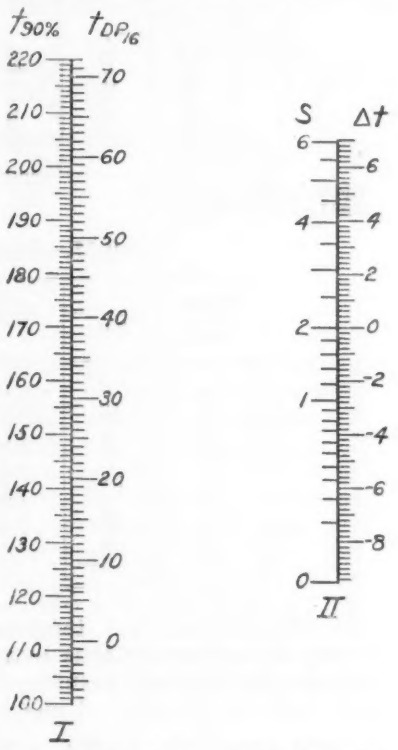

FIGURE 23.—*Duplex scales for evaluation of dew-point values from the temperature at 90 percent evaporated on the A.S.T.M. evaporation curve and from the slope of the evaporation curve at this percent evaporated.*

4. COMPLETE EXAMPLE OF EVALUATION OF VOLATILITY DATA

A further illustration of the method of obtaining volatility data from distillation data is outlined in detail below. The distillation data on a gasoline are given in table 16. These data are plotted in the form of an evaporation curve as explained previously. At every 10 percent evaporated from 10 to 90 percent evaporated, the temperatures are read off the evaporation curve and are listed in the second column of table 17 opposite the appropriate values of the percentage evaporated. The slopes of the A.S.T.M. evaporation curve at these even percentages are obtained in the manner previously outlined and are given in the third column of the table. The fourth column represents the values of C read from figure 20, using the corresponding values of S in the third column and of P in the first column. The fifth column shows the temperatures in centigrade degrees for the 16:1 resultant air-vapor mixture, obtained from figure 21, using the A.S.T.M. evaporation data in the second column and the values of C in the fourth column. The last column lists the temperatures corresponding to an 8:1 resultant air-vapor mixture. The difference in temperature between the last two columns of figures is obtained from the duplex scale in figure 22.

TABLE 16.—*Distillation data on fuel RPC*

Percent distilled	Temperature	Percent distilled	Temperature	Percent distilled	Temperature
	° *C*		° *C*		° *C*
I.B.P.	38	35	113	70	163
5	57	40	121	75	172
10	69	45	128	80	181
15	79	50	135	85	190
20	88	55	142	90	200
25	97	60	148	95	212
30	105	65	156	E.P.	222

Distillation loss=1.0 percent.
Residue=1.5 percent.

TABLE 17.—*Volatility data for fuel RPC*

Percent evaporated	Temperature	Slope	Value of *C*	16:1 temperature	8:1 temperature
	° *C*			° *C*	° *C*
0			24	−31	−18
10	66	2.3	47	−15	−2
20	86	1.8	45	−3	10
30	104	1.7	43	9	22
40	119	1.5	41	18	31
50	134	1.3	39	25	38
60	147	1.4	37	32	45
70	162	1.6	33	39	52
80	180	1.8	28	47	60
90	198	2.2	17	52	65
100			25	58	71

If desired, the 16:1 temperatures may be plotted against the corresponding percentages evaporated and a smooth curve drawn through the plotted points. From this curve the 16:1 temperatures may be obtained at any value of the percentage evaporated.

X. VOLATILITY DATA AT A TOTAL PRESSURE LOWER THAN STANDARD ATMOSPHERIC PRESSURE

The general volatility equations given in preceding sections and all of the experimental volatility data which are presented in this paper are applicable to conditions where the total pressure of the air-vapor mixture is 1 standard atmosphere. In an engine manifold, however, the pressure is normally below 760 mm and may become as low as half an atmosphere in an automobile engine manifold under idling conditions. In the manifold of an unsupercharged airplane engine at high altitudes the pressure may even be below half an atmosphere. In order to make possible the application of volatility data to vaporization in an ideal engine manifold under such conditions of reduced pressure it is desirable to know the temperatures of formation of various resultant air-vapor mixtures at any total pressure below that of the standard atmosphere, 760 mm of mercury.

Although no volatility data have been obtained at pressures other than 760 mm, it is possible to compute similar data at any reduced pressure with sufficient accuracy from the normal atmospheric values.

Consider first the problem of finding the air-vapor mixture M_R' which will be formed at any reduced total pressure p, any percentage

evaporated P, and at the temperature t, which corresponds to an air-vapor mixture M_R, at the same percentage evaporated and at a total pressure of 1 atmosphere. The relation between the mixture ratio and the total pressure is given by equation 23.
Rearranging equation 23, it becomes

$$\frac{760-p_f}{p_f}=M_R\cdot\frac{M_f}{M_A} \tag{39}$$

The analogous relation for any total pressure p is

$$\frac{p-p_f}{p_f}=M_R'\cdot\frac{M_f}{M_A} \tag{40}$$

Dividing equation 40 by equation 39, there results

$$\frac{M_R'}{M_R}=\frac{p-p_f}{760-p_f} \tag{41}$$

The desired air-vapor mixture M_R' can be computed from this relation at any reduced total pressure p if the vapor pressure p_f of the gasoline is known under the stated conditions of temperature and percentage evaporated. In general p_f is, however, not known, but an approximate value can be assumed without introducing much error. For example, for values of M_R from 8 to 20, p_f lies within the limits 5 to 50 mm of mercury for any percentage evaporated. Taking $p_f=5$ mm, $p=380$ mm and $M_R=16$, the value of M_R' from equation 41 is 7.95. For $p_f=50$ mm, $p=380$ mm and $M_R=16$, M_R' becomes 7.45. The difference in temperature between these two mixtures is only 1° C which is negligible in this case, and also for any value of M_R from 8 to 20, as long as the total pressure is not much lower than 380 mm.

Assuming an average value $p_f=30$ and limiting M_R to the range from 8 to 20, equation 41 can be written

$$M_R'=M_R\left[1.04\frac{p}{760}-0.04\right] \tag{42}$$

Suppose a gasoline forms a 16:1 resultant air-vapor mixture at 30 C when 50 percent is evaporated under a total pressure of 760 mm. Then at 30 C and 50 percent evaporated under a total pressure of 380 mm, M_R' is found from equation 42 to equal 7.7, which is the air-vapor mixture formed at this lower pressure.

It should be pointed out that the resultant mixture M_R' given by equation 41 is dependent to a slight extent upon the percentage evaporated, since the vapor pressure p_f changes somewhat with the percentage evaporated along a constant air-vapor mixture line M_R. However, the variations in p_f are within the limits of 5 to 50 mm stated above, and hence for all practical purposes the computed value of M_R' from equation 42 may be considered as independent of the percentage evaporated.

The first problem considered was to find the air-vapor mixture formed at reduced pressure under otherwise similar conditions of temperature and percentage evaporated to those at which a known air-vapor mixture was formed at atmospheric pressure. The second problem is to find the temperature at which a given air-vapor mixture will be formed at any reduced pressure when the temperature is known at which the same air-vapor mixture is formed at atmospheric

pressure. This can be easily solved by means of equation 42 supplemented by figure 7 or the duplex scale in figure 22.

Suppose a 16:1 resultant air-vapor mixture is formed at 30 C when 50 percent of a gasoline is evaporated in air at a total pressure of 1 atmosphere. Then at 380 mm total pressure when 50 percent of the gasoline is evaporated M_R is found from equation 42 to be 33.3. This is the mixture formed at 760 mm corresponding to a 16:1 mixture at 380 mm at the same temperature and percentage evaporated. From the curve in figure 7, it is found that a 33.3:1 mixture is formed at a temperature 13° C lower than a 16:1 mixture. Hence, a 16:1 mixture at 380 mm total pressure and at 50 percent evaporated will be formed at $(30-13)=17$ C.

The effect of reduction in total pressure is to enrich the air-vapor mixture formed when the same percentage is evaporated at the same temperature from the same supplied air-fuel mixture. Reduction in pressure under these conditions to one-half an atmosphere makes the mixture approximately twice as rich. In order to obtain the same air-vapor mixture at reduced pressure from the same supplied mixture, when the same percentage is evaporated as at atmospheric pressure, a lower temperature is required. The temperature difference in the two cases is constant for different gasolines and independent of the percentage evaporated. It is also independent of the particular mixture considered, within a range of M_R from 8 to 20, but is dependent upon the reduction in pressure. If a set of volatility curves have been obtained from the distillation data which are applicable to 760 mm total pressure, it is only necessary to lower all of them by a constant temperature difference of 13° C in order that they may be applicable to a total pressure of 380 mm. For application to other pressures, the temperature differences may be computed in the manner outlined or they may be obtained from table 18, by interpolation, if necessary.

TABLE 18.—*Temperature differences between the same resultant mixture curves at 760 mm pressure and at lower pressures*

p, mm mercury	$t_{760}-t_p$	p, mm mercury	$t_{760}-t_p$
	° C		° C
760	0	500	8.1
700	1.5	400	12.6
600	4.5	300	18.6

XI. CONCLUSIONS

The large volume of volatility data which have been obtained on 38 fuels of widely differing characteristics has indicated certain basic principles of fuel volatility. The correlation of the results with the A.S.T.M. distillation data has not only furnished an interpretation of the significance of the distillation data but has also furnished a simple means for the evaluation of equilibrium volatility values from gasoline distillation data. While the information obtained forms a fundamental basis for the investigation of the effect of fuel volatility in connection with numerous problems dealing with engine performance and operation, the precise application to these problems is very limited due to the lack of adequate information on the departure from equilibrium

vaporization in engine manifolds. Such information is urgently needed and when obtained should lead to a much better understanding of the relation between fuel volatility, operating conditions, and engine design factors. In a later paper there will be considered the application of the volatility relations to the problems of engine starting, acceleration, mixture distribution, and crankcase dilution on the basis of existing information.

Acknowledgment is made to the Cooperative Fuel Research Steering Committee of the automotive and petroleum industries for its active cooperation and financial support in connection with this investigation. Acknowledgment is also made to the late T. S. Sligh, who started the investigation and designed some of the apparatus used, and to D. C. Ritchie, who made a large number of the observations of experimental data herein reported.

WASHINGTON, May 14, 1934.

U.S. DEPARTMENT OF COMMERCE NATIONAL BUREAU OF STANDARDS

RESEARCH PAPER RP695

Part of Journal of Research of the National Bureau of Standards, vol. 13, July 1934

VARIATIONS IN REFRACTIVE INDEX OF CO_2-FREE DRY AIR AND A STATISTICAL CORRELATION WITH SOLAR ACTIVITY[1]

By L. W. Tilton

ABSTRACT

Existing data on refractive indices of dry air as measured by various observers show disagreements larger than the errors that seem probable in many of the recent measurements. Chemical (volumetric) data relating to the constancy of composition of the atmosphere at the earth's surface do not suggest that any appreciable variations in refractivity should be found, but gravimetric data show small variations that have never been satisfactorily explained.

All refractive-index data taken on air since 1857 have been examined for evidences of systematic variations and a correlation between refractivity and annual sunspot number has been found, the Pearson r being -0.48 (± 0.08 probable error) as determined from 40 pairs of values.

Degree of storminess of the earth's atmosphere has already been (positively) correlated with yearly relative sunspot number and thus it seems possible that a decrease in the average rate of stirring and mixing of the air, such as occurs during times of low sunspot numbers, allows certain denser components (perhaps associated molecules or isotopes) to settle and produce at the earth's surface a gaseous mixture having a slightly higher index of refraction. In addition to simple sunspot periodicity of 11 years, however, a superimposed 23-year periodicity, corresponding to a magnetic cycle of sunspots, also seems indicated.

Although the value $\mu = 1.0002925$ at 0 C and 760 mm pressure is a fair general average for the sodium lines index of air, it appears unsafe to rely implicitly on the constancy of μ over a period of years. It may be preferable to make estimates from the equation $(\mu_D - 1) \times 10^7 = 2932.2 - 0.15\ S$, where S is the relative annual sunspot number, and the constants are provisional values derived from all available data. Further experiments should precede the adoption of any radiation in air as a standard of length.

CONTENTS

	Page
I. Introduction	112
II. Gravimetric evidence of variation	112
III. Chemical analyses (chiefly volumetric)	113
1. Oxygen content	113
2. Argon content	114
3. Hydrogen content	114
4. Nitrogen content	114

[1] In this investigation of possible periodicity in the refractive index of air, sunspot numbers are employed primarily as a well-known comparison standard of established periodicity that in an empirical manner is found suitable for use in making a numerical estimate of the probability that certain discrepancies among published indices of air are, or are not, the result of chance or accidental error. Far from implying a causal relation, a correlation coefficient can, of course, indicate nothing about the nature of a relationship or even show whether it is direct or indirect. The correlation of a phenomenon with sunspot numbers permits a rough pseudo comparison with a number of other phenomena that also have been correlated with such numbers, and these rough comparisons or associations in thought serve to suggest partial explanations which may lead to fruitful experiments.

64093—34—8

Page
IV. Refractometric evidence of variation 115
1. Accuracy of the data 115
2. Character and significance of the variations 116
V. Quantitative discussion of composition and constitution of air 117
VI. Refractivity and sunspot number 118
1. Average refractivity during magnetic cycle of sunspots 119
2. Normal range in refractivity and a statistical correlation 120
VII. Concluding discussion 122

I. INTRODUCTION

In previous papers [2] discussing the errors of refractive-index measurement attention has been confined almost exclusively to goniometry and to other geometrical considerations. In these it has thus been assumed that the velocity of light in any given medium has a constant value for a given wave length, whether measurements are made simultaneously or follow after successive time intervals and whether the observations are made along the same or different paths. This, of course, can be true only when all pertinent physical and chemical conditions are well understood and under complete control.

It has long been assumed that our knowledge of the earth's atmosphere and its properties is sufficiently complete to justify the making of precise optical measurements in CO_2-free dry air. However, in view of the very high precision that is currently sought, and since certain small but definite variations have been found in the apparent weight of a normal liter of CO_2-free dry air, it is evident that a comprehensive survey of refractive-index errors should include careful consideration of possible variations in the composition and constitution of the atmosphere. Three well-known types of measurement that are frequently made on air and which have a direct bearing on this question are (1) density determinations, (2) chemical (chiefly volumetric) analyses, and (3) refractive-index determinations. Evidence from all three of these sources will be summarized before proceeding to a general discussion of interrelationships and possible periodic tendencies among variations in the properties of air.

II. GRAVIMETRIC EVIDENCE OF VARIATION

Approximately 50 years' work in precise weighings shows that observed densities of standard air are not as constant as similar results obtained by the same observers on certain other gases. Because of this lack of constancy in the normal density of air, the specific gravities of gases are now given in the Landolt-Börnstein Physikalisch-Chemische Tabellen [3] as referred to oxygen instead of to air.

The weight in grams of a liter of (chemically prepared) oxygen, under standard conditions,[4] has been determined by 13 observers, the mean value being 1.42893 with a total variation of approximately 2 parts in 10,000. Similar observations on the weight of a liter of CO_2-free dry air yield average values varying systematically from 1.29266 and 1.29284, for samplings at or near sea level, to 1.29301

[2] L. W. Tilton, B.S. Jour. Research, vol. 2 (RP64), p. 909–930, 1929; vol. 6 (RP262), p. 59–76, 1931; vol. 11 (RP575), p. 25–57, 1933.
[3] Erster Ergänzungsband, p. 160–163, 1927.
[4] A temperature of 0 C and a pressure of 760 mm of mercury (at 0 C, g=980.616) was used by E. Moles (Jour. de chim. phys., vol. 19, p. 100, 1921; Zeits. f. Phys. Chem., vol. 115, p. 61, 1925) in his critical review leading to the average value which was adopted for oxygen in the Landolt-Börnstein Tabellen.

and 1.29332 g for those made at altitudes of 700 and 1,960 meters, respectively. Also, as time varies at a single place of sampling, the total range of values obtained by a given observer is at least 5 and in some cases [5] 10 or 12×10^{-4} g; that is, from 2 to 5 times the variation among results by all observers on pure oxygen. Moreover it appears that these variations with time of sampling at given latitudes and altitudes are more or less systematically related to certain weather conditions existing at the time the sample is taken. In particular there is considerable evidence [6] to show that minima of density are often obtained on air sampled at or very soon after maxima of atmospheric pressure. It should also be mentioned that Paya and Moles [7] have made several weighings of atmospheric nitrogen and find similar but smaller systematic variations with pressure existing at times of sampling. In brief, it seems fairly well established that the bona fide time variations in the weight of a liter of CO_2-free dry air approximate 1 part in 1,000.

III. CHEMICAL ANALYSIS (CHIEFLY VOLUMETRIC)

Attempts have been made to explain the observed gravimetric variations as arising mainly from variations in the oxygen content of air. According to the Loomis-Morley [8] hypothesis, cold air which is less rich in oxygen should descend from upper regions during periods of high barometric pressure. Possibly atmospheric nitrogen should be less rich in argon when sampled under these same conditions. Important fluctuations at least as large as ±0.2 percent oxygen (i.e., ±1 percent of the oxygen content), together with ±0.02 percent argon (i.e., ±2 percent of the argon content), seemed required in order to explain the gravimetric data (including only the time variations and excluding those ascribed to altitude); but during the very early experiments in connection with this problem the variations in composition as found by chemical analysis were of a magnitude not altogether inconsistent with acceptance of this hypothesis.

1. OXYGEN CONTENT

The development of improved technique in volumetric gas analysis soon led, however, to a decidedly narrower range in the observed variations in composition, and the fluctuations in (averaged) oxygen content within the North Temperate Zone do not appear [9] to exceed ±1 part in 1,000 volumes. They are scarcely ±3 parts in 1,000 even if one considers both maxima and minima and includes the joint investigation by Morley, Hempel, and Kreussler on air collected simultaneously in 1886 at Cleveland, Bonn, Dresden, Para, and Tromsö.[10] Moreover, the greater normal densities found upon sampling at higher altitudes do not seem in accord with the Loomis-Morley hypothesis. The possible connection between such high densities and certain variations in atmospheric ozone, as suggested

[5] Recent data are given by A. Stock, H. Ramser, and G. Eyber, Zeits. f. Phys. Chem., vol. 163, p. 82–90, 1933.

[6] Ph. A. Guye, Jour. de chim. phys., vol. 15, p. 561–576, 1917; A. Jaquerod and Ch. Borel, Jour. de chim. phys., vol. 19, p. 11–28, 1921.

[7] M. Paya and E. Moles, Anales soc. españ. fís. y quím., vol. 20′, p. 247–254, 1922; 24′, p. 564, 1926.

[8] E. W. Morley, Amer. Jour. Sci., vol. 18, p. 168, 1879.

[9] M. S. Blanchard and S. F. Pickering, B.S. Scientific Papers, vol. 21 (S529), p. 167, 1926.

[10] For collected data and bibliography see F. G. Benedict, The Composition of the Atmosphere, publication no. 166 of the Carnegie Institution of Washington, 1912.

for the vicinity of Madrid,[11] may be untenable as a general and satisfactory explanation, not only because of the very small ozone concentrations that are usually found by direct tests but also because the presence at the earth's surface of the required amounts of from 0.01 to 0.02 percent of such an active agent as ozone should be chemically noticeable. If 20.94 ± 0.05 is adopted as the range in volume percentage of oxygen in CO_2-free dry air, then comparatively few reliable analyses on normal air are found in disagreement therewith. Those analyses made by Moles [12] on air sampled at Valencia and at Madrid are certainly exceptions. Possibly it is worth noting that Moles used a gravimetric method of analysis, whereas all air analyses considered by Blanchard and Pickering,[13] and also those made by Stock, Ramser, and Eyber,[14] were effected by volumetric procedures.

2. ARGON CONTENT

Very few direct determinations of argon in air seem to have been made. The writer has noticed those by Schloesing,[15] by Kellas,[16] and by Moissan.[17] A value of 0.936 ± 0.003 percent is suggested as a range in good agreement with the evidence which they present.

3. HYDROGEN CONTENT

Concerning the proportion of hydrogen in the air it is well known that Rayleigh [18] and other investigators [19] have reported negligible amounts. On the other hand, Gautier,[20] whose work was quite elaborate but has received little notice, finds at least 2 parts of hydrogen per 10,000 of ocean air taken near sea level 40 kilometers off the French coast. Rayleigh considered Gautier's work as very carefully and thoroughly done and expressed his embarrassment and a temptation to suppress his own results. A hydrogen percentage of 0.01 ± 0.005 seems, therefore, in fair agreement with these data and the range as thus expressed is probably ample.

4. NITROGEN CONTENT

If all constituents of CO_2-free dry air other than nitrogen, oxygen, argon, and hydrogen are negligibly small, it then follows from the estimates listed above that the range in nitrogen content is expressible as 78.114 ± 0.058 percent. This, of course, is only indirect evidence for the nitrogen content of air and the range depends almost entirely on the variations that are found in oxygen. Unfortunately no constituent except oxygen has been satisfactorily investigated by numerous experiments over periods of time sufficiently long to reliably establish the constancy or variability in its volume percentage.

[11] E. Moles, T. Batuecas, and M. Paya, Anales Soc. españ. fís. y quím., vol. 20, p. 34–40, 1922. The fluctuations in density and in oxygen content that these observers find at an altitude of 685 meters are somewhat greater than have been found elsewhere (lower altitudes) since von Jolly's experiments at Münich (altitude 515 meters) in 1879.

[12] E. Moles, Gazetta chimica Italiana, vol. 56, p. 938, 1926.

[13] See footnote 9, p. 113.

[14] See footnote 5, p. 113.

[15] Th. Schloesing, Comptes Rendus, vol. 121, p. 525, 1895; vol. 123, p. 696, 1896.

[16] Alex. Kellas, Proc. Royal Soc. London, vol. 59, p. 66, 1896.

[17] H. Moissan, Bull. Soc. chim. de Paris, (3) vol. 31, p. 729–735, 1904.

[18] Lord Rayleigh, Phil. Mag. (6) vol. 1, p. 100–103, 1901; (6) vol. 3, p. 416–422, 1902, obtained results varying from negative values up to 6 parts of hydrogen per 100,000 of air with an average of approximately 3 parts per 100,000.

[19] G. Claude, for example, Comptes Rendus, vol. 148, p. 1454, 1909, finds less than 1 part of hydrogen per million parts of air. See also A. Krogh, Vidensk. Selsk. Math-fysiske Medd., vol. 1 (nr. 12), p. 1–19, 1919.

[20] A Gautier, Annales de Chimie et de Physique, (7), vol. 22, p. 5–110, 1901; Bull. Soc. chim. de Paris (3) vol. 29, p. 108–116, 1903.

Consequently, aside from the values for oxygen, the ranges suggested in the above summary are simply tentative estimates. Even for oxygen it seems possible that further work by gravimetric methods may lead to some revision.

IV. REFRACTOMETRIC EVIDENCE OF VARIATION

In comparison with densities and chemical analyses, direct optical measurements on air have been less frequently made. Nevertheless, since 1857 the index of refraction of dry air has been determined in at least 40 distinct series of experiments. The general average of these data [21] is, for sodium light, $\mu = 1.0002925_4$ at a temperature of 0 C and a pressure of 760 mm of mercury. Only 21 of these 40 values fall within $\pm 5 \times 10^{-7}$ of the mean, 11 values being lower and 8 higher than this range. Since these data have not hitherto been collectively analyzed it is appropriate to remark concerning their possible accuracy and significance.

1. ACCURACY OF THE DATA

It is, of course, true that many of these observers did not remove CO_2 from the air, but the total variations on that account can scarcely be as large as 1×10^{-7} in index. Also, various values of wave lengths are assumed and various values of gravity have been used (or neglected) in the corrections to standard pressure; but, with one or two exceptions, these uncertainties are likewise very small, being matters of approximately $\pm 1 \times 10^{-7}$ in index.

Sources of error that are of somewhat more importance are inadequate care in removing moisture, the use of different temperature coefficients of index of air, and perhaps the assumption that, even for low pressures, the rate of shift of interference fringes is constant as observed pressure varies uniformly. These errors, so far mentioned, do not affect μ directly, but have their proportionate influence on $(\mu-1)$ only. The effect of pressure on the apparatus is a different matter, not often explicitly considered, and the error in μ itself may be proportional to certain compressive changes in length. Fortunately, with some experimental procedures, for example with the Jamin interferometer which is the one most frequently used for these measurements, the compressibility error is effectually compensated by corresponding variation in the air paths outside the tubes. For the Fabry-Perot type of apparatus, however, it would seem that such an effect may be appreciable, although even here the error can be (as in the Meggers and Peters apparatus) reduced by a choice of

[21] The Landolt-Börnstein Tabellen (fifth edition) list and give references to 27 of these values, the average for that restricted group as therein listed being 1.0002925_5. The other references are:
J. Jamin, Annales de Chimie et de Physique, (3) vol. 49, p. 282-303, 1857.
E. Mascart, Comptes Rendus, vol. 78, p. 617-679, 1874.
L. Magri, Physikalische Zeits., vol. 6, p. 629-632, 1905.
S. Loria, Annalen d. Phys. (4) vol. 29, p. 605-622, 1909.
I. M. Mathews, Jour. Franklin Inst., vol. 177, p. 673-686, 1914.
V. Posejpal, Annalen d. Phys. (4) vol. 53, p. 629-646, 1917.
V. Posejpal, Jour. de Phys. (6) vol. 2, p. 85-92, 1921.
A. Pérard, Procés-Verbaux des Séances, vol. X, p. 16, 1923.
A. Zwetsch, Zeits. f. Phys., vol. 19, p. 398-413, 1923.
Tausz und Görlacher, Zeits. f. techn. Phys., vol. 12, p. 19-24, 1931.
Sears and Barrell, Phil. Trans. Royal Soc. London, vol. (A) 231, p. 126-127, 1932.
Kösters und Lampe, result obtained in 1932 at the Phys. Techn. Reichsanstalt and privately communicated to the writer.
C. G. Peters, unpublished result obtained in 1917 at the National Bureau of Standards with apparatus different from that used by Meggers and Peters.

suitable separating posts and perhaps to some extent compensated by air film and certain differential compressibilities.

The writer has reviewed many of these observations and has applied tentative corrections in those cases where the necessary data are given or have been readily obtained. The general average of all values remained essentially unchanged by these corrections, however, and the only important individual changes are a possible reduction of 9×10^{-7} in Mascart's (second) result [22] and an increase of 5×10^{-7} in index after reanalyzing and applying the Mascart index-pressure equation to the data given by Chapuis and Rivière.

2. CHARACTER AND SIGNIFICANCE OF THE VARIATIONS

If the variations among all of these indices of air could reasonably be considered as accidental errors in measurements, the mean could probably be accepted as establishing the refractivity of air within a very few units of the seventh decimal place. Some careful workers have, however, obtained results that differ from the mean by amounts that materially exceed the estimated errors. In particular, Lorentz (1870–75), Scheel (1906), and Meggers and Peters (1917) give values which are lower than the mean by 15, 9, and 8×10^{-7}, respectively, while Ketteler (1865) and Quarder (1924) find results which are high by 22, and 7×10^{-7} in index. In this connection it should be remembered that air is compared with vacuum in these measurements and that differences of $\pm 10 \times 10^{-7}$ in refractive index correspond to variations as large as ± 1 part in 300 in the quantity actually determined, namely the (excess) refractivity, $\mu - 1$. In view of these facts and the known variations in air density, it appears possible that a similar uncertainty of approximately $\pm 1 \times 10^{-6}$ may exist in the index of refraction of air.

If the index of air varies slowly to this extent then it is easily shown that relative indices of refraction of very dense glass cannot (over a period of several years) be redetermined or checked with a precision better than $\pm 2 \times 10^{-6}$. If, in addition, these variations should prove to be functions of daily meteorological conditions some further question would arise concerning possible fluctuations of similar magnitude in index over relatively short periods of time. Recently, however, it has been reported [23] that measurements made on μ at the Reichsanstalt to 1×10^{-8} show no noticeable vacillations with meteorological conditions, and this result is in agreement with the constancy which Stoll [24] found in his precise experiments at Zurich.

Any uncertainties in index of refraction of air are of great importance, moreover, in correcting to vacuum values all wave lengths that are measured in air. An error of 1×10^{-6} in index of air corresponds to an error of 0.005 A in such a correction for a wave length of 5,000 A. Standard wave lengths are often given to 4 decimals and it was, no doubt, this state of affairs that in 1931 prompted a Subcommittee of the International Committee on Weights and Measures to sponsor further work on the refractivity of air.

[22] This is chiefly a temperature coefficient correction. Analysis of Mascart's data indicates that his temperature investigation was systematically in error when data were taken at other than room temperatures. On the other hand, Perreau, who afterwards used the same apparatus, considered Mascart's result as independent of Mascart's value for the temperature coefficient.

[23] Kösters and Lampe, Zeits. f. Instrumentenkunde, vol. 35, p. 201–2, 1933.

[24] E. Stoll, Annalen d. Phys. (4), vol. 69, p. 81–111, 1922.

V. QUANTITATIVE DISCUSSION OF COMPOSITION AND CONSTITUTION OF AIR

The variations evidenced by gravimetric, volumetric, and refractometric data can now be readily compared. Using the percentages adopted in section III, and taking the means of published [25] values for the densities and refractivities of the various constituents of CO_2-free dry air, some interesting computations can be made (by the additive rule for gaseous solutions) concerning the possible variations in these properties for atmospheric nitrogen and for air itself. The results are given as table 1 and the arrangement is such that the entries therein are self-explanatory. The most important result of these computations is the conclusion that known variations in the chemical composition of air, while they are sufficiently large to account for some [26] of the known variations in the normal density of air, are wholly inadequate to cause any appreciable variation in the refractivity of CO_2-free dry air. Even ozone, in amounts up to 0.02 percent can only cause variations beyond the seventh decimal place of the refractive index of air.

TABLE 1.—*Composition, density, and refractivity of CO_2-free dry air under standard conditions* (*see footnote 4, p. 112*)

Chemical substance	Percentage composition by volume (based on published data)		Density (mg per liter)		Refractivity ($\mu_D - 1$) $\times 10^6$	
	Average	Normal variation	Average from published data	Net weight equivalent of normal variation in composition	Average from published data	Net refractivity equivalent of normal variation in composition
N_2	78.11	$\begin{cases} -0.058 \\ +0.048 \end{cases}$ [1]	1,250.52	$\begin{cases} +0.025 \\ -0.020 \end{cases}$	297.8	$\begin{cases} -0.0034 \\ +0.0028 \end{cases}$
O_2	20.94	±0.05	1,428.93	±0.068	270.9	∓0.0105
A	0.93	±0.003	1,781	±0.015	282	∓0.0003
H_2	0.01	±0.005	90	∓0.060	140	∓0.0076
O_3	0.00	(+0.01)?	2,220	(+0.093)	519	(+0.0227)
Air	Computed from above		1,292.73	$\begin{cases} +0.26 \\ -0.16 \end{cases}$	292.0	$\begin{cases} +0.04 \\ -0.02 \end{cases}$
	Average of published observations.		1,292.75 [2]	±0.5	292.5	±1
Atmospheric nitrogen	Computed from above: Including H_2		1,256.65	±0.10	297.6	±0.01
	Neglecting H_2		1,256.80	±0.03	297.6	±0.003
	Average of published observations		1,256.67 [2]	±0.10	----------	----------

[1] Considering the ozone variation as tabulated herein.
[2] Near sea level.

In this connection, however, the isotopes of oxygen and of nitrogen may require consideration. Recent measurements [27] have shown that the ratio of O^{18} to O^{16} is approximately 1: 630 and the ratio of N^{15} to N^{14} seems to be almost twice that value.[28]

[25] The Landolt-Börnstein Tabellen have been used as the principal source for these data. For argon see also E. Moles, Ber. Deutschen Chem. Gesellschaft, vol. 60, p. 134–138, 1927.
[26] In general it may be said that, excluding ozone, all other variations in chemical composition that appear possible in view of accumulated (volumetric) chemical data do not explain more than 30 percent of the established density variations. Moreover, +0.01 percent ozone can account for only 10 percent of the increases in density even if unaccompanied by a depletion of O_2.
[27] H. Kallmann and W. Lasareff, Zeits. f. Physik, vol. 80, pp 237–241, 1933.
[28] G. M. Murphy and H. C. Urey (Phys. Rev., vol. 41, pp 141–148, 1932) find 1 : 346 for the ratio N^{15} to N^{14}.

The possible presence of oxygen in the forms $(O_2)_x$ must also be remembered,[29] particularly in connection with the reported increased normal densities of air sampled at higher altitudes. Perhaps the degree of existing association may be influenced by various meteorological conditions.

Presumably then a change in the rate of general stirring and mixing of the atmosphere could produce changes in density, and probably in refractivity, that would exceed those predictable from data given by the purely (volumetric) chemical methods of analysis which of late have been used almost exclusively in investigations of this problem. On the other hand, gravimetric methods of analysis would, of course, be sensitive to variations in molecular association and in ratios of isotopes. This may partially account for the agreement that Moles [30] finds between fluctuations in density and those in composition; also for the fact that Stock, Ramser, and Eyber,[31] who used a volumetric method, do not find such an agreement.

Unfortunately no refractivities of the isotopes of oxygen and nitrogen are as yet available for computations concerning these questions. Insofar as density [32] is concerned it is readily shown that variations of ± 10 or 15 percent in the above-mentioned ratios of these particular isotopes of oxygen and nitrogen would cause variations of ±0.03 or 0.04 mg in the weight of a normal liter of air, that is, only 6 or 8 percent of the established density variations with time in a given locality.

VI. REFRACTIVITY AND SUNSPOT NUMBER

With these general ideas in mind, the data on refractive indices of air as determined by various observers were examined with particular reference to the time sequence in which the observations were made. Considering only the data published in the last two decades it was at once evident that 8 of a total of 10 values obtained between the years 1912 and 1923 were lower than the general average (of $\mu_D = 1.0002923_7$) for the 20 years, while 8 of the 9 subsequent values have equaled or exceeded the general average. It happens that these 2 groups lie within the 2 opposite phases of the current 23-year magnetic cycle of sunspots. Consequently, since degree of storminess of the earth's atmosphere (at least in North America) has been correlated [33] with the Wolf-Wolfer series of annual relative sunspot numbers, and since sunspot numbers were appreciably higher during the first half of this 23-year period, a partially explainable correlation between sunspot number and variations in the refractivity of air was suggested. For the 19 indices determined between 1912 and 1932, and for the corresponding sunspot numbers, computation gave a Pearson correlation coefficient,[34] $r = -0.52$ (±0.11 probable error), and this preliminary result has been published.[35]

[29] Oliver R. Wulf, Phys. Rev., vol. 41, pp 375-376, 1932, discusses the presence of O_4 in the atmosphere and its effect on the formation of O_3 in the lower air at moderately high altitudes.
[30] See footnote 12, p. 114.
[31] See footnote 5, p. 113.
[32] This reference to densities should not, of course, be construed as relevant evidence concerning refractivities. For example, it is readily seen from the data of table 1 that both oxygen and argon are denser than either nitrogen or air but have lower refractive indices.
[33] Ellsworth Huntington, Earth and Sun, p. 29; Yale University Press, 1923. See also the Julius Hann Handbuch der Klimatologie, 4th ed., p. 406, 1932; and Shaw's Manual of Meteorology, vol. 2, p. 336.
[34] See any text on the theory of statistics.
[35] L. W. Tilton, Nature (London), vol. 132, p. 855, 1933.

1. AVERAGE REFRACTIVITY DURING MAGNETIC CYCLE OF SUNSPOTS

In the present examination of all available data on the refractive index of air it was assumed that the "double sunspot periods" 1844 to 1866, 1867 to 1889, and 1889 to 1911 are comparable with the present magnetic cycle from 1912 to 1934 and in each of these 4 cycles the years were numbered from 1 to 23. Each observed index of air was then tabulated in one of 23 columns as determined by the date of first publication or by a more precise date if such has been noticed.[36] In order to simplify the presentation and the discussion, and also to avoid the element of personal choice, no instrumentally determined absolute values published since 1857 have been intentionally rejected and results have been used as they are computed and published by the observers.[37]

In obtaining values of the index for the sodium lines, the computed rather than the observed values have been favored, provided there are accompanying dispersion equations which seem reliable; and necessary interpolations have been made with such equations. All extrapolations and some interpolations have been made by comparison between the observers' data and those computed by the Meggers and Peters dispersion equations which are based on observations for a very large number of wave lengths. Where temperature reductions have been necessary they have been made by the Meggers and Peters coefficients which, for lines near the middle of the visible region, are approximately equal to averages from the work of Benoit and of Pérard, both of whom observed at a large number of temperatures between 0 and 100 C.

Simple averages were formed in each of the 23 columns in which indices were tabulated and then these results were plotted in figure 1 for comparison with the Wolf-Wolfer series of annual relative sunspot numbers, which were similarly averaged over the 4 magnetic cycles of 23 years each. Each plotted point depends on from 1 to 5 series of experiments as indicated by the numbers shown near the small circles. No experiments occurred in the years 1, 2, 3, 9, or 10 of any cycle.

Similar attempts to compare sunspot numbers and refractive-index data over a single or 11-year sunspot period are not quite as satisfactory as for the double or 23-year cycle which has been used. It seems, at least for the current cycle from 1912 to 1934, that those factors which tend to produce low refractivity during high sunspot numbers are not so potent during the second half of the double period, or else that their effect is masked. This, of course, may mean that two distinct causes having different periodicities are operating to produce the observed variations in refractivity.

[36] For example, L. Lorentz, publishing first in 1875, states that his experiments on air were begun in 1870 and often repeated through the years because he obtained such a low value. His result has been tabulated as of 1872. Benoit, in 1889, gives dates from July 1882 to January 1883. Stoll, in 1922 (see footnote 24 p. 116), lists some data as of 1920 and says his experiments were in progress when the Meggers and Peters paper appeared. (That paper was issued in October 1918 and appeared in B.S. Bulletin as of July 1919.)

[37] A similar analysis based on selected and corrected data has been carefully considered but in most instances and in all general respects there is insufficient difference in final results to justify detailed presentation. In the case of data by A. Zwetsch, however (see footnote 21, p. 115), his "corrected" value has been ignored in favor of the uncorrected value which he himself lists as comparable with those of other observers. Dickey's results cannot be used because of the large arbitrary correction which he applies to all his data after a comparison with indices given by certain other observers.

2. NORMAL RANGE IN REFRACTIVITY AND A STATISTICAL CORRELATION

The points plotted in figure 1 suggest a normal range in refractivity between upper and lower limits such as those which have been sketched above and below all the points. Certainly a curve of average

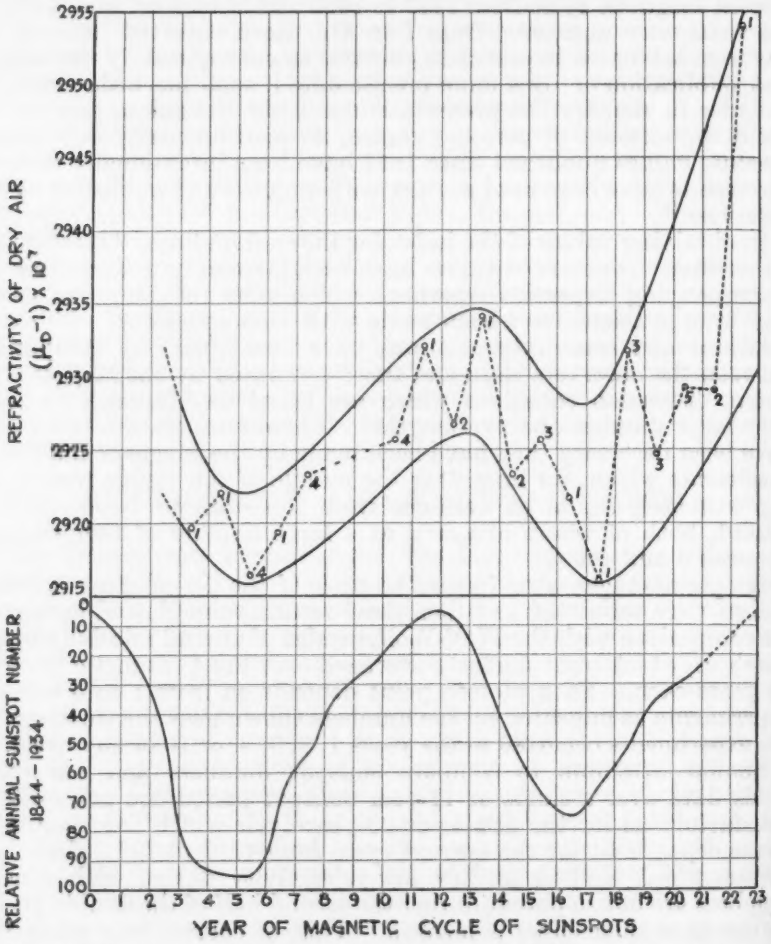

FIGURE 1.—*Average refractivity of dry air (at 0 C and 760 mm pressure) compared with average of sunspot numbers.*

The interval 1844 to 1934 has been divided into 4 periods of approximately 23 years each. The figures near the small circles indicate the number of experimental results that are available for averaging as of corresponding years during any of the 4 cycles. No experiments occurred in the years 1, 2, 3, 9, or 10 of any cycle. For the years 22 and 23 only 3 values of annual sunspot number are available for estabilshing the curve of average sunspot number (Wolf-Wolfer series).

refractivity is remarkably similar to that of average sunspot number but it must be remembered that some of the individual results depart widely from the averages, both for index and for sunspots. Consequently, in order to investigate further the matter of a normal range in refractivity the individual values were plotted in figure 2 for a

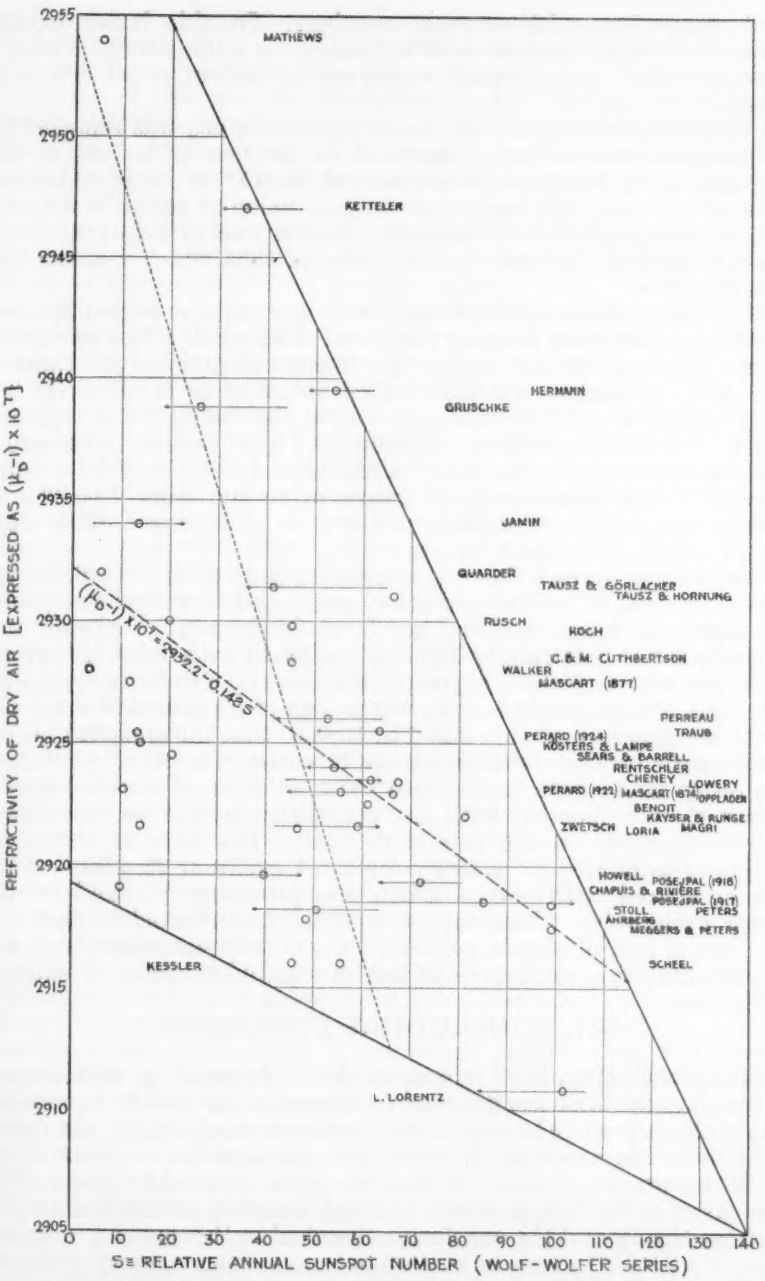

FIGURE 2.—*Correlation between refractivity of dry air and sunspot number.*

The Pearson coefficient of correlation is $r=-0.48$ (±0.08 probable error) as determined from 40 pairs of values. Except where the magnitude and direction of annual change in sunspot number is indicated by arrows, the uncertainty in determining such number is estimated as ±6 or less. Note that all observations are located in a triangular area having the broad base $\mu_D=1.000292$ to 1.000296 for $S=0$ with the apex near $\mu_D=1.000290_8$ for $S=140$ which is the upper limit for the whole period from 1844 to 1934.

direct comparison with sunspot numbers. In this latter exhibit arrows have been drawn to show the change in solar activity during a period (usually 1 year) within which an experiment is not definitely dated.

It should be noted that the lowest value of index was reported by Lorentz and that he began his work in the year of largest annual sunspot number which has been observed since 1778. Miss Mathews, on the other hand, who reports the highest value on record is the only observer who has taken data during the last year of a 23-year cycle. Ketteler reported the next highest index in 1864 which was the 21st year of a cycle.

All of these data are distributed over a triangular region forming considerably less than half the total area of figure 2. This particular distribution suggests that during the "disturbed periods", at times of high sunspot number, the index of refraction of air is relatively low and approaches a fairly constant value, the range being approximately 1.000291 to 1.000292. During the "quiet periods", when sunspot numbers are low, the index is higher and there may be a much wider variation with a normal range extending from 1.000292 to 1.000294 or higher, depending perhaps on the elapsed time since marked atmospheric disturbances.

Computation gives a Pearson correlation coefficient, $r = -0.48$ with a probable error of ± 0.08; and the characteristic (or regression) lines have also been determined and are shown in figure 2. Although this value of r is not particularly high (as compared with unity for perfect correlation) it suggests a degree of relationship far from negligible. The value of r approximates six times that of its probable error and thus it is rather improbable (say 1 in 10,000) that the apparent degree of systematic trend in refractivity can be entirely the result of chance. This result for all data taken since 1857 (40 series of experiments) is in very close agreement with the previously mentioned correlation ($r = -0.52$) based on the data since 1912. The slope of -0.15 for the line of estimated refractivity for the 4 cycles of 23 years each is large compared with -0.08 which was previously[38] found for the current cycle only. This may, of course, be attributed in part to a coincidental irregularity in certain of the older measurements, but it suggests that the current cycle has not included times of extreme conditions.

VII. CONCLUDING DISCUSSION

Before concluding, brief references should be made to variations in the measurements of the dielectric constant of air and to determinations of absolute wave lengths which have been made in air. In regard to the dielectric constant, it seems that the number of observations and the accuracies obtained do not warrant a detailed analysis. The value given in the International Critical Tables is $1.000585 \pm 5 \times 10^{-6}$ and from theory and the conclusions reached in this paper a variation of about $\pm 2 \times 10^{-6}$ would be written to express the necessary minimum range in values for this constant.

If the index of refraction of air varies as suggested by this analysis of existing data, then all determinations made in standard dry air on the relationships between wave lengths of light and other standards

[38] See footnote 35, p. 118. For estimating refractive indices of air during the current cycle, 1912 to 1934, the previously published provisional equation $(\mu_D - 1) \times 10^{-7} = 2927.5 - 0.0798$ is probably preferable to the equation given in figure 2, for the complete interval since 1857.

of length are subject to a periodic error, having an amplitude of about ±1 part per million. In the limited amount of published data concerning these relationships, the agreements are better than this estimate of the possible discrepancies but further consideration [39] shows that this should be the case, since no experiments of this nature have been conducted at such times that extremes in the average refractivity of air would necessarily be expected according to the curves of figure 1.

When considering refractivity as a possible function of general turbidity (on a large scale) and subsequent very gradual settling, it must be remembered that changes in the oxygen and argon volume content of air are not important because their optical densities differ but little from that of air, the small changes in refractivity being, in fact, of opposite sign to those produced in density (m/v). On the other hand, until something more is known regarding the relative proportions and refractivities of the various isotopes and associated molecules which may be present in air, it seems impossible to say that appreciable variations in the index of air may or may not be occasioned by simple storminess and turbidity of the atmosphere, and the subsequent gradual settling of certain components which are heavier and also have higher refractive indices.

The apparent time lag required for the highest indices seems to favor such views as compared with some electrical hypotheses relating to changes in refractivity. Moreover, the excellent consistency between the individual values in Stoll's series of measurements, and the recent report regarding the constancy of air indices obtained at the Reichsanstalt [40] do not accord with certain electrical considerations (such, for example, as an appreciable change produced at low altitudes in the degree of association of molecules), because data on other electrical and magnetic conditions usually show pronounced variations over short periods of time. The views herein presented do not seem, however, to conflict with the possibility that some electrical hypothesis (perhaps increase in ionization) may account in part for those small decreases in the apparent normal density of air that are often found if samplings follow rather promptly after sudden increases in barometric pressure.

All of the experimental evidence, considering both density and refractive index, does accord with the possibility of a small electrical, magnetic, or ultraviolet light effect (say, by means of a change, produced more effectively at increased altitudes, in the degree of association of molecules) which may increase with altitude but is otherwise relatively constant in value except for a slight 23-year variation which is superposed on the 11-year cycles of storminess.

In any event it appears unsafe to rely on the constancy of μ, the refractive index of air, over a period of years, or even when sampled simultaneously in different regions. The average of all measurements, namely 1.0002925 at 0 C and 760 mm pressure, still appears to be a

[39] For example, Benoit, Fabry, and Perot (Travaux et Mémoires du Bureau int., 15, p. 1–134, 1913) observed in 1906, the 18th year of a cycle, and the Sears and Barrell (see footnote 21, page 115) provisional values were obtained in 1931, the twentieth year of the present period.

[40] See footnote 23, p. 116. Presumably this refers to constancy over a relatively short period as compared with the very long times required for appreciable segregation by settling out of heavier components.

fair general value for the sodium lines index, but it may be preferable for any given year to estimate the index from the equation

$$(\mu_D - 1) \times 10^7 = 2932.2 - 0.148S \quad (1)$$

where S is the relative annual sunspot number according to the Wolf-Wolfer series of sunspot observations and the constants are provisional values derived from all available data taken since 1857. The probable error of the estimates derived from this equation is $\pm 5 \times 10^{-7}$.

Since the annual sunspot numbers commonly vary from 0 to 100 it appears from equation 1 and its probable error that variations in index of air may frequently extend over a range of about $\pm 12 \times 10^{-7}$ from the average value. Consequently, since $n = \frac{\overline{n}}{\mu}$ is the definitive relation between the relative index, n, of a medium and its absolute index, $\overline{n}$, one may write, $\Delta n = \pm 12n \times 10^{-7}$ to express approximately the corresponding uncertainty frequently present in carefully corrected indices of refraction which in the course of years are measured with respect to the CO_2-free dry atmosphere of the earth. Similarly, it is found that this same degree of uncertainty in air index is approximately equivalent to ± 0.4 percent variation in the 4 and 5 figure values of $(\mu\lambda - \lambda)$ which are tabulated and used in correcting wave lengths from air to vacuum values. Obviously, then, this question of possible variability in the optical density of air should receive careful consideration whenever one discusses the subject of defining or using radiation in air as a standard of length. The uncertainty can be avoided if such a standard is defined and used in vacuum but with air involved it seems that further experiments over a period of years should precede international agreements.

WASHINGTON, February 20, 1934.

U.S. DEPARTMENT OF COMMERCE NATIONAL BUREAU OF STANDARDS

RESEARCH PAPER RP696

Part of Journal of Research of the National Bureau of Standards, vol. 13, July 1934

CORROSION OF FERROUS METALS IN ACID SOILS

By I. A. Denison and R. B. Hobbs

ABSTRACT

Corrosion of ferrous metals in acid soils is influenced largely by the acidity of the soil. A definite correlation was obtained between the average rates of pitting of ferrous specimens exposed to acid soils for 8 and 10 years and the total acidity of the soils. A similar correlation was also obtained between the total acidity of soils and losses of weight of steel specimens in a laboratory test. The effect of acidity in inducing corrosion is attributed to its action in preventing the formation of protective layers of ferrous and ferric hydroxides. The pitting factor, defined as the ratio of the maximum depth of pits to the average depth of penetration, is shown to be roughly proportional to the ratio of the uncorroded to corroded areas on a metal surface. Measurements of several physical properties of soils which determine their permeability were correlated with the pitting factor, indicating that the more permeable the soil, exclusive of sands, the greater is the tendency for corrosion to take the form of pitting, other conditions being the same. Certain soils may be so impermeable that the rate of pitting in them is very low.

CONTENTS

	Page
I. Introduction	125
II. Influence of acidity in submerged corrosion	127
III. Influence of acidity on corrosion of steel in synthetic soil	128
IV. Influence of acidity on corrosion in natural soils	130
1. Relation between rates of pitting of buried specimens and total acidity of soils	130
2. Relation between rates of penetration of steel in laboratory test and total acidity of soils	135
V. Distribution of corroded and uncorroded areas as indicated by the pitting factor	137
VI. Relation of the physical properties of soils to corrosion	140
1. Methods of measuring physical properties of soils	141
2. Correlations between physical properties of soils and pitting factor	146
VII. Summary	149

I. INTRODUCTION

One of the most important conclusions which has been drawn from the National Bureau of Standards investigation of underground corrosion is that corrosion is determined by the nature of the soil rather than by the kind of ferrous material exposed to the soil. Consequently, efforts are being made to correlate the important physical and chemical properties of the soils at the test sites with their corrosiveness, as indicated by their behavior toward buried specimens of the commonly used pipe materials. Although these studies have not been completed, the results have indicated the influence of several

properties of the soil in producing corrosion and have led to methods for estimating the corrosive action of soils.

Since the soils of the United States are diverse, it is to be expected that the causes of corrosion would differ in different classes of soils, and that methods used in estimating corrosiveness should be adapted to the general class of soil to be tested. It has been shown that in certain arid and semiarid regions measurements of the electrical resistivity of soils are useful as one means of predicting corrosion (1).[1] In more humid regions, such as the eastern United States, where the soils have developed varying degrees of acidity, a relation between corrosiveness and soil acidity might be expected, as has been suggested by one of the authors (2, 3).

The development of acidity in soils is a result of natural processes of weathering under humid conditions. In the soils of arid and semiarid regions of the West and Southwest accumulations of soluble salts are of frequent occurrence, but in the more humid regions the rainfall has been sufficient to remove such salts to a considerable extent. In regions of high rainfall not only have the soluble salts and the difficultly soluble carbonates been removed but also the absorbed bases normally present in the colloidal material of the soil have been partly removed and replaced by hydrogen ions. This process eventually gives rise to the condition known as soil acidity. The depth to which this replacement of bases has occurred varies with rainfall, drainage, type of vegetation, and nature of the parent material. The fully developed soils of the prairie region have become acid to a considerable depth, while soils whose development has been retarded by imperfect drainage or by other conditions are alkaline and may even contain appreciable quantities of salts. East of the prairies, the well developed soils are generally acid throughout the soil profile.

Although many important soils occupying extensive areas are known to be very acid at the depth at which pipe lines are laid, little is definitely known concerning their action on ferrous metals, especially with regard to the mechanism of corrosion in such soils. In fact, a systematic study of the properties of acid soils which influence corrosion has not hitherto been possible owing to lack of adequate experimental data. However, with data now available from examination of specimens which have recently been removed from a large number of the National Bureau of Standards test sites after exposure to the soil for 10 years, the corrosiveness of the soils under study has been fairly well established.

The properties of acid soils which appear to be of primary importance in corrosion are the following: Hydrogen-ion concentration, total acidity, texture and the permeability to air and water. Although any one of these factors may possibly exert a predominant influence on corrosion in certain soils it would seem that in well-drained soils of similar texture a single factor such as hydrogen-ion concentration or total acidity might be correlated with corrosiveness. However, before considering the influence of acidity on the corrosiveness of the soils at the test sites, it is preferable first to review certain investigations of corrosion of submerged specimens in which the influence of the acidity of natural waters was specifically studied, and, secondly,

[1] Figures in parenthesis here and throughout the text indicate references and notes given in the "References" at the end of this paper.

to study the relation between acidity and corrosion in a synthetic "soil" in which acidity is the only variable.

II. INFLUENCE OF ACIDITY IN SUBMERGED CORROSION

It is generally recognized that the acidity of the solution in contact with the metal surface is a factor of great importance in the corrosion of submerged ferrous materials. Baylis (4) has pointed out that the tendency for iron to go into solution would be a function of the H-ion concentration if there were rapid displacement of the solution in contact with the metal and no tendency to form a surface coating. From a large number of tests Baylis has determined the quantities of iron which can remain dissolved in natural waters at various pH values. Practically no iron was found in solution at pH 8 in the absence of oxygen, whereas at pH 6.5 several hundred parts of (ferrous) iron per million remained in solution. The effect of oxygen on such a system in equilibrium is, according to Baylis, to precipitate iron as ferric hydroxide, and to establish an equilibrium at a much lower pH. Baylis has further pointed out that the tendency for iron to go into solution is so great at the pH values of natural waters that the life of iron pipe depends almost entirely on the factors which retard corrosion. The most important of these factors is, of course, the formation of films or protective layers of corrosion products.

The influence of the acidity of water containing oxygen on the protectiveness of rust films has been extensively studied by Whitman, Russell, and Altieri (5) and by Whitman and Russell (6). Employing the oxygen absorption method, these investigators studied the rate of corrosion of iron in a natural water at various pH values and at several oxygen concentrations. They found that between approximately pH 9.5 and 4 the rate of corrosion was unaffected by the H-ion concentration of the main solution, but was determined by the rate at which oxygen diffused to the cathodic surface, and by the protectiveness of the hydroxide film formed on the metal surface. The protective action of this film in water having a pH value as low as 4 was attributed to the fact that the quantity of hydrogen ions coming in contact with the metallic surface was insufficient to neutralize and dissolve the film. However, when carbon dioxide was introduced, rapid corrosion occured at pH 5.4, because then the increased total acidity of the water was sufficient to neutralize the hydroxide film. This result led to the conclusion that total acidity is more important in corrosion by natural waters than is the actual concentration of dissociated hydrogen ions in the solution, i.e., the pH value.

In applying to corrosion in soils the relations between acidity and corrosion which were observed by Whitman and Russell, it should be noted that the acids present in soils are extremely weak. Because of the very slight dissociation of the soil acids, the pH value of a soil may offer no indication of the capacity of the acidic material to prevent the formation of an otherwise protective layer of the hydroxides of iron. A soil having a high pH value and a high total acidity would be expected to be more corrosive than a soil having a low pH value and a low total acidity, because of the greater ability of the soil with the high total acidity to prevent the formation of a protective hydroxide layer.

64093—34——9

Further information concerning the influence of total acidity in submerged corrosion can be obtained from the study of systems in which the pH value of the solution was sustained by adequate buffering. Shipley and McHaffie (7) introduced iron filings into solutions buffered at several pH values and found that the rate of hydrogen evolution in the absence of oxygen was directly proportional to the hydrogen-ion concentration of the solution.

Holler (8), as a result of his study of hydrogen evolution from iron filings in contact with soil in the absence of oxygen, found a logarithmic relation between the total acidity of the Bureau soils and the volume of hydrogen evolved, and suggested that the corrosiveness of soils in humid regions might be predicted from their total acidity.

It is seen from these studies that the rate of corrosion of ferrous materials under certain conditions is definitely related to the acidity of natural waters and of soils. It has also been noted that with a definite oxygen concentration the rate of corrosion is determined by the total quantity of ionizable hydrogen which comes in contact with the metal surface, rather than by the hydrogen ion concentration of the corrosive medium. Unless the quantity of acid which comes in contact with the metal surface is sufficient to prevent the formation of protective hydroxide films, these films will tend to form regardless of the H-ion concentration (within the range of natural waters). Although the work of Shipley and of Holler, previously cited, leaves no doubt concerning the relation between total acidity and the corrosion of iron in soils in the absence of oxygen, the influence of acidity in soils in the presence of oxygen is not well understood. Since oxygen is usually present in moderately drained soils, it is important to ascertain the influence of acidity on the rate of corrosion of iron in the presence of oxygen.

III. INFLUENCE OF ACIDITY ON CORROSION OF STEEL IN SYNTHETIC SOIL

The influence of acidity on the corrosion of steel in soil in the presence of oxygen was studied by means of a laboratory corrosion test, which has been described in a previous publication (2). The test consisted in determining the loss of weight of a steel disk in contact with moist soil for a period of 2 weeks.

For the present study a synthetic soil consisting of quartz flour with 10 percent of agar was employed. The acidity of the material was regulated by additions of a mixture of *N* sodium acetate and *N* acetic acid in such proportions and concentrations as to produce the desired pH and total acidity. The latter was computed from pH 8.3, the neutral point of sodium acetate. These mixtures were employed because of their marked buffer capacities, which allowed large changes in total acidity with relatively small change in hydrogen-ion concentration. The use of buffer solutions gave the added advantage of allowing the pH range to be confined to that normally shown by soils.

The corrosion cells were prepared in triplicate according to the following procedure. The surface of each specimen, which consisted of a disk of cold rolled steel 1.74 in. (44.5 mm) in diameter and 12 mils[2] (0.3 mm) thick, was prepared by rubbing with 1G French

[2] 1 mil=0.001 inch or 0.025 mm.

emery paper and cleaning with ether and alcohol. After weighing, one face of the disk was lacquered in order to confine corrosion to one face only, and the disk was placed in a straight-side crystallizing dish of slightly greater diameter with the unprotected face uppermost. The disk was then covered with 20 g of a quartz flour-agar mixture which had been previously prepared by saturating the material with water, drying slowly on a steam bath, and then crushing the lumps to pass a no. 20 sieve. The material was then compacted by rotating on its surface a brass cylinder weighing about 500 g. A sufficient quantity of the buffer solution was added to produce the desired acidity in terms of milliequivalents of hydrogen per 100 g of soil and to bring the moisture content of the soil up to 40 percent of its dry weight. Each corrosion cell was then inserted in a 1-pint (500 ml) preserving jar in which a small amount of water had been added to produce a saturated atmosphere, and the jars were seled and placed

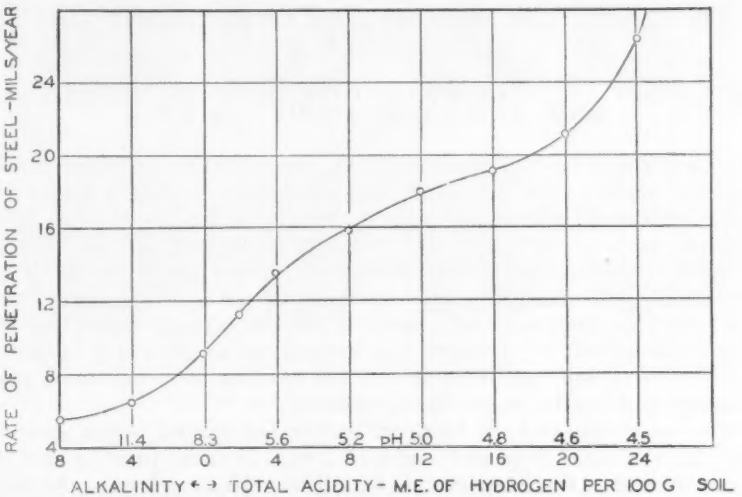

FIGURE 1.—*Relation between acidity and corrosion of steel in synthetic soil.*

in a chamber maintained at 25 C. In order to maintain the partial pressure of oxygen within the jars approximately the same as that in the outside atmosphere the jars were opened for a few minutes every 5 days. At the end of the test period the disks were removed and cleaned by alternate brushing and immersion in warm 10 percent ammonium citrate solution made alkaline with ammonium hydroxide. The loss of weight was calculated as average rate of penetration in mils per year. Most of the values shown in figure 1 are the averages of three (others of two) concordant results. The agreement of duplicates was usually within about 10 percent.

The changes in the rate of corrosion shown in figure 1 can be explained according to the electrolytic theory of corrosion. In the extreme alkaline range, in which the rate of corrosion is very low, it is probable that local anodic areas set up by differential aeration could not develop rapidly because of the protective action of a layer formed by precipitation of ferrous and ferric hydroxide in immediate contact with the metal surface. In the range of slight alkalinity,

where there is evidence of partial film protection, it is probable that ferrous and hydroxyl ions migrating along the surface in opposite directions between anodic and cathodic areas were precipitated over some intermediate area when their concentrations became sufficiently great, and thus reduced the accessibility of air to the active cathodic surface. In the acid range, diffusion of ferrous and hydroxyl ions was not restricted to directions parallel to the metal surface, but also occurred outward into the soil, where they came into contact with oxygen, which caused precipitation as ferric hydroxide. Accumulation of the metal hydroxides on the metal surface and in the soil mass, with consequent reduction in the access of air to the cathodic surface, would explain the diminution in the rate of increase of corrosion with respect to acidity. The sharp increase in the rate of corrosion in acid concentrations greater than 16 m.e. of hydrogen, at pH 4.8, accompanies rapid evolution of hydrogen gas in such soils.

IV. INFLUENCE OF ACIDITY ON CORROSION IN NATURAL SOILS

1. RELATION BETWEEN RATES OF PITTING OF BURIED SPECIMENS AND TOTAL ACIDITY OF SOILS

In a paper previously referred to (3) a correlation between the total acidity of soils at the National Bureau of Standards test sites and the rates of pitting of the ferrous specimens was indicated. Although the importance of soil acidity as a factor in corrosion was evident from this study, the nature of the relationship was indefinite because of uncertainty concerning the corrosiveness of the soils. However, with data available from measurements of corrosion made on buried specimens removed after 10 years, the corrosiveness of many of the soils becomes fairly well established and the relation between total acidity and corrosion can be more clearly defined.

From each site at each biennial inspection period, eight specimens of 1.5 in. (38 mm) pipe and eight of 3 in. (75 mm) pipe of each kind were removed. Each specimen was 6 in. (15 cm) long. As the results with pure open-hearth iron, wrought iron, Bessemer steel, open-hearth steel, and steel containing 0.2 percent of copper, were practically the same, the average values for the five kinds of pipe were used in the calculations. Similar results with cast-iron pipes were less concordant and were hence not included in these averages. The tendency for the depth of pits to increase with the area of the specimen was compensated for by averaging the single deepest pits on the 1½-in. specimens and the two deepest pits on the 3-in. specimens as described by Logan and Grodsky (9). The total area represented by the 24 measurements was 4.7 sq ft (44 dm^2).

In calculating the rates of pitting and of average penetration of the specimens the data for the five inspection periods were used. By plotting the depth of pits on the specimens from each site against the time of exposure and drawing a smooth curve through the points, a value is obtained for the average pitting rate during the first 10 years, which is based on 80 measurements instead of only the 16 measurements that would have been available if only the specimens removed after 10 years had been considered. The benefit of the larger number of measurements in the final result is that it minimizes the effects of

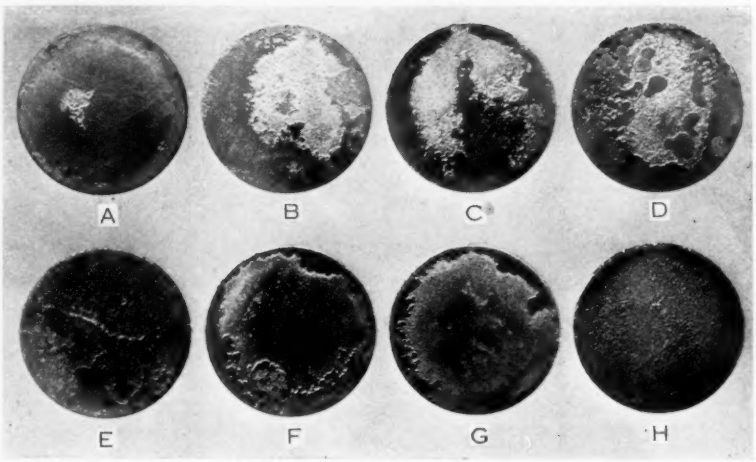

FIGURE 2.—*Appearance of specimens exposed to various soils in laboratory corrosion test.*

Specimen	Soil number	Soil type	Loss of weight	Specimen	Soil number	Soil type	Loss of weight
			gm				*gm*
A	20	Mahoning silt loam	0.074	E	3	Cecil clay loam	0.310
B	9	Genesee silt loam	.101	F	42	Susquehanna clay	.461
C	18	Knox silt loam	.186	G	7	Fairmount silt loam	.496
D	39	Sassafras silt loam	.201	H	43	Tidal marsh	.564

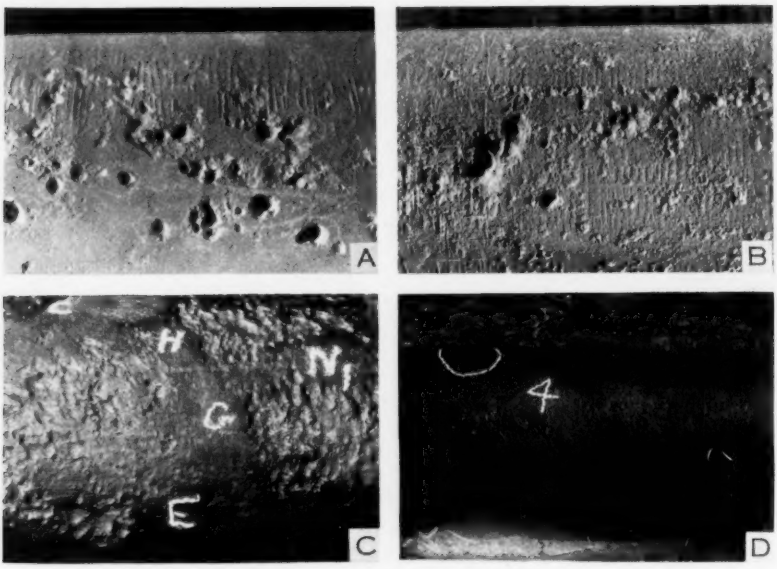

FIGURE 6.—*Types of corrosion observed on pipe lines.*

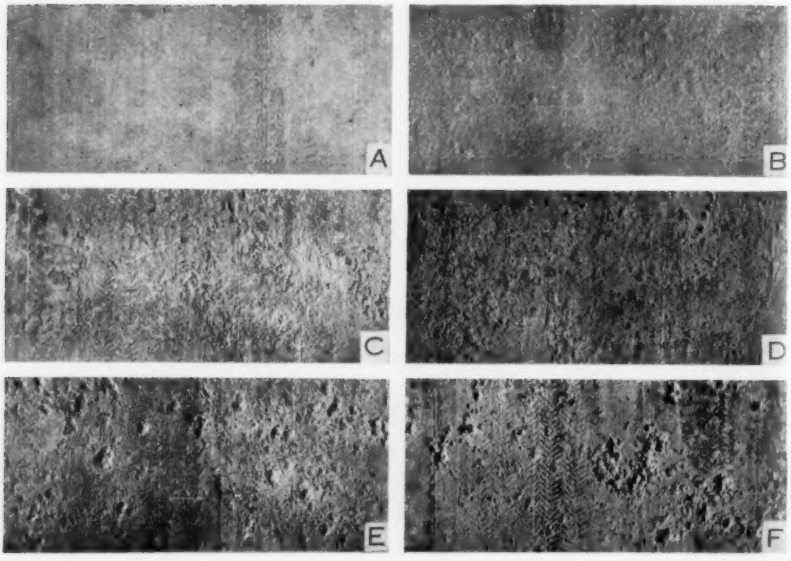

FIGURE 7.—*Types of corrosion shown by ferrous specimens in various soils.*

abnormal variations in the corrosiveness of the soil at any given site. An added advantage of this procedure is that it becomes possible to include in this comparison data of 8 years' exposure in soils from which the 10-year specimens have not yet been removed.

To supplement the data on the field specimens, laboratory studies were made of the corrosion of steel disks in samples of soil from the same test sites. The laboratory test was conducted as described in a previous section with a few modifications. Instead of protecting one surface of the disk with lacquer both surfaces were exposed to the soil. Five grams of soil were placed in the dish, the soil was compacted, and a definite quantity of water was added. The weighed disk was then placed in position, and two 10-g portions of soil were added with successive compression and addition of water. The quantity of water to be used for each soil was determined in preliminary tests by adding increasing amounts of water to corrosion cells and selecting the concentration which produced maximum corrosion. Since the moisture content for maximum corrosion did not differ by more than 5 percent from the moisture equivalent (the percentage of moisture retained by a definite weight of soil under a centrifugal force of 1,000 times gravity), it was sufficient in testing soils by this method to set up cells with only three moisture contents, namely, moisture equivalent, and 5 percent above and below moisture equivalent. In order to avoid corrosive action from the carbon dioxide produced by bacterial activity, a saturated solution of thymol instead of distilled water was used. This precaution was especially necessary in testing calcareous soils containing large quantities of organic matter.

As preliminary studies showed that the losses in weight of specimens in different soils were in about the same ratio for periods from 2 to 8 weeks, a 2-weeks period was adopted for the tests. The values in table 1 are averages of two or more concordant results. In most soils duplicate results were concordant. Except for very small values and occasional erratic results the agreement between duplicates was within 15 percent. The effects of different soils on steel specimens in the laboratory test are shown in figure 2 (for one month instead of the customary 2-weeks contact).

Determinations of total acidity were made by the methods described in previous publications (3, 10). The general method was based on the principle of electrometric titration. Soil extracts were prepared by adding to 10-gram samples of soil increasing amounts of a saturated solution (0.045 *N*) of $Ca(OH)_2$ in NaCl, and the pH values of these extracts, determined colorimetrically, were plotted against the quantity of alkali added. The inflection in the titration curve (usually at about pH 7.8) was taken as the end point of neutralization. For organic soils an indirect method was employed to avoid consumption of alkali by processes other than neutralization of acidity.

Determinations of hydrogen-ion concentration were made by the colorimetric method using a 1: 2 soil-water ratio. Each indicator was adjusted isohydrically to its acid, midpoint and alkaline range to avoid altering the pH value of the tested extract.

The electrical resistivity of the soils was determined by means of the wheatstone bridge, using alternating current. The soil samples were saturated with water, mixed thoroughly, and allowed to stand several hours before being tested. The values were corrected to

60 F (15.6 C). Descriptions of the soils have been given in a previous publication (11). It should be noted that soil 7, though so designated in table 1, is not Fairmount silt loam. Soils of the Fairmount series are alkaline below the surface, whereas the soil in question is very acid to a depth of 40 inches. The data obtained from the laboratory and field tests are summarized in table 1.

TABLE 1.—*Relation of soil properties to corrosion*

Soil number	Soil type	Depth	Location	Corrosion rates			Soil properties		
				Average rate of pitting of wrought specimens at 10 years	Rate of average penetration of wrought specimens at 10 years	Rate of average penetration of steel in laboratory	pH	Total acidity (milli-equivalents per 100 grams of soil)	Resistivity of soil at 60 F.
		In.		*Mils/yr*	*Mils/yr*	*Mils/yr*			*Ohms-cm*
1	Allis silt loam	90	Cleveland, Ohio	7.2	1.4	7.0	7.0	11.4	1,215
2	Bell clay	40	Dallas, Tex	4.5	.8	2.3	7.3	3.5	800
3	Cecil clay loam	32	Atlanta, Ga	7.5	.6	9.9	5.2	11.5	30,000
4	Chester loam	36	Jenkintown, Pa	6.0	1.0	6.8	5.6	7.6	6,670
6	Everett gravelly sandy loam.	36	Seattle, Wash	2.0	.2	1.8	5.9	12.8	45,100
7	Fairmount silt loam	40	Cincinnati, Ohio	3.4	.7	13.8	4.4	29.8	2,120
9	Genesee silt loam	22	Sidney, Ohio	[1]	.5	3.6	6.8	7.2	2,820
10	Gloucester sandy loam	30	Middleboro, Mass	4.4	.7	3.4	6.6	3.6	7,460
11	Hagerstown loam	60	Baltimore, Md	7.0	.3	9.2	5.3	10.8	11,000
14	Hempstead silt loam	60	St. Paul, Minn	11.5	.7	4.0	6.2	5.6	3,520
15	Houston black clay	36	San Antonio, Tex	6.0	1.1	5.9	7.5	5.0	570
16	Kalmia fine sandy loam.	30	Mobile, Ala	6.9	1.0	10.6	4.4	11.8	8,290
17	Keyport loam	36	Alexandria, Va	3.9	1.2	15.2	4.5	19.1	5,980
18	Knox silt loam	48	Omaha, Nebr	5.7	.5	5.9	7.3	1.4	1,410
19	Lindley silt loam	36	Des Moines, Iowa	6.0	.5	7.4	4.6	10.9	1,970
20	Mahoning silt loam	50	Cleveland, Ohio	4.1	.7	4.5	7.5	1.5	2,870
21	Marshall silt loam	36	Kansas City, Mo	6.5	.9	9.5	6.2	9.5	2,370
22	Memphis silt loam	33	Memphis, Tenn	6.0	1.1	6.9	4.9	9.7	5,150
24	Merrimac gravelly sandy loam.	33	Norwood, Mass	2.0	.2	3.0	4.5	12.6	11,400
25	Miami clay loam	36	Milwaukee, Wis	4.5	.3	3.1	7.2	4.7	1,780
26	Miami silt loam	48	Springfield, Ohio	[1]	.3	2.8	7.3	2.6	2,980
27	Miller clay	30	Bunkie, La	4.0	.8	4.4	6.6	3.7	500
29	Muck	24	New Orleans, La	10.9	2.3	11.1	4.2	28.1	1,270
30	Muscatine silt loam	36	Davenport, Iowa	4.1	.7	6.3	7.0	2.6	1,300
31	Norfolk sand	24	Jacksonville, Fla	4.0	.4	3.2	4.7	1.8	20,500
32	Ontario loam	48	Rochester, N.Y	4.5	.4	2.7	7.3	.5	5,700
33	Peat	24	Milwaukee, Wis	9.7	1.7	5.9	6.8	36.0	850
34	Penn silt loam	34	Norristown, Pa	6.5	.7	5.6	6.7	7.0	4,900
36	Ruston sandy loam	36	Meridian, Miss	4.7	.4	4.2	4.5	4.6	11,200
37	St. Johns fine sand	30	Jacksonville, Fla	7.3	1.3	7.2	3.8	15.3	11,200
38	Sassafras gravelly sandy loam.	30	Camden, N.J	3.0	.4	3.2	4.5	1.7	38,600
39	Sassafras silt loam	36	Wilmington, Del	5.7	.8	7.6	5.6	6.6	7,440
40	Sharkey clay	30	New Orleans, La	7.3	1.2	8.1	6.0	9.4	970
41	Summit silt loam	36	Kansas City, Mo	6.4	.8	9.7	5.5	11.0	1,320
42	Susquehanna clay	30	Meridian, Miss	9.7	1.6	17.9	4.7	28.2	13,700
43	Tidal marsh	36	Elizabeth, N.J	10.0	1.8	18.1	3.1	36.8	60
44	Wabash silt loam	30	Omaha, Nebr	7.1	.5	7.3	5.8	8.8	1,000

[1] Not determined.

It will be seen from the table that the soils differ widely with respect to their corrosiveness and their acidity and resistivity. The rate of average penetration of the field specimens is seen to range from 0.2 to 2.3 mils per year (soils 6 and 29) and the rate of pitting from 2 to 11.5 mils (soils 6 and 14). Although the soils that show extreme pitting, i.e., 29, 33, 42, 43, also show large average penetration, there is no consistent relation between pitting and average penetration. The pH varies from 7.5 in soils 15 and 20 to 3.1 in the very acid tidal marsh soil, 43. The total acidity ranges from 0.5 m.e. in soil 32, to 36.8 m.e. in soil 43. There is no consistent relation between the values for hydrogen ion concentration and total acidity; soil 31, having a pH of 4.3, contains 1.8 m.e. of ionizable hydrogen, while soil 42, having the same pH value, contains 28.2 m.e. of hydrogen. Although the influence of the texture of the soil on corrosion will be discussed in a succeeding section, it may be noted at this time that the sandy soils, 6, 10, 24, 31, and 38, are relatively noncorrosive. The data for resistivity cannot be correlated with the corrosion data.

Although there are many exceptions, certain definite trends can be observed between corrosion, as indicated by the field and laboratory tests, and acidity, as indicated by the values for hydrogen-ion concentration and for total acidity. Soils having pH values above 7 (2, 15, 18, 20, 25, 26, 30, and 32) are relatively noncorrosive, while soils having low pH values (29, 37, 42, and 43) are corrosive. The well-drained sandy soils (6 and 24) do not conform to this relation.

If the values for total acidity are now compared with the rates of pitting, a fairly satisfactory correlation is seen. Thus, soils 1 and 33, which are corrosive in spite of their high pH values, have high total acidities. The pitting tendencies are more clearly indicated by the values for total acidity than by their pH values. Thus, according to pH, soils 1, 3, 4, 11, 16, 21, 39, and 41 would be grouped simply as moderately pitting soils. However, when arranged in the order of increasing total acidity, they stand in the order of their corrosiveness with respect to pitting.

In the light of the theoretical considerations advanced earlier in this paper it would be expected that the total acidity of soils would indicate their relative corrosiveness more exactly than would values for H-ion concentration. If it is assumed that corrosion is inhibited by films of hydrated oxides formed on the metal surface, then the formation of such films would be determined by the total quantity of ionizable hydrogen in contact with the corroding metal rather than by the concentration of hydrogen ions. If the quantity of ionizable hydrogen (that is, the total acidity) is sufficient to neutralize hydroxyl ions as they are formed at the cathode, then a protective hydroxide layer will not be produced and corrosion will continue unrestricted. On the other hand, if a high concentration of hydrogen ions is not accompanied by a high total acidity, then the production of hydroxyl ions at the cathode will ultimately result in a decrease in hydrogen ion concentration and in the precipitation of metal ions as hydroxide in the form of a protective film.

The relation between the average rate of pitting of the ferrous specimens and total acidity is best illustrated graphically. In plotting the data shown in figure 3, the values for sandy soils were

omitted. The data for certain other soils, nos. 9 and 26, which conformed well to the acidity relation after 8 year's burial, are not shown in the figure since some doubt exists as to their rates of pitting at 10 years.

The relation between pitting and total acidity shown in figure 3 can be explained by assuming that the protective effect of the products of corrosion varies with the acidity of the soil. The relatively slight corrosion observed in the soils having low total acidities, such as 20, 30, and 32, would then be accounted for by assuming that precipitation of ferrous and ferric hydroxides in immediate contact with the metal surface produced a dense rust layer which tended to inhibit further corrosion. The higher corrosion rates in the moderately acid soils, such as 3, 16, 21, and 41, would then be ascribed to the lessened protectiveness of the rust layer with increasing acidity. Because of the greater solubility of the hydroxides of iron in these soils there was probably appreciable diffusion of the metallic and hydroxide ions outward into the soil, precipitation occurring at an appreciable distance from the metal surface when the concentrations of the reacting ions became sufficiently great. Accumulation of the precipitated corrosion products in the pore spaces of the soil would tend to restrict the movement of air through the soil to the cathodic areas, and would result in a reduced rate of corrosion. In the very acid soils, 29, 33, 42, and 43, it is probable that precipitation of the hydroxides in quantities sufficient to affect the rate of corrosion does not take place until a large loss of metal has occurred.

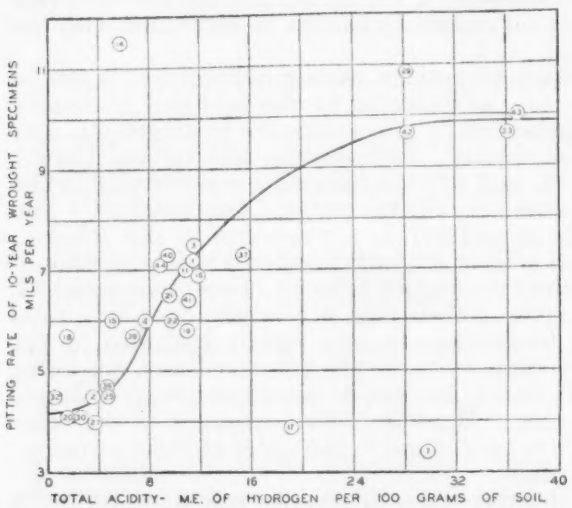

FIGURE 3.—*Relation between pitting rates of 10-year specimens and total acidity of soils.*

It is of interest to note in figure 3 that the rates of pitting in two very acid soils, 7 and 17, are even lower than the rates of pitting in the least acid of the soils. This fact may be taken to indicate the predominating influence of some factor other than acidity in the corrosiveness of these soils. As will be seen in a succeeding section on the physical properties of the soils, the failure of these soils to conform to the acidity relation may be ascribed to their natural impermeability to air. No explanation can be offered at this time for the high-pitting rate in soil 14.

Although the low acidities of soils 2, 15, 20, 30, and 32 are sufficient to account for their relatively low corrosiveness, the presence of calcium carbonate in these soils also probably tends somewhat to inhibit corrosion. Since the solutions in contact with the metal

surface in these soils are in equilibrium with calcium carbonate, an increase in the hydroxyl ion concentration at the cathode would result in the precipitation on the metal of a thin layer of calcium carbonate which would have some protective action. Precipitation of this kind is known to occur in the interior of pipes carrying water saturated with calcium carbonate.

Although a correlation exists between rate of pitting and total acidity, no correlation is evident between acidity and the average penetration of the specimens in the field test, and, in fact, none should be expected. Examination of the specimens shows that much of the surface of the specimens from certain soils remains uncorroded even after 10 years' exposure to the soil. Since the unit area on which the calculation of average penetration is based includes uncorroded as well as corroded area, it is evident that the greater the uncorroded area the lower will be the value for average penetration, other things being equal. As will be brought out later, the distribution of corrosion or the relative proportion of corroded to uncorroded area depends largely upon certain physical properties of the soil. According to this view, soil acidity has no effect on the distribution of corrosion and hence affects the average penetration only as it influences the rate at which the corroded areas deepen. If, however, the average penetration were calculated on the basis of the corroded area rather than of the total area, it is reasonable to expect that a correlation between acidity and the average penetration would be obtained.

In considering the application of the total acidity and corrosion tests to estimate the probable corrosive action of soils on a pipe line it should be especially noted that the electrical currents flowing along a pipe line may seriously affect the rates of corrosion which would occur if the pipe were unconnected. Thus the rate of corrosion of a section of pipe line which is discharging current would be expected to be greater than that on a single length of unconnected pipe in the same location. It may therefore be necessary in connection with corrosion surveys to supplement the acidity measurements with data from other tests, such as soil resistivity.

2. RELATION BETWEEN RATES OF PENETRATION OF STEEL IN LABORATORY TEST AND TOTAL ACIDITY OF SOILS

The relation between the rates of penetration of the steel disks in the laboratory test and the total acidity of the soils is shown in figure 4. It will be noted that although this curve has the same general shape as figure 1, in which the relation between acidity and corrosion in synthetic soil was shown, a given value for acidity in a soil corresponds to a much lower rate of corrosion than does the same value of acidity in the acetic acid-sodium acetate mixture. This result is to be expected from the fact that in soils the acid is difficultly soluble and hence, slowly diffusible, whereas in the buffer mixture the reverse is the case.

It is of special interest to note that soils 14 and 17, which departed widely from the relation between pitting and total acidity, conform well when the values from the laboratory corrosion test and total acidity are plotted. Although the plotted value for soil 7 does not lie near the curve, this soil is shown to be corrosive, probably because of its high acidity. Acid soils high in organic matter, namely, soils

29 and 33, did not conform to the relation. It was observed that in these soils the corrosion products of steel formed with the organic matter a dense layer which could be removed from the surface of the disk only with great difficulty. The layer probably excluded oxygen and so checked further corrosion. The rather wide scattering of the points shown in figure 4 indicates the importance of factors other than acidity that influence corrosion.

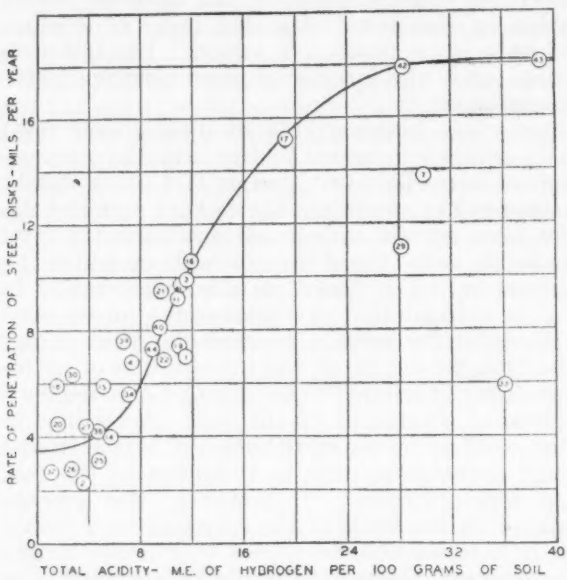

FIGURE 4.—*Relation between rates of penetration of steel in laboratory test and total acidity of soils.*

In order to show the degree of correspondence between the pitting data from the field specimens and the corrosion losses sustained in the same soils in the laboratory, the 10-year rates of pitting were plotted against the average rate of penetration of the disks (see fig. 5). A fairly satisfactory correlation is indicated. The exceptions to the relation are either poorly drained soils in which deficiency of oxygen inhibited pitting at the test site, or organic soils the corrosiveness of which is not well indicated by the laboratory test in its present form. In consideration of the many factors influencing corrosion in the field which cannot be evaluated in a laboratory corrosion test, it would seem that the correlation obtained is as good as could be expected. For most normally developed acid soils, the laboratory test appears to be of

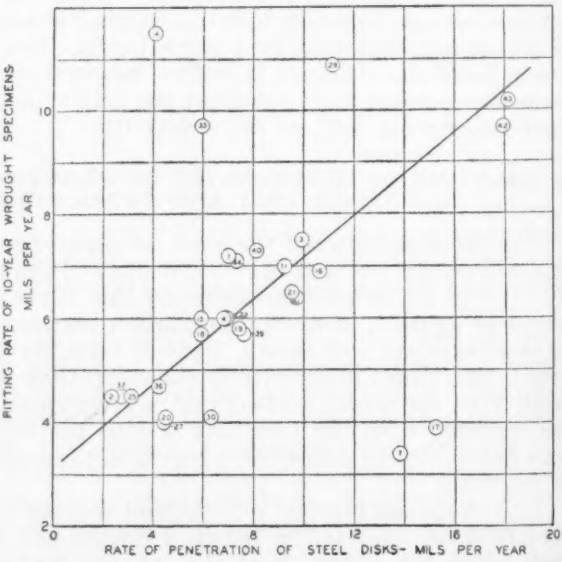

FIGURE 5.—*Relation between rates of pitting of 10-year wrought specimens and rates of corrosion of steel in laboratory test.*

value, at least to determine whether some form of protection against corrosion is needed.

The laboratory corrosion test indicates roughly whether the average penetration over the surface of the buried specimens would be large or small; but no correlation is evident or to be expected between the rates of average penetration of the field and laboratory specimens. A close correlation between rates of average penetration in the field and in the laboratory could occur only if the corroded areas of the two sets of specimens were always in the same ratio. This is known not to be the case. Corrosion occurred more or less generally over the surface of the disks, but the corroded areas of the field specimens varied greatly, from the relatively small area occupied by sharp pits on certain specimens to the entire surface of others. As will be shown later, the corroded area of the specimens is influenced largely by the physical characteristics of the soils in the field. When the soils are brought into the laboratory and prepared for testing, these characteristics are necessarily modified.

V. DISTRIBUTION OF CORRODED AND UNCORRODED AREAS AS INDICATED BY THE PITTING FACTOR

It has been observed in inspecting underground pipe lines that corrosion may take widely different forms, from the production of sharp isolated pits to a uniform attack of the metal surface. This range in the form of corrosion is illustrated by photographs of sections of operating pipe lines (fig. 6). In figure 6 (A) in which pitting is especially pronounced, it will be observed that the corroded area is relatively small, whereas in figure 6 (D) there is very little pitting, although practically the entire surface has been attacked.

The variation in the type of corrosion which may occur in soils is exhibited especially well by the specimens of ferrous materials which have been removed from the National Bureau of Standards test sites. Figure 7 illustrates corrosion patterns on steel specimens ranging from a uniform attack of the metal surface with entire absence of pitting (7 A) to a highly localized attack in the form of deep, well-marked pits (7 F). It will be especially noted from table 2, in which the essential data relative to figure 7 are shown that, although the weight of metal lost from the specimens is roughly the same, the maximum depth of pits ranges from zero to 107 mils. Accordingly, the pitting factor, defined as the ratio of the maximum depth of pit to the average penetration, varies from 1 to 24.5.

TABLE 2.—*Variation of maximum pit and pitting factor at the same stage of corrosion*

Number	Soil number	Soil type	Loss of weight	Average penetration	Depth of maximum penetration	Pitting factor
			Oz/ft²	*Mils*	*Mils*	
1	47	Unidentified silt loam	2.11	3.2	3.2	1
2	27	Miller clay	3.73	5.7	36	6.3
3	20	Mahoning silt loam	2.99	4.6	34	7.4
4	16	Kalmia fine sandy loam	4.23	6.5	60	9.3
5	3	Cecil clay loam	3.43	5.3	63	11.8
6	14	Hempstead silt loam	2.86	4.4	107	24.5

The fact that the ferrous specimens removed from any one soil exhibit essentially the same corrosion pattern regardless of the nature of the material, suggests immediately that the physical or chemical properties of the soil control the character of corrosion. It has been observed, for instance, that the specimens which have been in contact with poorly drained soils for a number of years are usually corroded uniformly, but those in well-drained soils show a greater tendency toward localized attack. These observations indicate a relation between the type of corrosion and the permeability of the soil.

In order to correlate the ratio of corroded and uncorroded areas on the specimens with the physical characteristics of soils, it is necessary to have a suitable measure or index of these areas. Unfortunately, it was not practicable to measure the corroded and uncorroded areas on all of the specimens, but as will be shown, the pitting factor may be employed as a rough index of the ratio of these areas.

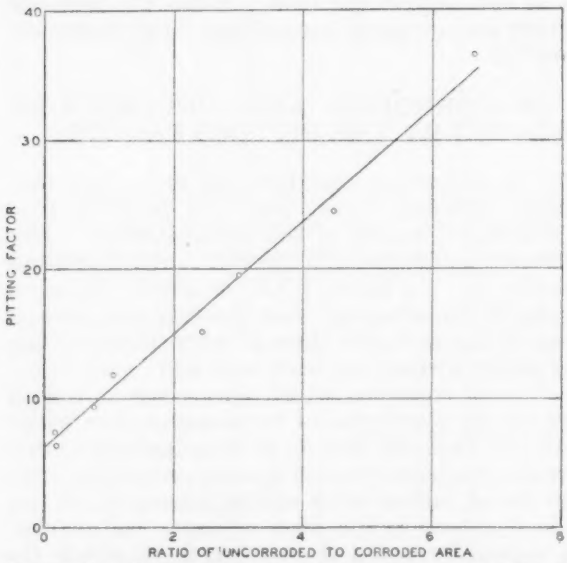

FIGURE 8.—*Relation between pitting factor and ratio of uncorroded to corroded area.*

As the pitting factor is defined as the depth of the deepest pit divided by the average depth of penetration, if a single pit of uniform depth (and no other corrosion) occurs on a specimen of unit area, the area of the pit can be readily calculated from the pitting factor. In this case the pitting factor would correspond to the depth of the pit divided by its volume, and the area of the pit, which would be equal to the volume divided by the depth, would therefore be the reciprocal of the pitting factor.

It is evident that this simple relation cannot be used to calculate the corroded area of actual specimens because pits have irregular shapes and because the average depth of all the pits on a specimen is unknown. However, since visual examination of the corroded specimens indicates a possible relation between the pitting factor and the ratio of uncorroded and corroded areas, it seemed worth while to devise a method which would test this relation experimentally. The method consisted in making on paper impressions in ink of a group of corroded specimens and measuring the total area covered by ink, which corresponded to the uncorroded area. The corroded area was then obtained by subtraction from the total area. If the corroded area was small, it was directly measured and the uncorroded area was obtained by difference. The areas were measured by placing trans-

parent coordinate paper over the ink impression and counting the number of squares covering the black or white areas.

In order to produce a firm pressure as the specimen was rolled over the paper a 2-foot (60-cm) length of 1½-inch (38-mm) pipe was attached firmly to the specimen in such a manner that the projecting ends of the pipe could be used as handles. It was found that sharp outlines of the pits could be obtained by making the impression on paper resting on a resilient rubber pad. Seven steel specimens with pitting factors from 6.3 to 36.6 were employed. In figure 8 it is seen that the pitting factors are roughly proportional to the ratio of the uncorroded to the corroded areas.

In order to account for the distribution of the corroded and uncorroded areas on the test specimens it may be assumed that they coincide respectively in a general way with the anodic and cathodic areas set up by the action of the soil. It is recognized that there may have been a certain shifting of the anodic and cathodic areas as a result of changes in soil moisture and aeration, but these temporary effects probably produced only a superficial roughening of the specimens.

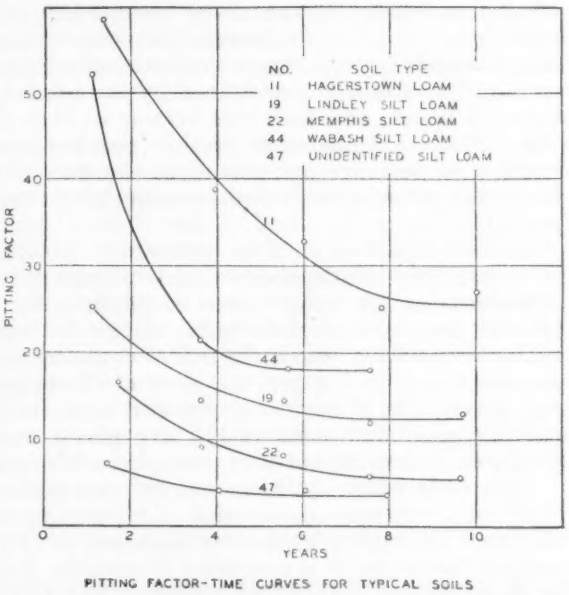

FIGURE 9.—*Pitting factor time curves of various soils.*

Figure 9 shows the change with time of the pitting factors for typical acid soils. After about 8 years these pitting factors become approximately constant; that is, the ratios of the rates of average and maximum penetration remain the same. These constant pitting factors (based on 10 years' observations) are listed in table 3 for most of the soils considered in this investigation.

TABLE 3.—*Pitting factors of acid soils*

Soil number	Pitting factor	Soil number	Pitting factor	Soil number	Pitting factor
1	5.7	17	4.5	33	5.5
2	7.5	18	12.5	35	7.5
3	10.0	19	12.5	36	13.5
4	5.5	20	5.5	37	6.0
5	4.7	21	10.0	39	7.5
6	11.7	22	5.5	40	6.5
7	4.5	24	10.0	41	8.0
8	10.0	25	12.5	42	8.0
10	5.3	27	5.0	43	5.0
11	25.5	29	5.0	44	18.0
14	15.0	30	6.0	47	3.0
15	6.0	31	11.0		
16	9.8	32	10.5		

VI. RELATION OF THE PHYSICAL PROPERTIES OF SOILS TO CORROSION

The influence of the physical properties of soils on their corrosiveness has not hitherto been systematically studied, although the importance of physical factors in soil corrosion has been recognized. The relation of the mechanism of the corrosion of lead in soils to the size of soil particles has been explained by Burns and Salley (12). These investigators found that the rate of corrosion increased with increase in particle size. The corrosion was attributed to the operation of oxygen concentration cells, which originated from partial or complete exclusion of oxygen at the points of contact of the metal and the soil particles. Such areas became anodic to the surrounding parts of the metal surface that were more accessible to air. (Potential differences of approximately 1 volt have been obtained by Shepard in this laboratory with iron under conditions involving differential aeration.) Burns and Salley point out that the ratio of cathodic to anodic area on a metal surface is determined by the total area of contact between soil and metal, and that this area is in turn determined by particle size. Since a decrease in particle size permits contact of a greater number of particles per unit area, the area of contact increases, and hence the ratio of cathodic to anodic area decreases with decrease in particle size.

In their explanation of the mechanism of corrosion Burns and Salley point out that the resistance and potential difference in the cell under consideration are independent of particle size. Hence the cathodic current density and the degree of polarization must vary inversely with particle size. Since the rate of corrosion depends upon the rate of depolarization by oxygen, the amount of oxygen required to maintain any given rate of corrosion per unit area increases with decrease in particle size, and conversely, any given concentration of oxygen produces increasing rates of corrosion with increase in particle size.

This explanation by Burns and Salley was reached from a laboratory study of the effects on corrosion of mineral particles of a limited range of size. In applying this explanation to corrosion in soils under natural conditions it is necessary to consider that the units of structure in soils are not individual particles but relatively large masses or aggregates of particles. These aggregates range in physical condition from dense, compact masses impermeable to air and water to porous masses through which water and air penetrate readily. According to the mechanism of corrosion just described, in dense, impermeable soils, in which air would be excluded from a relatively large area, the area of contact between soil and metal would be large and the anodic area would be relatively great, hence corrosion would take the form of large uniformly attacked areas. Since the cathodic current density and polarization would be relatively great because of the small cathodic area, and the oxygen concentration would be low because of the denseness of the soil, it follows that the rate of penetration by corrosion would be low. On the other hand, in porous, highly permeable soils, the area from which oxygen is excluded would necessarily be small, and hence the anodic area would also be small. Since the cathodic current density and the polarization would be low, the rate of penetration by corrosion would be relatively great, unless it was reduced by the accumulation of corrosion products. Under these conditions corrosion would take the form of pitting.

From the foregoing considerations it is evident that the permeability of soils to air determines to a large extent the rate of corrosion and the distribution of corroded areas on the metal surface. Hence it should be possible to correlate those properties of soil which determine their permeability with expressions of the distribution of corroded areas, such as the pitting factor.

It is well known that the permeability of a soil is largely dependent on its texture, illustrated by the excessive drainage of sands and the poor drainage of many heavy clay soils. With decreasing size of particles the size of the capillary spaces in soils tends to diminish, so that considerable resistance may be offered to the movement of fluids, especially in the usual moist condition of soils several feet below the surface. It has been shown by previous investigators that over a definite range of size of spherical particles the volume rate of flow varies directly with the square of the average diameter of the particle (other conditions being the same). This simple relation, however, cannot be applied generally to soils, partly because the particles of clay and silt are not spherical and are not of approximately uniform size.

Although, as previously stated, heavy clay soils tend to be impermeable, some soils containing a high percentage of clay are porous and well aerated. Impermeable clay soils are usually characterized by the presence of a clay fraction which, in the presence of water, shows characteristic colloidal properties such as high dispersability and absorptiveness and a marked tendency to swell. In relatively permeable clays, these properties are not pronounced. Because of the marked retentiveness of highly colloidal soils for water the interstitial spaces are largely filled with water, and offer considerable resistance to the movement of air.

The permeability of a soil is influenced not only by the texture (i.e., the size distribution of the particles) and by the colloidal behavior, but also by the degree of compactness or denseness of the soil, which is determined by the average diameter of the pores.

1. METHODS OF MEASURING PHYSICAL PROPERTIES OF SOILS

The physical properties of soils which influence their permeability have been recently studied by Slater and Byers (13). It was found that the relative permeability of soils was indicated by measurements of several physical properties and also by expressions derived from these measurements. Thus the percentage of silt, the dispersability of the silt and clay and an expression obtained by dividing the percentage of readily dispersed silt and clay by the colloid-moisture equivalent ratio were correlated with the measured permeability of undisturbed cores of various surface soils. None of these properties, however, appeared to be correlated with the observed percolation rates for the subsoils. It is evident that the swelling of a mass of soil which is associated with the dispersiveness of the individual particles would tend to reduce the size of interstitial spaces, thereby increasing the resistance to the movement of air.

Since the rate of movement of air in soils is controlled largely by the total space through which air may diffuse, it was thought that comparison of the relative volumes occupied by air under specified conditions in the different soils might provide an index to their permeability. Such measurements to have the greatest significance

should be made under conditions which simulate the natural condition of the soil with respect to moisture content and degree of packing as indicated by the apparent density. By means of centrifugal force the moistened samples of soil were compacted until their volume weights approached closely the volume weights of undisturbed lumps of soil from the corresponding test sites. The moisture contents of the centrifuged samples also approximated the average moisture contents of the soils at the test sites so far as these values could be determined. The volume of the compressed sample which is occupied by air will be referred to in the succeeding discussion by the term "volume of voids", following the practice of Boyd (14).

1. Mechanical analysis including colloid content was made by the method now employed at the Bureau of Chemistry and Soils of the United States Department of Agriculture (15). This method depends upon the relation of settling velocity to particle size, as given by Stokes' formula for the fall of a solid sphere in a viscous fluid.

2. Water-holding capacity was determined by the method employed by Slater (13). A 30 g sample of soil contained in the screen-bottom box also used for the moisture equivalent determination was saturated with water, centrifuged for 40 minutes at 1,000 times gravity to produce a standard packing and again saturated with water. After draining for 18 hours in a saturated atmosphere the box containing the soil was wiped dry, weighed, dried in an oven at 105 C and reweighed. The loss in weight was expressed as percentage of the weight of the oven-dried soil.

3. Moisture equivalent (16), defined as the moisture retained by a moist soil under a centrifugal force of 1,000 times gravity, was determined on the samples of soil which had previously been compacted to various degrees corresponding to the volume weights of undisturbed lumps of soil from the same test site. Because of the previous treatment of the samples the values obtained were lower in the case of most soils than the values for the moisture equivalent as conventionally determined.

4. *Volume weight* (*apparent specific gravity*).—The volume weight of the compacted soil was determined at the moisture equivalent and after drying in the oven at 105 C. To do so sufficient mercury was added to the soil contained in the moisture-equivalent box to fill the box, and the box containing the soil and mercury was weighed and the volume of the soil was calculated. The volume weight of undisturbed lumps from the test sites was determined by immersing the dry lumps in a dish filled with mercury, calculating the volume of the lump from the weight of the mercury displaced. The value selected for volume weight of lumps of each soil was the average of 6 to 8 closely agreeing determinations made on lumps selected at random.

5. *Volume of voids.*—The term "volume of voids" means the total space occupied by air in a mass of soil compacted by a definite force and having a definite moisture content. It was calculated by subtracting from the volume of moist soil the volume occupied by the soil particles plus the volume of water contained in the soil, and is expressed as percentage of the volume of the moist soil. The volume of the dried soil particles was calculated from their specific gravity as determined by the pycnometer method. The volume of the moist soil was determined on samples which had been compacted centrifugally in an attempt to reproduce for each soil the degree of compaction

indicated by the volume weight of the undisturbed samples from the test sites. The centrifugal force applied ranged from 1,000 to 2,000 times gravity, the samples being alternately saturated and centrifuged. In all soils the final centrifuging was made at 1,000 times gravity in order to insure that the moisture contents at the determination of the volume of voids would be comparable.

Comparison of the volume weights of the centrifuged samples with the volume weights of the soil in the field condition (table 4) shows that, with few exceptions, the latter were higher. However, in most of the soils the measured volume of voids was so low that, even if the material had been compressed to its field condition, the results would not have been significantly different.

6. Dispersiveness of silt and clay was determined by a slight modification of the method described by Middleton (17). A 10-g sample of soil contained in a 1-liter glass cylinder was moistened with distilled water and after 18 hours was suspended in 1 liter of water by shaking end over end 20 times. The suspension was then allowed to settle for 3 minutes and 45 seconds, when a 25-ml sample was pipetted at a depth of 30 cm. (Previous studies have shown that then the sample consisted of particles with a maximum diameter of 0.05 mm.) From the dry weight of the residue obtained by evaporating the pipetted fraction, the total weight of silt and clay in the suspension was calculated. This quantity, expressed as percentage of the weight of the sample, has been designated by Slater and Byers as the "suspension percentage." The ratio of the silt and clay so determined to the total silt and clay obtained by mechanical analysis is called the "dispersion ratio" (17). This value has been calculated for the clay soils in order to determine the relative dispersability of the silt and clay in these soils.

In view of the fact that the moisture equivalent is dependent upon the proportion of the finer capillary spaces to the total pore space, it was assumed that the relative permeability of the soil might be roughly indicated by the ratio of the saturation capacity of the soil (corresponding to the total pore space) to the moisture equivalent. Accordingly, these ratios were calculated and are shown in table 4.

64093—34— 10

TABLE 4.—*Comparison of physical properties of soils with pitting factor*

Soil no.	Soil type	Depth	Mechanical analysis				Water-holding capacity	Moisture equivalent of compacted soil	Volume weight		Volume of voids	Ratio of water-holding capacity to moisture equivalent	Suspension percentage	Dispersion ratio	Pitting factor
			Sand	Silt	Clay	Colloid			Field	Laboratory					
		Inches	*Percent*	*Percent*	*Percent*	*Percent*	*Percent*	*Percent*			*Percent*		*Percent*		
47	Unidentified silt loam	36	9.0	44.9	46.1	27.7	25.8	21.1	1.72	1.74	1.1	1.22	45.5	50.0	3.0
7	Fairmount silt loam	40	10.3	26.1	63.6	55.0	39.2	36.4	2.02	1.79	3.7	1.08	41.2	45.9	4.5
17	Keyport loam	36	9.6	38.6	51.7	39.6	32.8	27.7	1.72	1.60	4.4	1.18	43.5	48.1	4.5
5	Dublin clay adobe	30	25.6	38.6	35.8	30.2	29.2	27.5	2.00	1.85	4.9	1.06	40.8	54.8	4.7
27	Miller clay	30	1.4	10.8	87.8	71.5	48.6	44.6	2.01	1.78	1.9	1.09	30.2	30.6	5.0
4	Chester loam	36	29.3	53.0	17.7	9.9	34.5	22.9	1.78	1.66	7.0	1.51	27.9	----------	5.5
20	Mahoning silt loam	50	19.6	44.1	36.3	23.7	22.9	18.6	1.90	1.83	3.8	1.23	37.7	46.9	5.5
22	Memphis silt loam	33	1.2	76.5	22.3	18.3	43.5	28.4	1.67	1.64	9.6	1.53	38.7	----------	5.5
1	Allis silt loam	90	9.8	37.7	52.5	31.1	23.7	20.2	----------	1.83	1.1	1.18	38.0	42.1	5.7
15	Houston black clay	36	4.4	25.2	70.4	62.0	53.2	50.5	2.08	1.83	5.7	1.05	28.3	29.6	6.0
30	Muscatine silt loam	36	2.1	65.5	32.4	26.1	30.3	24.0	1.81	1.68	7.2	1.26	25.7	26.3	6.0
40	Sharkey clay	30	2.5	50.4	47.1	32.8	42.8	31.0	1.78	1.73	2.3	1.38	24.9	25.5	6.5
2	Bell clay	40	17.2	37.9	44.9	40.4	41.4	35.2	1.95	1.93	2.0	1.18	19.1	23.0	7.5
35	Ramona loam	36	35.9	37.3	26.0	19.3	20.4	15.8	1.88	1.77	10.9	1.29	22.2	----------	7.5
39	Sassafras silt loam	36	42.1	42.6	15.3	8.7	27.4	18.3	1.72	1.76	7.5	1.39	18.9	----------	7.5
41	Summit silt loam	36	3.0	56.7	40.3	35.0	36.7	28.1	1.61	1.61	6.9	1.31	24.7	25.5	8.0
42	Susquehanna clay	30	30.1	24.1	45.8	40.9	36.5	24.8	1.79	1.48	14.9	1.47	11.8	16.9	8.0
16	Kalmia fine sandy loam	30	50.4	23.1	26.5	21.8	21.3	16.5	1.65	1.66	12.0	1.29	11.1	----------	9.8
3	Cecil clay loam	32	29.0	24.9	46.1	37.8	47.6	29.9	1.60	1.32	18.2	1.59	4.4	6.2	10.0
21	Marshall silt loam	36	3.2	65.9	30.9	27.1	34.9	24.8	1.66	1.57	10.8	1.41	26.0	26.9	10.0
8	Fargo clay loam	48	2.2	27.7	70.1	50.7	50.8	34.8	1.56	1.57	8.7	1.46	20.2	20.6	10.0
32	Ontario loam	48	42.1	42.1	15.8	8.2	18.4	11.8	1.85	1.81	11.7	1.56	15.9	----------	10.5
19	Lindley silt loam	36	15.7	50.1	34.2	29.3	35.8	26.3	1.76	1.73	3.9	1.36	15.9	18.9	12.5
18	Knox silt loam	48	1.3	78.4	20.3	15.0	46.8	22.0	1.26	1.43	16.6	2.13	24.2	----------	12.5
25	Miami clay loam	36	21.0	43.0	36.0	21.8	22.4	18.6	1.95	1.81	9.5	1.31	24.8	31.4	12.5
36	Ruston sandy loam	36	60.6	21.8	17.6	14.8	32.1	14.9	1.62	1.62	16.0	2.15	17.0	----------	13.5
14	Hempstead silt loam	60	56.6	29.5	13.9	9.5	20.3	12.2	1.76	1.77	14.4	1.66	19.8	----------	15.0
44	Wabash silt loam	30	2.4	66.4	31.2	25.8	33.8	25.3	1.55	1.56	7.2	1.34	22.1	22.6	18.0
11	Hagerstown loam	60	25.8	21.1	53.1	45.9	49.8	31.3	1.49	1.41	15.5	1.59	7.9	10.6	25.5

SOILS CONTAINING LESS THAN 10 PERCENT OF CLAY

10	Gloucester sandy loam	30	64.0	29.4	6.6	2.8	22.8	9.0	1.58	1.58	27.8	2.53	16.4	5.3
37	St. Johns fine sand	30	90.6	4.9	4.5	4.3	35.9	7.0	1.30	1.30	41.4	5.13	3.3	6.0
24	Merrimac gravelly sandy loam	33	72.0	22.4	5.6	2.7	32.2	9.7	1.40	1.40	34.7	3.32	10.4	10.0
31	Norfolk sand	24	97.3	2.1	.6		21.9	2.3	1.55	1.55	38.1	9.52	1.8	11.0
6	Everett gravelly sandy loam	36	69.0	23.8	7.2	3.5	24.7	9.5	1.50	1.50	40.6	2.60	12.2	11.7

2. CORRELATIONS BETWEEN PHYSICAL PROPERTIES OF SOILS AND PITTING FACTOR

The data obtained from the various physical determinations are shown in table 4. In order to facilitate comparison with the pitting factor the data for the various soils have been arranged in the order of increasing pitting factor.

A comparison of the values for the pitting factor with the data on the physical properties of the soils containing more than 10 percent of clay indicates that the pitting factor is very largely determined by the permeability of the soil. It will be noted that increase in the pitting factor is generally accompanied by an increase in the volume of voids and the ratio of water-holding capacity to moisture equivalent. It will also be observed that there is a rough inverse relation between the pitting factor and the quantity of easily dispersed silt and clay, and also between the pitting factor and the dispersability of the clay and silt in the clay soils as indicated by the dispersion ratio. It will also be observed that there is a tendency for the pitting factor to increase inversely with the volume weight of the soils in the field condition, as might be expected.

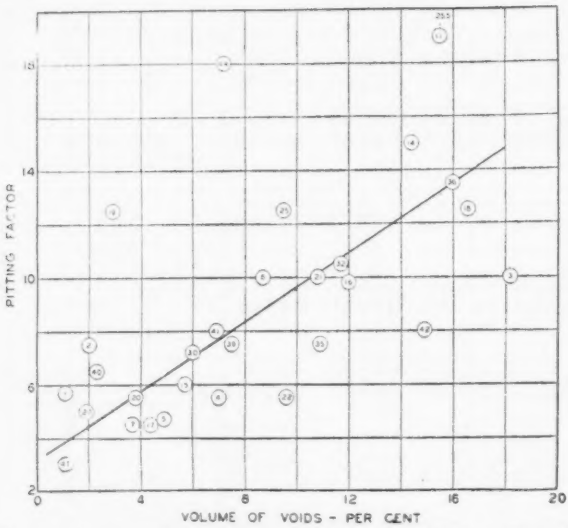

FIGURE 10.—*Relation between volume of voids in soils and pitting factor.*

In figure 10 the correlation between the pitting factor and the volume of voids is shown graphically. The significance of this relation may be best appreciated if it is assumed that the pitting factor is roughly proportional to the ratio of the cathodic to anodic areas on the specimens, as has been suggested. According to this assumption, a low volume of voids, which is associated with a relatively impermeable soil, would indicate a large anodic area corresponding to general corrosion of the metal surface. Conversely, a large value for the volume of voids, associated with a permeable soil would indicate a small total anodic area and hence localized corrosion or pitting. Furthermore, by reason of the large cathodic surface and the corresponding low cathodic current density, the concentration of oxygen required to maintain any given degree of depolarization would be small and deep pitting would result in the absence of interference from the accumulation of corrosion products or other inhibiting factors.

In view of the fact that the values for the volume of voids is determined by the moisture content of the soil, it is apparent that the

goodness of fit of the line drawn through the points (fig. 10) depends largely upon how well the moisture content of the soil at the time of measurement corresponds to the average moisture content of the soil in the field. Secondly, the gross structural features of the soil, such as the natural occurrence of cracks and fissures, affect the permeability to an extent which cannot be evaluated by the methods employed.

As previously indicated, a definite proportionality exists between the pitting factor and the ratio of water-holding capacity to moisture equivalent. The coefficient of correlation for this relation is 0.723 which according to the level of significance of Fisher (18) gives, for 30 observations, a probability somewhat better than 0.99 that the relation is significant. This value compares with 0.722 which is the coefficient of correlation calculated for the pitting factor volume of voids relation shown in figure 10.

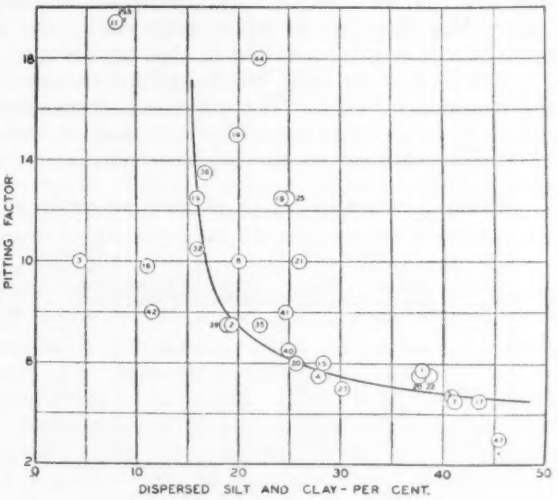

FIGURE 11.—*Relation between dispersed silt and clay in soils and pitting factor.*

The correlation observed between the pitting factor and the moisture ratio may be explained as follows. In a soil having a moisture ratio approaching unity it is evident that the amount of water retained by the soil under a force of 1,000 times gravity is nearly equal to the quantity required for saturation. Since the moisture is held so completely it follows that the capillary spaces through which air might move must be exceedingly fine and, therefore, offer high resistance to the diffusion of air. Under such conditions, which might amount to virtual exclusion of oxygen over a large part of the metal surface, the anodic area must be relatively great and the pitting factor correspondingly small. On the other hand, large values of the moisture ratio indicating large capillary spaces through which air may diffuse would be expected to produce relatively large cathodic areas, which would be indicated by high pitting factors.

The correlation between the quantity of silt and clay which is readily dispersed in water and the pitting factor is shown graphically in figure 11. As indicated by the figure, low pitting factors are associated with high concentrations of silt and clay, the pitting factor decreasing rapidly with the quantity of dispersed material. The explanation of the observed correlation evidently lies in the fact that dispersion of the soil material with the resultant swelling of the colloidal material results in diminution in size of the capillary spaces within the soil. The increased resistance to the diffusion of oxygen

produced in this manner would then tend to increase the anodic area with respect to the cathodic area.

It is apparent that the correlation shown in figure 11 becomes less satisfactory as the quantity of dispersed material decreases and at values below 10 to 15 percent it is probably without significance. It is likely that some minimum quantity of dispersed material is necessary for corrosion to be produced by differential aeration since concentration of dispersed silt and clay on parts of the metal surface may be essential to the effective exclusion of oxygen and so to the development of anodic areas. This observation may possibly have a bearing on the fact that relatively slight pitting has occurred in acid soils containing less than 10 percent of clay.

From the relation which has been developed between the permeability of the soil and the pitting factor, and explanation may now be offered for the failure of certain very acid soils to induce serious pitting. It will be recalled in this connection (fig. 3) that soils 7 and 17, although very acid, produced lower rates of pitting than any of the other acid soils. The physical characteristics of these soils are shown in table 5 for comparison with the characteristics of soils 3 and 11 which conform to the acidity relation.

TABLE 5.—*Comparison of physical properties of soils with pitting rate*

Soil number	Average pitting rate for 10 years	Total acidity	Clay content	Volume of voids	Saturation, moisture equivalent ratio	Suspension percentage	Permeability
	Mils/yr	*m.e.*	*Percent*	*Percent*		*Percent*	
7	3.4	29.8	63.6	3.7	1.08	41.2	Impermeable.
17	3.9	19.1	51.7	4.4	1.18	43.5	Do.
3	7.5	11.5	46.1	18.2	1.59	4.4	Permeable.
11	7.0	10.8	53.1	15.5	1.59	7.9	Do.

From the data shown in table 5 it is apparent that the two groups of soils which differ so widely in their rates of pitting differ also with respect to the physical characteristics which determine their permeability. By the criteria which have been employed, soils 7 and 17 are relatively impermeable, whereas soils 3 and 11 are permeable. It has been seen that highly impermeable soils tend to restrict the accessibility of oxygen over a large part of the metal surface and thus to produce relatively large anodic areas. Since the cathodic current density and hence the degree of polarization must be comparatively high, because of the small cathodic areas, it follows that in the absence of corrosive factors, such as high acidity or high salt content, the rate of penetration by corrosion under conditions of poor aeration would be expected to be low. This conclusion is confirmed by the low rates of pitting which have occurred in soils 7 and 17. These conditions are completely reversed in soils 3 and 11 where, because of their high porosity, air has ready access to the greater part of the metal surface, corrosion being confined to small anodic areas. Because of the large cathodic surface and resulting low current density, depolarization by oxygen is readily accomplished, and the rate of pitting is limited only by the accumulation of corrosion products. It is perhaps significant to note in connection with the present discussion that soil 47, which, by the criteria employed is the least permeable of all the soils, also has the lowest average pitting rate, approximately 1 mil per year.

So far as the data from the other soils are concerned, it is not possible to demonstrate a relation between permeability of the soil and rate of pitting. This might be taken to indicate that, except in very impermeable soils, differences in permeability do not have a marked effect on the pitting rate. However, it is more reasonable to assume that the available data on pitting rates are not suitable for testing this effect, since too few data are recorded for soils of the same acidity but differing permeability.

VII. SUMMARY

The corrosiveness of acid soils toward ferrous metals was studied by means of a laboratory corrosion test and by comparing corrosion data on specimens removed from the National Bureau of Standards test sites with certain physical and chemical properties of soils. The corrosion data from the field tests include measurements of loss of weight and depth of pits on specimens of a variety of ferrous materials removed after 8 and 10 years' exposure to 37 acid soils.

In a preliminary study of corrosion in a synthetic "soil" composed of pulverized quartz and agar it was found that the loss of weight of the test specimens increased markedly with increasing acidity within the range of acidity shown by soils. The low rate of corrosion in the range of mild alkalinity was attributed to the action of an adherent film or layer of ferrous and ferric hydroxides which tended to diminish the accessibility of oxygen to the cathodic surface. The high rate of corrosion in the acid range was explained by assuming that the metal ions diffused readily outward into the soil and that the acidity of the soil neutralized hydroxyl ions as they were formed at the cathode, thereby preventing the formation of a protective rust layer.

Comparison of the average rates of pitting of the field specimens at 10 years indicated that the rates of pitting at practically all of the test sites were determined chiefly by the total acidity of the soil. A similar correlation between the loss of weight of specimens and total acidity was obtained when samples of soils from the test sites were employed in the laboratory corrosion test. The correspondence between the field and laboratory data suggests the use of the laboratory test as a convenient means of testing the corrosiveness of acid soils. However, because of the effect of pipe-line currents it may be necessary to employ supplementary tests, such as the measurement of soil resistivity.

The pitting factor, defined as the ratio of the maximum depth of pit to the average penetration, diminishes with time and appears to approach a fairly constant value after 8 or 10 years. The pitting factor is shown to be roughly proportional to the ratio of the uncorroded to corroded area on a metal surface. This relation was employed in studying the influence of certain physical properties of the soil on the distribution of corrosion.

Measurements of several physical properties of the soil which determine its permeability to air were made in order to relate permeability to the rate of pitting and the distribution of corroded areas. These measurements included the following: (1) Percentage of the total volume of moist soil which is occupied by air; (2) ratio of the moisture required for saturation to the moisture equivalent; and (3) dispersability of silt and clay. Definite correlations were obtained between the values for these properties and the pitting factor, indicating that the greater the permeability of the soil, exclusive of sands, the greater

is the tendency for corrosion to be confined to pits, other conditions being the same. An explanation is suggested for the failure of certain very acid and impermeable soils to induce pitting.

REFERENCES

1. Field study of a long gas line. S. P. Ewing. Amer. Gas Assn. Monthly, vol. 13, pp. 70–76, 1931.
2. Correlation of certain soil characteristics with pipe-line corrosion. I. A. Denison. B. S. Jour. Research, vol. 7 (RP363), p. 631, Oct. 1931.
3. Methods for estimating the corrosiveness of acid soils in contact with iron and steel. I. A. Denison. Oil & Gas Jour., vol. 31, no. 19, pp. 83–87. Sept. 29, 1932.
4. Prevention of corrosion and "red water". J. R. Baylis. Jour. Amer. Water Works Assn., vol. 15, no. 6, pp. 596–633. June 1926.
5. Effect of hydrogen-ion concentration on the submerged corrosion of steel. W. G. Whitman, R. P. Russell, and V. J. Altieri. Ind. Eng. Chem., vol. 16, no. 7, pp. 665–670, 1924.
6. The submerged corrosion of iron. W. G. Whitman and R. P. Russell. Jour. Soc. Chem., Inc., vol. 43, no. 26, pp. 193–196T, 1924.
7. The relation of hydrogen-ion concentration to the corrosion of iron. J. W. Shipley and I. R. McHaffie. Can. Chem. and Met., vol. 8, pp. 121–124, May 1924.
8. Corrosiveness of soils with respect to iron and steel. H. D. Holler. Ind. Eng. Chem., vol. 21, pp. 750–764, 1929.
9. Soil Corrosion Studies, 1930. Rates of Corrosion and Pitting of Bare Ferrous Specimens. K. H. Logan and V. A. Grodsky. B.S. Jour. of Research, vol. 7 (RP329), 1931.
10. Methods for determining the total acidity of soils. I. A. Denison. B.S. Jour. Research, vol. 10 (RP539), 1933.
11. Bureau of Standards soil corrosion studies 1. Soils, materials, and results of early observations. K. H. Logan, S. P. Ewing, and C. D. Yeomans. B.S. Technologic Paper 368, 1928.
12. Particle size as a factor in the corrosion of lead by soils. R. M. Burns and D. J. Salley. Ind. Eng. Chem., vol. 22, pp. 293–297, 1930.
13. A laboratory study of the field percolation rates of soils. C. S. Slater and H. G. Byers. Tech. Bull. 232, U.S. Dept. of Agr., 1931.
14. Physical properties of subgrade materials. J. R. Boyd. Proc. Amer. Soc. Testing Materials, 22 (pt. 11), pp. 337–355, 1922.
15. A pipette method of mechanical analysis based on improved dispersion procedure. L. B. Olmstead and L. T. Alexander. Tech. Bull. 170, U.S. Dept. of Agr., 1930.
16. Moisture equiv lent determinations and their application. L. J. Briggs and J. W. McLane. Jour. Amer. Soc. Agron. 2, pp. 138–147, 1910.
17. Properties of soils which influence soil erosion. H. E. Middleton. Tech. Bull. 178, U.S. Dept. of Agr., 1930.
18. Statistical methods for research workers. R. A. Fisher. 3d edition. Oliver and Boyd, London, 1930.

WASHINGTON, April 4, 1934.

U.S. DEPARTMENT OF COMMERCE NATIONAL BUREAU OF STANDARDS

RESEARCH PAPER RP697

Part of Journal of Research of the National Bureau of Standards, vol. 13, July 1934

PHOTOCHEMICAL DECOMPOSITION OF SILK[1]

By Milton Harris [2]

ABSTRACT

The purpose of this investigation was to study the deterioration of silk on exposure to daylight under natural conditions of use.

The strength of silk cloth decreased and its ammonia nitrogen content increased on exposure to sunlight. Samples of the cloth treated with a tenth normal solution of sodium hydroxide showed smaller changes and samples treated with a tenth normal solution of sulphuric acid greater changes than the untreated cloth under the same conditions.

Similar results were obtained on exposure of samples to north skylight. Samples treated with sodium carbonate solution of 1 percent or less in concentration showed the greatest stability.

The amino nitrogen content was the same for silk stored in the dark and silk exposed to sunlight for 3 months. The rate of hydrolysis in 0.5 normal sodium hydroxide solution, measured by the formation of amino nitrogen, was the same for both samples.

The decrease in breaking strength and increase in ammonia nitrogen content of silk on exposure to light are brought about by atmospheric oxidation in the presence of light.

The results of these experiments are in accord with those obtained in the accelerated aging tests of silk, using the carbon arc lamp as a light source.

CONTENTS

	Page
I. Introduction	151
II. Experimental	152
III. Nature of the photochemical reaction	155

I. INTRODUCTION

Previous work [3] has shown that when silk is exposed to the radiation of a glass-enclosed carbon arc lamp, the extent to which it is weakened depends upon its "pH" (as defined by the pH of an aqueous extract). Silk was found to have maximum stability at about pH 10. As the pH was increased above pH 11 and decreased below pH 3, the stability of the silk decreased rapidly. Silk treated with 0.1 normal sodium-hydroxide solution was more stable to the action of light than untreated silk or silk treated with 0.1 normal sulphuric acid and the latter was the least stable.

[1] The work reported here was made possible by a grant from the Textile Foundation, Inc., to the American Association of Textile Chemists and Colorists.

[2] Research Associate for the American Association of Textile Chemists and Colorists at the National Bureau of Standards.

[3] M. Harris and D. A. Jessup. The Effect of pH on the Photochemical Decomposition of Silk. B.S. Jour. Research, vol. 17, p. 1179–1184, 1931.

The purpose of the present investigation was to study the deterioration of silk on exposure to daylight under natural conditions of use. Both the chemical and the physical breakdowns were followed. The experiments were designed to show something of the nature of the photochemical reaction.

II. EXPERIMENTAL

The general procedure was that used in the previous work and has been described.[4] The decrease in breaking strength of the cloth with duration of exposure was taken as a measure of the physical breakdown of the silk. The chemical breakdown was followed by analyzing specimens for ammonia nitrogen and amino nitrogen. The former is that portion of the nitrogen which is liberated when the silk is boiled in a saturated solution of magnesium oxide. The latter is the portion obtained when the silk is treated with nitrous acid, using the method of Van Slyke.[5]

One series of experiments was concerned with the effect of sunlight. Degummed silk was purified by successive extractions with alcohol and ether and then washed for one-half hour with water at 60 C to remove any adsorbed solvent. Some samples of the silk were soaked in 0.1 normal sodium-hydroxide solution and others in 0.1 normal sulphuric-acid solution for 10 minutes. The excess liquor was removed by centrifuging and the samples were air-dried. Samples of purified acid-treated and alkali-treated silk were then exposed to sunlight. The exposures were continuous day and night, regardless of the weather, under glass at an angle of 45°, facing south. At the end of 15 days the alkali-treated silk had a breaking strength of 53 pounds, the untreated sample 38 pounds, and the acid-treated sample 8 pounds. The strength of the original cloth was 55 pounds. At the end of 4 months the untreated and acid-treated silk had practically no strength but the alkali-treated silk still had 10 percent of its original strength.

At intervals of time samples were analyzed for ammonia nitrogen. The results are given in table 1. All of the exposed samples gave increasing amounts of ammonia nitrogen with increasing duration of exposure, the greatest amounts being present in the acid treated and untreated samples.

TABLE 1.—*Effect of sunlight exposure on ammonia nitrogen content of silk.*

[The number of milligrams of ammonia nitrogen per gram of silk is given]

Time of exposure, days	Untreated silk		Silk treated with	
	Not exposed	Exposed	0.1 N NaOH	0.1 N H_2SO_4
32	0.10	0.31	0.16	0.87
69	.08	.37	.22	1.03
90	.10	.64	.45	2.05
104	.09	.75	.52	2.09
130	.07	1.06	.64	2.81
150	.12	2.00	.95	2.92
175	.11	2.60	1.03	2.99

[4] See reference footnote 3.

[5] D. D. Van Slyke, The Quantitative Determination of Aliphatic Amino Groups, Jour. Biol. Chem., vol. 12, p. 275-84, 1912.

The total nitrogen content, amino-nitrogen content, and rates of hydrolysis of the purified silk (not treated with acid or alkali) which had not been exposed to strong light and which had been exposed to sunlight for 3 months were determined. The sample for analysis was ground to a fine powder. In order to determine rate of hydrolysis, about 5 grams of the powder was shaken in 200 ml of water for 4 hours, using an automatic shaker. The larger particles of silk were allowed to settle and the supernatant liquor was decanted and mixed with an equal volume of 1 normal sodium hydroxide solution. The mixture was kept in a bath at 37 C. Ten ml aliquots were withdrawn at definite intervals of time and analyzed for amino nitrogen and for total nitrogen. The results are shown in figure 1. Neither the unexposed nor the exposed silk contained an appreciable amount of amino nitrogen before hydrolysis. The rate of hydrolysis, measured by the formation of amino nitrogen, was the same for both samples.

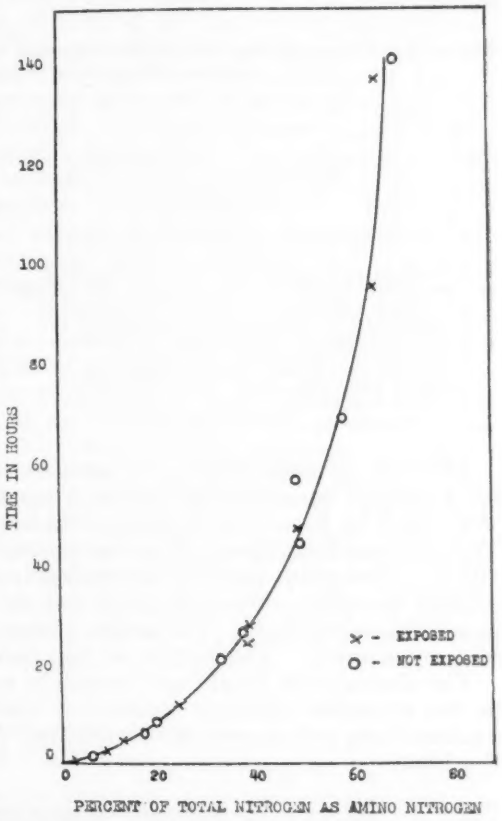

FIGURE 1.—*The rates of hydrolysis of silk which had not been exposed to strong light and which had been exposed to sunlight for 3 months.*

Another series of experiments was concerned with the deterioration of silk cloth treated with acid and alkaline solutions on exposure to north skylight. The samples were exposed continuously in a room behind window glass, vertical, facing north. Plain-weave cloth weighing approximately 1.6 ounces per square yard was cut into pieces about 1 yard square. These were purified by scouring in a 0.5 percent soap solution at 60 C for 20 minutes; rinsing in 3 successive baths of water at 60 C for 20 minutes each; extracting with alcohol and ether for 24 hours each; and finally washing with water at 60 C for 30 minutes. The individual cloths were soaked for 5 minutes in the solutions listed below, centrifuged, and dried at 70 F and at a relative humidity of 65 percent.[6]

(1) No treatment; (2) 0.01 *N* sulphuric acid; (3) 0.01 *N* acetic acid; (4) 0.1 percent sodium carbonate; (5) 0.5 percent sodium carbonate;

[6] The amount of reagent remaining on the fiber may be roughly estimated by assuming that after centrifuging, the silk retains its own weight of solution.

(6) 1.0 percent sodium carbonate; (7) 1.5 percent sodium carbonate; and (8) 0.75 percent sodium bicarbonate.

The breaking strength and appearance of each cloth after exposure for stated periods of time are given in table 2. The acid-treated samples showed the greatest deterioration, the untreated sample was much more stable, and the samples treated with sodium carbonate solutions in concentrations of 1 percent or less showed the greatest stability. These results are in accord with those obtained in the accelerated aging tests of silk, using the carbon-arc lamp as a light source.

TABLE 2.—*The appearance and breaking strength of silk treated with acid or alkaline solutions after exposure to north light*

Sample no.	Treatment	Appearance after exposure for 11 months	Breaking strength (1-inch strip) after—		
			5½ months	7½ months	11 months
			Pounds	*Pounds*	*Pounds*
1	Original (not exposed)	No change	37	37	36
2	0.1 percent Na_2CO_3	Very slightly yellow	34	30	30
3	1.0 percent Na_2CO_3	Slightly yellow	32	29	27
4	0.5 percent Na_2CO_3	Faint yellow	32	29	26
5	None (exposed)	No change	30	29	24
6	1.5 percent Na_2CO_3	Yellow	30	27	23
7	0.75 percent $NaHCO_3$	Faint yellow	28	24	20
8	0.01 N acetic acid	No change	17	16	14
9	0.01 N sulphuric acid	Faint yellow	14	13	12

After 11 months' exposure, samples of the cloth were analyzed for ammonia nitrogen and amino nitrogen. Portions of each cloth were dried for 6 hours at 105 C and the ammonia nitrogen determined. The silk was then thoroughly washed and again dried for 6 hours at 105 C. One-gram portions were dissolved in 20 ml of a 50 percent lithium bromide solution at 80 C and the solution diluted to 100 ml in a volumetric flask. The amino-nitrogen content of each solution was determined. The results of the analyses are given in table 3.

The decrease in breaking strength is accompanied by an increase in the ammonia nitrogen content of the silk. The amino-nitrogen content does not appear to be affected during the deterioriation of the fiber.

TABLE 3.—*The ammonia- and amino-nitrogen content of silk treated with acid or alkaline solutions after exposure to north light for 11 months*

Sample no.	Treatment	Ammonia nitrogen	Amino nitrogen
		Mg/g silk	*Mg/g silk*
1	None (not exposed)	0.07	1.5
2	0.1 percent Na_2CO_3	.15	1.6
3	1.0 percent Na_2CO_3	.15	1.4
4	0.50 percent Na_2CO_3	.23	1.4
5	None (exposed)	.44	1.4
6	1.5 percent Na_2CO_3	.19	1.4
7	0.75 percent $NaHCO_3$	.39	1.7
8	0.01 N acetic acid	.72	1.5
9	0.01 N sulphuric acid	1.08	1.4

III. NATURE OF THE PHOTOCHEMICAL REACTION

The photochemical decomposition of silk is a photo-oxidation reaction. Skeins of 20/22 Japanese silk have been exposed in vacuum and in atmospheres of moist and dry hydrogen and oxygen to north sky light for 4 months. The skeins in the vacuum and in the hydrogen retained their original strength. Those in the dry oxygen lost about 3 percent while those in moist oxygen lost about 10 percent of their strength.

The increase in ammonia nitrogen content of silk during the photochemical deterioration is further evidence that an oxidation reaction has taken place. Palit and Dhar [7] have shown that in the decomposition of most nitrogenous substances, ammonia is formed and the decomposition is accelerated by the presence of oxygen and light. The deterioriation of wool in the carbonizing process is also accompanied by the formation of ammonia, the amounts formed increasing with increasing acid and moisture contents of the wool and with increasing temperatures in the baking oven. When wool containing sulphuric acid is stored at ordinary temperatures, the ammonia-nitrogen content increases with increasing time of storage. When acid treated and untreated specimens of wool were baked in atmospheres of dry on moist air, oxygen, or carbon dioxide showed that both oxygen and moisture have an important influence on the deterioriation of wool. Sulphuric acid increases the rate of deterioration considerably.[8] Leiben and Urban [9] found that the splitting of ammonia from amino acids and other substances proceeds much more rapidly in acid than in alkaline or neutral solutions. Schanz [10] studied the action of ultraviolet rays on egg and serum proteins He found that the greatest change was produced in acid solution and that the reaction was accelerated by oxygen.

The experimental results of this research are in accord with those obtained by other workers in studying the action of light on protein materials. The decrease in breaking strength and increase in ammonia-nitrogen content of silk during exposure are caused by the action of the oxygen of the air in the presence of light.

WASHINGTON, May 4, 1934.

[7] Palit and Dhar. Oxidation of Carbohydrates, Fats, and Nitrogenous Products by Air in the Presence of Sunlight. Jour. Phys. Chem., vol. 32, p. 1263, 1928.
[8] M. Harris. The Carbonization Process: A Study of the System Wool-Sulphuric Acid-Water. B.S. Jour. Research, vol. 12, pp. 175–87, 1931.
[9] F. Lieben and F. Urban. The Splitting of Ammonia From Amino Acids and Other Substances in the Light of a Quartz Lamp. Biochem. Zs., vol. 239, pp. 250–56, 1931.
[10] Schanz. Arch. ges. Physiol., vol. 164, p. 445, 1916.

U.S. DEPARTMENT OF COMMERCE NATIONAL BUREAU OF STANDARDS

RESEARCH PAPER RP698

Part of Journal of Research of the National Bureau of Standards, vol. 13, July 1934

CONTRIBUTION TO THE DESIGN OF COMPRESSION MEMBERS IN AIRCRAFT

By Wm. R. Osgood

ABSTRACT

Compression members in riveted or in welded structures are columns with elastically restrained ends. Such members are usually designed as columns with a free length equal to or less than the distance between panel points. When the free length is taken as the distance between panel points, the design is likely to be safe but uneconomical. When it is taken less than this distance, however, though the economy may be evident, the safety is usually quite unknown. Bleich has shown what rational values are for the free lengths of compression members which occur in conventional types of bridges. His determination of these lengths (ratios of free length to panel-point length) is based on the theory of buckling of trusses or frameworks (*Stabnetze*). Unfortunately, Bleich's work does not carry over in its entirety to aircraft because some of the simplifying assumptions which he makes are not applicable here.

In this paper one of Bleich's analyses is carried a step further, resulting in a more general solution of the four-moment equation which applies to such problems.

CONTENTS

		Page
I.	Introduction	157
II.	Derivation of the condition of buckling	158
III.	Application to design	160

I. INTRODUCTION

Compression members in riveted or in welded structures are columns with elastically restrained ends. Such members are usually designed as columns with a free length equal to or less than the distance between panel points. When the free length is taken as the distance between panel points, the design is likely to be safe but uneconomical. When it is taken less than this distance, however, though the economy may be evident, the safety is usually quite unknown. Bleich [1] has shown what rational values are for the free lengths of compression members which occur in conventional types of bridges. His determination of these lengths (ratios of free length to panel-point length) is based on the theory of buckling of trusses or frameworks (*Stabnetze*). Unfortunately, Bleich's work does not carry over in its entirety to aircraft because some of the simplifying assumptions which he makes are not applicable here. In bridges, for example, diagonal members and vertical members frequently carry primarily tension and consequently are not made stiff; they may, therefore, be neglected as contributing to the restraints at the joints at their ends.

[1] Fr. Bleich, Theorie und Berechnung der eisernen Brücken, Berlin, Julius Springer, 1924, and Die Knickfestigkeit elastischer Stabverbindungen, Der Eisenbau, vol. 10, pp. 27 ff., Feb. 1919.

Corresponding members in the fuselage of an airplane, however, may be tubular and approximately as stiff as the other members meeting at the joints at their ends; to neglect such members results in a worthless analysis. It is the purpose of this paper to carry one of Bleich's analyses a step further.

II. DERIVATION OF THE CONDITION OF BUCKLING

Consider a loaded truss on the point of buckling in its own plane. Denote the lengths of any two of the members, ij and jk, meeting at any joint, j, by l_{ij} and l_{jk}, figure 1. In general, moments will be exerted on the joints by the members. Denote by M_{ij} the moment exerted on the joint i by the member ij and by M_{ji} the moment exerted on the joint j by the member ij, the first subscript indicating the joint acted on and the two together indicating the member acting. When the joints are fixed against translation but not against rotation, the moments in figure 1 are connected by the *equation of four moments*[2]

$$M_{ij}s'_{ij}+M_{ji}t'_{ij}+M_{jk}t'_{jk}+M_{kj}s'_{jk}=0 \tag{1}$$

where

$$s'=\frac{1}{v}s(\phi), \qquad t'=\frac{1}{v}t(\phi), \tag{2}$$

$$s(\phi)=\frac{\phi}{\sin\phi}-1, \quad t(\phi)=1-\frac{\phi}{\tan\phi}, \tag{3}$$

$$v=\frac{Pl}{E}, \qquad \phi=l\sqrt{\frac{\overline{|P|}}{EI\tau}} \tag{4}$$

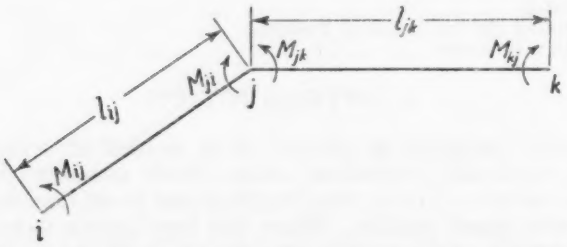

FIGURE 1.—*Two members of a framework meeting at a common joint*

I = the least moment of inertia of the cross-sectional area of a member with respect to an axis perpendicular to the plane of the truss.

$\tau=\frac{\overline{E}}{E}$, the ratio of the Considère-Engesser modulus for a member to Young's modulus.

[2] See footnote 1; also Alfred S. Niles and Joseph S. Newell, Airplane Structures, John Wiley and Sons, Inc., New York, 1929.

P = the axial load in a member, positive when compression. If $P=0$, then $\tau=1$, and $s(\phi)=t(\phi)=0$, but $s'=\frac{1}{6}\frac{l}{I}$ and $t'=\frac{1}{3}\frac{l}{I}$; and if P is negative, $s(\phi)=\frac{\phi}{\sinh\phi}-1$, $t(\phi)=1-\frac{\phi}{\tanh\phi}$.

The moments in equation 1 are positive when for an observer on one side of the members the moments tend to increase the angle on the side of the observer between the two members at any joint. The moments indicated in figure 1 are all positive for an observer below ijk.

The general method of analyzing a truss for buckling is to apply the equation of four moments successively to pairs of members meeting at joints and to determine in this way the "condition of buckling." The individual members can then be investigated, and preliminary designs may be modified.

Let it be desired to investigate a compression member ij, figure 2, in a riveted or a welded truss. We shall assume that the far ends of

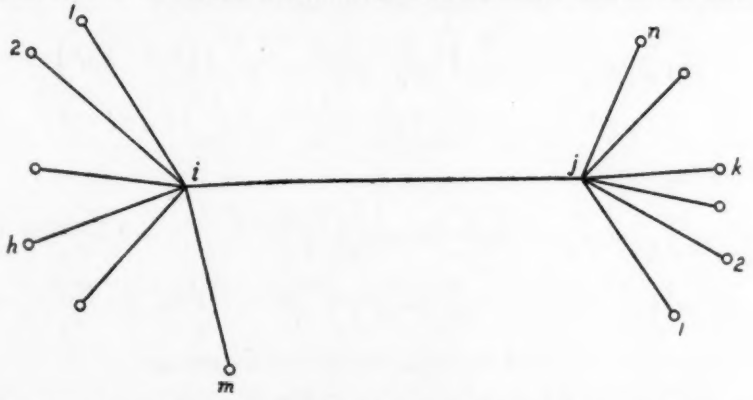

FIGURE 2.—*A member of a framework together with the members meeting it at its ends.*

all the members meeting at i and at j: i1, i2, ... ih, ... im and j1, j2, ... jk, ... jn, respectively, except the ends of the member ij itself are freely supported. This is one of Bleich's assumptions, it is on the safe side, and some such simplifying assumption is practically necessary in all except the simplest cases. In an ideal design, as a matter of fact, the condition would be approximated closely. We shall consider moments acting on the joints positive in the counterclockwise sense. Applying the equation of four moments successively to the pairs of members 1i and ij, 2i and ij, ... mi and ij, ij and j1, ij and j2, ... ij and jn, and making use of the condition of equilibrium that the sum of all the moments acting on a joint must be equal to zero, we obtain m equations of the type

$$-M_{ih}t'_{hi}+M_{ij}t'_{ij}-M_{ji}s'_{ij}=0, \tag{5a}$$

n equations of the type

$$M_{ij}s'_{ij}-M_{ji}t'_{ij}+M_{jk}t'_{jk}=0, \tag{5b}$$

and the two equations of equilibrium

$$M_{ij}+M_{i1}+M_{i2}+\ldots+M_{ih}+\ldots+M_{im}=0, \tag{6a}$$

$$M_{ji}+M_{j1}+M_{j2}+\ldots+M_{jk}+\ldots+M_{jn}=0. \tag{6b}$$

By substituting M_{ij} and M_{ji} from equations 6a and 6b, respectively, in equations 5a and 5b, we get $m+n$ linear homogenous equations in $m+n$ unknown moments, m equations being of the form,

$$\begin{aligned} &t'_{ij}M_{i1}+t'_{ij}M_{i2}+\cdots+(t'_{ij}+t'_{hi})M_{ih}+\cdots+t'_{ij}M_{im} \\ &-s'_{ij}M_{j1}-s'_{ij}M_{j2}-\cdots-s'_{ij}M_{jk}-\cdots-s'_{ij}M_{jn}=0, \end{aligned} \tag{7a}$$

and n equations of the form,

$$\begin{aligned} &-s'_{ij}M_{i1}-s'_{ij}M_{i2}-\cdots-s'_{ij}M_{ih}-\cdots-s'_{ij}M_{im} \\ &+t'_{ij}M_{j1}+t'_{ij}M_{j2}+\cdots+(t'_{ij}+t'_{jk})M_{jk}+\cdots+t'_{ij}M_{jn}=0. \end{aligned} \tag{7b}$$

The determinant of the coefficients of the set of $m+n$ equations, 7a and 7b, equated to zero is the condition for buckling. Upon evaluation of the determinant the condition becomes

$$\begin{aligned} &\left(\frac{1}{t'_{i1}}+\frac{1}{t'_{i2}}+\cdots+\frac{1}{t'_{im}}\right)\left(\frac{1}{t'_{j1}}+\frac{1}{t'_{j2}}+\cdots+\frac{1}{t'_{jn}}\right)\left(t'^{2}_{ij}-s'^{2}_{ij}\right) \\ &+\left(\frac{1}{t'_{i1}}+\frac{1}{t'_{i2}}+\cdots+\frac{1}{t'_{im}}+\frac{1}{t'_{j1}}+\frac{1}{t'_{j2}}+\cdots+\frac{1}{t'_{jn}}\right)t'_{ij}+1=0. \end{aligned} \tag{8}$$

By setting

$$T_i=\frac{1}{v_{ij}}\left(\frac{1}{t'_{i1}}+\frac{1}{t'_{i2}}+\cdots+\frac{1}{t'_{im}}\right)=\frac{1}{P_{ij}l_{ij}}\left(\frac{P_{i1}l_{i1}}{t_{i1}}+\frac{P_{i2}l_{i2}}{t_{i2}}+\ldots+\frac{P_{im}l_{im}}{t_{im}}\right) \tag{9a}$$

$$T_j=\frac{1}{v_{ij}}\left(\frac{1}{t'_{j1}}+\frac{1}{t'_{j2}}+\cdots+\frac{1}{t'_{jn}}\right)=\frac{1}{P_{ij}l_{ij}}\left(\frac{P_{j1}l_{j1}}{t_{j1}}+\frac{P_{j2}l_{j2}}{t_{j2}}+\ldots+\frac{P_{jn}l_{jn}}{t_{jn}}\right) \tag{9b}$$

(see equations 2, 3, and 4), equation 8 may be written

$$T_iT_j(t_{ij}^2-s_{ij}^2)+(T_i+T_j)t_{ij}+1=0. \tag{10}$$

III. APPLICATION TO DESIGN

The procedure in designing should be to make a preliminary design as at present, and then by means of equations 9a to 10 to check the design of individual compression members (ij) and modify it if necessary. The use of equations 9a to 10 is facilitated greatly by a nomographic chart due to L. B. Tuckerman and by tables of values of s and t for ϕ as argument, all of which it is hoped to publish in the near future. It may be pointed out that a considerable simplification on the safe side is effected by assuming the stress in tension members to be zero.

WASHINGTON, May 18, 1934.